MycoKeys 59: 1–26 (2019)
doi: 10.3897/mycokeys.59.37966
http://mycokeys.pensoft.net

RESEARCH ARTICLE

A peer-reviewed open-access journal
MycoKeys
Launched to accelerate biodiversity research

European species of *Dendrostoma* (Diaporthales)

Walter M. Jaklitsch[1,2], Hermann Voglmayr[1,2]

1 *Institute of Forest Entomology, Forest Pathology and Forest Protection, Department of Forest and Soil Sciences, BOKU-University of Natural Resources and Life Sciences, Franz Schwackhöfer Haus, Peter-Jordan-Straße 82/I, 1190 Vienna, Austria* **2** *Division of Systematic and Evolutionary Botany, Department of Botany and Biodiversity Research, University of Vienna, Rennweg 14, 1030 Vienna, Austria*

Corresponding author: *Walter M. Jaklitsch* (walter.jaklitsch@univie.ac.at)

Academic editor: *Huzefa Raja* | Received 4 July 2019 | Accepted 7 September 2019 | Published 16 October 2019

Citation: Jaklitsch WM, Voglmayr H (2019) European species of *Dendrostoma* (Diaporthales). MycoKeys 59: 1–26. https://doi.org/10.3897/mycokeys.59.37966

Abstract

European species of the genus *Dendrostoma* (Erythrogloeaceae, Diaporthales) occurring on *Castanea sativa* and *Quercus* spp. based on freshly collected material are presented. Using a matrix of sequences from ITS, LSU, *rpb2*, and *tef1*, five species are recognized, and their phylogenetic positions are determined. Four species are added to the 14 described species of *Dendrostoma*. *Dendrostoma atlanticum* on *Castanea sativa*, *D. creticum* on *Quercus coccifera* and *D. istriacum* on *Q. ilex* are described as new species, *Valsa castanea* is combined in *Dendrostoma*, and *D. leiphaemia* is redescribed and illustrated. A key to the European species of *Dendrostoma* is provided.

Keywords

Amphiporthe, *Cryptodiaporthe*, multi-gene phylogeny, pyrenomycetes, systematics

Introduction

The genus *Cryptodiaporthe*, based on *Cryptospora aesculi*, is one of several segregates from the large genus *Diaporthe* (Diaporthales), characterized by the lack of stromatic zones and with asexual morphs recognized by Petrak (1921) as *Septomyxa*. In 1933, Wehmeyer (1933) recognized the relatively large number of species with a simple type of stroma development having various asexual morphs as a heterogeneous grouping. Petrak (1971) removed *C. tiliae* (as *C. hranicensis*) to his new genus *Amphiporthe*, mainly due to its *Amphicytostroma* asexual morph, where subsequently several species were added. Using the phylogenetic markers ITS, LSU, and *rpb2*, Mejía et al. (2008)

detected that *C. aesculi* is congeneric with the generic type of *Plagiostoma*, *P. euphorbiae*. Thus, *Cryptodiaporthe* became a synonym of *Plagiostoma*. Subsequently (Mejía et al. 2011), several other species of *Cryptodiaporthe* were combined in *Plagiostoma*. Since the first phylogenetic treatment of the Diaporthales using DNA data (Castlebury et al. 2002), many old genera have been split and new ones described, and the proliferation of family names has forwarded a current number of 28, more than a half of which having been erected during the last three to four years (compare Jaklitsch et al. (2016), who listed 11 families). One of these families is the Erythrogloeaceae, whose members are based on phytopathogenic coelomycetous fungi (*Chrysocrypta*, *Disculoides*, *Erythrogloeum*). The only genus of this family for which sexual morphs are known is *Dendrostoma* (Fan et al. 2018). This genus is characterized by features common to many other diaporthalean genera forming pseudostromata lacking black stromatic margins, including *Amphiporthe* and *Plagiostoma* (*Cryptodiaporthe*). Rossman et al. (2015) already noted that *Amphiporthe castanea* and *A. leiphaemia* are not congeneric with *A. tiliae* (syn. *A. hranicensis*) and would need a new generic name. *Amphiporthe leiphaemia* was combined in *Dendrostoma* by Senanayake et al. (2018), based on ITS and LSU sequences of a CBS strain without giving any further information, whereas *A. castanea* has not been treated recently, although Jiang et al. (2019), who substantially enlarged the scope of the genus by describing 10 new species from *Castanea* and *Quercus* in China, recognized seven species on *Castanea mollissima*. Here we report on recently collected species of *Dendrostoma* occurring on *Castanea sativa* and *Quercus* spp. in Europe.

Materials and methods

Sample sources

All isolates included in this study originated from ascospores of freshly collected specimens derived from recently dead branches or twigs. Details of the strains including NCBI GenBank accession numbers of gene sequences used to compute the phylogenetic trees are listed in Table 1. Strain acronyms other than those of official culture collections are used here primarily as strain identifiers throughout the work. Representative isolates have been deposited at the Westerdijk Fungal Biodiversity Centre (CBS-KNAW), Utrecht, The Netherlands. Details of the specimens used for morphological investigations are listed in the Taxonomy section under the respective descriptions. Freshly collected specimens have been deposited in the Fungarium of the Department of Botany and Biodiversity Research, University of Vienna (WU).

Morphology

Microscopic observations were made in tap water except where noted. Morphological analyses of microscopic characters were carried out as described by Jaklitsch (2009).

Table 1. Isolates and accession numbers of sequences used in the phylogenetic analyses.

Species	Culture[1,2]	Country	Host	Host family	GenBank accession numbers[2]			
					ITS	LSU	*rpb2*	*tef1*
Chrysocrypta corymbiae	CBS 132528*	Australia	*Corymbia* sp.	Myrtaceae	JX069867	JX069851	MH545415	MH545457
Dendrostoma atlanticum	**D196** = CBS 145804*	France	*Castanea sativa*	Fagaceae	**MN447223**	**MN447223**	**MN432160**	**MN432167**
	D303	Spain	*Castanea sativa*	Fagaceae	**MN447224**	**MN447224**	**MN432161**	**MN432168**
Dendrostoma aurorae	CFCC 52753*	China	*Castanea mollissima*	Fagaceae	MH542498	MH542646	MH545405	MH545447
	CFCC 52754	China	*Castanea mollissima*	Fagaceae	MH542499	MH542647	MH545406	MH545448
Dendrostoma castaneae	CFCC 52745*	China	*Castanea mollissima*	Fagaceae	MH542488	MH542644	MH545395	MH545437
	CFCC 52746	China	*Castanea mollissima*	Fagaceae	MH542489	–	MH545396	MH545438
	CFCC 52747	China	*Castanea mollissima*	Fagaceae	MH542490	–	MH545397	MH545439
	CFCC 52748	China	*Castanea mollissima*	Fagaceae	MH542491	–	MH545398	MH545440
	CFCC 52749	China	*Castanea mollissima*	Fagaceae	MH542492	MH542645	MH545399	MH545441
	CFCC 52750	China	*Castanea mollissima*	Fagaceae	MH542493	–	MH545400	MH545442
	CFCC 52751	China	*Castanea mollissima*	Fagaceae	MH542494	–	MH545401	MH545443
	CFCC 52752	China	*Castanea mollissima*	Fagaceae	MH542495	–	MH545402	MH545444
Dendrostoma castaneicola	CFCC 52743*	China	*Castanea mollissima*	Fagaceae	MH542496	–	MH545403	MH545445
	CFCC 52744	China	*Castanea mollissima*	Fagaceae	MH542497	–	MH545404	MH545446
Dendrostoma castaneum	**D192** = CBS 145803	Austria	*Castanea sativa*	Fagaceae	**MN447225**	**MN447225**	**MN432162**	**MN432169**
	D230	Italy	*Castanea sativa*	Fagaceae	**MN447226**	**MN447226**	–	**MN432170**
	D260	Italy	*Castanea sativa*	Fagaceae	**MN447227**	**MN447227**	–	–
Dendrostoma chinense	CFCC 52755*	China	*Castanea mollissima*	Fagaceae	MH542500	MH542648	MH545407	MH545449
	CFCC 52756	China	*Castanea mollissima*	Fagaceae	MH542501	MH542649	MH545408	MH545450
	CFCC 52757	China	*Castanea mollissima*	Fagaceae	MH542502	MH542650	MH545409	MH545451
	CFCC 52758	China	*Castanea mollissima*	Fagaceae	MH542503	MH542651	MH545410	MH545452
Dendrostoma creticum	**D124** = CBS 145802*	Greece	*Quercus coccifera*	Fagaceae	**MN447228**	**MN447228**	**MN432163**	**MN432171**
Dendrostoma dispersum	CFCC 52730*	China	*Quercus* sp.	Fagaceae	MH542467	MH542629	MH545374	MH545416
	CFCC 52731	China	*Quercus* sp.	Fagaceae	MH542468	MH542630	MH545375	MH545417
Dendrostoma istriacum	**D122** = CBS 145801*	Croatia	*Quercus ilex*	Fagaceae	**MN447229**	**MN447229**	**MN432164**	**MN432172**
Dendrostoma leiphaemia	**D105** = CBS 145800	Austria	*Quercus robur*	Fagaceae	**MN447230**	**MN447230**	**MN432165**	**MN432173**
	D144	Poland	*Quercus robur*	Fagaceae	**MN447231**	**MN447231**	**MN432166**	**MN432174**
	CBS 187.37	NA	*Quercus* sp.	Fagaceae	MH855882	MH867393	–	–
Dendrostoma mali	CFCC 52102*	China	*Malus spectabilis*	Rosaceae	MG682072	MG682012	MG682032	MG682052
Dendrostoma osmanthi	CFCC 52106*	China	*Osmanthus fragrans*	Oleaceae	MG682073	MG682013	MG682033	MG682053
	CFCC 52107	China	*Osmanthus fragrans*	Oleaceae	MG682075	MG682015	MG682035	MG682055
	CFCC 52108	China	*Osmanthus fragrans*	Oleaceae	MG682074	MG682014	MG682034	MG682054
	CFCC 52109	China	*Osmanthus fragrans*	Oleaceae	MG682076	MG682016	MG682036	MG682056
Dendrostoma parasiticum	CFCC 52761	China	*Castanea mollissima*	Fagaceae	MH542480	MH542636	MH545387	MH545429
	CFCC 52762*	China	*Quercus wutaishanica*	Fagaceae	MH542482	MH542638	MH545389	MH545431
	CFCC 52763	China	*Castanea mollissima*	Fagaceae	MH542481	MH542637	MH545388	MH545430
	CFCC 52764	China	*Quercus aliena*	Fagaceae	MH542483	MH542639	MH545390	MH545432
	CFCC 52765	China	*Castanea mollissima*	Fagaceae	MH542484	MH542640	MH545391	MH545433
	CFCC 52766	China	*Quercus aliena* var. *acutiserrata*	Fagaceae	MH542485	MH542641	MH545392	MH545434
Dendrostoma qinlingense	CFCC 52732*	China	*Quercus wutaishanica*	Fagaceae	MH542471	MH542633	MH545378	MH545420
	CFCC 52733	China	*Quercus aliena* var. *acutiserrata*	Fagaceae	MH542472	MH542634	MH545379	MH545421
Dendrostoma quercinum	CFCC 52103*	China	*Quercus acutissima*	Fagaceae	MG682077	MG682017	MG682037	MG682057
	CFCC 52104	China	*Quercus acutissima*	Fagaceae	MG682078	MG682018	MG682038	MG682058
	CFCC 52105	China	*Quercus acutissima*	Fagaceae	MG682079	MG682019	MG682039	MG682059

Species	Culture[1,2]	Country	Host	Host family	GenBank accession numbers[2]			
					ITS	LSU	*rpb2*	*tef1*
Dendrostoma quercus	CFCC 52734	China	*Quercus* sp.	Fagaceae	MH542473	–	MH545380	MH545422
	CFCC 52735	China	*Quercus* sp.	Fagaceae	MH542474	–	MH545381	MH545423
	CFCC 52736	China	*Quercus* sp.	Fagaceae	MH542478	–	MH545385	MH545427
	CFCC 52737	China	*Quercus* sp.	Fagaceae	MH542475	–	MH545382	MH545424
	CFCC 52738	China	*Quercus* sp.	Fagaceae	MH542477	–	MH545384	MH545426
	CFCC 52739*	China	*Quercus* sp.	Fagaceae	MH542476	MH542635	MH545383	MH545425
	CFCC 52740	China	*Quercus* sp.	Fagaceae	MH542479	–	MH545386	MH545428
Dendrostoma shaanxiense	CFCC 52741*	China	*Castanea mollissima*	Fagaceae	MH542486	MH542642	MH545393	MH545435
	CFCC 52742	China	*Castanea mollissima*	Fagaceae	MH542487	MH542643	MH545394	MH545436
Dendrostoma shandongense	CFCC 52759*	China	*Castanea mollissima*	Fagaceae	MH542504	MH542652	MH545411	MH545453
	CFCC 52760	China	*Castanea mollissima*	Fagaceae	MH542505	MH542653	MH545412	MH545454
Disculoides eucalypti	CBS 132183*	Australia	*Eucalyptus* sp.	Myrtaceae	JQ685517	JQ685523	MH545413	MH545455
Disculoides eucalyptorum	CBS 132184*	Australia	*Eucalyptus viminalis*	Myrtaceae	JQ685518	JQ685524	MH545414	MH545456

[1] Ex-type strains marked by an asterisk.; [2] Abbreviations: **CBS:** Culture collection of the Westerdijk Fungal Biodiversity Institute, Utrecht, The Netherlands; **CCFC**: China Forestry Culture Collection Centre, Beijing, China; [3] Isolates/sequences in bold were isolated/sequenced in the present study.

Methods of microscopy included stereomicroscopy using a Nikon SMZ 1500 and Nomarski differential interference contrast (DIC) using the compound microscopes Nikon Eclipse E600 or Zeiss Axio Imager.A1 equipped with a Zeiss Axiocam 506 colour digital camera. Images and data were gathered using a Nikon Coolpix 4500 or a Nikon DS-U2 digital camera and measured by using the NIS-Elements D v. 3.0 or 3.22.15 or Zeiss ZEN Blue Edition software packages. For certain images of ascomata the stacking software Zerene Stacker v. 1.04 (Zerene Systems LLC, Richland, WA, USA) was used. Measurements are reported as maxima and minima in parentheses and the range representing the mean plus and minus the standard deviation of the number of measurements given in parentheses.

Culture preparation, DNA extraction, PCR, and sequencing

Ascospore isolates were prepared and grown on 2% corn meal dextrose agar (CMD; CMA: Sigma, St Louis, Missouri; supplemented with 2% (w/v) D(+)-glucosemonohydrate) or 2% malt extract agar (MEA; 2% w/v malt extract, 2% w/v agar-agar; Merck, Darmstadt, Germany). Cultures are illustrated in Figure 2. Growth of liquid cultures and extraction of genomic DNA was performed as reported previously (Voglmayr and Jaklitsch 2011; Jaklitsch et al. 2012) using the DNeasy Plant Mini Kit (QIAgen GmbH, Hilden, Germany). The following loci were amplified and sequenced: a ca 1.6 kb fragment containing the terminal part of the small subunit nuclear ribosomal DNA (nSSU rDNA), the complete internal transcribed spacer region (ITS1-5.8S-ITS2) and a ca 900 bp fragment of the large subunit nuclear ribosomal DNA (nLSU rDNA), amplified and sequenced as a single fragment with primers V9G (De Hoog and Gerrits van den Ende 1998) and LR5 (Vilgalys and Hester 1990); a ca 1.2 kb

fragment of the RNA polymerase II subunit 2 (*rpb2*) gene with primers fRPB2-5f and fRPB2-7cr (Liu et al. 1999) or dRPB2-5f and dRPB2-7r (Voglmayr et al. 2016); a ca 1.3–1.5 kb fragment of the translation elongation factor 1-alpha (*tef1*) gene with primers EF1-728F (Carbone and Kohn 1999) and TEF1LLErev (Jaklitsch et al. 2005). PCR products were purified using an enzymatic PCR cleanup (Werle et al. 1994) as described in Voglmayr and Jaklitsch (2008). DNA was cycle-sequenced using the ABI PRISM Big Dye Terminator Cycle Sequencing Ready Reaction Kit v. 3.1 (Applied Biosystems, Warrington, UK) and the PCR primers; in addition, primers ITS4 (White et al. 1990), LR2R-A (Voglmayr et al. 2012), and LR3 (Vilgalys and Hester 1990) were used for the SSU-ITS-LSU region, and TEF1_INTF (forward, Jaklitsch 2009) and TEFD_iR1 (reverse, 5' GAGTTYGAGGCYGGTATCTC 3') or TEF1_INT2 (Voglmayr and Jaklitsch 2017) for *tef1*. Sequencing was performed on an automated DNA sequencer (3730xl Genetic Analyzer, Applied Biosystems).

Phylogenetic analyses

The newly generated sequences were aligned with the sequences of Jiang et al. (2019), and a combined matrix of the three loci (partial SSU-ITS-LSU rDNA, *rpb2*, and *tef1*) was produced for phylogenetic analyses, with three species (*Chrysocrypta corymbiae*, *Disculoides eucalypti*, and *Disculoides eucalyptorum*) added as the outgroup according to Jiang et al. (2019). The GenBank accession numbers of sequences used in the analyses are given in Table 1. Sequence alignments were produced with the server version of MAFFT (http://mafft.cbrc.jp/alignment/server/), checked and refined using BioEdit v. 7.2.6 (Hall 1999). The combined data matrix contained 4194 characters, viz. 1637 nucleotides of SSU-ITS-LSU, 1075 nucleotides of *rpb2*, and 1482 nucleotides of *tef1*.

Maximum parsimony (MP) analyses were performed with PAUP v. 4.0a165 (Swofford 2002). All molecular characters were unordered and given equal weight; analyses were performed with gaps treated as missing data; the COLLAPSE command was set to MINBRLEN. MP analysis of the combined multilocus matrix was done using 1000 replicates of heuristic search with random addition of sequences and subsequent TBR branch swapping (MULTREES option in effect, steepest descent option not in effect). Bootstrap analyses with 1000 replicates were performed in the same way but using 10 rounds of random sequence addition and subsequent branch swapping during each bootstrap replicate.

Maximum likelihood (ML) analyses were performed with RAxML (Stamatakis 2006) as implemented in raxmlGUI 1.3 (Silvestro and Michalak 2012), using the ML + rapid bootstrap setting and the GTRGAMMA substitution model with 1000 bootstrap replicates. The matrix was partitioned for the different gene regions. In the Results and Discussion, bootstrap values below 70% are considered low, between 70–90% medium, and above 90% high.

Results

Phylogenetic analyses

Of the 4194 characters included in the phylogenetic analyses, 703 were parsimony informative (133 from the SSU-ITS-LSU, 247 from *rpb2*, 323 from *tef1*). MP analyses revealed eight MP trees 1552 steps long, one of which is shown as Figure 1. The tree backbone was identical in all MP trees, except for the position of *Dendrostoma castaneicola*, which was embedded within *D. castaneae* in some of the MP trees (not shown). The best ML tree (lnL = −13985.7598) revealed by RAxML was compatible with the MP strict consensus tree, except for an interchanged position of *D. atlanticum* and *D. shaanxiense* (not shown). The genus *Dendrostoma* received maximum and medium support in the MP and ML analyses, respectively, and most of the tree backbone received significant support as well (Fig. 1). Although *Dendrostoma* accessions from *Quercus* and *Castanea* were interspersed, host-related patterns were obvious in the various *Dendrostoma* subclades (Fig. 1). The basal subclade A (*D. castaneum*, *D. chinense*, *D. shandongense*) contains only accessions from *Castanea* and is followed by subclade B (*D. creticum*, *D. istriacum*) from *Quercus* and subclade C with the single species *D. aurorae* from *Castanea*. Subclade D contains four species from *Castanea* (*D. atlanticum*, *D. castaneae*, *D. castaneicola*, *D. shaanxiense*) and subclade E three species from *Quercus* (*D. dispersum*, *D. leiphaemia*, *D. quercinum*) plus *D. mali* from *Malus* (Rosaceae). Finally, subclade F contains *D. qinlingense* and *D. quercus* from *Quercus*, *D. parasiticum* from *Quercus* and *Castanea*, and *D. osmanthi* from *Osmanthus* (Oleaceae). Geographically, no patterns were obvious, as the European accessions were distributed amongst the phylogenetic tree and embedded within lineages described from Eastern Asia (China).

Taxonomy

***Dendrostoma* X.L. Fan & C.M. Tian, Persoonia 40: 126 (2018)**

Type species. *Dendrostoma mali* X.L. Fan & C.M. Tian.

Description, emended here. *Sexual morph*: *pseudostromata* immersed in bark and erumpent, causing a pustulate bark surface, consisting of an ectostromatic disc and entostroma with embedded ascomata. *Ectostromatic disc* flat or convex, surrounded by bark flaps. *Entostroma* light-coloured, prosenchymatous to nearly pseudoparenchymatous, mixed with bark cells, sometimes forming a more-or-less conical central column beneath the disc. *Stromatic zones* lacking or sometimes bark dorsally darkened. *Ascomata* perithecial, subglobose. *Ostioles* flat in the disc or slightly projecting, cylindrical, often with conical apical part. *Paraphyses* deliquescent. *Asci* oblong, fusoid, narrowly clavate or subellipsoid, with a refractive apical ring, containing (4–)6–8 ascospores in various arrangements, becoming detached at maturity. *Ascospores* hyaline, ellipsoid, fusoid, oblong to subacicular, often inequilateral, straight to curved,

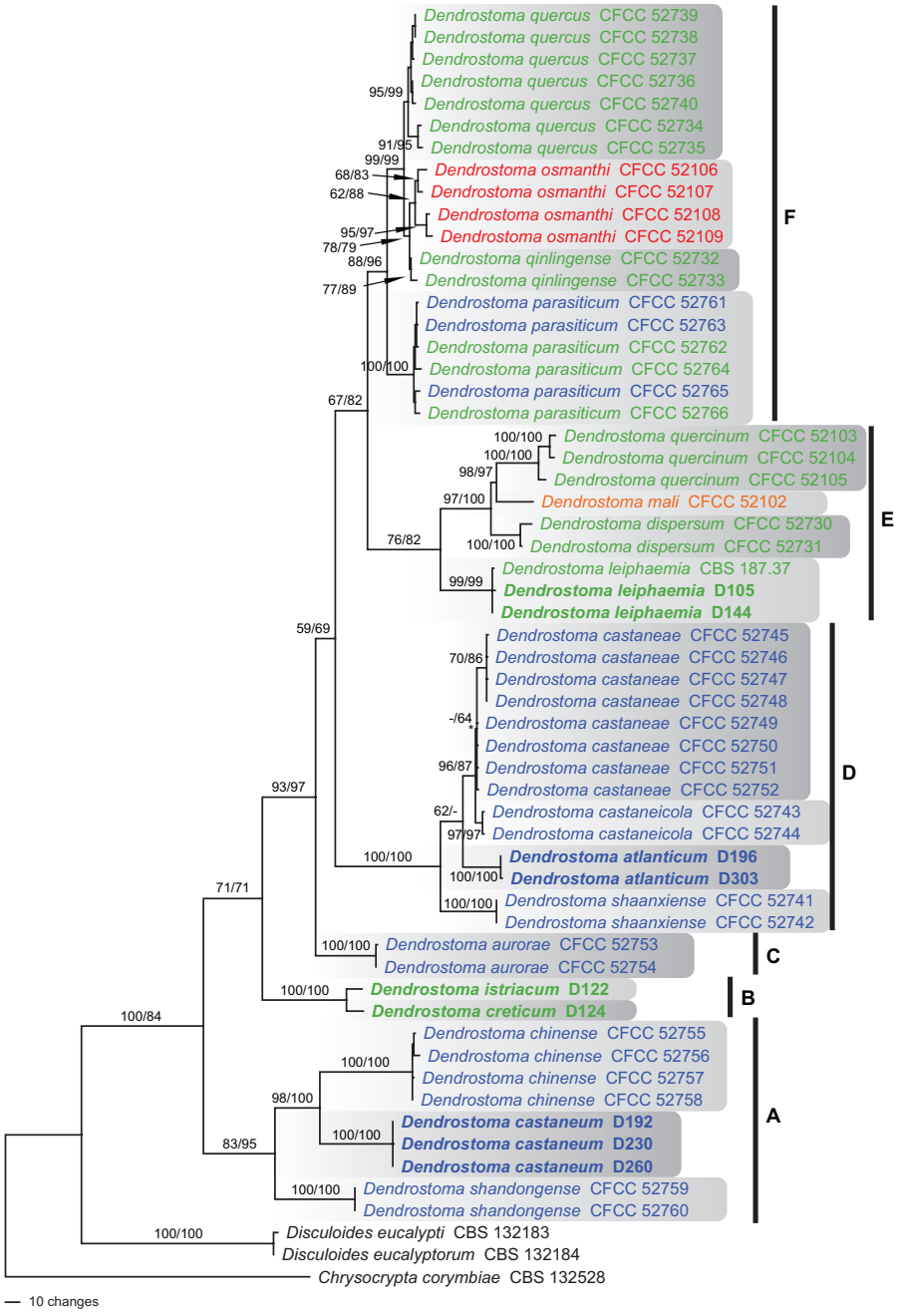

Figure 1. Phylogram showing one of 8 MP trees 1552 steps long revealed by PAUP from an analysis of the combined ITS-LSU-*rpb2-tef1* matrix of *Dendrostoma*, with *Chrysocrypta corymbiae*, *Disculoides eucalypti* and *D. eucalyptorum* added as outgroup taxa. MP and ML bootstrap support above 50% are given above or below the branches. The asterisk (*) denotes the node collapsed in the strict consensus of the eight MP trees. Accessions in bold were sequenced in the present study; accessions in blue were isolated from *Castanea*, those in green from *Quercus*, in orange from *Malus* and in red from *Osmanthus*.

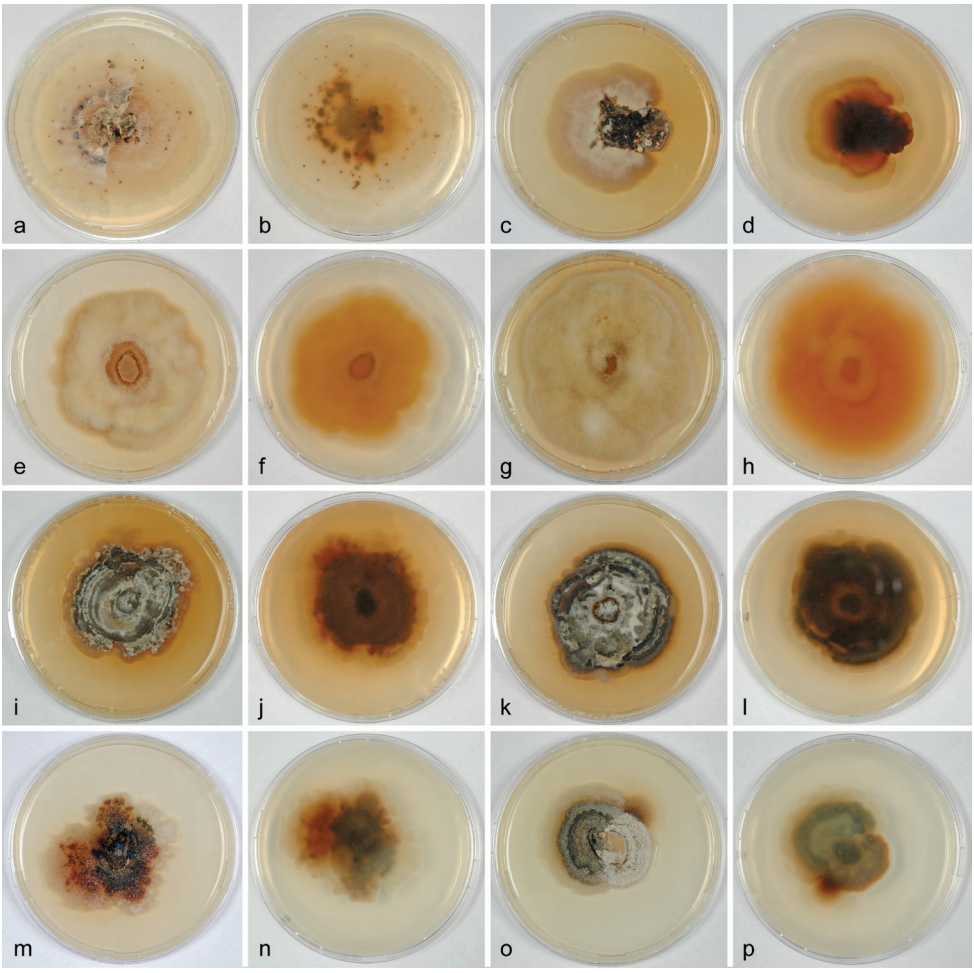

Figure 2. *Dendrostoma* cultures (CMD, 16 °C) after 20d (**e–h, m–p**), 54–58 d (**a–d, i–l**). **a–d** *D. atlanticum* (**a, b** D192; **c, d** D230) **e–h** *D. castaneum* (**a, b** D196; **c, d** D303) **i–j** *D. creticum* D124 **k–l** *D. istriacum* D122 **m–p** *D. leiphaemia* (**m, n** D105; **o, p** D144) **b, d, f, h, j, l, n, p** reverse side.

bicellular, more-or-less constricted at the median or eccentric septum, smooth, with 2–4 drops or multiguttulate, often with gelatinous terminal appendages. *Asexual morph*: *conidiomata* acervular, either forming lateral locules on the ostiolar level of sexual pseudostromata or separate, conical to pulvinate, immersed-erumpent from bark; wall pseudoparenchymatous. Often a pseudoparenchymatous conical central column present beneath the covering layer. *Conidiophores* non-differentiated, hypha-like or reduced to conidiogenous cells. *Conidiogenous cells* phialidic, lining the inner walls of cavities, subcylindrical to ampulliform, hyaline, shades of brown with age. *Conidia* hyaline, aseptate, smooth, multiguttulate or not, thin-walled, oblong, ellipsoid to fusoid, straight or curved.

***Dendrostoma atlanticum* Voglmayr & Jaklitsch, sp. nov.**
MycoBank: MB 832515
Figures 3, 4

Diagnosis. *Dendrostoma atlanticum* is recognized by clay-coloured ectostromatic discs and ascospores having large guttules and bristle-like appendages.

Holotype. FRANCE, Bretagne, Dépt. Morbihan (56), Saint Martin sur Oust, Beauvais, on twigs of *Castanea sativa*, soc. immature *Valsaria* sp., 15 Jan. 2016, A. Delannoy (WU 37024; ex-type culture CBS 145804 = D196).

Etymology. *Atlanticum*, referring to its occurrence in the Atlantic region.

Description. *Sexual morph*: *pseudostromata* 1–4.5 mm in their widest dimension in cross section, bluntly conical or pulvinate, circular, elliptic or irregular in outline, scattered, gregarious to confluent up to 7 mm length. *Ectostromatic discs* 0.4–2 mm in their widest dimension, distinct and conspicuous, projecting up to 0.5(–1) mm from the bark surface, pulvinate, circular, angular or fusoid in outline, with flat or convex top, initially whitish, turning pale to dark clay-coloured, splitting the periderm, often surrounded by bark flaps. *Ostioles* 1–40 per disc, often originating eccentrically from the perithecial venter, arranged in ring-like configuration or variably filling the disc, (44–)100–163(–195) µm (*n* = 42) in diameter at the tip, brown to black, cylindrical, sometimes attenuated towards tip, plane with the disc or projecting up to 300 µm; tip usually with dark umbilicate centre. *Entostroma* whitish, yellowish to pale bark coloured, consisting of thin-walled, hyaline to subhyaline 1–3 µm wide hyphae and bark cells. *Perithecia* (390–)480–660(–750) µm (*n* = 35) in diameter, depressed subglobose, collapsing upward upon drying; *peridium* ca 10–30 µm thick, colourless to pale olivaceous, consisting of hyaline to yellowish or pale brownish, thick-walled cells without clear contours, smaller and more-or-less isodiametric outside, larger and compressed inside, very variable, (3–)4–17(–38) in diameter (*n* = 66). *Paraphyses* of broad collapsing threads. *Asci* (64–)71–86(–90) × (11–)13–17(–19) µm (*n* = 35), fusoid to oblong, being released at maturity, containing 8 biseriate ascospores. *Ascospores* (13–)15–18(–20) × (4.3–)5.5–7(–8) µm, l/w (2.1–)2.4–2.9(–3.9) (*n* = 51), ellipsoid, often inequilateral, 2-celled, slightly constricted at the median septum, with the upper cell often slightly wider than the lower, hyaline, with 1–2 large and several small guttules per cell, smooth, with a hyaline, bristle-like, straight to curved appendage (10–)11.5–15.5(–21) × (1.5–)2–2.5(–2.8) µm (*n* = 101) at each end.

Asexual morph acervular. *Conidiomata* ca 1–2.2 mm in diameter, bluntly conical, width exceeding height, prosenchymatous. *Covering discs* 0.3–1.1 mm in diameter, flat to pulvinate, whitish cream to pale reddish brown. Central column whitish to reddish brown, usually darker toward the top; fertile chamber ring-like around the central column; walls and column consisting of pale yellowish brown *textura angularis*, outer wall and outer layer of the column containing numerous crystals. *Phialides* (3.7–)6.3–9.7(–11.5) × (2–)2.5–3.8(–4.7) µm (*n* = 46), arranged in a palisade on hyaline to yellowish, angular cells, ampulliform to lageniform, less commonly cylindrical. *Conidia* 1-celled, hyaline, smooth, dimorphic, both morphs formed in the same locule, either ellipsoid to oblong, (6.4–)7.7–10.2(–11.7)

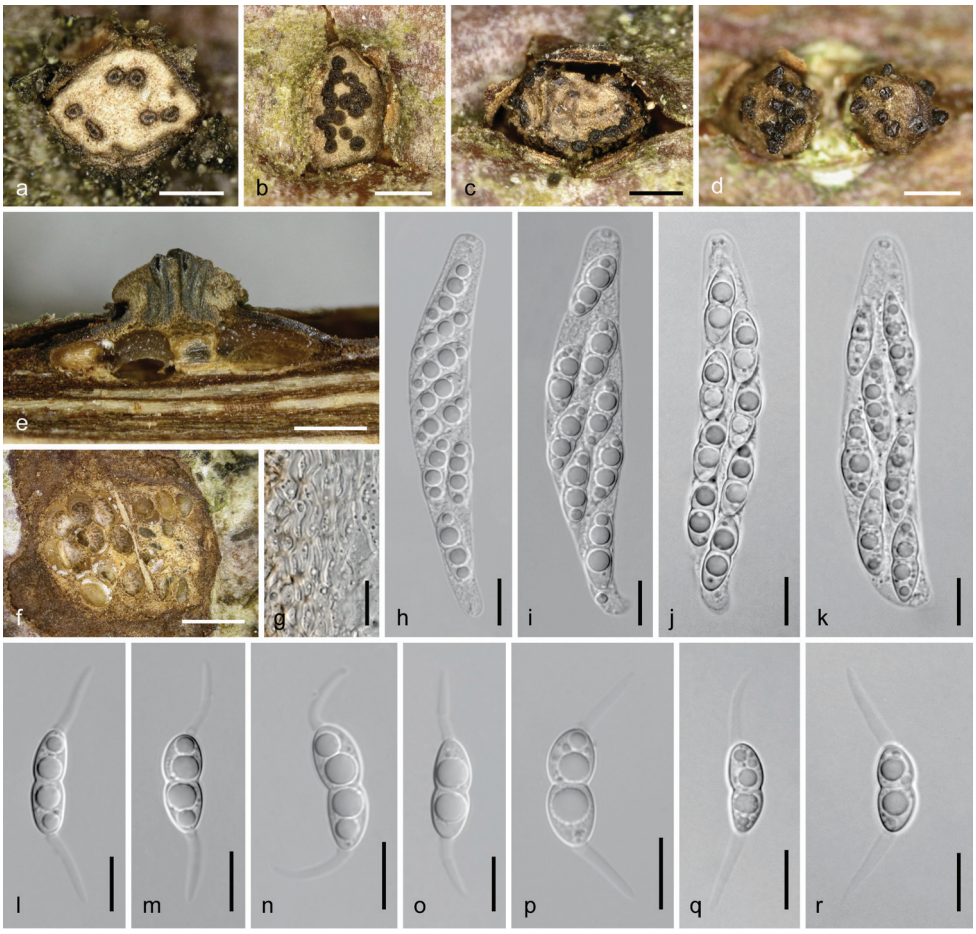

Figure 3. *Dendrostoma atlanticum*. Sexual morph **a–d** ectostromatic discs and ostioles **e** pseudostroma in vertical section **f** pseudostroma in cross section **g** peridium in cross section (in 3% KOH) **h–k** asci **l–r** ascospores. **a–c, f, h, i, k–p** WU 37024 = D196), **d, e, g, j, q, r** WU 37025 = D303. Scale bars: 1 mm (**f**), 500 µm (**a–e**), 10 µm (**g–r**).

× (4–)4.5–5.7(–6) µm, l/w (1.4–)1.4–2.2(–3) (*n* = 21), with a large guttule and often distinct abscission scar, or cylindrical, (7.7–)10.2–13.5(–15.3) × (2.3–)2.5–3.2(–3.5) µm, l/w (2.8–)3.6–4.7(–5.6) (n = 45), straight or curved, with mostly 3 or 4 confluent guttules.

Culture characteristics. On CMD at 16 °C in the dark colony more-or-less circular, of loose mycelium, first white, variably covered by white aerial hyphae, becoming dense, forming white and apricot to orange zones, darkening and turning black from the centre, sometimes forming reddish brown dots, spots or tubercles.

Other specimen examined. SPAIN, Galicia, Pontevedra, O Grove, 42°28'04"N, 08°53'14"W, on twigs of *Castanea sativa*, 4 Nov. 2018, M.A. Delgado (WU 37025; culture D303).

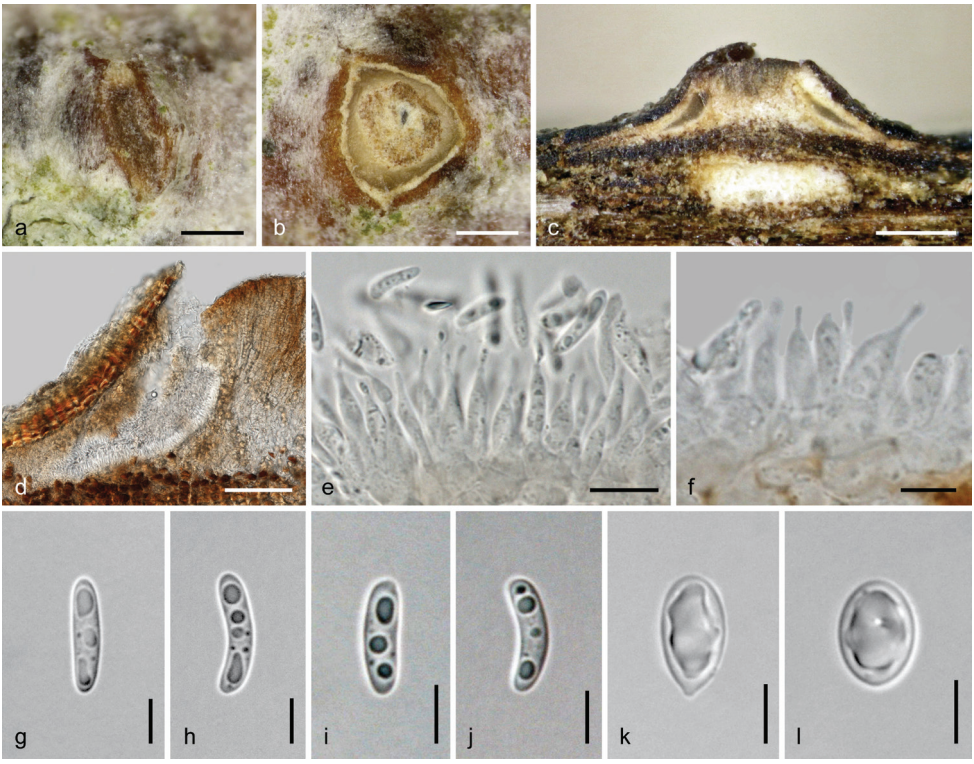

Figure 4. *Dendrostoma atlanticum* (WU 37024 = D196). Asexual morph **a, b** conidiomata in face view **c** conidioma in vertical section **d** vertical section through fertile chamber and part of the central column **e, f** phialides **g–l** conidia (cylindrical in **g–j**, ellipsoid in **k, l**). **d–l** In 3% KOH. Scale bars: 300 µm (**a–c**), 100 µm (**d**), 10 µm (**e**), 5 µm (**f–l**).

Notes. *Dendrostoma atlanticum* is easily recognized by its long-pedicellate ascospores having 2–4 large drops, setting it apart from *D. castaneum*, which has narrow, often curved ascospores with small drops and short appendages. All species described from *Castanea* in China are only known from asexual morphs (Jiang et al. 2019).

***Dendrostoma castaneum* (Tul. & C. Tul.) Voglmayr & Jaklitsch, comb. nov.**
MycoBank: MB 832516
Figures 5, 6

Valsa castanea Tul. & C. Tul., Select. fung. carpol. (Paris) 2: 202 (1863) (Basionym).
≡ *Amphiporthe castanea* (Tul. & C. Tul.) M.E. Barr, Mycol. Mem. 7: 142 (1978).
≡ *Cryptodiaporthe castanea* (Tul. & C. Tul.) Wehm., Trans. Br. mycol. Soc. 18(4): 284 (1934) [1933].
≡ *Diaporthe castanea* (Tul. & C. Tul.) Sacc., Syll. fung. (Abellini) 1: 624 (1882).

= *Cryptospora leiphaemoides* Fuckel, Jb. nassau. Ver. Naturk. 25–26: 323 (1871).
≡ *Diaporthe leiphaemoides* (Fuckel) Sacc., Syll. fung. (Abellini) 1: 624 (1882).

Diagnosis. *Dendrostoma castaneum* is recognized by KOH+ purple ostioles, slender ascospores with small drops and subfusiform conidia, and the presence of hyphal conidiophores.

Description. *Sexual morph*: *pseudostromata* 0.8–3(–5) mm in their widest dimension in cross section, very variable, flat subconical or lenticular, in outline circular, elliptic or elongate, scattered, gregarious or confluent, and forming elongate patches, lifting the periderm slightly and often becoming visible as a dark zone on the bark surface, causing bumps in bark, splitting the periderm. *Ectostromatic discs* 0.3–2.7 mm in their widest dimension, often ill-defined and variable, cream, yellowish brown to dark brown, flat, surrounded by bark flaps, first present as a covering layer with ostiolar necks subsequently bursting through it, soon crumbling away. *Ostioles* 1–25 per disc, usually arising eccentrically from the perithecial venter, (53–)71–125(–180) µm (*n* = 51) in diameter, bluntly conical or cylindrical with black sides and red, yellowish, or greenish tip, often attenuated to a minute, ca 20–40 µm wide dark centre, in section rounded to angular, sometimes sulcate, variably arranged in the disc, projecting to 0.2 mm, periphysate; red colour of the ostiolar tip turning purple in 3% KOH and yellow in lactic acid. *Entostroma* yellowish to shades of brown, consisting of bark cells and hyaline to yellowish, 1.5–4.5 wide, thin-walled hyphae becoming thicker-walled and forming a pseudoparenchyma in the vicinity of perithecia. *Perithecia* tightly aggregated, (265–)305–460(–600) µm (*n* = 47) in diameter, depressed subglobose to ellipsoid, collapsing upward; *peridium* ca 10–30 µm thick, hyaline, pale olivaceous to brown, in section outside of brown isodiametric to strongly compressed thick-walled cells, inside of compressed and elongated hyaline to brownish cells, in combination (3–)4–15(–28) µm (*n* = 57) in diameter. *Paraphyses* absent at maturity. *Asci* (49–)53–63(–65) × (7.8–)8.5–10.5(–12) µm (*n* = 35), narrowly clavate to subfusoid or oblong, floating freely in the centre, thick-walled at the apex containing a minute refractive ring invisible in 3% KOH, containing 4–8 biseriate ascospores. *Ascospores* (11.5–)14–18(–20) × (3–)3.5–4.5(–5.3) µm, l/w (2.7–)3.5–4.6(–5.4) (*n* = 76), 2-celled, not or slightly constricted at the median or slightly eccentric septum, oblong to inequilaterally ellipsoid, straight to mostly curved, with the upper cell often slightly wider than the lower, broadly rounded at the ends, hyaline, with several minute drops (confluent to 2 larger drops per cell in mounts), smooth, with or without a hyaline, subconical to filiform appendage (2.2–)2.8–4.5(–5.5) × (1.1–)1.3–1.6(–1.8) µm (*n* = 88) at each end invisible in 3% KOH.

Asexual morph co-occurring with the sexual morph, acervular, pulvinate, scattered to aggregated, 0.5–2.7 mm in diameter, appearing as superficial discs 0.3–2 mm in diameter, with undulate surface, cream to pale brown and becoming brittle in the centre and nearly black at the periphery and often also indicated as dark zone on the bark surface around the disc; inside consisting of a pale or yellowish brown, loose and brittle central column consisting of pale brown *t. prismatica* and a lateral ring-like, dense, white to distinctly yellow fertile part with even or undulating margin, the latter also

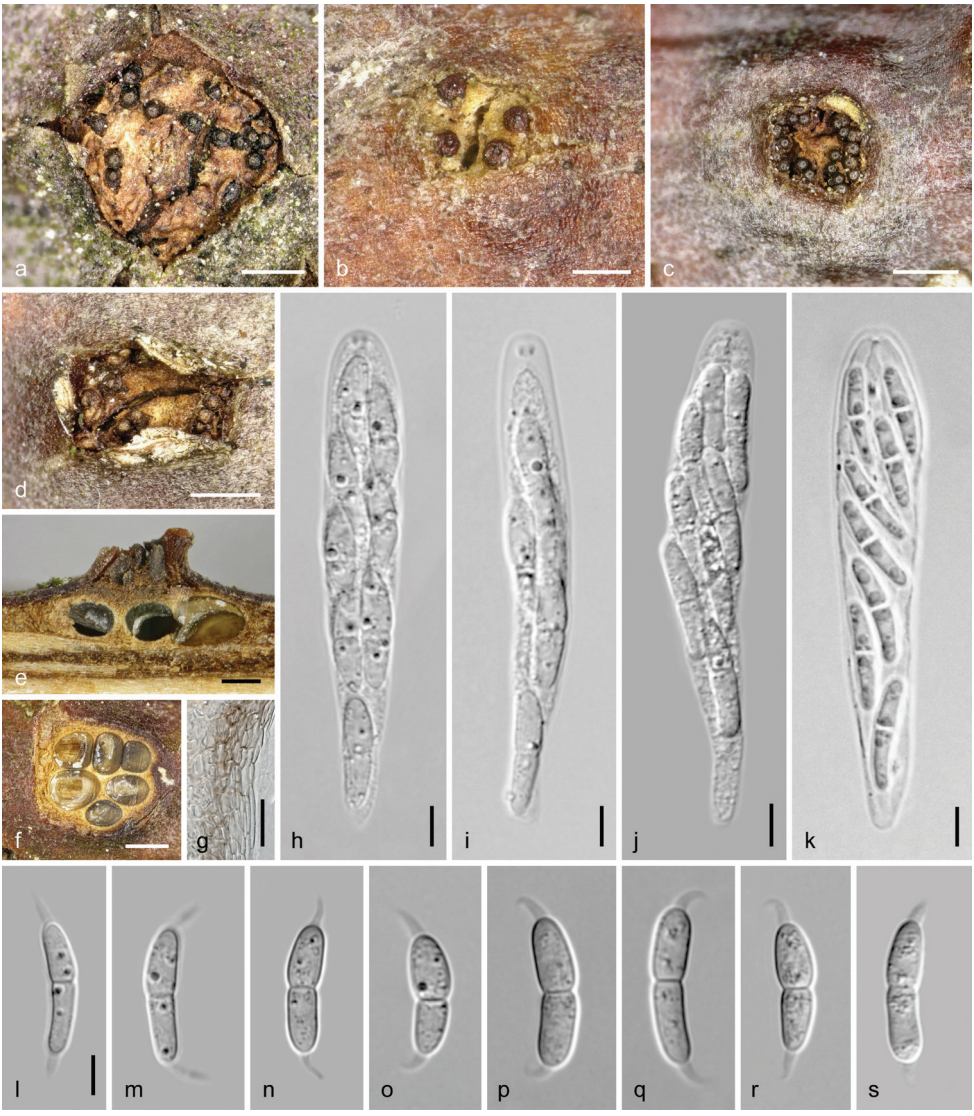

Figure 5. *Dendrostoma castaneum*. Sexual morph **a–d** ectostromatic discs and ostioles (in a ostioles breaking through covering layer) **e** pseudostroma in vertical section **f** pseudostroma in cross section **g** peridium in section (in 3% KOH) **h–k** asci **l–s** ascospores **a, c–g, j, k, s** WU 37030 = D230 **b, n–r** WU 37026 **h, i, l, m** WU 37028 = D192. Scale bars: 500 mm (**a, c, d, f**), 200 µm (**b, e**), 20 µm (**g**), 5 µm (**h–s**).

raising above the column, outside surrounded by a partly undulating, ca 20–25 µm thick black wall consisting of dark brown *textura angularis* of cells 4–10 µm in diameter at apical and upper peripheral regions, becoming paler downward and being absent at the base and lower sides. Interior of the fertile chambers consisting of isodiametric to elongate hyaline supporting cells and richly and irregularly branched hyphal conidiophores bearing phialides and conidia. Wall, supporting cells and phialides turn-

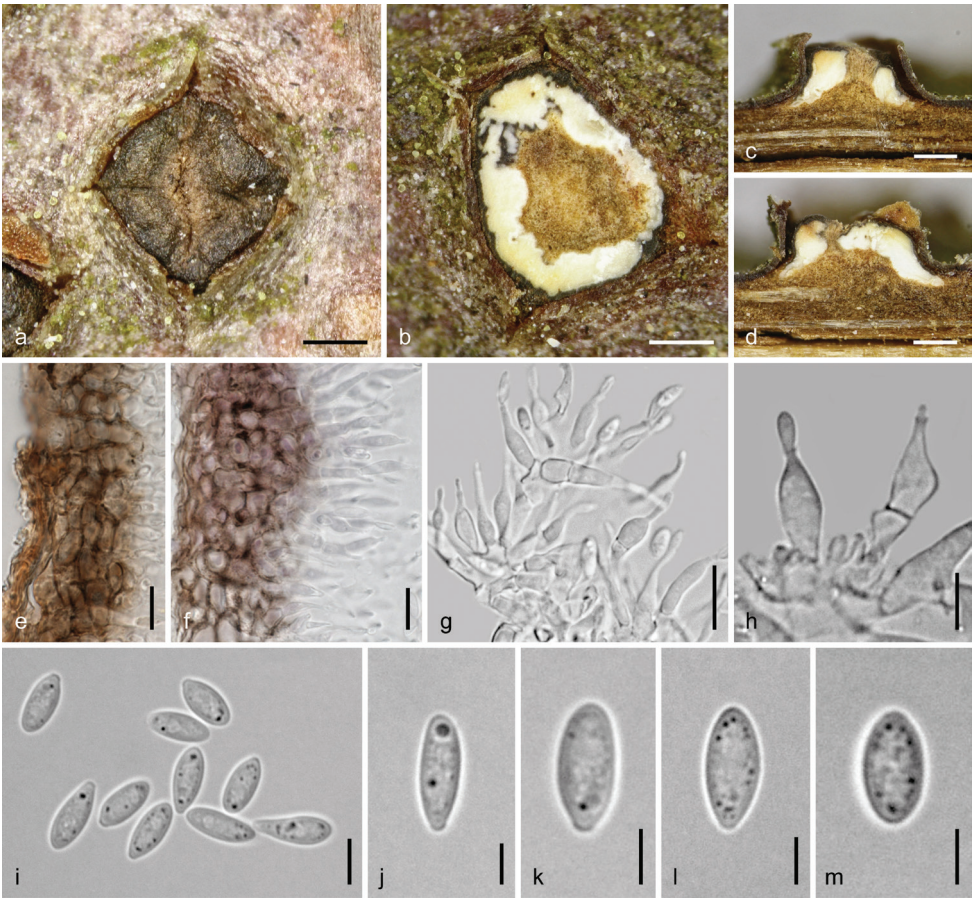

Figure 6. *Dendrostoma castaneum* (WU 37030 = D230). Asexual morph **a** conidioma in face view **b** conidioma in cross section **c, d** conidiomata in vertical section **e** outer upper wall of fertile chamber **f** wall, short conidiophores and phialides (note violaceous tone) **g, h** phialides and hyphal conidiophores **i–m** conidia **f–m** In 3% KOH. Scale bars: 300 µm (**a–d**), 10 µm (**e–g**), 5 µm (**h, i**), 3 µm (**j–m**).

ing dilute violaceous in 3% KOH. *Phialides* arranged on supporting cells in palisades along the walls and on conidiophores, (6–)8.2–12(–15.3) × (1.7–)2.5–3.5(–5) µm (*n* = 80), repetitive, mostly lageniform, often with long necks; conidia also formed on cylindrical pegs and denticles. *Conidia* (6–)6.7–8(–8.8) × (2.5–)3–3.5(–3.7) µm, l/w (1.7–)2.1–2.6(–3.1) (*n* = 85), subfusiform, subclavate or ellipsoid, scar often distinct, smooth, with few minute drops.

Culture characteristics. On CMD at 16 °C in the dark colony circular, dense, white, covered by white cottony aerial hyphae, partly turning pale apricot, reverse orange, not zonate.

Specimens examined (all on recently detached twigs of *Castanea sativa* on ground). AUSTRIA, Burgenland, Forchtenstein, Kohlstatt, 13 Feb. 2016, H. Voglmayr (WU 37026); Steiermark, near highway A2 exit Steinberg, grid square 9057/1,

26 Oct. 2000, W. Jaklitsch W.J. 1651 (WU 37027); same locality, soc. *Cytospora* sp., 3 Nov. 2015, W. Jaklitsch & H. Voglmayr (WU 37028; culture CBS 145803 = D192). ITALY, Sicilia, Etna, above Zafferana Etnea, soc. *Cytospora* sp. (*Valsa* morph), 17 June 2016, H. Voglmayr & W. Jaklitsch (WU 37029; culture D260); Veneto, Selva di Montello, 8 Apr. 2016, H. Voglmayr & W. Jaklitsch (WU 37030; culture D230).

Notes. Sizes of pseudostromata and acervuli strongly depend on twig thickness. Remarkably, red colour of the ostiolar tip, when present, turns purple in 3% KOH and yellow in lactic acid, a feature, which is typical of the Hypocreales and within the Diaporthales otherwise only found in the Cryphonectriaceae.

So far, confirmed records of *D. castaneum* are only known from Europe where the species is widely co-occurring with its host, *Castanea sativa*. Kobayashi (1970) reported and illustrated *D. castaneum* (as *Cryptodiaporthe castanea*) from *Castanea crenata* and *C. mollissima* in Japan. However, it is unlikely that these collections are conspecific with the European *D. castaneum*, considering their different spore shape and hosts. The 1 or 2 large guttules per ascospore cell and the ascospore appendages illustrated in Kobayashi (1970: fig. 32) are similar to *D. atlanticum* rather than to *D. castaneum*. Remarkably, he also reported and illustrated dimorphic conidia for the Japanese collections, which we also observed in *D. atlanticum*. Considering hosts and distribution, the Japanese collections likely represent one of the species described by Jiang et al. (2019) or an undescribed species.

Dendrostoma creticum **Voglmayr & Jaklitsch, sp. nov.**
MycoBank: MB 832517
Figure 7

Diagnosis. *Dendrostoma creticum* is recognized by long, subacicular ascospores.

Holotype. GREECE, Crete, near Askifou, 35°17'47"N, 24°12'33"E, on twigs of *Quercus coccifera*, soc. *Cytospora* (*Valsa* morph) sp., 6 June 2015, H. Voglmayr & W. Jaklitsch (WU 37031; ex-type culture CBS 145802 = D124)

Etymology. *Creticum*, referring to its occurrence, Crete.

Description. *Sexual morph*: *pseudostromata* 0.6–1.6 mm in their widest dimension in cross section, pulvinate, circular, elliptic or irregular in outline, scattered, gregarious to confluent up to 4 mm length, causing small bumps in the bark, splitting the periderm. *Ectostromatic discs* 0.25–1.4 mm in their widest dimension, medium to dark brown, flat or convex, surrounded by bark flaps. *Ostioles* 1–7 per disc, (31–)55–102(–135) µm (n = 40) in diameter at the rounded tip, dark brown to black, bluntly conical, plane with the disc or slightly prominent. *Entostroma* pale bark coloured, mottled. *Perithecia* (245–)320–445(–495) µm (n = 30) in diameter, depressed-subglobose, collapsing upward; *peridium* ca 10–50 µm thick, a dark brown *textura angularis* in face view, in section outside of dark brown *textura angularis* to strongly compressed cells (4–)7–14(–18) µm (n = 30) in diameter, inside of strongly compressed and elongated hyaline cells. *Paraphyses* absent at maturity. *Asci* (66–)71–85(–94) × (8.8–)9.5–11.2(–

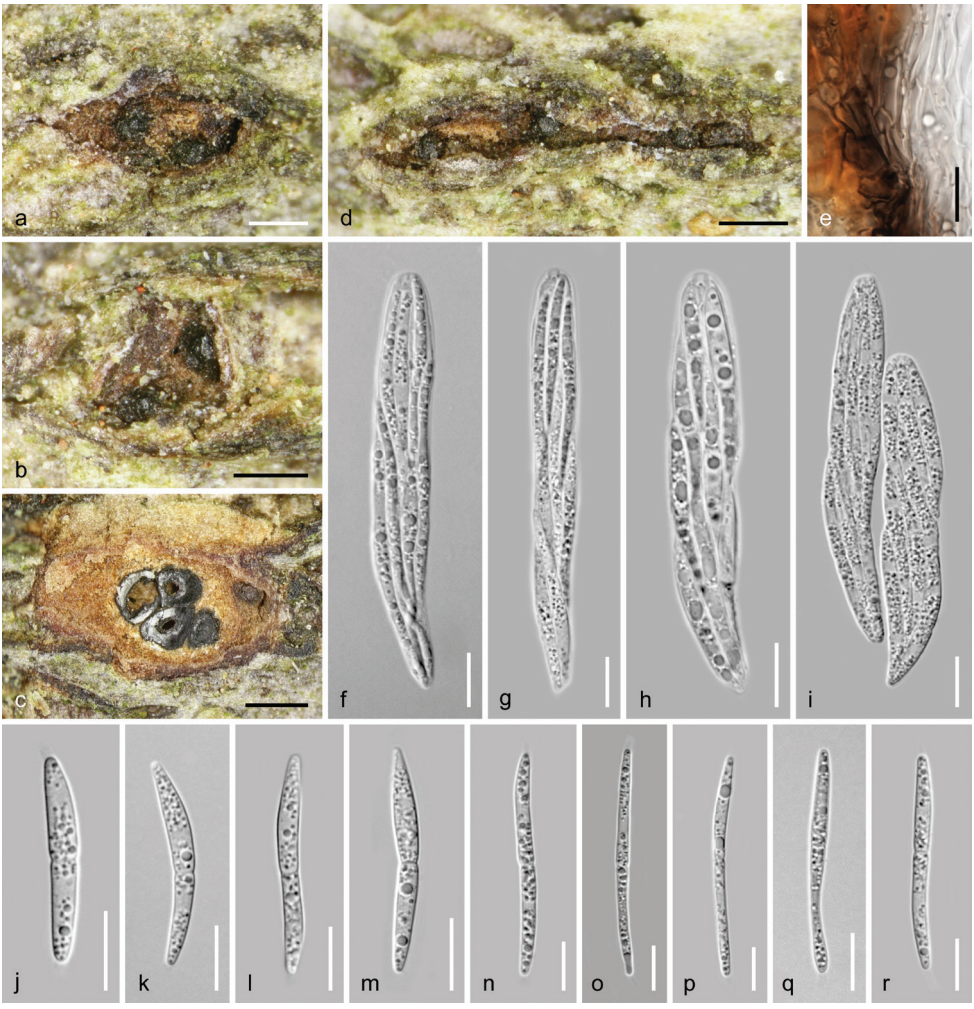

Figure 7. *Dendrostoma creticum* (WU 37031 = D124). **a, b, d** Ectostromatic discs and ostioles in face view **c** pseudostroma in cross section **e** peridium in cross section in 3% KOH **f–i** asci **j–r** ascospores. Scale bars: 200 µm (**a, b, d**), 500 µm (**c**), 10 µm (**e–r**).

12.3) µm (*n* = 44), narrowly clavate to subfusoid, floating freely in the centre, containing 8 bi- to triseriate ascospores. *Ascospores* (26–)33–45.5(–52) × (2.7–)3–3.7(–4.6) µm, l/w (6.8–)9.8–14.3(–17.5) (n = 40), 2-celled, slightly constricted at the median or often distinctly eccentric septum, oblong, straight to curved, with the upper cell often slightly wider than the lower, hyaline, multiguttulate, smooth, with or without a hyaline subconical appendage (1.4–)1.5–2.3(–3.2) × (0.6–)0.9–1.3(–1.5) µm (*n* = 25) at each end.

Asexual morph unknown.

Culture characteristics. On CMD at 16 °C in the dark colony circular to irregular, dense, white, partly covered by short, white aerial hyphae, zonate, soon turning

dark brown to black with pale apricot spots and margin and apricot to orange pigment diffusing into agar, reverse dark brown with orange margin.

Notes. *Dendrostoma creticum* is similar to the closely related *D. istriacum* but differs by distinctly longer ascospores, darker ectostromatic discs and a different host species.

***Dendrostoma istriacum* Voglmayr & Jaklitsch, sp. nov.**
MycoBank: MB 832518
Figure 8

Diagnosis. *Dendrostoma istriacum* is recognized by narrow, oblong ascospores with small drops.

Holotype. CROATIA, Istria, Rovinj, near Kamp Amarin, 45°06'33"N, 13°37'02"E, on twigs of *Quercus ilex*, soc. *Diplodia* sp., 14 May 2015, H. Voglmayr (WU 37032; ex-type culture CBS 145801 = D122).

Etymology. *Istriacum*, referring to its occurrence, Istria.

Description. *Sexual morph*: *pseudostromata* 0.6–1.5 mm in their widest dimension in cross section, pulvinate, circular or elliptic in outline, scattered or tightly aggregated in large numbers, causing bumps in the bark and bark lesions to ca 3.2 mm long parallel to the twig axis. *Ectostromatic discs* 0.15–0.7 mm in diameter, mostly inconspicuous, surrounded by bark flaps, flat or convex, prosenchymatous, first whitish, turning pale to dark brown, becoming disintegrated and replaced by black ostioles and perithecial tops. *Entostroma* whitish to pale bark coloured. *Stromatic tissues* consisting of bark cells and 2–4 µm wide, hyaline to brown hyphae. *Ostioles* 1–5 per disc, (45–)61–91(–103) µm (n = 30) in diameter, short cylindrical, slightly projecting from the disc, brown to black; wall consisting of dark brown *textura angularis*. *Perithecia* (230–)280–393(–443) µm (n = 20) in diameter, globose to subglobose; peridium ca 15–35 µm thick, pale olivaceous to dark brown, consisting of 2–4 cell layers of thick-walled, dark brown angular cells (3–)4–13.5(–20.5) µm (n = 40) in diameter outside and long compressed, thin-walled, hyaline to brownish cells inside. *Paraphyses* absent at maturity. *Asci* (59–)62–70(–74) × (7–)8.5–10(–11) µm (n = 30), fusoid to narrowly clavate, floating freely in the centre, containing 8 bi- to triseriate ascospores. *Ascospores* (19.3–)20.5–25.5(–29.5) × (3–)3.5–4.2(–5.1) µm, l/w (4.5–)5.3–7(–8.7) (n = 40), 2-celled, constricted at the more-or-less median septum, oblong, straight to curved, with the upper cell often slightly wider than the lower, hyaline, containing several small guttules concentrated towards the ends and the septum, smooth, with a hyaline subconical appendage (1.7–)2.5–3.5(–4.5) × (0.8–)1–1.3(–1.5) µm (n = 40) at each end, becoming elongated in mounts.

Asexual morph: *conidiomata* ca 250–520 µm in diameter, acervular, inconspicuous, immersed in bark, causing small bark bumps, becoming visible in fissures, whitish to brownish, flat or convex, bluntly conical, usually broader than high, consisting of a broad sterile greyish brown central column, a white outer fertile ring and a brown covering layer; also fertile between the latter and the top of the column. Cov-

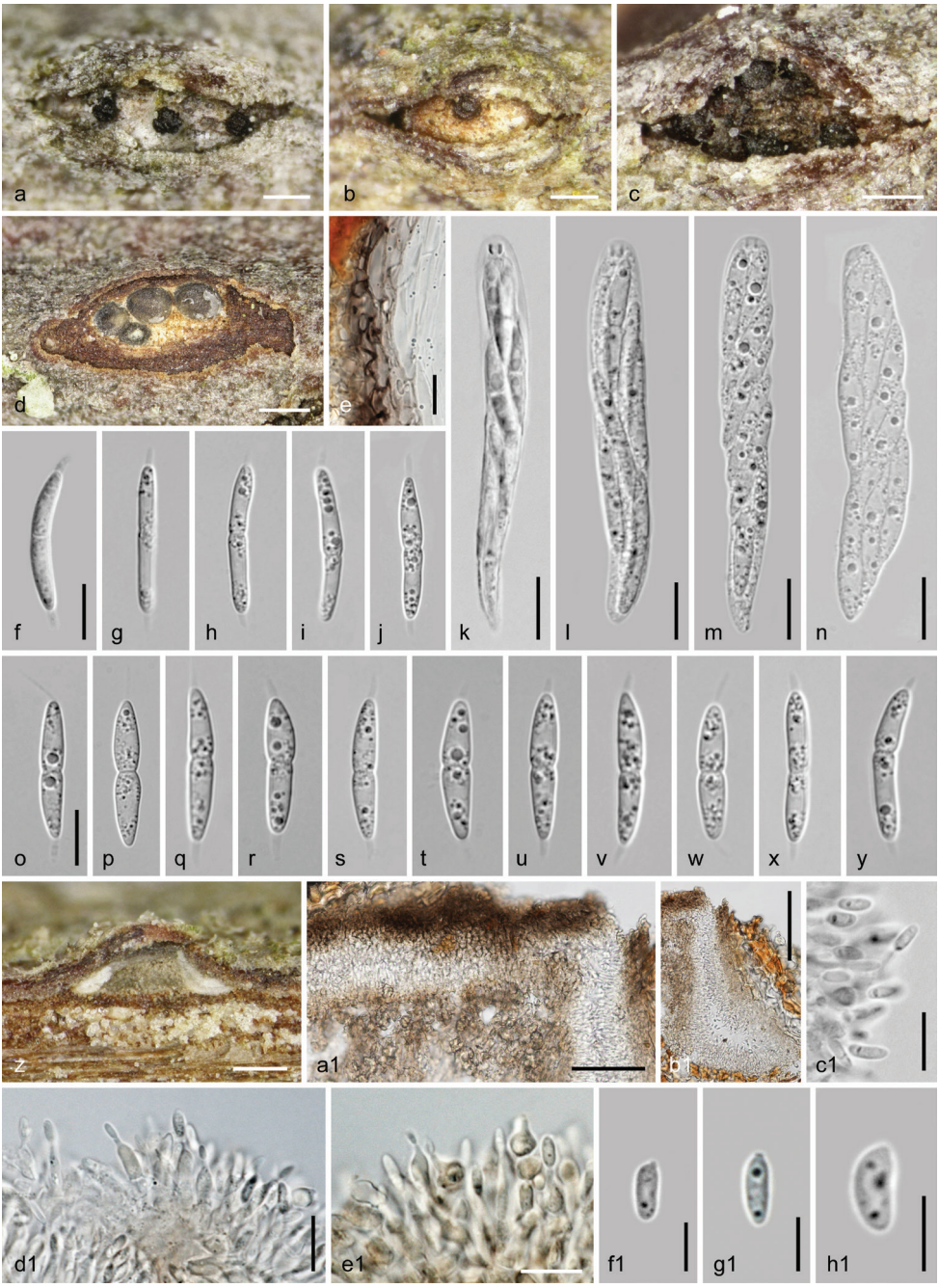

Figure 8. *Dendrostoma istriacum* (WU 37032 = D122). **a–y** Sexual morph **a–c** ectostromatic discs and ostioles **d** pseudostroma in cross section **e** peridium in cross section **f–j, o–y** ascospores **k–n** asci **z–h1** asexual morph **z** conidioma in vertical section **a1** upper part of conidioma showing covering layer, upper part of central column and fertile layers with opening at the upper right side **b1** peripheral fertile chamber in vertical section **c1** conidia attached to phialides **d1–e1** phialides **f1–h1** conidia; **e, c1–h1** In 3% KOH. Scale bars: 150 µm (**a–c, z**), 300 µm (**d**), 100 µm (**b1**), 50 µm (**a1**), 10 µm (**e–y, c1–e1**), 5 µm (**f1–h1**).

ering layer consisting of a dark brown *textura angularis* of 4–10 µm wide cells, turning paler to hyaline and more rounded downwards; column comprising pale brown *textura angularis-epidermoidea* of similarly sized cells; outer margin of the fertile ring consisting of a narrow layer of hyaline to pale brown, angular to compressed cells; gel surrounding rounded to angular, subhyaline to hyaline cells supporting phialides slowly turning pinkish in 3% KOH. *Phialides* forming palisades in fertile areas, tightly packed, cylindrical to ampulliform, often with long acute necks, (5.5–)6.3–9(–11) × (1.8–)2.2–3.7(–5.3) µm (*n* = 33). *Conidia* (4–)5–6.6(–7.4) × (1.9–)2.1–2.5(–2.7) µm, l/w (1.6–)2.1–3(–3.7) (n = 53), oblong to ellipsoid, 1-celled, hyaline, smooth, usually with distinct abscission scar.

Culture characteristics. On CMD at 16 °C in the dark, colony circular to irregular, dense, white, partly covered by short white aerial hyphae, zonate, soon turning dark brown to black with pale apricot to reddish brown spots and margin and some pale apricot pigment diffusing into agar, reverse dark brown with pale apricot margin.

Other specimen examined. CROATIA, Istria, Rovinj, near Kamp Veštar, 45°03'19"N, 13°40'55"E, on twigs of *Quercus ilex*, 30 May 2019, H. Voglmayr (WU 37033).

Notes. *Dendrostoma istriacum* is closely related to *D. creticum* but differs from that species by distinctly shorter ascospores and a different host species.

***Dendrostoma leiphaemia* (Fr.: Fr.) Senan. & K.D. Hyde, in Senanayake et al., Fungal Diversity 93: 317 (2018).**
Figure 9

Sphaeria leiphaemia Fr., Syst. mycol. (Lundae) 2(2): 399 (1823) (Basionym).
≡ *Amphiporthe leiphaemia* (Fr.) Butin, Sydowia 33: 22 (1980).
≡ *Diaporthe leiphaemia* (Fr. : Fr.) Sacc. [as 'leiphaema'], Atti Soc. Veneto-Trent. Sci. Nat. 2(1): 135 (1873).
≡ *Valsa leiphaemia* (Fr.) Fr., Summa veg. Scand., Sectio Post. (Stockholm): 412 (1849).

Diagnosis. *Dendrostoma leiphaemia* is recognized by conspicuous ectostromatic discs, broad conical ostiolar necks, and broad multiguttulate ascospores.

Description. *Sexual morph*: *pseudostromata* 1–5 mm in their widest dimension in cross section, pulvinate to conical, circular, elliptic or irregular in outline, scattered, aggregated to confluent, sometimes forming lines of up to 15 mm length, causing conspicuous bumps and lesions in the bark; dark brown dorsal zones present within the bark, absent in basal regions. *Ectostromatic discs* 0.35–2.5 mm in their widest dimension, conspicuous, whitish, cream, pale brown, pale yellowish brown to dull brown, fusoid, triangular to circular in section, flat or convex, often surrounded by bark flaps, elevated up to 1.3 mm beyond the bark surface, brittle to powdery, first present as a covering layer with ostiolar necks subsequently bursting through it, eventually crumbling away. *Ostioles* 1–30 per disc, (88–)124–220(–336) µm (*n* = 64) in diameter, dark brown, black, or reddish brown with black, rarely yellowish tip, cylindrical with coni-

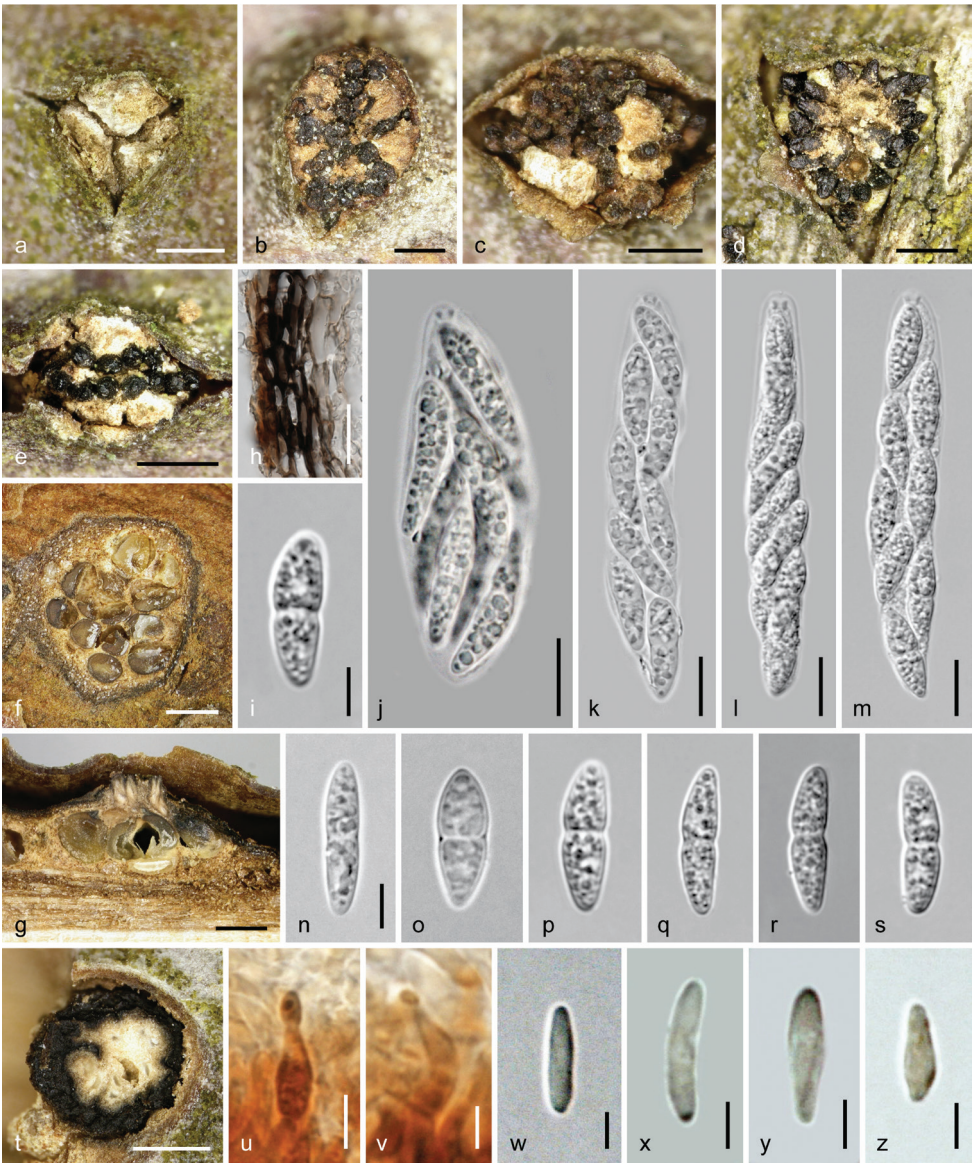

Figure 9. *Dendrostoma leiphaemia*. **a–s** Sexual morph **a–e** ectostromatic discs and ostioles **f** pseudostroma in cross section **g** pseudostroma in vertical section **h** peridium in cross section **i, n–s** ascospores **j–m** asci **t–z** asexual morph **t** conidioma in cross section **u, v** phialides **w–z** conidia; **a, d–g, t–z** WU 37037 (D105), **b** WU 37036 **c, h, j, k, n** WU 37038 **i, l, m, p–s** Mannersdorf **o** WU 37040. **h, j, k, n, o, u–z** In 3% KOH. Scale bars: 500 µm (**a–g, t**), 20 µm (**h**), 10 µm (**j–m**), 5 µm (**i, n–s, u**), 3 µm (**v–z**).

cal apical part, attenuated to 35–90(–180) µm at the rounded, compressed or coarsely sulcate tip, projecting to 250, less commonly 400 µm, white, in upper regions sometimes yellow inside, periphysate, arising centrally to eccentrically from the perithecial venter and slightly convergent above perithecia; turning partly yellow, partly brown in

3% KOH. *Entostroma* whitish to pale yellowish or pale bark-coloured, prosenchymatous to pseudoparenchymatous, the latter particularly in the vicinity of perithecia, consisting of 1.5–5 µm wide hyphae or angular cells, mixed with bark cells. *Perithecia* arranged in valsoid configuration, tightly aggregated, (292–)380–625(–700) µm (*n* = 21) in diameter, globose to depressed-subglobose, with gelatinous contents, collapsing upward; *peridium* ca 7–35 µm thick, pale olivaceous to dark brown, consisting of an outer layer of isodiametric to elongate, thick-walled dark brown cells and an inner layer of compressed elongate, hyaline to brownish, thin-walled cells (5–)6.5–16(–22.5) µm (*n* = 31). *Paraphyses* absent at maturity. *Asci* floating freely in the centre when mature, (49–)58–71(–80) × (9–)10–13.5(–17.5) µm (*n* = 56), clavate, oblong, fusoid to subellipsoid, with a refractive apical ring, containing 8 bi- to triseriate, fasciculate or obliquely uniseriate ascospores. *Ascospores* (15–)16–19(–21) × (3.8–)4.3–5.2(–5.8) µm, l/w (2.7–)3.3–4.1(–4.7) (*n* = 95), 2-celled, not or slightly constricted at the median or slightly eccentric septum, inequilaterally ellipsoid or oblong, straight or curved, with the upper cell sometimes slightly wider than the lower, hyaline, multiguttulate, smooth, lacking appendages.

Asexual morph co-occurring with the sexual morph, acervular, either present as locules in lateral regions of pseudostromata above perithecia or forming separate, conical to pulvinate, dorsally blackened *acervuli* 0.9–2.2 mm in diameter, with conical upper part or whitish to cream or brownish, more-or-less circular, continous or deeply fissured discs ca 0.4–1 mm in diameter and whitish-cream, partly hollow interior containing slightly darker fertile chambers meandering through it. Walls and interior consisting of brown or hyaline to pale yellowish brown *textura angularis*. *Phialides* lining inner wall of the cavity, sessile, (4.8–)6.5–11(–12.7) × (1.7–)2–3.8(–5.3) µm (*n* = 16), subcylindrical to lageniform, reddish brown in 3% KOH (when old). *Conidia* (4.8–)7–9.5(–11) × (1.5–)1.8–2.3(–2.5) µm, l/w (2.3–)3.3–4.9(–6.3) (*n* = 50), unicellular, cylindrical, oblong, subclavate, rhomboid or narrowly ellipsoid, straight to slightly curved, often with a truncate or acute end, hyaline, turning pinkish-yellowish in 3% KOH, smooth, with minute terminal drops, adhering together in masses when old.

Culture characteristics. On CMD at 16 °C in the dark, colony irregular or dimorphic, dense, white, partly covered by short white aerial hyphae, zonate, soon turning dark brown to black with red or reddish brown spots, reverse dark brown, reddish brown with white, pale apricot or reddish brown spots and margins.

Specimens examined. AUSTRIA, Kärnten, St. Margareten im Rosental, shrubs in front of the Stariwald, grid square 9452/4, on branches of *Quercus petraea*, 9 Jan. 1995, W. Jaklitsch W.J. 443 (WU 37034); same area, 31 Dec. 1997, W. Jaklitsch W.J. 1122 (WU 37035); Niederösterreich, Hagenbrunn, Bisamberg east side, grid square 7664/3, on twigs of *Quercus petraea*, 30 Oct. 1999, W. Jaklitsch W.J. 1396 (WU 37036); Mannersdorf am Leithagebirge, on twigs of *Quercus petraea*, 12 Mar. 2016, H. Voglmayr (specimen lost); Mühlleiten, Herrnau, on branches of *Quercus petraea*, 29 Mar. 2015, H. Voglmayr (WU 37037; culture CBS 145800 = D105); Oberösterreich, Unterach am Attersee, Stockwinkl, Egelsee, grid square 8147/3, on branch of *Quercus petraea*, 25 May 1996, W. Jaklitsch W.J. 880 (WU 37038); Steiermark, Wundschuh, Kaiserwald, at the Seerestaurant, grid square 9058/4, on branch of *Quercus petraea*, 10 Sep. 2002,

W. Jaklitsch W.J. 1936 (BPI 843342; culture A.R. 3874); Vienna, 19th district, at the Cobenzl, grid square 7763/2, on branches of *Quercus cerris*, 11 Feb 1995, W. Jaklitsch W.J. 482 (WU 37039); same area and host, 27 Feb. 1999, W. Jaklitsch W.J. 1286 (WU 37040). POLAND, E Grajewo, Kuligi, on branches of *Quercus robur*, 28 July 2015, H. Voglmayr (WU 37041; culture D144).

Notes. Asexual fructifications of this species are reported to have dimorphic conidia (Butin 1980; Wehmeyer 1933). However, for the description above only overmature material with a single type of conidia was available, the measurements of which agree with the cylindrical form given as 7–12 × 1.5–2 µm by Wehmeyer (1933), but their shape is more variable, possibly due to their age. As Butin (1980) observed, the asexual morph precedes the sexual morph and may still be present as separate acervuli among sexual pseudostromata or as locules within the periphery of the latter.

Key to European species of *Dendrostoma*

1	Ascospores without appendages, multiguttulate, 15–21 × 4–6 µm; on broad-leaved *Quercus* spp. ..... ***D. leiphaemia***
–	Ascospores with appendages..... **2**
2	Appendages 10–21 µm long, bristle-like; ascospores with 1–2 large guttules per cell, 13–19.5 × 4.5–8 µm; on *Castanea sativa*..... ***D. atlanticum***
–	Appendages <6 long, not bristle-like **3**
3	Ascospores 11.5–20 × 3–5.3 µm, oblong, often curved, with 2 minute guttules per cell; on *Castanea sativa*..... ***D. castaneum***
–	Ascospores longer..... **4**
4	Ascospores oblong, 19–30 × 3–5 µm; on *Quercus ilex*..... ***D. istriacum***
–	Ascospores oblong to subacicular, 26–52 × 2.7–4.5 µm; on *Quercus coccifera*... ..... ***D. creticum***

Discussion

Our phylogenetic analyses are largely congruent with those of Jiang et al. (2019), and different topological positions of, e.g., *D. aurorae* and *D. parasiticum* concern backbone nodes with low to medium support. A notable difference concerns the position of the generic type, *D. leiphaemia*, which in Jiang et al. (2019) is contained within the *D. osmanthi* – *D. qinlingense* – *D. quercus* clade with medium (80% MP) to high (90% ML) support, while in our analyses it is placed basal to the *D. dispersum* – *D. mali* – *D. quercinum* clade with medium support (76% MP, 88% ML). These differences may be due to different taxon and marker sampling, as in the analyses of Jiang et al. (2019) only the ITS and LSU rDNA were available for *D. leiphaemia*.

Previous authors recorded phytopathogenic potential in all species of *Dendrostoma* studied by them (Fan et al. 2018; Jiang et al. 2019). As an example, *Dendrostoma castaneicola*, *D. castaneae*, and *D. shaanxiense* were reported to cause

chestnut canker (termed "Dendrostoma canker") on *Castanea mollissima* in China (Jiang et al. 2019). It is remarkable that almost all Chinese *Dendrostoma* species recorded as canker pathogens by Jiang et al. (2019) were only found as asexual morphs, which were abundantly produced on the dead twigs. This may, at least partly, be linked to the fact that Jiang et al. (2019) mainly investigated chestnut plantations, in which asexual reproduction of virulent pathotypes may be particularly favoured by genetically uniform host cultivars. However, pathogenicity of these species has not been confirmed by inoculation experiments. Défago (1937) observed canker disease symptoms of *Castanea sativa* after artificial inoculation with *Dendrostoma castaneum*, and Kobayashi (1970) mentioned unpublished inoculation experiments showing pathogenicity of *Dendrostoma* sp. (as *Cryptodiaporthe castanea*) on cultivated Japanese chestnut varieties. Phillips and Burdekin (1982) considered *D. castaneum* to be a weak wound pathogen. In our studies, we have not seen any obvious disease symptoms exhibited by *Castanea* and *Quercus* species infected by species of *Dendrostoma*. The typical habitat of species like *D. castaneum* or *D. leiphaemia* are cut branches piled up on the ground. Species on evergreen *Quercus* spp. may occur on dead branchlets attached to trees, but their appearance is rather inconspicuous, and specific searches are necessary to spot them. However, as our observations have not been conducted to specifically study disease symptoms, it is premature to make predictions about potential pathogenicity, which thus cannot be excluded. Frequent association of *Dendrostoma* spp. with *Cytospora* spp. may suggest weak or facultative parasitism, but inoculation experiments are required to prove pathogenicity by fulfilling Koch's postulates.

Although other genera of the Erythrogloeaceae produce acervuli, asexual morphs of *Dendrostoma* have been termed pycnidia (Fan et al. 2018; Jiang et al. 2019). This may be due to studies in culture, as asexual fructifications on agar may easily be interpreted as pycnidia, even when no true ostioles are present. However, none of the asexual morphs of the European species we have seen on natural substrates have preformed openings that may be termed ostioles. Therefore, we recognize asexual fructifications of *Dendrostoma* on natural substrates generally as acervuli. Jiang et al. (2019) found dimorphic conidia in a single species of *Dendrostoma*, *D. quercus*. Here we add another such species, *D. atlanticum*. These forms occur at the same time in the same asexual fructifications. However, to gain a complete picture of asexual morphs and elucidate entire life cycles of *Dendrostoma* species, long-term studies may be required, as certain asexual fungi have two different morphs, which may not occur at the same time (Butin 1980).

Most species of *Dendrostoma* are only known as asexual morphs. Only one of the 10 species described by Jiang et al. (2019), *D. quercus*, has a sexual morph. However, it is unclear whether in these species sexual morphs are absent, only rarely produced or have not yet been recorded, e.g., due to unfavourable weather conditions for development, unsuitable substrates or an untimely sampling season. Other species, for which sexual morphs are known are *D. mali* on *Malus spectabilis*, *D. osmanthi* on *Osmanthus fragrans*, and *D. quercinum* on *Quercus acutissima* (Fan et al. 2018). All five species of *Dendrostoma* we describe or redescribe from Europe, two from *Castanea sativa* and three from *Quercus* spp., have sexual morphs and in all but one (*D. creticum*) we found also an asexual morph on the natural hosts.

The high species biodiversity of *Dendrostoma* recorded from Eastern Asia as well as the phylogenetic patterns indicate that the group may have originated in this area. This is also supported by the fact that the European species do not form a monophyletic group, but are embedded within Eastern Asian lineages, indicating that Europe has been colonised from Asia several times independently. In addition, evolutionary radiation may have started on *Castanea* as the basal subclade A exclusively contains accessions from that host (Fig. 1). However, detailed additional studies including other areas as well as hosts are necessary to vigorously test these hypotheses.

Acknowledgments

We thank Alain Delannoy, Miguel Angel Delgado, and Joseba Castillo for providing fresh material of *Dendrostoma atlanticum* and Irmgard Greilhuber and Walter Till (WU) for incorporating the specimens in the herbarium. The financial support by the Austrian Science Fund (FWF; project P27645-B16) to HV is gratefully acknowledged.

References

Butin H (1980) Über einige *Phomopsis*-Arten der Eiche einschließlich *Fusicoccum quercus* Oudemans. Sydowia 33: 18–28. https://www.zobodat.at/pdf/Sydowia_33_0018-0028.pdf

Carbone I, Kohn LM (1999) A method for designing primer sets for speciation studies in filamentous ascomycetes. Mycologia 91: 553–556. https://doi.org/10.1080/00275514.1999.12061051

Castlebury LA, Rossman AY, Jaklitsch WM, Vasilyeva LN (2002) A preliminary overview of the Diaporthales based on large subunit nuclear ribosomal DNA sequences. Mycologia 94: 1017–1031. https://doi.org/10.1080/15572536.2003.11833157

De Hoog GS, Gerrits van den Ende AHG (1998) Molecular diagnostics of clinical strains of filamentous basidiomycetes. Mycoses 41: 183–189. https://doi.org/10.1111/j.1439-0507.1998.tb00321.x

Défago G (1937) *Cryptodiaporthe castanea* (Tul.) Wehmeyer, parasite du châtaignier. Phytopathologische Zeitschrift 10: 168–177.

Fan XL, Bezerra JD, Tian CM, Crous PW (2018) Families and genera of diaporthalean fungi associated with canker and dieback of tree hosts. Persoonia 40: 119–134. https://doi.org/10.3767/persoonia.2018.40.05

Hall TA (1999) BioEdit: a user-friendly biological sequence alignment editor and analysis program for Windows 95/98/NT. Nucleic Acids Symposium Series 41: 95–98.

Jaklitsch WM (2009) European species of *Hypocrea* – Part I. The green-spored species. Studies in Mycology 63: 1–91. https://doi.org/10.3114/sim.2009.63.01

Jaklitsch WM, Baral HO, Lücking R, Lumbsch HT, Frey W (2016) Syllabus of plant families – A. Engler's Syllabus der Pflanzenfamilien Part 1/2: Ascomycota. 13th edition. Borntraeger, Berlin, 1–322.

Jaklitsch WM, Komon M, Kubicek CP, Druzhinina IS (2005) *Hypocrea voglmayrii* sp. nov. from the Austrian Alps represents a new phylogenetic clade in *Hypocrea*/*Trichoderma*. Mycologia 97: 1365–1378. https://doi.org/10.1080/15572536.2006.11832743

Jaklitsch WM, Stadler M, Voglmayr H (2012) Blue pigment in *Hypocrea caerulescens* sp. nov. and two additional new species in sect. *Trichoderma*. Mycologia 104: 925–941. https://doi.org/10.3852/11-327

Jiang N, Fan X-L, Crous PW, Tian C-M (2019) Species of *Dendrostoma* (Erythrogloeaceae, Diaporthales) associated with chestnut and oak canker diseases in China. MycoKeys 48: 67–96. https://doi.org/10.3897/mycokeys.48.31715

Kobayashi T (1970) Taxonomic studies of Japanese Diaporthaceae with special reference to their life-histories. Bulletin of the Government Forest Experimental Station Meguro 226: 1–242.

Liu YL, Whelen S, Hall BD (1999) Phylogenetic relationships among ascomycetes: evidence from an RNA polymerase II subunit. Molecular Biology and Evolution 16: 1799–1808. https://doi.org/10.1093/oxfordjournals.molbev.a026092

Mejía LC, Castlebury LA, Rossman AY, Sogonov MV, White JF (2008) Phylogenetic placement and taxonomic review of the genus *Cryptosporella* and its synonyms *Ophiovalsa* and *Winterella* (Gnomoniaceae, Diaporthales). Mycological Research 112: 23–35. https://doi.org/10.1016/j.mycres.2007.03.021

Mejía LC, Castlebury LA, Rossman AY, Sogonov MV, White Jr JF (2011) A systematic account of the genus *Plagiostoma* (Gnomoniaceae, Diaporthales) based on morphology, host-associations, and a four-gene phylogeny. Studies in Mycology 68: 211–235. https://doi.org/10.3114/sim.2011.68.10

Petrak F (1921) Mykologische Notizen. II. Annales Mycologici 19: 17–128.

Petrak F (1971) Über *Diaporthe hranicensis* Petr. Sydowia 24: 256–260. https://www.zobodat.at/pdf/Sydowia_24_0256-0260.pdf

Phillips DH, Burdekin DA (1982) Diseases of forest and ornamental trees. Macmillan Press, London, 1–581. https://doi.org/10.1007/978-1-349-06177-8_1

Rossman AY, Adams GC, Cannon PF, Castlebury LA, Crous PW, Gryzenhout M, Jaklitsch WM, Mejia LC, Stoykov D, Udayanga D, Voglmayr H, Walker DM (2015) Recommendations of generic names in Diaporthales competing for protection or use. IMA Fungus 6: 145–154. https://doi.org/10.5598/imafungus.2015.06.01.09

Senanayake IC, Jeewon R, Chomnunti P, Wanasinghe DN, Norphanphoun C, Karunarathna A, Pem D, Perera RH, Camporesi E, McKenzie EHC, Hyde KD, Karunarathna SC (2018) Taxonomic circumscription of Diaporthales based on multigene phylogeny and morphology. Fungal Diversity 93: 241–443. https://doi.org/10.1007/s13225-018-0410-z

Silvestro D, Michalak I (2012) raxmlGUI: a graphical front-end for RAxML. Organisms Diversity & Evolution 12: 335–337. https://doi.org/10.1007/s13127-011-0056-0

Stamatakis E (2006) RAxML-VI-HPC: maximum likelihood-based phylogenetic analyses with thousands of taxa and mixed models. Bioinformatics 22: 2688–2690. https://doi.org/10.1093/bioinformatics/btl446

Swofford DL (2002) PAUP* 4.0b10: phylogenetic analysis using parsimony (*and other methods). Sinauer Associates, Sunderland, Massachusetts.

Vilgalys R, Hester M (1990) Rapid genetic identification and mapping of enzymatically amplified ribosomal DNA from several *Cryptococcus* species. Journal of Bacteriology 172: 4238–4246. https://doi.org/10.1128/jb.172.8.4238-4246.1990

Voglmayr H, Akulov OY, Jaklitsch WM (2016) Reassessment of *Allantonectria*, phylogenetic position of *Thyronectroidea*, and *Thyronectria caraganae* sp. nov. Mycological Progress 15: 921. https://doi.org/10.1007/s11557-016-1218-4

Voglmayr H, Jaklitsch WM (2008) *Prosthecium* species with *Stegonsporium* anamorphs on *Acer*. Mycological Research 112: 885–905. https://doi.org/10.1016/j.mycres.2008.01.020

Voglmayr H, Jaklitsch WM (2011) Molecular data reveal high host specificity in the phylogenetically isolated genus *Massaria* (Ascomycota, Massariaceae). Fungal Diversity 46: 133–170. https://doi.org/10.1007/s13225-010-0078-5

Voglmayr H, Jaklitsch WM (2017) *Corynespora*, *Exosporium* and *Helminthosporium* revisited – new species and generic reclassification. Studies in Mycology 87: 43–76. https://doi.org/10.1016/j.simyco.2017.05.001

Voglmayr H, Rossman AY, Castlebury LA, Jaklitsch WM (2012) Multigene phylogeny and taxonomy of the genus *Melanconiella* (Diaporthales). Fungal Diversity 57: 1–44. https://doi.org/10.1007/s13225-012-0175-8

Wehmeyer LE (1933) The genus *Diaporthe* and its segregates. University of Michigan Studies: Scientific Series 9: 1–349.

Werle E, Schneider C, Renner M, Völker M, Fiehn W (1994) Convenient single-step, one tube purification of PCR products for direct sequencing. Nucleic Acids Research 22: 4354–4355. https://doi.org/10.1093/nar/22.20.4354

White TJ, Bruns T, Lee S, Taylor J (1990) Amplification and direct sequencing of fungal ribosomal RNA genes for phylogenetics. In: Innis MA, Gelfand DH, Sninsky JJ, White TJ (Eds) PCR protocols: A guide to methods and applications, Academic Press, San Diego. 315–322. https://doi.org/10.1016/B978-0-12-372180-8.50042-1

MycoKeys 59: 27–45 (2019)
doi: 10.3897/mycokeys.59.38359
http://mycokeys.pensoft.net

RESEARCH ARTICLE

A peer-reviewed open-access journal
MycoKeys
Launched to accelerate biodiversity research

Two new species of *Lactifluus* (Fungi, Russulales) from tropical *Quercus* forest in eastern Mexico

Leticia Montoya[1], Abraham Caro[1], Antero Ramos[1], Victor M. Bandala[1]

1 *Red Biodiversidad y Sistemática, Instituto de Ecología A.C., P.O. Box 63, Xalapa, Veracruz, 91000, México*

Corresponding author: *Victor M. Bandala* (victor.bandala@inecol.mx)

Academic editor: *María P. Martín* | Received 18 July 2019 | Accepted 9 September 2019 | Published 16 October 2019

Citation: Montoya L, Caro A, Ramos A, Bandala VM (2019) Two new species of *Lactifluus* (Fungi, Russulales) from tropical *Quercus* forest in eastern Mexico. MycoKeys 59: 27–45. https://doi.org/10.3897/mycokeys.59.38359

Abstract

Two new species of *Lactifluus* subgenus *Lactifluus* were discovered during a three-year monitoring of the ectomycorrhizal fungi in a tropical oak forest from central Veracruz, Mexico. Systematic sampling of basidiomes allowed recording of the morphological variation of fruit-bodies in different growth stages along with their fructification season. Both new species were distinguished, based on macro- and micromorphological features and on molecular data. A phylogenetic analysis of a concatenated nuc rDNA ITS, D1 and D2 domains of nuc 28S rDNA (LSU) and the 6–7 region of the second largest subunit of the RNA polymerase II (*rpb2*) sequence dataset of species of *Lactifluus* is provided. In the phylogeny inferred, one of the new species is sister to *L. dissitus* Van de Putte, K. Das & Verbeken and the other belongs to the group of species of *L. piperatus* (L.) Kuntze, sister to an unidentified species from U.S.A. The studied taxa grow under *Quercus oleoides* in the study site. The species are presented and illustrated here.

Keywords

Ectomycorrhizal fungi, milkcaps new taxa, Neotropical fungi, oak forests

Introduction

Mexico is one of the worldwide centres for oak (*Quercus*) diversity. It hosts around 174 species, over 60% of which are endemic (Valencia 2004, Oldfield and Eastwood 2007, Villaseñor 2016). Most members of the genus grow in subtropical and temperate montane forests (1000–3500 m a.s.l.) and very few in lowland tropical areas (below 1000 m a.s.l.) (Valencia 2004). Some lowland tropical areas from central Veracruz (eastern Mexico) harbour oak forest patches, part of them being considered Pleistocene relicts and formally recognised amongst "main land regions" of the country ("Región Terrestre Prioritaria 104") (Arriaga et al. 2000). These forests are important wildlife

refuges, including fungi and endemic species of cycads and orchids (Castillo-Campos et al. 2005). The high biodiversity of the tropical oak forest and the ecosystem services provided are important for protecting prevailing relicts. Ectomycorrhizal (ECM) fungi, such as *Lactifluus* species, are undoubtedly a key to the growth and survival of *Quercus* seedlings and trees in such patches of native tropical forest under drought conditions and adverse edge effects, through greater water and nutrient absorption in degraded soils. Despite their importance, ECM fungi in such a Mexican ecosystem have received scarce taxonomic attention, excepting reports, from the area or surroundings, of a few Boletales, *Lactarius* s.l., *Cantharellus* (Guzmán and Sampieri 1984; García et al. 1987; Singer et al. 1991; Montoya and Bandala 1996, Herrera et al. 2018a, b).

The genus *Lactifluus* contains around 190 species based on Index Fungorum (http://www.indexfungorum.org) and recent publications and is widespread in a variety of ecosystems worldwide but with a clear predominance in the tropics, especially in tropical Africa, Asia and the Neotropical region (De Crop et al. 2017). Within subgenus *Lactifluus*, De Crop et al. (2017) recognised six sections molecularly and morphologically well-supported. Recent advances on the study of this genus in the tropics are indeed revealing high species diversity. For example, in at least two surveys related with *L. volemus* sensu lato, Van de Putte et al. (2010, 2012) discovered 24 phylogenetic species in a small area of northern Thailand and in Sikkim Himalaya. Dealing with section *Piperati*, the revision by De Crop et al. (2014), based on morphology and molecular data, threw light on its wide worldwide diversity and the possible existence of cryptic species. Moreover, they found that the European *L. glaucescens* and *L. piperatus* are not conspecific with species of the section from other regions.

In Mexico, around 19 species of *Lactifluus* (as *Lactarius*) have been recorded, most of them from montane (above 1200 m elevation) subtropical and temperate forests, in comparison with the higher proportion of surveys focused on the subtropical and temperate diversity in this country. In western Mexico, at elevations between 2200–2550 m, the ECM community of *Quercus* spp. (including *Q. laurina* and *Q. crassifolia*), studied by Morris et al. (2008, 2009), included five species of milkcaps belonging to the genus *Lactarius* but none to *Lactifluus*. In our weekly monitoring of two tropical *Quercus* forests in eastern Mexico, we have noticed the presence of milkcaps, including *Lactifluus* species. One of our interests is to continue documenting their taxonomic identity and, in parallel with research, such as Herrera et al. (2018b), to provide morphological and molecular evidence of their association, at root tips level, with the native *Quercus* species. In this paper, we describe two new species found in these forests, recognised with morphological information and a multilocus phylogeny.

Materials and methods

Study area, sampling, morphological and colour study of basidiomes

Random visits were conducted during June-October of 2015–2017 to a remnant of the tropical *Quercus* forest from Central Veracruz (eastern Mexico). The site is privately

owned, at Alto Lucero Co. (450–500 m elevation). Sampling of the two *Lactifluus* species studied was developed in monodominant stands of *Q. oleoides*, surrounded by a coffee trees plantation or land used for livestock.

Macro-morphological features and colours were recorded from fresh samples in different growth stages. Alpha-numeric colour codes in descriptions follow Kornerup and Wanscher (1967) (e.g. 7C8) and Munsell (1994) (e.g. 10YR 8/6). Basidiomes were dried with a hot air dehydrator (45 °C) over a week. Measurements and colours of micromorphological structures were recorded in 3% potassium hydroxide (KOH) and Melzer´s solution. Methods to determine basidiospore ranges are those used by Montoya et al. (2019). Thirty five basidiospores per collection were measured (length and width of the spore in lateral view, excluding the ornamentation). These measurements are presented in taxonomic descriptions accompanied by the symbols: $\bar{X}$ representing the range of X (where X is the average of basidiospores length and width in each collection) and $\bar{Q}$ refers to the range of Q (where Q is the average of the ratio of basidiospore length/basidiospore width in each collection). The methods used to produce scanning electron microscope (FEI, Quanta 250 FEG.) images of their basidiospores are those used by Montoya and Bandala (2003). Twenty five basidia and cystidia per collection were measured. Line drawings were made with the aid of a drawing tube. Collections are part of the herbarium of the Institute of Ecology, A.C., Xalapa, Mexico (XAL) (Thiers B. [continuously updated] Index Herbariorum: a global directory of public herbaria and associate staff. New York Botanical Garden's Virtual Herbarium. http://sweetgum.nybg.org/science/ih/ accessed June 2019).

DNA extraction, PCR amplification and sequencing

Genomic DNA was extracted from fresh and dried basidiome tissue, according to Cesar et al. (2018). PCR was performed to amplify the nuc rDNA ITS (Internal Transcribed Spacer) and D1–D2 domains of nuc 28S rDNA (28S), using primers ITS1F and ITS5/ITS4 and LR0R/LR21 and LR7, respectively (Vilgalys and Hester 1990, White et al. 1990, Gardes and Bruns 1993). Regions 6 and 7 of the nuclear gene that encode the second largest subunit of RNA polymerase II (*rpb*2) were amplified with primers bRPB2 6f/fRPB2 7CR (Liu et al. 1999, Matheny 2005). The thermal cycler conditions for ITS and *rpb*2 markers were (i) initial denaturation at 95 °C for 5 min; (ii) 35 cycles of 30 sec at 95 °C, 30 sec at 55 °C and 40 sec at 72 °C (for LSU this condition was for 60 sec); and (iii) a 5 min final elongation at 72 °C. Amplified PCR products were sequenced using a Genetic Analyzer 3730XL (Applied Biosystems). Once sequences were assembled and edited, they were deposited at GenBank (Benson et al. 2017) and the accession numbers are indicated in Table 1.

Phylogenetic methods

Following preliminary analyses that placed the new species within *Lactifluus* subgenus *Lactifluus*, phylogenetic analyses were performed with the newly generated sequenc-

Table 1. Fungal names, specimen vouchers, locations and GenBank accession numbers (for ITS, 28S and *rpb2*), with newly sequenced collections of *Lactifluus* subgenera *Lactifluus* and *Piperati* in bold.

Taxa	Voucher	Locality	ITS	LSU	*rpb2*
Lactifluus* sect. *Lactifluus					
Lactifluus acicularis	K. Van de Putte 08-029 – Type	Thailand	HQ318239	HQ318147	HQ328884
Lactifluus corrugis	AV05-290	USA	JN388976	JN388997	JN375600
Lactifluus crocatus	KVP08-035 – Type	Thailand	JN388985	HQ318152	HQ328889
Lactifluus dissitus	AV-KD-KVP09-134	India	JN388978	JN389026	JN375628
Lactifluus distantifolius	D. Stubbe 07-461 – Type	Thailand	HQ318223	HQ318124	HQ328866
Lactifluus leptomerus	AV-KD-KVP09-131 – Neotype	India	NR_119981	NG_060275	JN375625
Lactifluus longipilus	H.T. Le 168 – Type	Thailand	HQ318235	HQ318143	HQ328880
Lactifluus mexicanus	Montoya 5189	Mexico	MK211179	MK211188	MK258869
	Montoya 5266	Mexico	MK211180	MK211189	MK258870
	Montoya 5276 – Type	Mexico	MK211181	MK211190	MK258871
Lactifluus pallidilamellatus	Montoya 4716	Mexico	JQ753824	JQ348268	-
Lactifluus oedematopus	KVP 12-001 – Type	Germany	KR364100	KR364232	KR364319
Lactifluus pinguis	H.T. Le 117 – Type	Thailand	HQ318211	HQ318111	HQ328858
Lactifluus subvolemus	Kobeke Van de Putte 08-49 – Type	Slovenia	JQ753928	JQ348380	JQ348242
Lactifluus versiformis	AV-KD-KVP09-006 – Type	India	NR_119980	JN389033	JN375633
Lactifluus vitellinus	K. Van de Putte 08-024 – Type	Thailand	HQ318236	HQ318144	HQ328881
Lactifluus volemus	KVP 11-002	Belgium	JQ753948	KR364175	KR364360
Lactifluus* sect. *Tenuicystidiati					
Lactifluus aff. *tenuicystidiatus*	KUN:F75810	China	KC154105	KC154131	KC154157
Lactifluus subpruinosus	KUN:F73639 – Type	China	NR_155312	NG_060288	KC154161
Lactifluus tropicosinicus	KUN:F59627 – Type	China	NR_155322	NG_060321	KP347670
Lactifluus* sect. *Gerardii					
Lactifluus atrovelutinus	D.Stubbe 06-003	Malaysia	GU258231	GU265588	GU258325
Lactifluus bicolor	DS06-247	Malaysia	JN388955	JN388987	JN375590
Lactifluus gerardii	A.Verbeken 05-375	USA	GU258254	GU265616	GU258353
Lactifluus genevievae	G.G./D.K. 17-02-05 Type	Australia	GU258294	GU265657	GU258397
Lactifluus aff. *ochrogalactus*	AV-KD-KVP09-120	India	JN388956	JN388990	JN375593
Lactifluus parvigerardii	KUN:F61367 – Type	China	JF975641	NG_060270	JF975643
Lactifluus petersenii	A.Verbeken 05-300	USA	GU258281	GU265642	GU258382
Lactifluus* sect. *Ambicystidiati					
Lactifluus ambicystidiatus	KUN:F57008 – Type	China	NR_155311	NG_060287	KC154148
Lactifluus* sect. *Allardii					
Lactifluus allardii	J. Nuytinck 2004-008	USA	KF220016	KF220125	KF220217
Lactifluus* sect. *Piperati					
Lactifluus aff. *glaucescens*	AV 05-374	North America	KF220049	KF220150	KF220236
Lactifluus aff. *piperatus*	A. Verbeken 04-202	USA	KF220021	KF220127	KF220220
	A. Verbeken 05-295	USA	KF220048	KF220149	KF220235
	A. Verbeken 05-393	USA	KF220050	KF220151	KF220237
	H.T. Le 198	Thailand	KF220099	KF220194	KF220268
	H.T. Le 242	Thailand	KF220100	KF220195	KF220269
	H.T. Le 293	Thailand	KF220101	KF220196	KF220270
	H.T. Le 378	Thailand	KF220102	KF220197	KF220271
	H.T. Le 51	Thailand	KF220076	KF220175	KF220253
	J. Nuytinck 2011-036	Vietnam	KF220105	KF220200	KF220274
	J. Nuytinck 2011-072	Vietnam	KF220106	KF220201	KF220275
	TENN 064342	USA	KR364103	KR364234	KR364324
Lactifluus dwaliensis	H.T. Le 67	Thailand	KF220108	KF220203	KF220277
Lactifluus leucophaeus	A.Verbeken 97-382 – Type	Papua New Guinea	GU258299	GU265640	GU258379
Lactifluus lorenae	Caro103	Mexico	MK211187	MK211196	MK258874
	Montoya 5190 – Type	Mexico	MK211185	MK211194	MK258872
	Montoya 5191	Mexico	MK211186	MK211195	MK258873

Taxa	Voucher	Locality	ITS	LSU	*rpb2*
Lactifluus piperatus	A. Fraiture 2584	Belgium	KF220080	KF220176	KF220254
	J. Vesteholt 96-144	Denmark	KF220081	KF220177	KF220255
	M. Lecomte:2000 10 07 01	France	KF220033	KF220135	KF220225
	R. Walleyn 25-08-92b	Germany	KF220082	KF220178	KF220256
	UE09.08.2004-6	Sweden	DQ422035	DQ422035	DQ421937
	GENT:78111 – Type	France	KF220122	KF220215	-
Lactifluus roseophyllus	J. Nuytinck 2011-076	Vietnam	KF220107	KF220202	KF220276
Outgroup					
Auriscalpium vulgare	PBM 944	North America	DQ911613	DQ911614	AY218472
Bondarzewia montana	AFTOL 452	No data	DQ200923	DQ234539	AY218474
Stereum hirsutum	AFTOL 492	No data	AY854063	AF393078	AY218520

es and the sequences retrieved from GenBank (Benson et al. 2017) derived from the BLAST search (best match) of related *Lactifluus* species, complemented with other GenBank sequences of species of all the sections within *Lactifluus* subgenus *Lactifluus*, considered by De Crop et al. (2017) (Table 1). We constructed a concatenated sequence dataset (ITS+LSU+*rpb*2 sequences), with final length of 2,423 bp, in PhyDE v.0.9971 (Müller et al. 2010), aligned with MUSCLE algorithm (Edgar 2004) and corrected inconsistencies manually. Using the IQ-Tree (Nguyen et al. 2015) in an interface online (Trifinopoulos et al. 2016), we calculated the evolutionary model with a partitioning analysis (Kalyaanamoorthy et al. 2017; Chernomor et al. 2016) and Edge-unlinked partition model (Lopez et al. 2002), using the Bayesian Information Criterion (BIC), the Akaike Information Criterion (AIC) and corrected AIC to select the best-fit model. This later was used to generate a phylogenetic tree with the Maximum Likelihood (ML) method, with a Nearest Neighbour Interchange (NNI) heuristic, with TNe+I+G evolutionary model and Ascertainment Bias Correction (ASC). We also generated a consensus tree, calculating the Robinson-Foulds distance between the ML tree and the consensus tree, the branches being tested by means of Ultrafast Approach Bootstrap (UFBoot), SH-like approximate Likelihood Ratio Test (SH-aLRT), Approximate Bayes test (aBayes) and Bootstrap Standard (BS). A phylogenetic tree was generated also by Bayesian Inference (BI), using MrBayes v. 3.2.6 (Ronquist et al. 2012). The phylogenies from ML and BI analyses were displayed using FigTree v1.4.3 (Rambaut 2016).

Results

We generated 18 new sequences from *Lactifluus* species studied, six from each of ITS, nLSU regions of rDNA and *rpb*2 (Table 1 and alignment deposited in TreeBASE S23676). The dataset built included a total of 54 sequences and *Auriscalpium vulgare*, *Bondarzewia montana* and *Stereum hirsutum* as the outgroups. In the phylogenetic trees, inferred using both ML and BI, terminal clades were concordant amongst topologies and internal nodes that had significant BS score (≥ 70%), BI (≥ 0.90), UFBoot

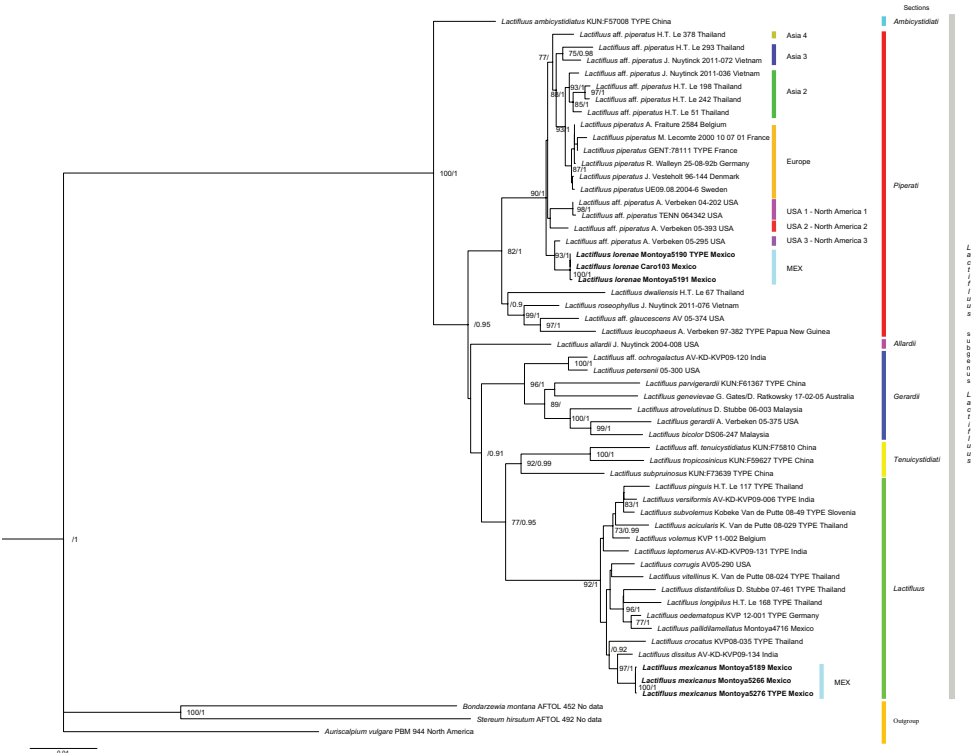

Figure 1. Concatenated three-locus (nuc rDNA ITS, nrLSU and *rpb2*) phylogenetic analysis by maximum likelihood of *Lactifluus* species. Bootstrap scores (only values ≥ 70) / Posterior probabilities (only values ≥ 0.90) are indicated above branches. New species are indicated in bold letters.

(≥ 95%), aBayes (≥ 0.90) and SH-aLRT (≥ 80%). The ML tree with the two former values for the nodes is presented here (Fig. 1). The generated sequences from the Mexican specimens clustered with strong support in two terminal clades.

Based on morphological features and supported with the grouping displayed in the phylogenetic tree, we recognised two groups of the Mexican samples studied representing two distinct new species of *Lactifluus.* One of them, *Lactifluus mexicanus*, appears sister (with strong support) to *L. dissitus* from India and the other one, *L. lorenae*, clusters in a clade with *L. piperatus* (L.) Kuntze from Europe and related species from North America and Asia, sister (with strong support) to an undescribed species from U.S.A.

Taxonomy

Below, we present a key to facilitate the morphological recognition of the species here described. It is based on information from the specimens studied and on research dealing with subgenus *Lactifluus* (Hesler and Smith 1979; Verbeken and Horak 1999; Das et al. 2003; Van de Putte et al. 2010, 2012, 2016; De Crop et al. 2014, 2017).

Basidiomes staining brown or brownish when bruising or cut, especially the lamellae, context and latex; pleurolamprocystidia present ....**II. Sect. *Lactifluus***
Basidiomes not staining as above; pleuromacrocystidia present..... .....**I. Sect. *Piperati***

I. Sect. *Piperati*

1 Lamellae pink salmon to pale orange-brownish.....***L. roseophyllus***
– Lamellae whitish or cream colour.....**2**
2 Pileus brownish grey; latex drying bluish-green.....***L. leucophaeus***
– Basidiomes whitish **3**
3 Lamellae distant; latex white, slowly becoming light greenish-yellow on exposure.....***L. dwaliensis***
– Lamellae crowded **4**
4 Basidiomes staining orange-brown when bruised; basidiospores with $\bar{Q}$ = 1.20–1.27; Pleuromacrocystidia 40–53 µm length.....***L. lorenae***
– Basidiomes not staining orange-brown; basidiospores more ellipsoid, with $\bar{Q}$ = 1.26–1.40; pleuromacrocystidia 50–90 length µm **5**
5 Basidiospores with $\bar{Q}$ = 1.28–1.40, may form incomplete reticulum; suprapellis 80–120 µm thick; lamellae margin heterogeneous, cheilomacrocystidia 35–55 × 5–10 µm..... ***L. piperatus***
– Basidiospores with $\bar{Q}$ = 1.26–1.33, ornamentation never forming a reticulum; suprapellis 10–30 µm; lamellae margin almost composed of emergent cheilomacrocystidia 55–70 × 7–9 µm .....***L. glaucescens***

II. Sect. *Lactifluus*

1 Lamellae moderately distant to distant.....**2**
– Lamellae close or crowded **4**
2 Smell mild .....***L. oedematopus***
– Smell of seafood.....**3**
3 Interlamellae distance a relation of up to 5L+l/cm; basidiospores ornamentation up to 2.1 µm high; pleurolamprocystidia 45–155 × 5–7 µm; wall up to 3 µm thick; Cheilolamprocystidia 25–90 × 4–5.5 µm.....***L. distantifolius***
– Interlamellae distance denser (up to 8L+l/cm); basidiospores ornamentation up to 1.7 (–1.8) µm high; pleurolamprocystidia 60–145 × 7–9(–10) µm; wall up to 4 (–4.5) µm thick; Cheilolamprocystidia 15–80 × (4-) 6–10 µm ..... ***L. dissitus***
4 Lamellae crowded (interlamellae distance a relation of up to 35L+l/cm) .... ***L. leptomerus***
– Lamellae with a less dense arrangement **5**

5	Odour mild **6**
–	Odour of seafood **7**
6	Pileus surface smooth to rugose; basidiospores (7.7–)7.8–9.9(–10.1) µm wide ..... ***L.versiformis***
–	Pileus surface clearly wrinkled, even merulioid or with gyrose-reticulate wrinkles; basidiospores wider (8.5–)9–11(– 12) µm wide ..... ***L. corrugis***
7	Pileus in pale and dull colours **8**
–	Pileus more pigmented with darker or brighter tonalities, pileus including orange, brown, reddish or vinaceous colours **9**
8	Pileus colour pale brownish-yellow ..... ***L. subvolemus***
–	Pileus pale yellowish-white or straw-coloured ..... ***L. pinguis***
9	Pileus mostly reddish-brown to vinaceous, brown with pinkish tinges **10**
–	Pileus mostly in yellowish-orange to orange-brown tinges **11**
10	Stipe with pinkish-orange, pinkish-brown tinges; suprapellis elements and pleurolamprocystidia up to 63 µm long; basidiospores ornamentation up to 1.5 µm high ..... ***L. mexicanus***
–	Stipe brownish-orange; suprapellis elements up to 130 µm long, thus pileus surface with a more velvety appearance; pleurolamprocystidia up to 115 µm long; basidiospores ornamentation up to 2.3 µm high ..... ***L. longipilus***
11	Basidiomes mostly in light yellowish-orange or orange tinges; basidiospores ornamentation up to 2(–2.4) high **12**
–	Basidiomes with orange colouration but including darker brown colours; basidiospores ornamentation shorter **13**
12	Basidiospores with a $\bar{Q}$ = 1.10–1.14; pleurolamprocystidia 64–120 × 6.4 – 9.6 µm; pileipellis terminal elements 16–40.8 × 2.4–12.8 µm ..... ***L. pallidilamellatus***
–	Basidiospores with a $\bar{Q}$ = 1.07–1.09; pleurolamprocystidia 55–105 × 6–13 µm; pileipellis terminal elements 10–70 (–85) × 5–15 µm ..... ***L. vitellinus***
13	Pileipellis terminal elements 10–70(–75) × 4–11 µm ..... ***L. crocatus***
–	Pileipellis terminal elements slender up to 100–130 × 2.5–8 µm **14**
14	Basidiospores 7.7–11.3 × 7.1–10.3 (–10.6) µm; pleurolamprocystidia 55–145(–160) × (6–)7–12 µm; cheilolamprocystidia 20–115 µm long ..... ***L. volemus***
–	Basidiospores 7.0–9.1(–9.3) × 6.5–8.5 µm; pleurolamprocystidia 35–100 × 6–9(–11.5) µm; cheilolamprocystidia 15–85 µm long ..... ***L. acicularis***

Lactifluus lorenae **Montoya, Caro, Ramos & Bandala, sp. nov.**
MycoBank: MB 829060
Figs 2a, b, 3, 5a, b

Holotype. MEXICO, Veracruz State, Alto Lucero Co., 12 km SW Palma Sola (road Veracruz-Nautla) 25 June 2015, Montoya 5190 (XAL). Ectomycorrhizal, under *Quercus oleoides*.

Figure 2. *Lactifluus* species basidiomes and pileipellis **a, b** *L. lorenae*; **c, d** *L. mexicanus*. Scale bars: 40 mm (**a**), 20 mm (**c**), 2 µm (**b, d**).

Diagnosis. *Lactifluus lorenae* is clearly distinguished by white basidiomes, staining orange-brown, latex staining white paper yellow, odour somewhat chlorine-like, basidiospores broadly ellipsoid, pleuromacrocystidia 40–53 × 7–9 µm and pileipellis a hyphoepithelium with a gelatinzied hyphoid layer, 30–60 µm wide.

Gene sequences ex-holotype. MK211185 (ITS), MK211194 (LSU), MK258872 (*rpb2*).

Etymology. In honour of Dr. Lorena E. Sánchez Higueredo because of her interest in the conservation of tropical oak forest relicts in Veracruz, Mexico.

Pileus 25–114 mm diam., convex when young, expanded to broadly infundibuliform, undulate, depressed at centre when old, smooth to irregular when old, dull whitish with yellow tinges (3A2–3A5), staining orange-brown (5C6–C7) when bruised; margin decurved when young, with edge faintly decurved to straight when old, continuous to irregular. **Lamellae** adnate to subdecurrent, crowded to very close, 0.5–1.8 mm broad, edge entire, bifurcate at different levels, yellowish (3–4A2), staining orange-brown when handled, with lamelullae of different sizes, approximately 1 lamelullae per two lamellae. **Stipe** 20–90 × 11–35 mm, eccentric, cylindrical, attenuated or broadened towards the base, robust but at times flattened; surface smooth to irregular, faintly velvety under lens, more evident towards the base, whitish to cream-white, with yellow stains (5Y8/6), staining orange-brown when handled. **Context** cream colour, changing to brownish-orange when exposed, compact. Odour somewhat like chlorine; taste acrid. **Latex** whitish, milky, at times somewhat serous, staining white paper yel-

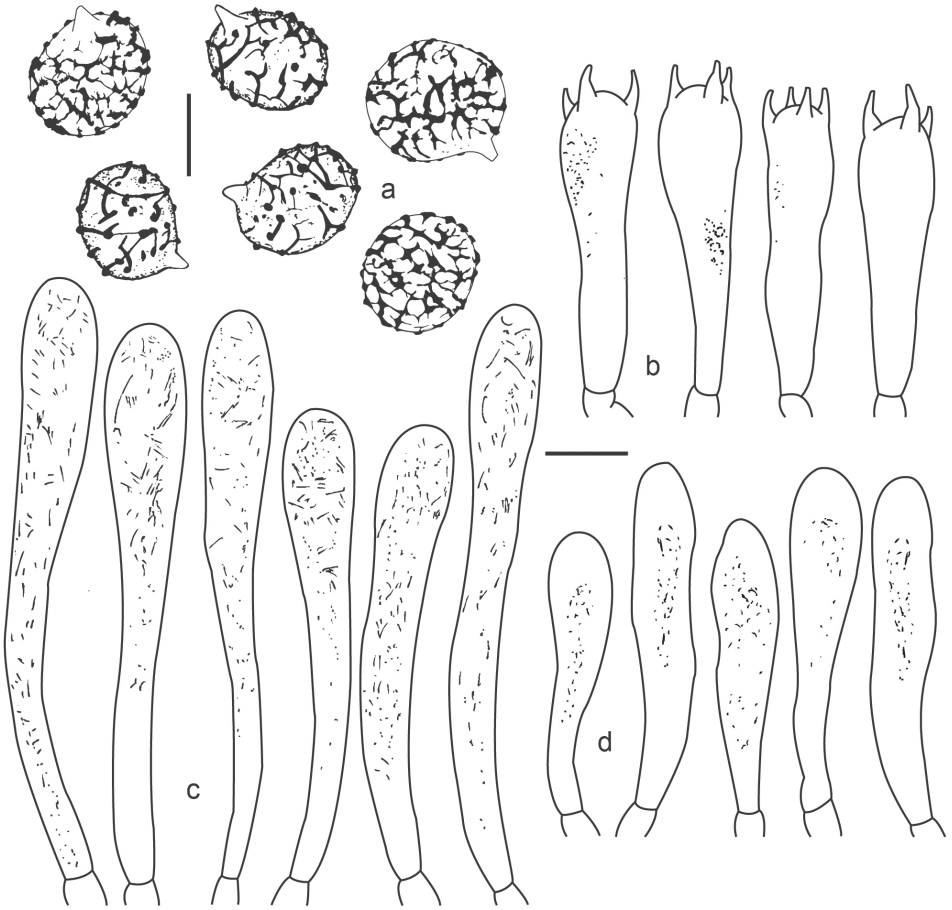

Figure 3. *Lactifluus lorenae* microscopical characteristics **a** basidiospores **b** basidia **c** pleurocystidia **d** cheilocystidia. Scale bars: 5 µm (**a**), 10 µm (**b–d**).

low (5Y 8/2), brownish after some minutes; taste burning acrid. KOH staining the pileus and stipe yellow to pale reddish.

Basidiospores (6–)6.5–8(–10) × (5–)5.5–6.5(–9) µm; $\bar{X}$ = 7.0–7.3(–9.2) × 5.5–6.0(–7.6) µm; $\bar{Q}$ = 1.20–1.27, broadly ellipsoid, thin-walled; ornamentation 0.2–0.4 µm high (measured under SEM), an incomplete reticulum, composed of thick and thin bands and some isolated warts, others ornamented almost with isolated warts and some unconnected bands, plage inamyloid; under SEM the relief of the bands of the basidiospores ornamentation appear with an irregular inflated shape and the plage area with reminiscences of ornamentation. **Basidia** 30–45 × 8–11 µm, clavate, some subcylindrical, with refractive contents, thin-walled, with 2, 4 or at times 3 sterigmata. **Pleuromacrocystidia** 40–53 × 7–9 µm, clavate, some cylindrical and faintly broadened towards the middle area, thin-walled, with refractive needle-like and granular

contents. **Cheilomacrocystidia** 34–54 × 7–9 µm, cylindrical, some clavate at base, thin-walled, with refractive contents. **Pseudocystidia** absent. **Pileipellis** a hyphoepithelium; suprapellis layer of 30–60 µm thick, gelatinized, composed of periclinally orientated hyphae, in some areas the hyphae are loosely intermixed or at times projected in mounds of up to 85 µm thick, the gelatinized matrix dissolved in KOH after some minutes; hyphae 2–4 µm broad, cylindrical, septate, wall up to 0.5 µm thick, sinuous; subpellis of 50–130 µm thick, composed of subisodiametric cells, 12–35 × 10–38 µm diam., yellowish in KOH, wall up to 1.0 µm thick; dermatocystidia 37–128 × 6–8 µm, 3.6–4.8 µm diam. at base, clavate, with refractive needle-like and granular contents, wall up to 0.5 µm thick, scarce, arising from subisodiametric cells of the subpellis layer. **Context** hyphae 5–7 µm broad, cylindrical, thin-walled, some with walls 0.5 µm thick, with faint refractive contents, sphaerocytes 12–26 µm diam., pale yellowish, wall 0.5(–1) µm thick, frequent, laticiferous hyphae 4–7 µm diam., infrequent. **Hymenophoral trama** composed of hyphae which are 4–6 µm diam., septate, wall 0.5 µm thick, with sphaerocytes of 10–25 µm diam., pale yellowish, wall 0.5 µm thick, laticiferous hyphae 4–6 µm diam., infrequent. Clamp connections absent.

Habitat. Gregarious, under *Quercus oleoides*, infrequent.

Additional studied material. MEXICO, Veracruz, Alto Lucero Co., 12 km SW Palma Sola (road Veracruz-Nautla) 25 June 2015, Corona 1127, Montoya 5191; October 11, 2016, Caro 103 (all at XAL).

Lactifluus mexicanus **Montoya, Caro, Bandala & Ramos, sp. nov.**
MycoBank: MB 829061
Figs 2c, d, 4, 5c, d

Holotype. MEXICO, Veracruz State, Veracruz, Alto Lucero Co., 12 km SW Palma Sola (road Veracruz-Nautla) 11 July 2016, Montoya 5276 (XAL). Ectomycorrhizal, under *Quercus oleoides*.

Diagnosis. Recognised by the combination of pileus disc faintly rugose, margin rugose to strongly venous-rugose, lamellae close to very close, the stipe including pinkish tinges and by the size of lamprocystidia and pileipellis terminal elements.

Gene sequences ex-holotype. MK211181 (ITS), MK211190 (LSU), MK258871 (*rpb2*).

Etymology. referring to Mexico.

Pileus 33–125 mm diam., convex, plano convex to depressed at centre, subvelvety, smooth or at times faintly rugose at centre, at remaining disc surface smooth, vinaceous-brown or vinaceous (7D6–8; 7E8; 8C7; 8D4–8) when young, then ferruginous-brown, cinnamon-brown, frequently pale vinaceous (7C4–6), dull vinaceous (7D6) or pinkish-wine over a yellowish base, other reddish-brown to vinaceous (7C8–E8, 7D7–8; 2.5YR 4–5/6), at times with orange-brown (6C7; 6D7–8; 5YR 5/6–6/6; 7.5YR 5/4, 5/6–8) areas; margin decurved, straight in age, at times undulated, rugose to strongly venous-rugose. **Lamellae** 2–9 mm broad, close to very close,

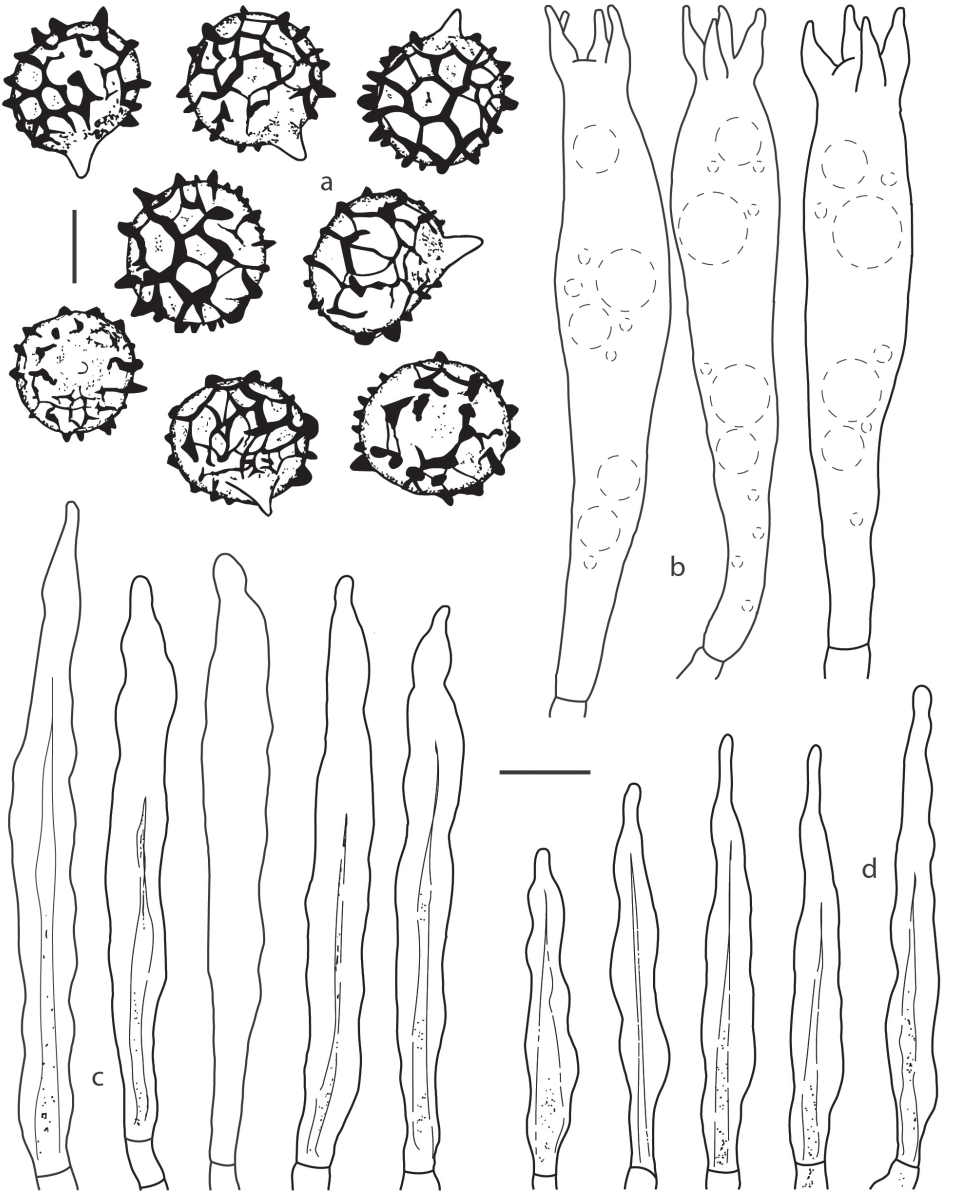

Figures 4. *Lactifluus mexicanus* microscopical characteristics **a** basidiospores **b** basidia **c** pleurocystidia **d** cheilocystidia. Scale bar: 5 μm (**a**), 10 μm (**b–d**).

adnate to subdecurrent, arcuate, with entire edge, some furcate at different levels, at times sinuous especially towards the stipe attachment, pale yellowish to yellowish (2.5Y 8/1–3, 8/6; 7.5YR 8/4; 10YR 8/3–6), straw-yellow, yellow-orange (4A2–6 surfaces, 5A3–5 edges in group) with brown to cinnamon-brown tinges, with faint

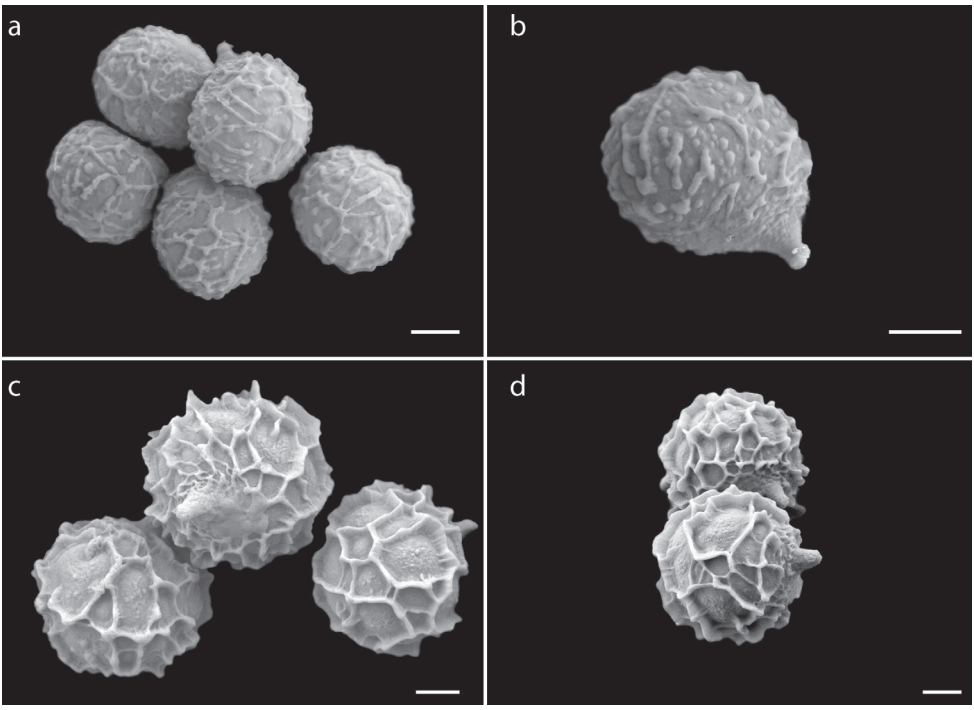

Figures 5. SEM microphotographs of *Lactifluus* species **a, b** *Lactifluus lorenae* **c, d** *L. mexicanus*. Scale bar: 2 µm.

vinaceous stains or brown colour (2.5YR 5/3; 7.5YR 5/4) when handled; lamelullae of different sizes, 1–4 per lamellae. **Stipe** 35–115 × 9–27 mm, cylindrical, faintly broadened towards the base, subtomentose, dry, solid, in general concolorous but paler than pileus surface, at apex pale pinkish-orange (5YR 8/3–4), pinkish-brown, pale orange-brown or pinkish-red (6B3–4, 6B6–C6; 5YR 7/4–6, 8/2), continuing in pale orange (6A2–3), brown-orange with pinkish-grey tinges (6B2–5, 6C2) and pinkish-brown (6–7B3, 6–7B4) colours, becoming darker towards the base (7C4–6) (2.5YR 4/6; 5YR 6/4; 5YR 6/6; 7.5YR 6/3, 5/4, 8/4, 8/6), with some dark brown areas; base whitish and with whitish mycelium. **Context** compact, whitish to yellowish, staining brown-vinaceous. Odour faintly disagreeable, fishy; taste mild to somewhat bitter. **Latex** whitish to cream colour (2.5Y 8/3–6), milky, abundant, secreting from the whole basidiome, staining the lamellae and white paper pale brown; taste mild. KOH darkens the pileus surface.

Basidiospores 8–10(–11) × 7–9(–10) µm, $\bar{X}$= 8.7–9.2 × 7.5–9.0 µm, $\bar{Q}$ = 1.1–1.2, subglobose to broadly ellipsoid, thin-walled; ornamentation up to 0.2–1.2 µm high (measured under SEM), a rather complete reticulum with irregular ridges, at times with thin connecting lines, rarely with some isolated ridges; plage in most spores inamyloid, rarely faintly amyloid; under SEM, the basidiospores wall appears rugose and with some isolated verrucae, with a complete reticulum composed of continuous

regular or irregular ridges, some parts of the reticulum having rounded or irregular nodulose elevations, these later seen in the light microscope as verrucae, plage area smooth or with ornamentation reminiscences. **Basidia** 38–47 × 8–13 µm, clavate to faintly cylindrical, with 3–4 sterigma (at times with 2), thin-walled, with refractive contents. **Pleurolamprocystidia** 47–63 × 5–8 µm, lanceolate, at times mucronate, with wall 1.0–2.0 (–3.0) µm thick (in some elements, the wall is so thick that the lumen is very narrow). **Cheilolamprocystidia** 40–55 × 5–8 µm, lanceolate, some subcylindrical, at times mucronate, with wall up to 1.0 µm thick, without dense contents, hyaline. **Pseudocystidia** absent. **Pileipellis** a lampropalisade, elements of the suprapellis 45–63 × 3–6 µm, most cylindrical, others clavate, ventricose or even ovoid 10–12 × 5–6 µm, without dense contents, some septate, hyaline, compact, at times, the elements arranged in mounds, wall up to 0.5 µm thick; subpellis 42–70 µm thick, composed of cells 9–30 × 7–20 µm, inflated, some subisodiametric, others irregular in form, wall 0.5–1.0 µm thick, not gelatinzied, pale yellowish in KOH. **Context** hyphae in an irregular arrangement, 5.0–8.0 µm diam., cylindrical, septate, wall up to 0.5 µm thick, laticiferous hyphae 4–7 µm diam., with refractive contents, yellowish in KOH; sphaerocytes 14–20 × 16–22 µm, yellowish, wall 1–1.5 µm thick scarce. **Hymenophoral trama** with hyphae 4–8 µm diam., cylindrical, septate, wall up to 0.5 µm thick, with scarce refractive contents, intermixed with laticiferous hyphae 4–8 µm diam., with refractive contents, yellowish in KOH; sphaerocytes 19–27 µm diam., hyaline, with a faint yellowish tinge. Clamp connections absent.

Habitat. Solitary or gregarious, under *Quercus oleoides*.

Additional studied material. MEXICO, Veracruz, Alto Lucero Co., 12 km SW Palma Sola (road Veracruz-Nautla) 25 June 2015, Montoya 5189, 5192; 3 July 2015, Montoya 5193; 5 July 2016, Montoya 5266; 4 October 2016, Montoya 5294, 5295; 29 June 2017, Caro 109, Montoya 5329, 5330, 5331; 4 July 2017, Corona 1370, 1371; 10 July 2017 Montoya 5340; 12 September 2017, Montoya 5398; 16 September 2017, Montoya 5411, 5412; 19 September 2017, Caro125, 126; 25 September 2017 Corona 1423, 1424 (all at XAL).

Discussion

The results inferred in the multilocus phylogeny (Fig. 1), strongly support the recognition of the two new species, *Lactifluus lorenae* and *L. mexicanus*. Although we faced difficulties to amplify *rpb*2 region, fortunately, the Mexican collections processed allowed us to recover with success, this and also ITS and 28S regions. The resolution obtained in our phylogeny may be related to the vouchers selection, mostly having sequences of the three regions (ITS, 28S and *rpb*2). The strong support of the clades, especially of *L. mexicanus* and *L. lorenae* allow us to complement morphological results and, on this basis, we decided to describe them. Both species are members of subgenus *Lactifluus*, the first one falling in section *Piperati* and the second in section *Lactifluus*, according to the classification proposed by De Crop et al. (2017).

Lactifluus lorenae is a white milkcap, with basidiomes showing macromorphological similarities with *L. piperatus*, as narrowly cicumscribed by De Crop et al. (2014). When comparing the macro- and micromorphological variation displayed in the Mexican samples and the information provided by De Crop et al. (2014) about *L. piperatus* in the strict sense, significant differences between the two taxa are detected. Basidiomes of the Mexican species show a uniform tendency to develop an orange-brown colouration on the surfaces when handled and in the context when exposed. The latex can be somewhat serous, staining white paper yellow and becoming brownish after some minutes. When comparing micromorphological features between *L. lorenae* and *L. piperatus* (according to the later authors), in the former, the basidiospores are more globose ($\bar{Q}$ = 1.20–1.27 vs. $\bar{Q}$ = 1.28–1.40) and pleurocystidia are distinctly shorter (40–53 × 7–9 µm vs. 50–70(–90) × 8–11 µm). Another difference between the taxa is the pileipellis structure, which in the Mexican species presents a thicker hyphoid suprapellis (30–60 µm thick vs. 10–30 µm thick) and with abundant dermatocystidia in the suprapellis in *L. piperatus*, while scarce in the subpellis in the Mexican taxon. Organoleptic differences may be noted between both taxa too, because in *L. lorenae*, the odour is somewhat like chlorine, while in *L. piperatus*, it is slightly acidic, distinctly honey- or apple-like when drying. In the inferred phylogeny (Fig. 1), *L. lorenae* clusters sister to an unidentified species, *L.* aff. *piperatus* USA 3-North America 3, but unfortunately, there is no information available on its morphological features and habitat from the U.S.A. to compare with the Mexican species.

Lactifluus mexicanus can be recognised by the combination of close to very close lamellae, pileus in vinaceous, reddish-brown, ferruginous-brown and pinkish-wine tinges, with a paler stipe, mostly including pinkish-orange to pinkish-brown tinges, short cystidia and pileipellis terminal elements (Pleurolamprocystidia 47–63 × 5–8 µm, cheilolamprocystidia 40–55 × 5–8 µm, terminal cells 45–63 × 3–6 µm). *Lactifluus mexicanus*, is recovered as sister species of *L. dissitus* from India, this latter differs by having more distant gills arrangement and clearly larger cystidia [pleurocystidia: 60–145 × 7.0–9 (–10) µm vs. 47–63 × 5–8 µm; cheilocystidia: 15–80 × (4–) 6–10 µm vs. 40–55 × 5–8 µm] (Van de Putte et al. 2012). *Lactifluus mexicanus* is a macro- morphological look-alike of the American *L. corrugis* (Peck) Kuntze. According to the original description of *L. corrugis* (Peck 1880), for which sequences of the type specimen are not available and based on information by Hesler and Smith (1979), the two species share the velvety cap surface and, to some extent, the general basidiome colour. However, in the latter, the basidiomes tend to be darker, especially the stipe ("… at times tinged reddish brown") and the pileus surface is definitively more conspicuously wrinkled, even "...merulioid or corrugated with gyrose-reticulate wrinkles...". In *L. mexicanus*, the cap surface at the disc centre is smooth or only faintly rugose, with the remaining surface smooth, except for the margin, which may appear rugose to strongly venose-rugose, but never with the merulioid aspect depicted in *L. corrugis*. Based on the information of Hesler and Smith (1979), micromorphological differences between both taxa also exist. *Lactifluus mexicanus* has shorter and narrower basidiospores [8–10 (–11) × 7.0–9.0 (–10) µm vs. 9–12 × (8.5–)9–11(–12) µm], with the basidiospore ornamentation up to

1.5 µm high vs. (0.2–) 0.4–0.7 (–0.8) µm high in *L. corrugis*. The cystidia and pileipellis terminal elements are shorter in the Mexican species (pleurocystidia: 4– 63 × 5–8 µm vs. (48–) 60–125 (–204) × 6–10 (16) µm; cheilocystidia: 40–55 × 5.0–8.0 µm vs. (25–) 35–78 × (2) 4–8 µm; pileipellis terminal elements 45–63 × 3–6 µm vs. 45–80 (–128) × 2.5–6 µm]. The pleurocystidia in *L. corrugis*, according to Hesler and Smith (1979), even have a thicker wall up to 7 µm thick. Moreover, this latter species appears to have a more temperate habit, growing in deciduous and mixed woods in U.S.A.

From the weekly sampling in tropical *Quercus* forest, during 2015–2017, we conclude that basidiomes of the studied species are produced in June-October, with those of *Lactifluus mexicanus* being more abundant. Although close to other edible species (Boa 2004, Borah et al. 2018), we have no records of edibility for *L. mexicanus* in the area.

Considering the high diversity of *Quercus* and *Pinus* species in Mexico, they represent important ECM hosts, related with the milkcaps in the country. *Quercus oleoides*, with a wide distribution from Mexico to Costa Rica, especially represents a key ECM host for this group of fungi in its range. In Costa Rica, however, at an elevation around 215 m, associated with *Q. oleoides*, Desai et al. (2016) found 37 ECM species belonging to different genera, three of which were determined as *Lactarius* but no *Lactifluus* was recorded. Considering that the two *Lactifluus* species, here studied, were found in a monodominant area of *Q. oleoides*, we consider them as putative mycobionts of this tree species. However, this will need to be confirmed at root tip level with molecular evidence, as in other milkcaps, such as *Lactarius trichodermoides* Montoya, Bandala & M. Herrera and *L. subplinthogalus* Coker (Herrera et al. 2018b). The two latter species associate with *Q. sapotifolia* and *Q. glaucescens*, respectively, in the relicts of the tropical oak forests from central Veracruz, Mexico.

Acknowledgements

We recognise the support given by CONACYT (CB 252431) to study the ECM fungi associated with tropical species of *Quercus* in Veracruz, Mexico. We appreciate the support given by CONACYT (225382) to the Laboratorio de Presecuenciación, Red Biodiversidad y Sistemática, INECOL. Biol. D. Ramos and M.Sc. Bertha Pérez assisted us in the field and in some molecular procedures, respectively. We appreciate the kind observations made to the manuscript by Dr. A. Vovides (all at INECOL). A special recognition to the owners of the private areas where the study was developed.

References

Arriaga L, Espinoza JM, Aguilar C, Martínez E, Gómez L, Loa E (2000) Regiones terrestres prioritarias de México. Comisión Nacional para el Conocimiento y uso de la Biodiversidad. México.

Benson DA, Cavanaugh M, Clark K, Karsch-Mizrachi I, Lipman DJ, Ostell J, Sayers EW (2017) GenBank. Nucleic Acids Research 45 (Database issue): D37–D42. https://doi.org/10.1093/nar/gkw1070

Boa E (2004) Wild edible fungi a global overview of their use and importance to people. FAO, Rome.

Borah N, Semwal RL, Garkoti SC (2018) Ethnomycological knowledge of three indigenous communities of Assam, India. Indian Journal of Traditional Knowledge 17: 327–335.

Castillo-Campos G, Medina-Abreo ME, Dávila PD, Zavala JA (2005) Contribución al conocimiento del endemismo de la flora vascular en Veracruz, México. Acta Botánica Mexicana 73: 19–57. https://doi.org/10.21829/abm73.2005.1004

Cesar E, Bandala VM, Montoya L, Ramos A (2018) A new *Gymnopus* species with rhizomorphs and its record as nesting material by birds (*Tyrannideae*) in the subtropical cloud forest from eastern Mexico. MycoKeys 42: 21–34. https://doi.org/10.3897/mycokeys.42.28894

Chernomor O, Haeseler A, Minh BQ (2016) Terrace aware data structure for phylogenomic inference from supermatrices. Systematic Biology 65: 997–1008. https://doi.org/10.1093/sysbio/syw037

Das K, Sharma JR, Verbeken A (2003) New species of *Lactarius* from Kumaon Himalaya, India. Mycotaxon 88: 333–342.

De Crop E, Nuytinck J, Van de Putte K, Lecomte M, Eberhardt U, Verbeken A (2014) *Lactifluus piperatus* (Russulales, Basidiomycota) and allied species in Western Europe and a preliminary overview of the group worldwide. Mycological Progress 13: 493–511. https://doi.org/10.1007/s11557-013-0931-5

De Crop E, Nuytinck J, Van de Putte K, Lecomte M, Eberhardt U, Verbeken A (2014) *Lactifluus piperatus* (Russulales, Basidiomycota) and allied species in Western Europe and a preliminary overview of the group worldwide. Mycol Progress 13: 493–511. https://doi.org/10.1007/s11557-013-0931-5

De Crop E, Nuytinck J, Van de Putte K, Wisitrassameewong K, Hackel J, Stubbe D, Hyde KD, Halling R, Moreau PA, Eberhardt U, Verbeken A (2017) A multi-gene phylogeny of *Lactifluus* (*Basidiomycota*, *Russulales*) translated into a new infrageneric classification of the genus. Persoonia 38: 58–80. https://doi.org/10.3767/003158517X693255

Desai NS, Wilson AW, Powers JS, Mueller GM, Egerton-Warburton1 LM (2016) Ectomycorrhizal diversity and community structure in stands of *Quercus oleoides* in the seasonally dry tropical forests of Costa Rica. Environmental Research Letters 11: 125007. https://doi.org/10.1088/1748-9326/11/12/125007

Edgar R (2004) MUSCLE: Multiple Sequence Alignment with High Accuracy and High Throughput. Nucleic Acids Research 32: 1792–1797. https://doi.org/10.1093/nar/gkh340

García J, Castillo J, Guzmán G (1987) Segundo registro de *Boletellus jalapensis* en México. Biotica 12: 291–295.

Gardes M, Bruns D (1993) ITS primers with enhanced specificity for basidiomycetes application to the identification of mycorrhizae and rusts. Molecular Ecology 2: 113–118. https://doi.org/10.1111/j.1365-294X.1993.tb00005.x

Guzmán G, Sampieri A (1984) Nuevos datos sobre el hongo comestible *Cantharellus odoratus* en México. Boletín de la Sociedad Mexicana de Micología 19: 201–205.

Herrera M, Bandala VM, Montoya L (2018a) *Cantharellus violaceovinosus*, a new species from tropical *Quercus* forests in eastern Mexico. MycoKeys 32: 91–109. https://doi.org/10.3897/mycokeys.32.22838

Herrera M, Bandala VM, Montoya L (2018b) Two *Lactarius* species (subgenus Plinthogalus) in ectomycorrhizal association with tropical *Quercus* trees in eastern Mexico. Mycologia 110: 1033–1046. https://doi.org/10.1080/00275514.2018.1521685

Hesler LR, Smith AH (1979) North American Species of *Lactarius*. University of Michigan, Ann Arbor.

Kalyaanamoorthy S, Minh BQ, Wong TKF, Haeseler A, Jermiin LS (2017) ModelFinder: Fast model selection for accurate phylogenetic estimates. Nature Methods 14: 587–589. https://doi.org/10.1038/nmeth.4285

Kornerup A, Wanscher JH (1967) Methuen Handbook of Colour. 2nd edn. Methuen, London, 243 pp.

Liu YJ, Whelen S, Hall BD (1999) Phylogenetic relationships among ascomycetes: evidence from an RNA polymerase II subunit. Molecular Biology and Evolution 16: 1799–1808. https://doi.org/10.1093/oxfordjournals.molbev.a026092

Lopez P, Casane D, Philippe H (2002) Heterotachy, an Important Process of Protein Evolution. Molecular Biology and Evolution 19: 1–7. https://doi.org/10.1093/oxfordjournals.molbev.a003973

Matheny PB (2005) Improving phylogenetic inference of mushrooms with RPB1 and RPB2 nucleotide sequences (*Inocybe*; Agaricales). Molecular Phylogenetics and Evolution 35: 1–20. https://doi.org/10.1016/j.ympev.2004.11.014

Montoya L, Bandala VM (1996) Additional new records on *Lactarius* from Mexico. Mycotaxon 57: 425–450.

Montoya L, Bandala VM (2003) Studies on *Lactarius* a new combination and two new species from Mexico. Mycotaxon 85: 393–407.

Montoya L, Garay-Serrano E, Bandala VM (2019) Two new species of *Phylloporus* (Fungi, Boletales) from tropical *Quercus* forests in eastern Mexico. MycoKeys 51: 107–123. https://doi.org/10.3897/mycokeys.51.33529

Morris MH, Pérez-Pérez MA, Smith ME, Bledsoe CS (2008) Multiple species of ectomycorrhizal fungi are frequently detected on individual oak root tips in a tropical cloud forest. Mycorrhiza 18: 375–383. https://doi.org/10.1007/s00572-008-0186-1

Morris MH, Pérez-Pérez MA, Smith ME, Bledsoe CS (2009) Influence of host species on ectomycorrhizal communities associated with two co-occurring oaks (*Quercus* spp.) in a tropical cloud forest. FEMS Microbiology Ecology 69: 274–287. https://doi.org/10.1111/j.1574-6941.2009.00704.x

Müller J, Müller K, Neinhuis C, Quandt D (2010) PhyDE – Phylogenetic Data Editor, version 0.9971. Program distributed by the authors. http:\\www.phyde.de

Munsell Soil Colour Charts (1994) Macbeth, New Windsor, 10 pp.

Nguyen LT, Schmidt HA, Haeseler A, Minh BQ (2015) IQ-TREE: A Fast and Effective Stochastic Algorithm for Estimating Maximum-Likelihood Phylogenies. Molecular Biology and Evolution 32: 268–274. https://doi.org/10.1093/molbev/msu300

Oldfield S, Eastwood A (2007) The Red List of Oaks. Flora and fauna International, Cambridge, UK.

Peck Ch (1880) Annual Report New York State Museum Natural History 32: 31 pp. [1879]

Rambaut A (2016) FigTree v1.4.3 software. Institute of Evolutionary Biology, University of Edinburgh. http://tree.bio.ed.ac.uk/software/figtree/

Ronquist F, Teslenko M, van der Mark P, Ayres DL, Darling A, Höhna S, Larget B, Liu L, Suchard MA, Huelsenbeck JP (2012) MrBayes 3.2: efficient Bayesian phylogenetic inference and model choice across a large model space. Systematic Biology 61: 539–542. https://doi.org/10.1093/sysbio/sys029

Singer R, García J, Gómez LD (1991) The Boletineae of Mexico and Central America III. J. Cramer, Stuttgart. Nova Hedwigia, Beihefte, 102 pp.

Trifinopoulos J, Nguyen LT, Haeseler A, Minh BQ (2016) W-IQ-TREE: a fast online phylogenetic tool for maximum likelihood analysis. Nucleic Acids Research 44(W1): W232–W235. https://doi.org/10.1093/nar/gkw256

Valencia S (2004) Diversidad del género *Quercus* (Fagaceae) en México. Boletín de la Sociedad Botánica de México 75: 33–53. https://doi.org/10.17129/botsci.1692

Van de Putte K, Nuytinck J, Stubbe D, Le HT, Verbeken A (2010) *Lactarius volemus* sensu lato (Russulales) from northern Thailand: morphological and phylogenetic species concepts explored. Fungal Diversity 45: 99–130. https://doi.org/10.1007/s13225-010-0070-0

Van de Putte K, Nuytinck J, Das K, Verbeken A (2012) Exposing hidden diversity by concordant genealogies and morphology – a study of the *Lactifluus volemus* (Russulales) species complex in Sikkim Himalaya (India). Fungal Diversity 55: 171–194. https://doi.org/10.1007/s13225-012-0162-0

Van de Putte K, Nuytinck J, De Crop E, Verbeken A (2016) *Lactifluus volemus* in Europe: Three species in one Revealed by a multilocus genealogical approach, Bayesian species delimitation and morphology. Fungal Biology 120: 1–25. https://doi.org/10.1016/j.funbio.2015.08.015

Verbeken A, Horak E (1999) *Lactarius* (Basidiomycota) in Papua New Guinea. 1. Species of Tropical Lowland Habitats. Australian Systematic Botany 12: 767–779. https://doi.org/10.1071/SB98026

Vilgalys R, Hester M (1990) Rapid genetic identification and mapping of enzymatically amplified ribosomal DNA from several Cryptococcus species. Journal of Bacteriology 172: 4239–4246. https://doi.org/10.1128/jb.172.8.4238-4246.1990

Villaseñor JL (2016) Checklist of the native vascular plants of Mexico. Revista Mexicana de Biodiversidad 87: 559–902. https://doi.org/10.1016/j.rmb.2016.06.017

White TJ, Bruns TD, Lee SB, Taylor JW (1990) Amplification and direct sequencing of fungal ribosomal RNA genes for phylogenetics. In: Innis MA, Gelfand DH, Sninsky JJ, White TJ (Eds) PCR protocols: a guide to methods and applications. Academic Press, San Diego, 315–322. https://doi.org/10.1016/B978-0-12-372180-8.50042-1

MycoKeys 59: 47–65 (2019)
doi: 10.3897/mycokeys.59.36823
http://mycokeys.pensoft.net

RESEARCH ARTICLE

A peer-reviewed open-access journal
MycoKeys
Launched to accelerate biodiversity research

Additions to the knowledge of *Ganoderma* in Thailand: *Ganoderma casuarinicola*, a new record; and *Ganoderma thailandicum* sp. nov.

Thatsanee Luangharn[1,2,3,4], Samantha C. Karunarathna[1,3,4], Peter E. Mortimer[1,4], Kevin D. Hyde[3,5], Jianchu Xu[1,3,4]

1 *Key Laboratory for Plant Diversity and Biogeography of East Asia, Kunming Institute of Botany, Chinese Academy of Sciences, Kunming 650201, Yunnan, China* **2** *University of Chinese Academy of Sciences, Beijing 100049, China* **3** *East and Central Asia Regional Office, World Agroforestry Centre (ICRAF), Kunming 650201, Yunnan, China* **4** *Centre for Mountain Futures (CMF), Kunming Institute of Botany, Kunming 650201, Yunnan, China* **5** *Center of Excellence in Fungal Research, Mae Fah Luang University, Chiang Rai 57100, Thailand*

Corresponding author: *Jianchu Xu* (jxu@mail.kib.ac.cn); *Peter E. Mortimer* (peter@mail.kib.ac.cn)

Academic editor: *Bao-Kai Cui* | Received 5 June 2019 | Accepted 5 September 2019 | Published 16 October 2019

Citation: Luangharn T, Karunarathna SC, Mortimer PE, Hyde KD, Xu J (2019) Additions to the knowledge of *Ganoderma* in Thailand: *Ganoderma casuarinicola*, a new record; and *Ganoderma thailandicum* sp. nov. MycoKeys 59: 47–65. https://doi.org/10.3897/mycokeys.59.36823

Abstract

Ganoderma is a cosmopolitan genus of mushrooms, which can cause root and butt rot diseases on many tree species. Members of this genus are particularly diverse in tropical regions. Some *Ganoderma* spp. are medicinally active and therefore are used to treat human diseases or as a dietary supplement. In this study, three *Ganoderma* strains were collected in tropical southern Thailand. Phylogenetic analyses of combined ITS, LSU, TEF1α and RPB2 sequence data indicated that the three strains grouped in a distinct lineage within laccate *Ganoderma*. One strain was collected from Surat Thani Province clustered in the *G. casuarinicola* clade with high statistical support (MLBS = 100% / MPBS = 98% / PP = 0.96), while the other two strains of *Ganoderma*, collected from Nakhon Si Thammarat Province, formed a distinct well-supported clade (MLBS = 100% / MPBS = 100% / PP = 1.00) and are described here as a new species. *Ganoderma casuarinicola* is reported here as a new record to Thailand. Morphological differences of the two taxa and their closely related taxa are discussed. Colour photographs of macro and micro morphological characteristics and a phylogenetic tree to show the placement of the new record and new species are provided.

Keywords

Ganodermataceae, medicinal mushroom, molecular phylogeny, morphological characteristics, new species, white rot

Introduction

Ganoderma, a genus of the Ganodermataceae, was established by Karsten (1881) with *G. lucidum* (Curtis) P. Karst. as the type species. Justo et al. (2017) treated Ganodermataceae as a synonym of Polyporaceae, while Cui et al. (2019) state that *Ganoderma* was not included in Polyporaceae because their double-walled basidiospores are quite different from Polyporaceae. Relevant characteristics for *Ganoderma* species delimitation are unique to laccate and non-laccate basidiocarps: truncated double walled basidiospores, an apical germinal pore, a thin and colourless external wall (exosporium) and a dark brown internal wall (endosporium) (Moncalvo and Ryvarden 1997; Zhao 1989; Núñez and Ryvarden 2000; Ryvarden 2004). *Ganoderma* is a cosmopolitan genus and some of the species are pathogenic, causing white rot diseases on rotting stumps, roots and living trunks (Moncalvo and Ryvarden 1997; Pilotti et al. 2004). *Ganoderma* are distributed in both tropical and temperate regions, but are particularly diverse in the tropical regions (Cao and Yuan 2013). Index Fungorum records 451 taxa (http://www.indexfungorum.org/; accessed date: 1 June 2019) and MycoBank records 387 taxa (http://www.mycobank.org/; accessed date: 1 June 2019). *Ganoderma* can be a confusing genus to study due to the highly variable morphological features of the species in this group, including intra-species variations (Ryvarden 2000; Papp et al. 2017; Hapuarachchi et al. 2018a, c; Hapuarachchi et al. 2019a, b).

The genus *Ganoderma* is economically important, as the members of the genus are regarded as valuable medicinal mushrooms (Dai et al. 2009; Hapuarachchi et al. 2018b). *Ganoderma* spp. have been used in traditional medicines for hundreds of years in Asian countries. Several *Ganoderma* species are known to be prolific sources of highly active bioactive compounds such as polysaccharides, proteins, steroids and triterpenoids, such as ganoderic acids (Shim et al. 2004; Qiao et al. 2005; Wang and Liu 2008; Teng et al. 2011; De Silva et al. 2012a, b; De Silva et al. 2013; Li et al. 2018). Those bioactive compounds have a therapeutic potential to treat and remedy many pathological diseases (Sanodiya et al. 2009; Richter et al. 2015; Hapuarachchi et al. 2018b).

Most members of *Ganoderma* are regarded as plant pathogens for trees, such as *G. australe* (Jungh.) Bres., which is associated with *Castanopsis* spp. (Luangharn et al. 2017); *G. boninense* Pat., which is the causal agent of oil palm basal stem rot (Pilotti 2005); *G. dunense*, which is associated with *Acacia cyclops* (Tchoumi et al. 2018); *G. leucocontextum* T.H. Li, W.Q. Deng, Sheng H. Wu, Dong M. Wang & H.P. Hu, which causes problems to *Cyclobalanopsis glauca* (Li et al. 2015); *G. philippii* (Bres. & Henn. ex Sacc.) Bres., which causes problems to tea and rubber (Zakaria et al. 2009); *G. tropicum*, which grows in a solitary manner on living *Dipterocarpus* spp. (Luangharn et al. 2019); and the holotype of *G. casuarinicola*, which was found associated with a living *Casuarina equisetifolia* tree (Xing et al. 2018).

In Thailand, several *Ganoderma* species have been reported based on both morphological characteristics and molecular data, including *G. australe* (Luangharn et al. 2017), *G. sichuanense* (Thawthong et al. 2017) and *G. tropicum* (Luangharn et al. 2019). The aims of the present study are to report *G. casuarinicola* as a new record to Thailand and describe *G. thailandicum* as a new species from Thailand, based on both morphological characteristics and phylogenetic data.

Methods

Mushroom collections and morphological study

Three specimens of *Ganoderma* were photographed at the collecting sites: one from a tropical climate at Surat Thani Province and the other two from Prachuap Khiri Khan Province in Thailand during the rainy season. The detailed morphological characteristics of the specimens were recorded, based on fresh materials (Luangharn et al. 2017). Specimens were subsequently dried at 40 °C for 24 hours, covered with wax papers, kept in sealed plastic bags with anhydrous silica gel (Luangharn et al. 2017) and deposited in the Mae Fah Luang University herbarium (MFLU herb.), while being duplicated in the Herbarium of Cryptogams, Kunming Institute of Botany Academia Sinica (HKAS).

Morphological characteristics were determined following the methodology described by Lodge et al. (2004). Colour changes on bruising were recorded in the field. Colours were recorded following Ridgeway (Ridgeway 1912). Micro-morphological characteristics were observed using a compound Carl Zeiss™ SteREO Discovery.V8 Microscope, while basidiospores were photographed using a Scanning Electron Microscope (SEM). Microscopic features and measurements were made from glass slide preparations, staining the tissues with 3–5% potassium hydroxide (KOH), 2% Melzer's reagent and 3% Congo red reagent (Kreisel and Schauer 1987). Measurements were made using the Tarosoft Image Framework programme v. 0.9.0.7. Basidiospore features, hyphal system, colour, sizes and shapes were recorded and photographed. The description of basidiospore measurements was done by using at least 50 basidiospores from each basidiomata (Miettinen and Larsson 2006). The basidiospore quotient was followed [$Q = L/W$], where Q, the quotient of basidiospore length to width (L/W) of a basidiospore in side view and Qm, the mean of Q-values ± SD, was calculated considering the mean value of the lengths and widths of basidiospores (Tulloss 2005). The basidiospore size was measured with and without the myxosporium and given as (*a*–)*b*–*c*(–*d*) (Tulloss 2005).

DNA extraction, PCR amplification and sequencing

Dried internal tissues of the fruiting bodies were used to extract DNA by using the Biospin Fungus Genomic DNA Extraction Kit (BioFlux), following the manufacturer's instructions. Total reaction mixtures (25 µl) contained 9.5 µl ddH_2O, 12.5 µl of PCR master mix, 1 µl of DNA template and 1 µl of each primer (10 µM). The primers used in PCR amplification were: ITS4/ITS5 for internal transcribed spacer gene region (ITS); LROR/LR5 for partial large subunit rDNA gene region (LSU) (Vilgalys and Hester 1990; White et al. 1990); 983F/2218R for partial translation elongation factor 1-alpha gene region (TEF1α) (Sung et al. 2007); and fRPB2-5f/fRPB2-7cR for partial RNA polymerase II second largest subunit gene (RPB2) (Liu et al. 1999). PCR amplification conditions were 3 min at 94 °C, followed by 35 cycles of 95 °C for 30 s, 55 °C for 1 min, 72 °C for 1 min, followed by a final extension at 72 °C for 10 min for ITS and LSU. The amplification condition for TEF1α consisted of initial denaturation at 5.30 min at 95 °C, followed by 35 cycles of

94 °C for 1 min, 57 °C for 30 s and 72 °C for 1.30 min, followed by a final extension at 72 °C for 10 min and 3 min at 94 °C followed by 35 cycles of 95 °C for 1 min, 52 °C for 2 min and 72 °C for 1 min, followed by a final extension at 72 °C for 10 min for RPB2. PCR products were sequenced by Sangon Biotech (Shanghai) Co., Ltd., Shanghai, China.

Phylogenetic analyses

Sequence data, retrieved from GenBank based on previous studies, are listed in Table 1. The sequences were subjected to standard BLAST searches in GenBank to determine the primary identity of the fungal isolates. *Amauroderma rugosum* Cui 9011 (Li and Yuan 2015) and *Tomophagus colossus* (Zhou et al. 2015) were selected as the outgroup taxa. All the newly generated sequences were aligned with the combined datasets of ITS, LSU and TEF1α with MAFFT v. 7.309 (Katoh and Standley 2013) and manually adjusted using Bioedit v. 7.2.5 (Hall 1999). Gaps were treated as missing data. Maximum parsimony (MP) analysis was performed with PAUP v. 4.0b10 (Swofford 2002). Maximum likelihood analyses (ML) were estimated by using the software on the CIPRES Gateway platform (Miller et al. 2010) and performed using RAxML-HPC2 on XSEDE (v. 8.2.8) (Stamatakis 2014), then carried out using the raxmlGUI version v. 1.3.1 (Silvestro and Michalak 2011).

MrModeltest v. 2.3 was used to determine the best-fitting substitution model for each single gene partition and the concatenated dataset for Bayesian analyses (Nylander 2004). Bayesian inference posterior probabilities (PP) with a GTR+I+G model was used for each partition. MrBayes v. 3.2.2 (Huelsenbeck and Ronquist 2001) was used to evaluate PP by Markov Chain Monte Carlo sampling (BMCMC) (Rannala and Yang 1996; Zhaxybayeva and Gogarten 2002). The number of generations was set at 4,000,000, with trees being sampled every 100 generations and a total of 40,000 trees obtained, resulting in an average standard deviation of split frequencies below 0.01. Based on the tracer analysis (Rambaut et al. 2014), the first 20% of trees (8,000 trees) were discarded as the burn-in phase of the analyses represented. The remaining 32,000 trees were used for calculating PP in the majority rule consensus tree (Larget and Simon 1999). ML and MP bootstrap values, equal to or greater than 70% and Bayesian Posterior Probabilities (BP) equal to or greater than 0.95 are presented above each node (Fig. 1). Trees were figured in the FigTree v. 1.4.0 programme (Rambaut 2012), edited using Microsoft Office PowerPoint 2010 and exported to Adobe Illustrator CS v. 3 (Adobe Systems, USA). Sequences derived in this study were deposited in GenBank (http://www.ncbi.nlm.nih.gov).

Results

Phylogenetic analyses

The phylogenetic analyses included 56 taxa (including the three new sequence data) and the tree was inferred from the combined ITS, LSU, TEF1α and RPB2 sequences, which comprise 3,360 characters with gaps; 623 characters for ITS, 930 characters for LSU,

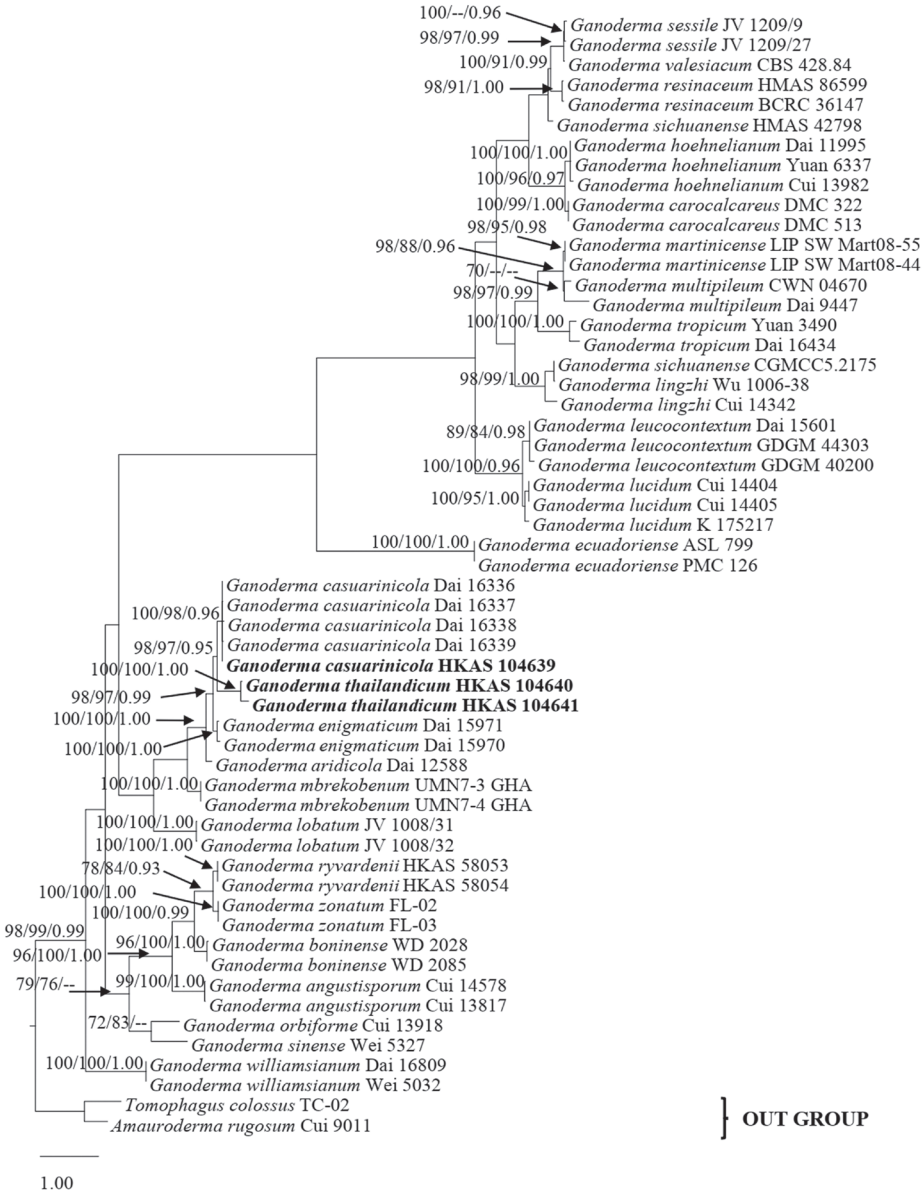

Figure 1. Phylogram of *Ganoderma thailandicum*, obtained from maximum likelihood (RAxML) of combined ITS, LSU, TEF1α and RPB2 datasets. Bootstrap values (BS) from maximum likelihood (ML, left) and Maximum parsimony (MP, middle) greater than 70% and Bayesian posterior probabilities (PP), greater than 0.95, are indicated above the nodes as MLBS/MPBS/PP. The tree is rooted with *Amauroderma calcitum* Cui 9011 and *Tomophagus colossus* TC-02. New species and new records are indicated in black bold.

859 characters for TEF1α and 948 characters for RPB2. The best scoring ML tree is shown in Fig. 1. Tree topologies of the ML and MP were similar to the Bayesian analysis. The dataset represents 26 *Ganoderma* species, with *Amauroderma rugosum* Cui 9011 and

Table 1. Details of the taxa used in the phylogenetic analysis of this study. The newly generated sequences are in bold.

Fungal species	Voucher	GenBank accession no.				References
		ITS	LSU	TEF1α	RPB2	
Ganoderma angustisporum	Cui 13817	MG279170	–	MG367563	MG367507	Xing et al. 2018
G. angustisporum	Cui 14578	MG279171	–	MG367564	–	Xing et al. 2018
G. aridicola	Dai 12588	KU572491	–	KU572502	–	Xing et al. 2016
G. boninense	WD 2028	KJ143905	KU220015	KJ143924	KJ143964	Zhou et al. 2015
	WD 2085	KJ143906	–	KJ143925	KJ143965	Zhou et al. 2015
G. carocalcareus	DMC 322	EU089969	–	–	–	Douanla-Meli and Langer 2009
	DMC 513	EU089970	–	–	–	Douanla-Meli and Langer 2009
G. casuarinicola	Dai16336	MG279173	–	MG367565	MG367508	Xing et al. 2018
	Dai16337	MG279174	–	MG367566	MG367509	Xing et al. 2018
	Dai16338	MG279175	–	MG367567	MG367510	Xing et al. 2018
	Dai16339	MG279176	–	MG367568	MG367511	Xing et al. 2018
G. casuarinicola	**HKAS 104639**	**MK817650**	**MK817654**	**MK871328**	**MK840868**	**This study**
G. thailandicum	**HKAS 104640 (holotype)**	**MK848681**	**MK849879**	**MK875829**	**MK875831**	**This study**
	HKAS 104641 (paratype)	**MK848682**	**MK849880**	**MK875830**	**MK875832**	**This study**
G. ecuadoriense	ASL799	KU128524	KX228350	–	–	Crous et al. 2016
	PMC126	KU128525	KU128529	–	–	Crous et al. 2016
G. enigmaticum	Dai 15970	KU572486	–	KU572496	MG367513	Xing et al. 2016
	Dai 15971	KU572487	–	KU572497	MG367514	Xing et al. 2016
G. heohnelianum	Dai 11995	KU219988	–	MG367550	MG367497	Song et al. 2016
	Yuan 6337	MG279160	–	MG367551	MG367498	Xing et al. 2018
	Cui 13982	MG279178	–	MG367570	MG367515	Xing et al. 2018
G. leucocontextum	Dai 15601	–	–	–	MG367516	Xing et al. 2016
	GDGM 44303	KJ027607	–	–	–	Li et al. 2015
	GDGM 40200	KF011548	–	–	–	Li et al. 2015
G. lobatum	JV 1008/31	KF605671	–	MG367553	MG367499	Xing et al. 2018
	JV 1008/32	KF605670	–	MG367554	MG367500	Xing et al. 2018
G. lucidum	K175217	KJ143911	–	KJ143929	KJ143971	Zhou et al. 2015
	Cui 14404	MG279181	–	MG367573	MG367519	Xing et al. 2018
	Cui 14405	MG279182	–	MG367574	MG367520	Xing et al. 2018
G. lingzhi	Wu1006-38	JQ781858	–	JX029976	JX029980	Cao et al. 2012
	Cui 14342	MG279179	–	MG367571	MG367517	Xing et al. 2018
G. martinicense	LIP SWMart 08-55	KF963256	–	–	–	Welti and Courtecuisse 2010
	LIP SWMart 08-44	KF963257	–	–	–	Welti and Courtecuisse 2010
G. mbrekobenum	UMN7-3 GHA	KX000896	KX000897	–	–	Crous et al. 2016
	UMN7-4 GHA	KX000898	KX000899	–	–	Crous et al. 2016
G. multipileum	CWN 04670	KJ143913	–	KJ143931	KJ143972	Zhou et al. 2015
	Dai 9447	KJ143914	–	MG367588	KJ143973	Zhou et al. 2015
G. orbiforme	Cui 13918	MG279186	–	MG367576	MG367522	Xing et al. 2018
G. resinaceum	HMAS86599	AY884177	–	–	JF915435	GenBank
	CBS 194.76	KJ143916	–	KJ143934	–	Zhou et al. 2015
G. ryvardenii	HKAS 58053	HM138671	–	–	–	Kinge and Mih 2011
	HKAS 58054	HM138672	–	–	–	Kinge and Mih 2011
G. sessile	JV1209/9	KF605629	–	KJ143936	-	Li et al. 2015
	JV 1209/27	KF605630	–	KJ143937	KJ143976	Li et al. 2015
G. sichuanense	HMAS 42798	JQ781877	–	–	–	Li et al. 2015
	CGMCC 5.2175	KC662402	–	–	–	Yao et al. 2013

Fungal species	Voucher	GenBank accession no.				References
		ITS	LSU	TEF1α	RPB2	
G. sinense	Wei5327	KF494998	KF495008	KF494976	MG367529	Xing et al. 2018
G. tropicum	Yuan 3490	JQ781880	–	KJ143938	–	Cao et al. 2012
	Dai 16434	MG279194	–	MG367585	MG367532	Xing et al. 2018
G. valesiacum	CBS428.84	JQ520218	–	–	–	Park et al. 2012
G. williamsianum	Dai 16809	MG279183	–	MG367588	MG367535	Xing et al. 2018
	Wei5032	KU219994	KU220024	–	–	Song et al. 2016
G. zonatum	FL-02	KJ143921	–	KJ143941	KJ143979	Zhou et al. 2015
	FL-03	KJ143922	–	KJ143942	KJ143980	Zhou et al. 2015
Amauroderma rugosum	Cui 9011	KJ531664	–	KU572504	–	Li and Yuan 2015
Tomophagus colossus	TC-02	KJ143923	–	KJ143943	MG367506	Zhou et al. 2015

Tomophagus colossus TC-02 as the outgroup taxa. The dataset comprised 3361 total characters, of which 2378 were constant, 782 variable characters were parsimony-informative and 201 characters were parsimony-uninformative. Phylogenetic analyses indicated the placement of three isolates (HKAS 104639, HKAS 104640 and HKAS 104641) within the laccate *Ganoderma* clade. Phylogenetic results showed that the tree has two main distinct clades. The phylogenetic tree gave considerably high support for the *G. casuarinicola* strain HKAS 104639 and is closely related to the laccate *G. casuarinicola*, as well as the isolates of Guangdong, China, with good support (MLBS = 100% / MPBS = 98% / PP = 0.96), while the two newly isolated strains from this study (HKAS 104640 and HKAS 104641) formed a distinct clade (MLBS = 100% / MPBS = 100% / PP = 1.00) with a sister clade with *G. casuarinicola* clade (MLBS = 98% / MPBS = 97% / PP = 0.95).

Taxonomy

Ganoderma casuarinicola **J.H. Xing, B.K. Cui & Y.C. Dai., MycoKeys 34: 93–108 (2018)**
Faces of fungi number: FoF 06130
Fig. 2

Description. Basidiocarps: Substipitate to stipitate. **Pileus shape.** Annual, applanate and dimidiate when becoming mature, up to 10–16 cm in length, 4– 9 cm in width, up to 0.7–1.2 cm thick. **Pileus surface.** Distinctively zonate from the base to the margin where the new hyphae are in active development, orange, golden yellow at the base, slightly to reddish-orange, orange red, brownish-red, extended to reddish-brown, red at centre, orange to deep orange extending to the upper margin surface, with yellowish-white to pale yellow under margin surface, strongly laccate, glabrous, glossy, shiny, smooth, spathulate, shallow sulcate when fresh, thin crust overlies the pellis, thicker at the base than the margin, light in weight when dried, non-woody when dried. **Context.** Mostly yellow to light orange, orange close to crust, reddish-golden, light brown,

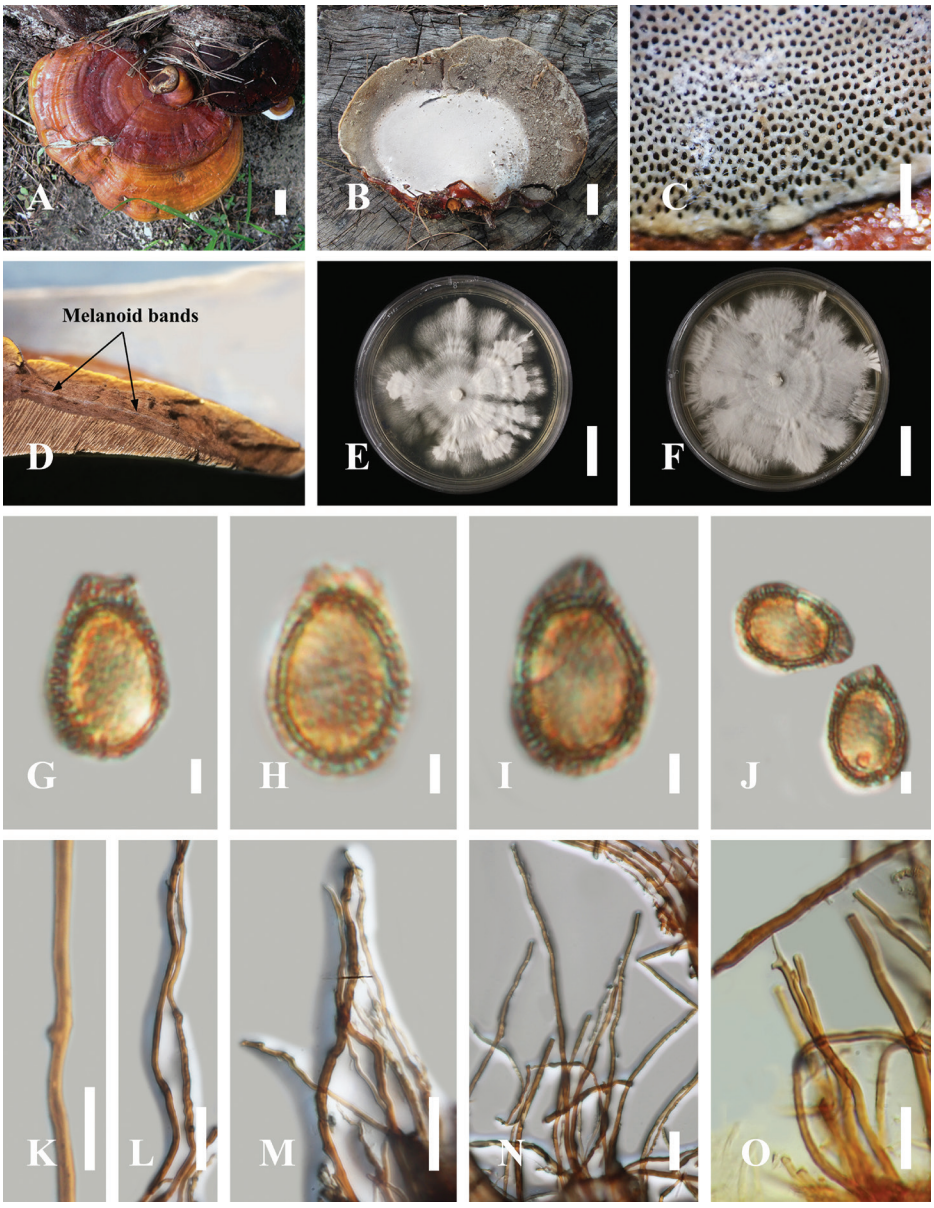

Figure 2. Morphology of *Ganoderma casuarinicola* (HKAS 104639) **A** The upper surface of mature basidiocarp **B** the lower surface of mature basidiocarp **C** pore characteristics **D** melanoid bands in the context tissue **E, F** culture after incubation at 25 °C for 10–14 days on Potato Dextrose Agar (PDA) **G–J** basidiospores in KOH **K** clamp connections **L** thick walled unbranched generative hyphae of context in KOH **M, N** thin-thick-walled unbranched generative and flexuous skeletal hyphae **O** thick-walled generative and skeletal hyphae of the tube layers. Scale bars: 2 cm (**A, B**); 500 µm (**C**); 2 cm (**E, F**); 2 µm (**G–J**); 5 µm (**K**); 3 µm (**L–O**).

brown near the tube layers, dense context layer but not fully homogeneous, thick near the base, tough to break when dried; generative hyphae up to 2.10–4.92 µm ($\bar{x}$ = 3.34, n = 50) in diam., thin walled, almost colourless, some expanded at the apex, unbranched,

with clamp connections; binding hyphae 3.67–5.93 µm ($\bar{x}$ = 4.85, *n* = 50), almost colourless, thin to thick-walled, branched, with clamp connections; skeletal hyphae abundant, up to 3.49–7.34 µm ($\bar{x}$ = 5.34, *n* = 50), almost colourless, thick-walled, unbranched or with very few branches in the distal end, without clamp connections. **Hymenophore.** Trimitic, heterogeneous, up to 1.4 cm thick, generally yellow slightly to light orange, up to 4 mm thick, the lower layer (close to the tubes) on the upper layers, light brown to brown close to the tubes, presented dark brown, melanoid band. **Basidiospores.** Ellipsoid to broadly ellipsoid with double wall (ganodermoid) at maturity, yellowish brown, (*8.7*)*10.8–13.5*(*14.4*) × (*6.6*)*7.6–8.9*(*9.8*) µm ($\bar{x}$ = 12.05 × 7.8 µm, *n* = 50), with Q = 1.38 – 1.45, L = 11.68 µm, W = 8.25 µm (including myxosporium), (*7.1*)*9.9–11.2*(*12.1*) × (*5.2*)*6.7–7.3*(*8.9*) µm ($\bar{x}$ = 10.2 × 6.4 µm, *n* = 50) µm, with Q = 1.48–1.52, L = 10.65 µm, W = 7.10 µm (excluding outer myxosporium). **Tubes.** Up to 6–14 mm long, dark brown, hard, woody when dried; generative hyphae 1.0–3.7 µm in diam., occasionally with simple septa, almost colourless, thin-walled with occasionally thick walls, with clamp connections, occasionally branched; skeletal hyphae 2.7–5.1 µm in diam., thick-walled frequently branched at apex; binding hyphae 1.1–3.0 µm in diam., thin to thick-walled, frequently branched at apex. **Stipe.** Lateral, golden yellow, orange red, up to 8 cm long, 1.8 cm in diam. **Margin.** Obtuse from the substrate, soft, slippery to the touch when young, tough to break. **Pores.** Angular to round, 4–6 per mm, up to 128–195 × 148–266 µm ($\bar{x}$ = 162 × 220 µm, *n* = 50). **Pore surface.** White when fresh, turning yellowish-white to pale yellow when dry, reddish-grey when touched, greyish-brown, brownish-grey when wet. **Hyphal system.** Trimitic, generative hyphae, 2–5 µm in diam., almost colourless, thin-walled or occasionally thick-walled, with clamp connections, occasionally with irregular cuticle cells, light brown to brown in KOH; binding hyphae 3–5 µm, almost colourless, thin to thick-walled, branched, with clamp connections; skeletal hyphae abundant, up to 3–7 µm, almost colourless, thick-walled, unbranched, without clamp connections.

Habitat. Solitary on *Pinus kesiya* stumps in pine forests.

Specimen examined. THAILAND, Surat Thani Province, Phanom District, Khao Sok national park, 8°54'32"N, 98°31'09"E, 427 m elev., 25 June, 2018, LT2018-103 (HKAS 104639).

Ganoderma thailandicum **T. Luangharn, P.E. Mortimer, S.C. Karunarathna & J.C. Xu, sp. nov.**

Faces of Fungi number: FoF 06129
Index Fungorum number: IF 556535
MycoBank MB 831323
Fig. 3

Diagnosis. *Ganoderma thailandicum* is characterised by its laccate deep magenta close to stipe, brownish-red at centre and light yellow of active development towards the margin on pileal surface, white pore surface, brownish-red context and absence of melanoid band.

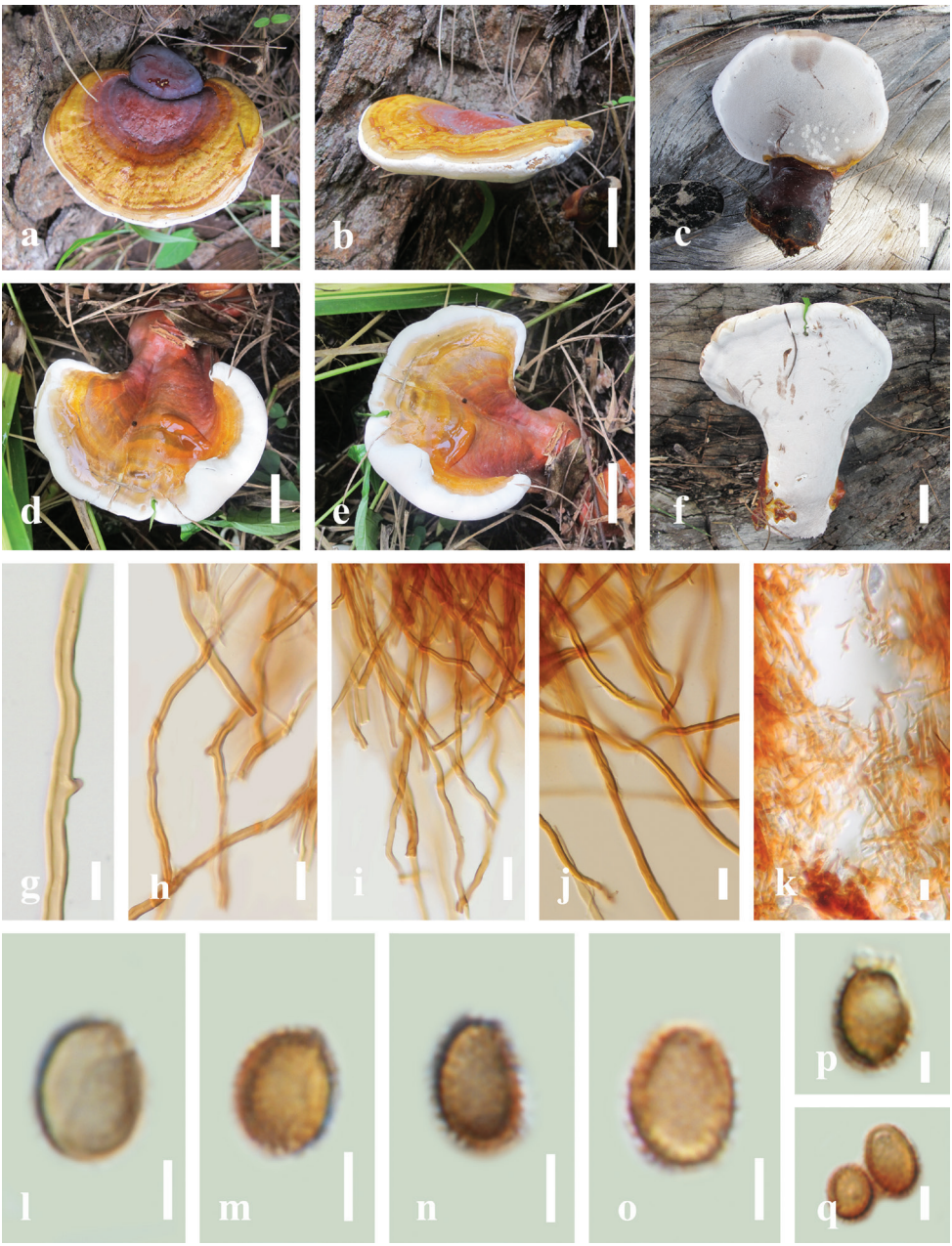

Figure 3. Morphological characteristics of *Ganoderma thailandicum* (HKAS 104640, HKAS 104641). **A, B** Mature basidiocarps (HKAS 104640) **C** lower surface of mature basidiocarp (HKAS 104640) **D, E** development of young to mature fruiting bodies (HKAS 104641) **F** lower surface (HKAS 104641) **G** clamp connections **H** thick-walled unbranched generative hyphae with clamp connections of context in KOH **I** thick-walled, skeletal hyphae in KOH without septa **J** thick-walled sparingly branched skeletal hyphae in Melzer's reagent **K** hyphae of tube layers **L–Q** basidiospores in 3% Congo red reagent. Scale bars: 2 cm (**A–F**); 10 µm (**G**); 15 µm (**H–K**); 3 µm (**L–P**); 5 µm (**Q**).

Holotype. THAILAND, Nakhon Si Thammarat Province, Khanom District, solitary on stump of *Pinus merkusii*, 10 December 2018, LT2018-105 (HKAS 104640).

Etymology. The species epithet "*thailandicum*" refers to the country where the holotype was collected.

Description. Basidiocarps. Dimidiate, laccate, substipitate to stipitate. **Pileus shape.** Annual and dimidiate when mature, up to 3–9 cm in length, 3–6 cm in width, up to 0.4–1.8 cm thick at centre of pileus close to the stipe, obtuse from the substrate. **Pileus surface.** Laccate, glabrous, glossy, smooth, soft, umbonate, distinctly concentrically zonate, greyish-magenta to deep magenta at stipe, greyish-ruby, greyish-red to brownish-red at centre, extended to reddish-orange to slightly pale red with light yellow to vivid yellow of active development towards the margin, thin crust overlaying the pileus, sometimes convex sulcate extending at centre, with distinct concentric zones, with fine furrows at centre extended to the margin, thicker at the base than the margin, consistency hard when young to mature, some cracked when old, non-woody, light in weight when dried. **Hymenophore.** Trimitic, up to 0.4–2.4 cm thick, heterogeneous with greyish-red close to the upper layers slightly to brownish-red to reddish-brown close to the tubes. **Context**. Mostly brownish-red to reddish-brown in Melzer's reagent, absent of melanoid band, with dense context layer. **Basidiospores.** Ellipsoid to broadly ellipsoid with some globose with double wall (ganodermoid) at maturity, light brown to reddish-brown in Congo red reagent, (*6.8*)*8.4–9.7*(*10.2*) × (*5.8*)*6.5–7.3*(*7.7*) µm ($\bar{x}$ = 9.1 × 6.9 µm, *n* = 50), with Q = 1.29–1.35, L = 9.13 µm, W = 6.96 µm (including myxosporium), (*5.4*)*7.6–9.6*(*10.0*) × (*4.7*)*5.8–6.9*(*7.4*) µm ($\bar{x}$ = 7.6 × 6.0 µm, *n* = 50) µm, with Q = 1.32–1.38, L = 8.64 µm, W = 6.42 µm (excluding outer myxosporium). **Tubes.** Up to 0.5 mm close to margin to 7 mm at centre in length, brown to dark brown, hard, woody when dried; generative hyphae 2.73–4.74 µm in diam., almost colourless, thin-walled with occasionally thick walls, with clamp connections, occasionally branched; skeletal hyphae 3.76–5.81 µm in diam., thick-walled frequently branched at apex; binding hyphae 3.24–5.84 µm in diam., thin to thick-walled, frequently branched at apex. **Stipe.** Lateral, pale red to vivid red, greyish-red to red when present, with violet brown when mature, different from and darker than pileus, up to 3–5 cm long, 2.5–3.0 cm in diam., 1.8–2.7 cm thick. **Margin.** Up to 0.4–0.8 cm thick when becoming mature, active growing margin white on the upper and under margin surface when fresh, with a yellow line under the pileus, round, soft, smooth, slippery when touched when young to mature stage, without any zonation, tough when broken. **Pores.** Angular to round, 4–8 per mm, up to 121–176 × 174–247 µm ($\bar{x}$ = 155 × 209 µm, *n* = 50). **Pore surface.** White when fresh, grey at centre, slightly orange grey at margin, brownish-grey when touched, turning brownish-orange when dry, grey when wet. **Hyphal system.** Trimitic, light orange to deep orange, reddish-brown in Melzer's reagent; generative hyphae, 2.65–4.58 µm ($\bar{x}$ = 3.82, *n* = 50) in diam., almost colourless, mostly thick-walled, occasionally thin-walled, bearing clamp connections, occasionally with irregular cuticle cells; binding hyphae 3.32–6.28 µm ($\bar{x}$ = 5.53, *n* = 50), almost colourless, thin-walled, occasionally branched in the distal end, with clamp connections; skeletal hyphae abundant, up to 3.40–6.78 µm ($\bar{x}$ = 5.73,

n = 50), almost colourless, thick-walled and unbranched. **Context**. Mostly brownish-red in Melzer's reagent, reddish-brown, with greyish-red close to crust, dense context layer, agglutinate mass, usually solid in basal part, thick near the base, tough to break when dried; generative hyphae up to 2.80–5.75 µm ($\bar{x}$ = 4.36, n = 50) in diam., mostly colourless, thick-walled, with clamp connections, occasionally with simple septa; binding hyphae 1.23–4.75 µm ($\bar{x}$ = 2.49, n = 50), colourless, thin-walled or with a very few branches in the distal end, with clamp connections; abundant skeletal hyphae up to 3.30–7.51 µm ($\bar{x}$ = 5.75, n = 50), almost colourless, thick-walled, unbranched, with clamp connections and occasionally with simple septa. **Cuticle cells.** Clavate to narrowly clavate, tuberculate, occasionally with irregular cuticle cells, mostly thick-walled, occasionally thin-walled with simple septa. **Basidia.** Clavate, with 4 sterigmata, 12.2–19.6 × 8.3–10.9 µm, light brown (5D6) to yellowish in Melzer's reagent.

Material examined. THAILAND, Nakhon Si Thammarat Province, Khanom District, solitary on stump of *Pinus merkusii*, 11°45'58"N, 99°47'43"E, 499 m elev., 10 December 2018, LT2018-105 and LT2018-106, specimens no. HKAS 104640 and HKAS 104641.

Discussion

In this study, we describe a new species of *Ganoderma* growing on *Pinus* sp. in tropical southern Thailand, in a well-researched genus. This is not surprising as Hyde et al. (2018) found that up to 96% of species discovered in northern Thailand were new to science. *Ganoderma casuarinicola* was collected on a *Pinus kesiya* stump in a pine forest at Surat Thani Province in Thailand, while two collections of *Ganoderma thailandicum* were collected on *Pinus merkusii* stumps from Kanom District, Nakhon Si Thammarat Province in Thailand. All three collections grouped as sister taxa to the laccate *Ganoderma* clade, their morphological characteristics and molecular analyses providing insights to resolve species delimitation. In this study, we introduce *G. casuarinicola* (HKAS 104639) as a new record to Thailand which grouped with the holotype from Guangdong, China (Fig. 1) with high statistical support (MLBS = 100% / MPBS = 98% / PP = 0.96) and *G. thailandicum* is described as a new species, the two collections of *G. thailandicum* (HKAS 104640 and HKAS 104641) grouping together as a distinct clade with 100% ML, 100% MP and 1.00 PP support.

Our findings are consistent with Xing et al. (2018), who demonstrated that *G. casuarinicola* forms a sister clade with *G. aridicola* J.H. Xing & B.K. Cui, from South Africa and *G. enigmaticum* M.P.A. Coetzee, Marinc., M.J. Wingf., from Africa (Coetzee et al. 2015). The morphological differences of these three *Ganoderma* species were detailed in Xing et al. (2018). Moreover, our study allows us to compare the holotypes of *G. casuarinicola* from Guangdong and our collection from Thailand. The Guangdong's *G. casuarinicola* shows its distinctive sectorial to shell-shaped, 10 cm long and 7 cm wide pileus (Xing et al. 2018), while the Thai *G. casuarinicola* shows its annual, applanate to dimidiate shape, 3–16 cm long and 1.5–3 cm wide pileus, larger than the

Guangdong collection. Our *G. casuarinicola* collections show longer tubes of 6–14 mm, while the tubes of the Guangdong collection are 9 mm long; however, our collections show a thinner margin (0.8–1.2 cm thick) than the Guangdong collection (2 cm thick) (Xing et al. 2018). Macro-morphological characteristics of our *G. casuarinicola* share similarities with the holotype collection, such as strongly laccate, shallow sulcate, reddish-brown pileus surface, lateral stipe shape, white pore surface and brown context.

Micro-morphological characteristics of the context layers of both Guangdong and Thai *G. casuarinicola* share similar characteristics, such as the dense light brown to brown context layers; thin to thick-walled generative hyphae; thin-walled binding hyphae; and thick-walled skeletal hyphae. Although both type specimens and our collection of *G. casuarinicola* collection have mostly distinctive yellowish-brown basidiospores, Thai *G. casuarinicola* collections have a smaller size range of (*8.7*)*10.8–13.5*(*14.4*) × (*6.6*)*7.6–8.9*(*9.8*) µm than the type of *G. casuarinicola* (*8.3–*)*9.0–10.2*(*–11.5*) × (*4.5–*)5.*0–6.0*(*–7.0*) µm (including myxosporium). However, the type of *G. casuarinicola* does not have the melanoid band (Xing et al. 2018), while our collection has a dark brown, melanoid band. Although both type specimens and our *G. casuarinicola* collections are grouped in the same clade, macro-morphologically, their pilei are very different, most probably due to geographical and climatic changes. Boddy et al. (2014) also mentioned that climate change and geography affect fungi in many ways, especially regarding phenological changes of fungal fruiting and the spatial and temporal distribution of hosts.

According to our phylogenetic analyses (Fig. 1), collections of *G. thailandicum* were grouped as a sister to *G. aridicola*, *G. casuarinicola*, and *G. enigmaticum* as a well-supported clade of 100% ML, 100% MP and 1.00 PP statistical supports. *Ganoderma aridicola*, *G. casuarinicola*, *G. enigmaticum* and *G. thailandicum* share morphological similarities of laccate to strong laccate upper pileus surface and ellipsoid to broadly ellipsoid basidiospores at maturity. *Ganoderma aridicola* (Xing et al. 2016), *G. casuarinicola* (Xing et al. 2018) and *G. enigmaticum* (Coetzee et al. 2015) are considered as members of the *G. lucidum* complex and our *G. thailandicum* is also clustered within the *G. lucidum* complex, according to the results of the phylogenetic analyses. Our phylogenetic tree showed *G. thailandicum* clustered together with *G. casuarinicola*. Although *G. thailandicum* and *G. casuarinicola* form a distinctive laccate pileus surface, their macro- and micro-morphological characteristics are quite different. *Ganoderma thailandicum* can be easily distinguished from *G. casuarinicola*, by its deep magenta colour near the stipe, brownish-red colour at the centre of the pileus surface and vivid yellow colour at the actively-developed margin, while the fruiting bodies of *G. casuarinicola* are homogenously brownish-red to reddish-brown at maturity. *Ganoderma thailandicum* also has a smaller sized pileus (3–9 cm long, 3–6 cm width, 0.4–1.8 cm thick), while *G. casuarinicola* has a larger pileus (up to 10 cm long, 4–9 cm width, up to 2 cm thick). *Ganoderma thailandicum* has a smaller pore size (4–8 per mm) than *G. casuarinicola* (4–6 per mm) and *G. thailandicum* has narrower basidiospores (6.93 × 9.11 µm; including myxosporium) than *G. casuarinicola* (8.25 × 11.68 µm; including myxosporium). The basidiopore shapes of *G. thailandicum* are distinctive, with

ellipsoid to broadly ellipsoid or some globose, while basidiospores of *G. casuarinicola* are mostly ellipsoid to broadly ellipsoid at maturity. Both *G. thailandicum* and *G. casuarinicola* are quite similar by having angular to round pore shapes. The differences of *G. aridicola* and *G. enigmaticum* have been described in Xing et al. (2016). *Ganoderma mbrekobenum* can be differentiated from *G. casuarinicola* and *G. thailandicum* by its woody to corky texture when dried, with dimitic hyphal system, ovoid and bitunicate basidiospores (Crous et al. 2016).

Casuarina has been reported as a host genus for *G. casuarinicola* (Xing et al. 2018), which is found in coastal areas, while our *G. casuarinicola* collection was found on dead *Pinus kesiya* wood, thus this is the first *Pinus* host recorded for *G. casuarinicola*. Based on comprehensive morphological characteristics and molecular analyses, we report *G. casuarinicola* as a new record to Thailand, with *G. thailandicum* as a new species from Thailand.

Acknowledgements

We appreciate the kind support given by the Key Laboratory for Plant Diversity and Biogeography of East Asia, Kunming Institute of Botany, Chinese Academy of Sciences, Kunming 650201, Yunnan, China; Key Laboratory for Economic Plants and Biotechnology, Kunming Institute of Botany, Chinese Academy of Sciences, Kunming 650201, Yunnan, China and Centre for Mountain Futures (CMF), Kunming Institute of Botany, Kunming 650201, Yunnan, China. We thank the Germplasm Bank of Wild Species, Kunming Institute of Botany, Kunming 650201, Yunnan, China for enabling our molecular laboratory work. Kasiphat Limsakul and Wilawan Punyaboon are acknowledged for their invaluable assistance. Samantha C. Karunarathna thanks the CAS President's International Fellowship Initiative (PIFI) for funding his postdoctoral research (No. 2018PC0006) and the National Science Foundation of China (NSFC) for funding this work under the project code 31750110478. Peter E. Mortimer thanks the National Science Foundation of China (NSFC) project codes 41761144055 and 41771063 and the South East Asia Biodiversity Resources Institute, CAS, project code Y4ZK111B01. The authors also thank William A. Julian for his editing contributions.

References

Boddy L, Büntgen U, Egli S, Gange AC, Heegaard E, Kirk PM, Mohammad A, Kauserud H (2014) Climate variation effects on fungal fruiting. Fungal ecological 10: 20–33. https://doi.org/10.1016/j.funeco.2013.10.006

Cao Y, Wu SH, Dai YC (2012) Species clarification of the prize medicinal *Ganoderma* mushroom "Lingzhi". Fungal Diversity 56: 49–62. https://doi.org/10.1007/s13225-012-0178-5

Cao Y, Yuan HS (2013) *Ganoderma mutabile* sp. nov. from southwestern China based on morphological and molecular data. Mycological Progress 12: 121–126. https://doi.org/10.1007/s11557-012-0819-9

Coetzee MPA, Marincowitz S, Muthelo VG, Wingfield MJ (2015) *Ganoderma* species, including new taxa associated with root rot of the iconic *Jacaranda mimosifolia* in Pretoria, South Africa. IMA Fungus 6(1): 249–256. https://doi.org/10.5598/imafungus.2015.06.01.16

Crous PW, Wingfield MJ, Richardson DM, Le Roux JJ, Strasberg D, Edwards J, Roets F, Hubka V, Taylor PWJ, Heykoop M, Martín MP, Moreno G, Sutton DA, Wiederhold NP, Barnes CW, Carlavilla JR, Gené J, Giraldo A, Guarnaccia V, Guarro J, Hernández-Restrepo M, Kolařík M, Manjón JL, Pascoe IG, Popov ES, Sandoval-Denis M, Woudenberg JHC, Acharya K, Alexandrova AV, Alvarado P, Barbosa RN, Baseia IG, Blanchette RA, Boekhout T, Burgess TI, Cano-Lira JF, Čmoková A, Dimitrov RA, Dyakov MY, Dueñas M, Dutta AK, EsteveRaventós F, Fedosova AG, Fournier J, Gamboa P, Gouliamova DE, Grebenc T, Groenewald M, Hanse B, Hardy GEJ, Held BW, Jurjević Z, Kaewgrajang T, Latha KPD, Lombard L, Luangsa-ard JJ, Lysková P, Mallátová N, Manimohan P, Miller AN, Mirabolfathy M, Morozova OV, Obodai M, Oliveira NT, Ordóñez ME, Otto EC, Paloi S, Peterson SW, Phosri C, Roux J, Salazar WA, Sánchez A, Sarria GA, Shin HD, Silva BDB, Silva GA, Smith MT, Souza-Motta CM, Stchige AM, Stoilova-Disheva MM, Sulzbacher MA, Telleria MT, Toapanta C, Traba JM, Valenzuela-Lopez N, Watling R, Groenewald JZ (2016) Fungal planet description sheets: 400–468. Persoonia 36: 316–458. https://doi.org/10.3767/persoonia.2018.40.10

Cui BK, Li HJ, Ji X, Zhou JL, Song J, Si J, Yang ZL, Dai YC (2019) Species diversity, taxonomy and phylogeny of Polyporaceae (Basidiomycota) in China. Fungal Diversity 97: 137-392. https://doi.org/10.1007/s13225-019-00427-4

Dai YC, Yang ZL, Cui BK, Yu CJ, Zhou LW (2009) Species diversity and utilization of medicinal mushrooms and fungi in China. International Journal of Medicinal Mushrooms 11: 287–302. https://doi.org/10.1615/IntJMedMushr.v11.i3.80

De Silva DD, Rapior S, Fons F, Bahkali, AH, Hyde KD (2012a) Medicinal mushrooms in supportive cancer therapies: an approach to anti-cancer effects and putative mechanisms of action. Fungal Diversity 55: 1–35. https://doi.org/10.1007/s13225-012-0151-3

De Silva DD, Rapior S, Hyde KD, Bahkali AH (2012b) Medicinal mushrooms in prevention and control of diabetes mellitus. Fungal Diversity 56: 1–29. https://doi.org/10.1007/s13225-012-0187-4

De Silva DD, Rapior S, Sudarman E, Stadler M, Xu J, Alias SA, Hyde KD (2013) Bioactive metabolites from macrofungi: ethnopharmacology, biological activities and chemistry. Fungal Diversity 62: 1–40. https://doi.org/10.1007/s13225-013-0265-2

Douanla-Meli C, Langer E (2009) *Ganoderma carocalcareus* sp. nov., with crumbly-friable context parasite to saprobe on *Anthocleista nobilis* and its phylogenetic relationship in *G. resinaceum* group. Mycological Progress 8: 145–155. https://doi.org/10.1007/s11557-009-0586-4

Hall TA (1999) BioEdit: a user-friendly biological sequence alignment editor and analysis program for Windows 95/98/NT. Nucleic Acids Symposium Series 41: 95–98.

Hapuarachchi KK, Elkhateeb WA, Karunarathna SC, Phengsintham P, Cheng CR, Bandara AR, Kakumyan P, Hyde KD, Daba GM, Wen TC (2018a) Current status of global *Ganoderma* cultivation, products, industry and market. Mycosphere 9: 1025–1052. https://doi.org/10.5943/mycosphere/9/5/6

Hapuarachchi KK, Karunarathna SC, Phengsintham P, Kakumyan P, Hyde KD, Wen TC (2018b) *Amauroderma* (*Ganodermataceae*, Polyporales) – bioactive compounds, beneficial properties and two new records from Laos. Asian Journal of Mycology 1: 121–136. https://doi.org/10.5943/ajom/1/1/10

Hapuarachchi KK, Karunarathna SC, Raspé O, De Silva KHWL, Thawthong A, Wu XL, Kakumyan P, Hyde KD, Wen TC (2018c) High diversity of *Ganoderma* and *Amauroderma* (Ganodermataceae, Polyporales) in Hainan Island, China. Mycosphere 9: 931–982. https://doi.org/10.5943/mycosphere/9/5/1

Hapuarachchi KK, Karunarathna SC, McKenzie EHC, Wu XL, Kakumyan P, Hyde KD, Wen TC (2019a) High phenotypic plasticity of *Ganoderma sinense* (Ganodermataceae, Polyporales) in China. Asian Journal of Mycology 2: 1–47. https://doi.org/10.5943/ajom/2/1/1

Hapuarachchi KK, Karunarathna SC, Phengsintham P, Yang HD, Kakumyan P, Hyde KD, Wen TC (2019b) Ganodermataceae (Polyporales): diversity in Greater Mekong Subregion countries (China, Laos, Myanmar, Thailand and Vietnam). Mycosphere 10: 221–309. https://doi.org/10.5943/mycosphere/10/1/6

Huelsenbeck JP, Ronquist F (2001) MRBAYES: Bayesian inference of phylogenetic trees. Bioinformatics 17: 754–755. https://doi.org/10.1093/bioinformatics/17.8.754

Hyde KD, Norphanphoun C, Chen J, Dissanayake AJ, Doilom M, Hongsanan S, Jayawardena RS, Jeewon R, Perera RH, Thongbai B, Wanasinghe DN, Wisitrassameewong K, Tibpromma S, Stadler M. (2018) Thailand's amazing diversity – up to 96% of fungi in northern Thailand are novel. Fungal Diversity 93: 215–239. https://doi.org/10.1007/s13225-018-0415-7

Index Fungorum (2019) http://www.indexfungorum.org/names/names.asp [Accessed on: 2019-6-1]

Justo A, Miettinen O, Floudaas D, Ortiz-Santana, B, Sjökvist E, Lindner D, Nakasone K, Niemela D, Nakasone K, Niemelö T, Larsson KH, Ryvarden L, Hibbett DS (2017) A revised family-level classification of the Polyporales (Basidiomycota) 121: 798–894. https://doi.org/10.1016/j.funbio.2017.05.010

Karsten PA (1881) Enumeralio boletinearum et polyporearum fennicarum, systemate novo dispositarum. Revue de Mycologie 3: 16–19.

Katoh K, Standley DM (2013) MAFFT multiple sequence alignment software version 7: improvements in performance and usability. Molecular Biology and Evolution 30: 772–780. https://doi.org/10.1093/molbev/mst010

Kinge TR, Mih AM (2011) *Ganoderma ryvardense* sp. nov. associated with basal stem rot (BSR) disease of oil palm in Cameroon. Mycosphere 2: 179–188.

Kreisel H, Schauer F (1987) Methoden des mykologischen Laboratoriums. VEB Gustav Fischer Verlag, Jena, 181 pp.

Larget B, Simon DL (1999) Markov Chain Monte Carlo Algorithms for the Bayesian analysis of phylogenetic trees. Molecular Biology and Evolution 16: 750–759. https://doi.org/10.1093/oxfordjournals.molbev.a026160

Li TH, Hu HP, Deng WQ, Wu SH, Wang DM, Tsering T (2015) *Ganoderma leucocontextum*, a new member of the *G. lucidum* complex from southwestern China. Mycoscience 56: 81–85. https://doi.org/10.1016/j.myc.2014.03.005

Li LF, Liu HB, Zhang QW, Li ZP, Wong TL, Fung HY, Zhang JX, Bai SP, Lu AP, Han QB (2018) Comprehensive comparison of polysaccharides from *Ganoderma lucidum* and *G. sinense*: chemical, antitumor, immunomodulating and gut-microbiota modulatory properties. Scientific Reports 8: 1–12. https://doi.org/10.1038/s41598-018-22885-7

Li MJ, Yuan HS (2015) Type studies on *Amauroderma* species described by J.D. Zhao et al. and the phylogeny of species in China. Mycotaxon 130: 79–89. https://doi.org/10.5248/130.79

Liu YJ, Whelen S, Hall BD (1999) Phylogenetic relationships among ascomycetes: evidence from an RNA polymerase II subunit. Molecular Biology and Evolution 16: 1799–1808. https://doi.org/10.1093/oxfordjournals.molbev.a026092

Lodge DJ, Ammirati FJ, O'Dell TE, Mueller GM (2004) Collecting and describing macrofungi. In: Mueller GM, Bills GF, Foster MS (Eds) Biodiversity of Fungi Inventory and Monitoring Methods. Elsevier Academic Press, London, 128–154 pp.

Luangharn T, Karunarathna SC, Khan S, Xu JC, Mortimer PE, Hyde KD (2017) Antibacterial activity, optimal culture conditions and cultivation of the medicinal *Ganoderma australe*, new to Thailand. Mycosphere 8: 1108–1123. https://doi.org/10.5943/mycosphere/8/8/11

Luangharn T, Karunarathna SC, Mortimer PE, Hyde KD, Thongklang N, Xu JC (2019) A new record of *Ganoderma tropicum* (Basidiomycota, Polyporales) for Thailand and first assessment of optimum conditions for mycelia production. MycoKeys 51: 65–83. https://doi.org/10.3897/mycokeys.51.33513

Miettinen O, Larsson KH (2006) *Trechispora elongata* species nova from North Europe. Mycotaxon 96: 193–198. http://hdl.handle.net/10138/42882

Moncalvo JM, Ryvarden L (1997) A nomenclatural study of the Ganodermataceae Donk. Synopsis Fungorum 11: 1–114.

MycoBank (2019) http://www.mycobank.org [Accessed on: 2019-6-1]

Núñez M, Ryvarden L (2000) East Asian Polypores: *Ganoderma taceae* and Hymenochaetaceae. Fungiflora, Oslo, Norway, 6–50.

Nylander JAA (2004) MrModeltest v.2 program distributed by the author. Evolutionary Biology Centre, Uppsala University.

Papp V, Dima B, Wasser SP (2017) What is *Ganoderma lucidum* in the molecular era? International journal of medicinal mushrooms abbreviation 19(7): 579–593. https://doi.org/10.1615/IntJMedMushrooms.2017021195

Park YJ, Kwon OC, Son ES, Yoon DE, Han W, Nam JY, Yoo YB, Lee CS (2012) Genetic diversity analysis of *Ganoderma* species and development of a specific marker for identification of medicinal mushroom *Ganoderma lucidum*. African Journal of Microbiology Research 6 (25): 5417–5425. https://doi.org/10.5897/AJMR12.846

Pilotti CA (2005) Stem rots of oil palm caused by *Ganoderma boninense*: pathogen biology and epidemiology. Mycopathologia 159(1): 129–137. https://doi.org/10.1038/s41598-018-22885-7

Pilotti CA, Sanderson FR, Aitken AB, Armstrong W (2004) Morphological variation and host range of two *Ganoderma* species from Papua New Guinea. Mycopathologia 158: 251–265. https://doi.org/10.1023/B:MYCO.0000041833.41085.6f

Qiao Y, Yang Y, Dong X, Qiu M (2005) 13C NMR in the application of new *Ganoderma* triterpenoids. Journal of Spectroscopy 22(4): 437–456.

Rambaut A (2012) FigTree version 1.4.0. http://tree.bio.ed.ac.uk/software/soft-ware/figtree/

Rambaut A, Suchard MA, Xie D, Drummond AJ (2014) Tracer v16. http://beast.bio.ed.ac.uk/Tracer

Rannala B, Yang Z (1996) Probability distribution of molecular evolutionary trees: a new method of phylogenetic inference. Journal of Molecular Evolution 43(3): 304–311. https://doi.org/10.1007/BF02338839

Richter C, Wittstein K, Kirk PM, Stadler M (2015) An assessment of the taxonomy and chemotaxonomy of *Ganoderma*. Fungal Divers 71: 1–15. https://doi.org/10.1007/s13225-014-0313-6

Ridgeway R (1912) Color Standards and Color Nomenclature. Ridgeway, Washington DC, 12–225. https://doi.org/10.5962/bhl.title.144788

Ryvarden L (2000) Studies in neotropical polypores 2: a preliminary key to neotropical species of *Ganoderma* with a laccate pileus. Mycologia 92: 180–191. https://doi.org/10.2307/3761462

Ryvarden L (2004) Neotropical polypores Part 1. Synopsis Fungorum. Fungiflora, Oslo, 1–227.

Sanodiya BS, Thakur GS, Baghel RK, Prasad GB, Bisen PS (2009) *Ganoderma lucidum*: a potent pharmacological macrofungus. Current Pharmaceutical Biotechnology 10: 717–742. https://doi.org/10.2174/138920109789978757

Shim SH, Ryu J, Kim JS, Kang SS, Xu Y, Jung SH, Lee YS, Lee S, Shin KH (2004) New lanostane-type triterpenoids from *Ganoderma applanatum*. Journal of Natural Products 67: 1110–1113. https://doi.org/10.1021/np030383p

Silvestro D, Michalak I (2011) raxmlGUI: a graphical front-end for RAxML. Organisms Diversity and Evolution 12 (4): 335–337. https://doi.org/10.1007/s13127-011-0056-0

Song J, Xing JH, Decock C, He XL, Cui BK (2016) Molecular phylogeny and morphology reveal a new species of *Amauroderma* (Basidiomycota) from China. Phytotaxa 260: 47–56. https://doi.org/10.11646/phytotaxa.260.1.5

Stamatakis A (2014) RAxML v. 8: A tool for phylogenetic analysis and post-analysis of large phylogenies. Bioinformatics 30: 1312–1313. https://doi.org/10.1093/bioinformatics/btu033

Sung GH, Sung JM, Hywel-Jones NL, Spatafora JW (2007) A multi-gene phylogeny of Clavicipitaceae (Ascomycota, Fungi): identification of localized incongruence using a combinational bootstrap approach. Molecular Phylogenetics and Evolution 44(3): 1204–1223. https://doi.org/10.1016/j.ympev.2007.03.011

Swofford DL (2002) PAUP*. Phylogenetic analysis using parsimony (*and Other Methods), Version 4.0 beta version. Sinauer Associates, Sunderland, Massachusetts.

Tchoumi JMT, Coetzee MPA, Rajchenberg M, Wingfield MJ, Roux J (2018) Three *Ganoderma* species, including *Ganoderma dunense* sp. nov., associated with dying *Acacia cyclops* trees in South Africa. Australasian Plant Pathology 47: 431–447. https://doi.org/10.1007/s13313-018-0575-7

Teng BS, Wang CD, Yang HJ, Wu JS, Zhang D, Zheng M, Fan ZH, Pan D, Zhou P (2011) A protein tyrosine phosphatase 1B activity inhibitor from the fruiting bodies of *Ganoderma lucidum* (Fr.) Karst and its hypoglycemic potency on streptozotocin-induced type 2 diabetic mice. Journal of Agricultural and Food Chemistry 59: 6492–6500. https://doi.org/10.1021/jf200527y

Thawthong A, Hapuarachchi KK, Wen TC, Raspé O, Thongklang N, Kang JC, Hyde KD (2017) *Ganoderma sichuanense* (Ganodermataceae, Polyporales) new to Thailand. MycoKeys 22: 27–43. https://doi.org/10.3897/mycokeys.22.13083

Tulloss RE (2005) Amaniteae: Amanita, Limacella, & Torrendia. by Pierre Neville & Serge Poumarat, etc. (Book Review). Mycotaxon 92: 474–484.

Vilgalys R, Hester M (1990) Rapid genetic identification and mapping of enzymatically amplified ribosomal DNA from several *Cryptococcus* species. Journal of Bacteriology 172(8): 4238–4246. https://doi.org/10.1128/jb.172.8.4238-4246.1990

Wang F, Liu JK (2008) Highly oxygenated lanostane triterpenoids from the fungus *Ganoderma applanatum*. Chemical and Pharmaceutical Bulletin 56: 1035–1037. https://doi.org/10.1248/cpb.56.1035

Welti S, Courtecuisse R (2010) The *Ganoderma taceae*, in the French West Indies (Guadeloupe and Martinique). Fungal Diversity 43: 103–126. https://doi.org/10.1007/s13225-010-0036-2

White TJ, Bruns T, Lee S, Taylor JW (1990) Amplification and direct sequencing of fungal ribosomal RNA genes for phylogenetics. In: Innis MA, Gelfand DH, Sninsky JJ, White TJ (Eds) PCR Protocols: a Guide to Methods and Applications. Academic Press, New York, 315–322. https://doi.org/10.1016/B978-0-12-372180-8.50042-1

Xing JH, Song J, Decock C, Cui BK (2016) Morphological characters and phylogenetic analysis reveal a new species within the *Ganoderma lucidum* complex from South Africa. Phytotaxa 266: 115–124. https://doi.org/10.11646/phytotaxa.266.2.5

Xing JH, Sun YF, Han YL, Cui BK, Dai YC (2018) Morphological and molecular identification of two new *Ganoderma* species on *Casuarina equisetifolia* from China. MycoKeys 34: 93–108. https://doi.org/10.3897/mycokeys.34.22593

Yao YJ, Wang XC, Wang B (2013) Epitypification of *Ganoderma sichuanense* J.D. Zhao and X.Q. Zhang (Ganodermataceae). Taxon 62(5): 1025–1031. https://doi.org/10.12705/625.10

Zakaria L, Ali NS, Salleh B (2009) Molecular analysis of *Ganoderma* species from different hosts in Peninsular Malaysia. Journal of Biological Sciences 9: 12–20. https://doi.org/10.3923/jbs.2009.12.20

Zhao JD (1989) The Ganodermataceae in China. Bibliotheca Mycologica 132: 1–176.

Zhaxybayeva O, Gogarten JP (2002) Bootstrap, Bayesian probability and maximum likelihood mapping: exploring new tools for comparative genome analyses. BMC Genomics 3(1): 4. https://doi.org/10.1186/1471-2164-3-4

Zhou LW, Cao Y, Wu SH, Vlasák J, Li DW, Li MJ, Dai YC (2015) Global diversity of the *Ganoderma lucidum* complex (*Ganoderma taceae*, Polyporales) inferred from morphology and multilocus phylogeny. Phytochemistry 114: 7–15. https://doi.org/10.1016/j.phytochem.2014.09.023

MycoKeys 59: 67–94 (2019)
doi: 10.3897/mycokeys.59.38055
http://mycokeys.pensoft.net

RESEARCH ARTICLE

A peer-reviewed open-access journal
MycoKeys
Launched to accelerate biodiversity research

Diaporthalean fungi associated with canker and dieback of trees from Mount Dongling in Beijing, China

Haiyan Zhu[1], Meng Pan[1], Guido Bonthond[2], Chengming Tian[1], Xinlei Fan[1]

1 *The Key Laboratory for Silviculture and Conservation of Ministry of Education, Beijing Forestry University, Beijing 100083, China* **2** *GEOMAR Helmholtz Centre for Ocean Research Kiel, Düsternbrooker Weg 20, 24105, Kiel, Germany*

Corresponding author: *Xinlei Fan* (xinleifan@bjfu.edu.cn)

Academic editor: *Kevin Hyde* | Received 8 July 2019 | Accepted 23 September 2019 | Published 16 October 2019

Citation: Zhu H, Pan M, Bonthond G, Tian C, Fan X (2019) Diaporthalean fungi associated with canker and dieback of trees from Mount Dongling in Beijing, China. MycoKeys 59: 67–94. https://doi.org/10.3897/mycokeys.59.38055

Abstract

Diaporthales is a fungal order comprising important plant pathogens, saprobes and endophytes on a wide range of woody hosts. It is often difficult to differentiate the pathogens in this order, since both the morphology and disease symptoms are similar among the various species. In the current study, we obtained 15 representative diaporthalean isolates from six tree hosts belonging to plant families Betulaceae, Fagaceae, Juglandaceae, Rosaceae, and Ulmaceae from Mount Dongling in China. Six species were identified residing in four families of Diaporthales (Diaporthaceae, Erythrogloeaceae, Juglanconidaceae and Melanconidaceae). Based on morphological comparison and the phylogenetic analyses of partial ITS, LSU, *cal*, *his3*, *rpb2*, *tef1-a* and *tub2* gene sequences, we identified five known species (*Diaporthe betulina*, *D. eres*, *D. rostrata*, *Juglamconis oblonga* and *Melanconis stilbostoma*) and one novel species (*Dendrostoma donglinensis*). These results represent the first study of diaporthalean fungi associated with canker and dieback symptoms from Mount Dongling in Beijing, China.

Keywords

Ascomycota, Diaporthales, new species, phylogeny, taxonomy

Introduction

Diaporthales is an important order in class Sordariomycetes containing taxa that have broad host ranges and widely distributed as plant pathogens, endophytes or saprobes (Fan et al. 2018a, Crous et al. 2019). Most families of the Diaporthales are responsible for diseases on a wide range of host plants, some of which are economically important worldwide, causing anthracnose, blights, cankers, dieback, leaf spots and rots of root and

fruit (Alvarez et al. 2016, Guarnaccia and Crous 2017, Voglmayr et al. 2017, Jiang et al. 2019a, Xavier et al. 2019, Fan et al. 2020). The order is characterized by perithecia often with elongate beaks, immersed in stromatic tissues, producing deliquescent paraphyses and unitunicate asci that generally deliquesce, become detached from the perithecial wall when mature, and have a characteristic refractive apical annulus in sexual morph; and acervuli, pycnidia or rarely synnemata, producing phialidic or annellidic conidiogenous cells with 0–1-septate conidia in asexual morph (Barr 1978, Rossman et al. 2007, Fan et al. 2020). The classification of Diaporthales has been confused over the past decades because of the wide variation in morphological characters. Several recent studies have helped to resolve taxonomic problems of Diaporthales by multigene phylogenetic analyses and accepted 30 families in the order (Senanayake et al. 2017, 2018, Braun et al. 2018, Fan et al. 2018a, Crous et al. 2019, Guterres et al. 2019, Xavier et al. 2019).

Mount Dongling has a high diversity of plant species in western Beijing, which is considered as a biodiversity hotspot with more than 1000 plant species (Ma et al. 1995). As more plant species were recorded in this region, the exploration of fungal diversity gradually increased as most fungi are often linked to particular host plants as parasites or endophytes. *Alternaria*, *Diaporthe*, *Leptostroma*, *Pestalotiopsis* and *Phoma* were the most commonly isolated endophytic fungi from *Pinus tabuliformis*, and later additional 38 endophytic taxa were identified from *Acer truncatum* from the Mount Dongling (Guo et al. 2008, Sun et al. 2011). Further, pathogens of Botryosphaeriales have been identified from Mount Dongling, including species from the genera *Aplosporella*, *Botryosphaeria* and *Phaeobotryon* (Zhu et al. 2018).

During the trips to collect forest pathogens causing canker or dieback symptoms in Mount Dongling in Beijing, several specimens associated with typical diaporthalean symptoms were collected from various tree hosts, i.e. *Betula dahurica* (Betulaceae), *Juglans regia*, *J. mandshurica* (Juglandaceae), *Prunus davidiana* (Rosaceae) and *Quercus mongolica* (Fagaceae). As the higher-level phylogeny of many genera within the diaporthalean taxa remains largely unresolved in this region, the current study aims to clarify the systematics and taxonomy of these diaporthalean fungi with detailed descriptions.

Materials and methods

Sampling and isolation

Fresh specimens of diaporthalean fungi were collected from infected branches of six hosts from Mount Dongling in Beijing, China (Table 1), during the course of cognitive practice at the Beijing Forestry University (**BJFU**). Diaporthalean canker symptoms include elongated, slightly sunken and discolored areas in the bark, which often splits along the canker margin, forming several prominent dark sporocarps immersed and erumpent through the surface of the bark (Fig. 1). A total of 15 isolates were obtained by removing the mucoid spore mass from conidiomata or ascomata of fresh material, which was cut horizontally with a sterile blade and mixed in a drop of sterile water on a

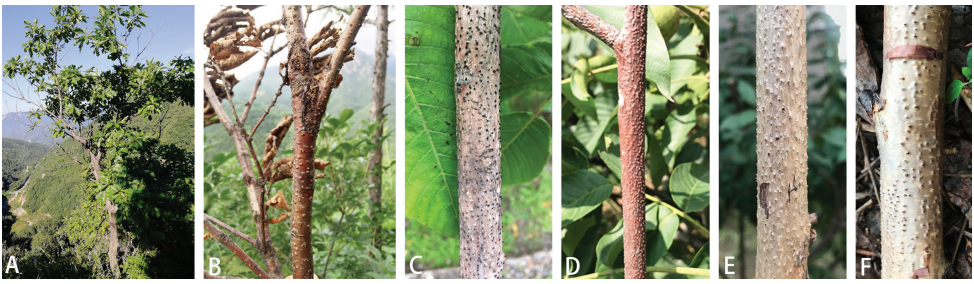

Figure 1. Disease symptoms associated with diaporthalean species. **A, B** *Quercus mongolica* **C** *Juglans regia* **D, E** *Juglans mandshurica* **F** *Betula dahurica*.

glass slide. The contents were broken up further with the blade until a spore suspension was obtained. The suspension was spread over the surface of 1.8 % potato dextrose agar (PDA). Single germinating spores were transferred on to fresh PDA plates. Specimens and isolates were deposited in the Key Laboratory for Silviculture and Conservation of the Ministry of Education in BJFU, and the working Collection of X.L. Fan (**CF**) housed at the BJFU. Axenic cultures are maintained in the China Forestry Culture Collection Centre (**CFCC**).

Morphology

Descriptions were performed based on morphological features of the ascomata or conidiomata from infected host materials. The macro-morphological photographs were captured using a Leica stereomicroscope (M205 FA) (structure and size of stromata, structure and size of ectostromatic disc and ostioles). Micro-morphological observations (shape and size of conidiophores, asci and conidia/ascospores) were determined under a Nikon Eclipse 80i microscope equipped with a Nikon digital sight DS-Ri2 high definition colour camera, using differential interference contrast (DIC) illumination and the Nikon software NIS-Elements D Package v. 3.00. Adobe Bridge CS v. 6 and Adobe Photoshop CS v. 5 were used for the manual editing. Over 10 conidiomata/ascomata, 10 asci and 30 conidia/ascospores were measured to calculate the mean size/length and respective standard deviations (SD). Colony diameters were measured and the colony features were described using the color charts of Rayner (1970). Nomenclatural novelties and descriptions were deposited in MycoBank (Crous et al. 2004).

DNA isolation, amplification and sequencing

Genomic DNA was extracted from colonies grown on cellophane-covered PDA using a modified CTAB method (Doyle and Doyle 1990). The primers and PCR conditions are listed in Table 2. DNA sequencing was performed using an ABI PRISM 3730XL

Table 1. Isolates and GenBank accession numbers obtained from Mount Dongling in the current study. (NA – not applicable).

Species	Strain	Host	GenBank accession numbers						
			ITS	LSU	*Cal*	*his3*	*rpb2*	*tef1-α*	*tub2*
Dendrostoma donglinensis	CFCC 53148	*Quercus mongolica*	MN266206	MN265880	NA	NA	MN315491	MN315480	NA
	CFCC 53149	*Quercus mongolica*	MN266207	MN265881	NA	NA	MN315492	MN315481	NA
	CFCC 53150	*Quercus mongolica*	MN266208	MN265882	NA	NA	MN315493	MN315482	NA
Diaporthe betulina	CFCC 53144	*Betula dahurica*	MN266200	MN265874	MN315462	MN315465	MN315498	MN315474	MN315470
Diaporthe eres	CFCC 53145	*Prunus davidiana*	MN266202	MN265876	NA	NA	MN315500	MN315476	MN315472
	CFCC 53146	*Prunus davidiana*	MN266201	MN265875	NA	MN315466	MN315499	MN315475	MN315471
	CFCC 53147	*Juglans regia*	MN266203	MN265877	NA	MN315467	MN315501	MN315477	MN315473
Diaporthe rostrata	CFCC 53142	*Juglans mandshurica*	MN266204	MN265878	MN315463	NA	MN315489	MN315478	MN315468
	CFCC 53143	*Juglans mandshurica*	MN266205	MN265879	MN315464	NA	MN315490	MN315479	MN315469
Juglanconis oblonga	CFCC 53151	*Juglans mandshurica*	MN266209	MN265883	NA	NA	MN315502	MN315483	NA
	CFCC 53152	*Juglans mandshurica*	MN266210	MN265884	NA	NA	MN315503	MN315484	NA
Melanconis stilbostoma	CFCC 53128	*Betula dahurica*	MN266211	MN265885	NA	NA	MN315494	MN315485	NA
	CFCC 53129	*Betula dahurica*	MN266212	MN265886	NA	NA	MN315495	MN315486	NA
	CFCC 53130	*Betula* sp.	MN266213	MN265887	NA	NA	MN315496	MN315487	NA
	CFCC 53131	*Betula* sp.	MN266214	MN265888	NA	NA	MN315497	MN315488	NA

Table 2. Genes used in this study with PCR primers, primer DNA sequence, optimal annealing temperature and corresponding references.

Locus	Definition	Primers	Primer DNA sequence (5'–3')	Optimal annealing temp (°C)	References of primers used
ITS	internal transcribed spacer of ribosomal RNA	ITS1	TCCGTAGGTGAACCTGCGG	51	White et al. 1990
		ITS4	TCCTCCGCTTTTGATATGC		
LSU	large subunit of ribosomal RNA	LR0R	ACCCGCTGAACTTAAGC	55	Vilgalys and Hester 1990
		LR7	TACTACCACCAAGATCT		
cal	Calmodulin	CAL-228F	GAGTTCAAGGAGGCCTTCTCCC	55	Carbone and Kohn 1999
		CAL-737R	CATCTTTCTGGCCATCATGG		
rpb2	RNA polymerase II second largest subunit	RPB2-5F	GA(T/C)GA(T/C)(A/C)G(A/T)GATCA(T/C)TT(T/C)GG	52	Liu et al. 1999
		RPB2-7cR	CCCAT(A/G)GCTTG(T/C)TT(A/G)CCCAT		
his3	histone H3	CYLH4F	AGGTCCACTGGGTGGCAAG	58	Crous et al. 2004
		H3-1b	GCGGGCGAGCTGGATGTCCTT		Glass and Donaldson 1995
tef-1a	translation elongation factor 1-alpha	EF1-668F	CGGTCACTTGATCTACAAGTGC	55	Alves et al. 2008
		EF1-1251R	CCTCGAACTCACCAGTACCG		
tub2	beta-tubulin	Bt2a	GGTAACCAAATCGGTGCTGCTTTG	55	Glass and Donaldson 1995
		Bt2b	ACCCTCAGTGTAGTGACCCTTGGC		

DNA Analyser with a BigDye Terminator Kit v.3.1 (Invitrogen, USA) at the Shanghai Invitrogen Biological Technology Company Limited (Beijing, China). The DNA sequences obtained from forward and reverse primers were combined using SeqMan v. 7.1.0 in the DNASTAR Lasergene Core Suite software (DNASTAR Inc., Madison, WI, USA). Reference sequences were selected based on ex-type or ex-epitype sequences available from relevant recently published literature (Rossman et al. 2007, Suetrong et al. 2015, Norphanphoun et al. 2016, Hongsanan et al. 2017, Senanayake et al. 2017, Voglmayr et al. 2017, Yang et al. 2018, Fan et al. 2018a, b, 2020) (Table 1). Subsequent alignments for each gene were generated using MAFFT v.7 (Katoh and Standley 2013) and manually improved where necessary using MEGA v. 6 (Tamura et al. 2013). Novel sequences generated in the current study were deposited in GenBank (Table 1, Suppl. materials 1–3: Tables S1–S3) and the aligned matrices used for phylogenetic analyses were submitted to TreeBASE (www.treebase.org; accession number: S24893).

Phylogenetic analyses

To infer the first phylogenetic relationships at the family level, an initial alignment combining the here generated and available ITS, LSU, *rpb2* and *tef1-a* sequences was compiled following Fan et al. (2018a). This alignment was analyzed based on Maximum Parsimony (MP), Maximum Likelihood (ML), and Bayesian Inference (BI) methods.

The MP analysis was conducted using a heuristic search (1,000 bootstrap) by PAUP v. 4.0b10 (Swofford 2003). The MP analysis was conducted with random sequence additions as option to stepwise-addition (1,000 bootstrap replicates and one tree held at each addition step), and maxtrees limited to 100 by replicate. The tree bisection and reconnection (TBR) was selected as option to the branch swapping algorithm (Swofford 2003). The branches of zero length were collapsed and all equally most parsimonious trees were saved. Other calculated parsimony scores were tree length (TL), consistency index (CI), retention index (RI) and rescaled consistency (RC). The ML analysis was performed using a GTR site substitution model, including a gamma-distributed rate heterogeneity and a proportion of invariant sites in PhyML v. 3.0 (Guindon et al. 2010). The BI analysis was conducted using the best-fit evolutionary models for each partitioned locus estimated in MrModeltest v. 2.3 (Posada and Crandall 1998) following the Akaike Information Criterion (AIC), with a Markov Chain Monte Carlo (MCMC) algorithm in MrBayes v. 3.1.2 (Ronquist and Huelsenbeck 2003). Two MCMC chains were run from random trees for 10 million generations and terminated when the average standard deviation of split frequencies dropped below 0.01. Trees were saved in each 1,000 generations. The first 25 % of trees were discarded at the burn-in phase of each analysis, and the Bayesian posterior probabilities (BPP) were calculated to assess the remaining trees (Rannala and Yang 1996). The MP bootstrap support (BS) equal to or above 50 were shown at the first and second position in branches. The branches with significant BPP equal to or above 0.95 were thickened in the phylogram.

In addition to the above analyses, we provided separate phylogenetic trees for two additional genera (*Dendrostoma* and *Diaporthe*) in Diaporthales, based on various gene regions (see below) including the same parameters as in the analyses described above. The branch support from MP and ML analyses was evaluated with a bootstrap support (BS) method of 1,000 replicates (Hillis and Bull 1993). Phylograms were plotted in Figtree v. 1.4.4 (http://tree.bio.ed.ac.uk/software/figtree) and edited in Adobe Illustrator CS6 v.16.0.0 (https://www.adobe.com/cn/products/illustrator.html).

Results

Phylogenetic analysis

The combined matrix (ITS, LSU, *rpb2* and *tef1-a*) of Diaporthales included 198 ingroup accessions (15 from the current study and 183 retrieved from GenBank) and two outgroup taxa. The aligned matrix comprised 4,047 characters including gaps (773 characters for ITS, 1,190 for LSU, 1,114 for *rpb2* and 970 for *tef1-a*), of which 2,002 characters were constant, 158 variable characters were parsimony-uninformative and 1,887 characters were variable and parsimony-informative. MP analyses generated 100 parsimonious trees of which the first tree is presented in Fig. 2 (TL = 12,631, CI = 0.313, RI = 0.792, RC = 0.248). The tree topologies of ML and BI analyses were mostly similar to the generated MP tree. The 15 isolates obtained in this study were clustered within the families Diaporthaceae, Erythrogloeaceae, Juglanconidaceae and Melanconidaceae in Diaporthales (Fig. 2). To delimitate to the species level, phylogenetic trees for *Dendrostoma* and *Diaporthe* were constructed separately based on different DNA datasets.

For the genus *Diaporthe* (Diaporthaceae), a concatenated ITS, *cal*, *his3*, *tef1-a* and *tub2* matrix was produced with 201 ingroup accessions (6 from this study and 195 retrieved from GenBank). The combined matrix comprised 3,237 characters including gaps (544 characters for ITS, 593 for *cal*, 587 for *his3*, 645 for *tef1-a* and 868 for *tub2*) of which 1,330 characters were constant, 442 variable characters parsimony-uninformative and 1,465 characters variable and parsimony-informative. The MP analysis generated 100 parsimonious trees and the first tree is presented in Fig. 3 (TL = 12,978, CI = 0.280, RI = 0.712, RC = 0.199). The isolates of *Diaporthe* clustered in three different clades, corresponding to the three known species in this genus. The second combined matrix (*cal*, *tef1-a* and *tub2*) focusing on the *Diaporthe eres* complex included 56 ingroup accessions (4 from this study and 52 retrieved from GenBank). The concatenated matrix comprised 1,198 characters including gaps (405 for *cal*, 363 for *tef1-a* and 430 for *tub2*) of which 933 characters were constant, 112 variable characters parsimony-uninformative and 153 characters variable and parsimony-informative. The MP analysis generated 100 parsimonious trees of which the first is presented in Fig. 4 (TL = 415, CI = 0.701, RI = 0.882, RC = 0.618). The tree topologies of the ML and BI analyses were almost similar to the MP tree.

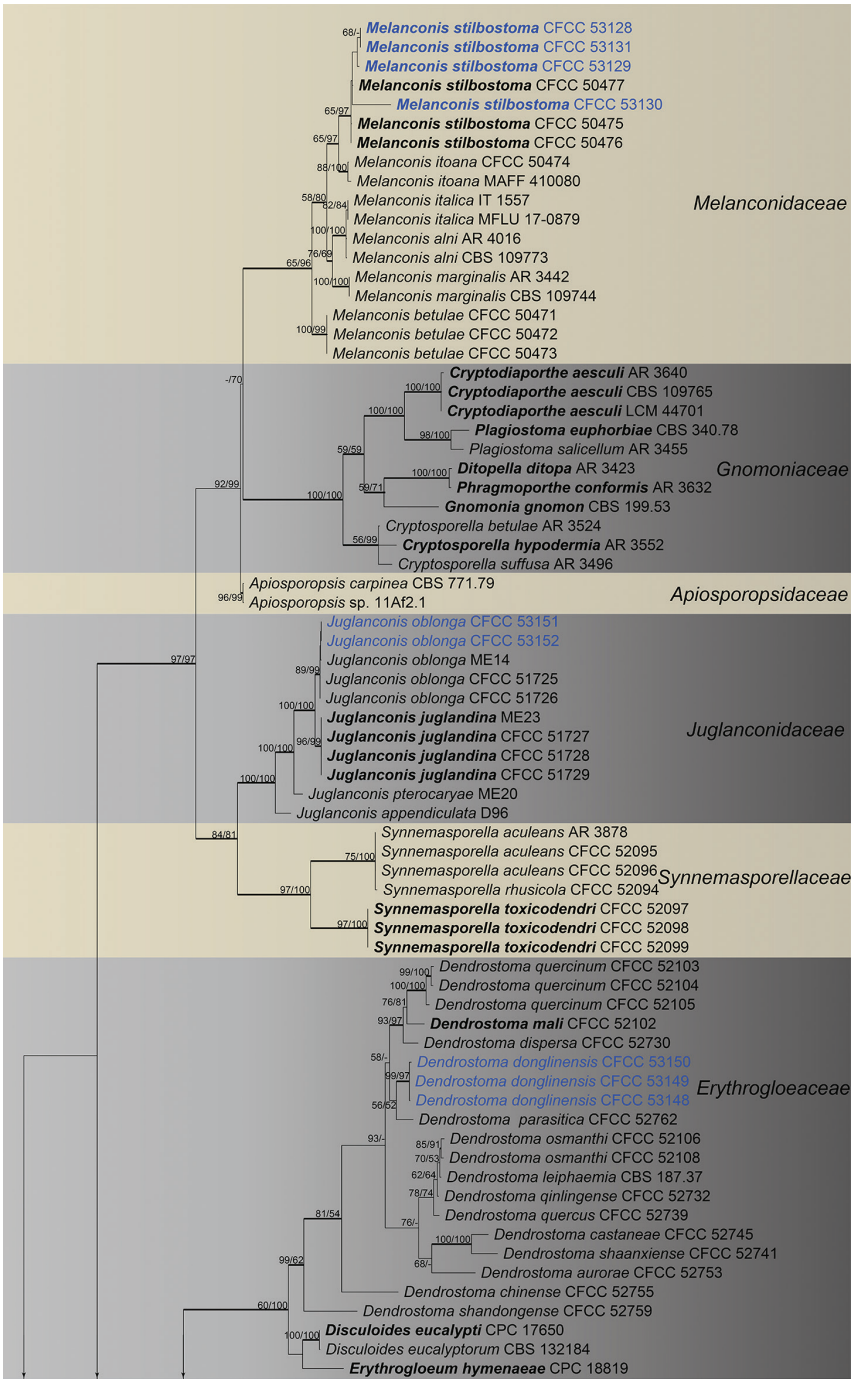

Figure 2. Phylogram of Diaporthales based on combined ITS, LSU, *rpb2* and *tef1-a* genes. The MP and ML bootstrap support values above 50 % are shown at the first and second position, respectively. Thickened branches represent posterior probabilities above 0.95 from the BI. Ex-type strains are in bold. Strains from the current study are in blue.

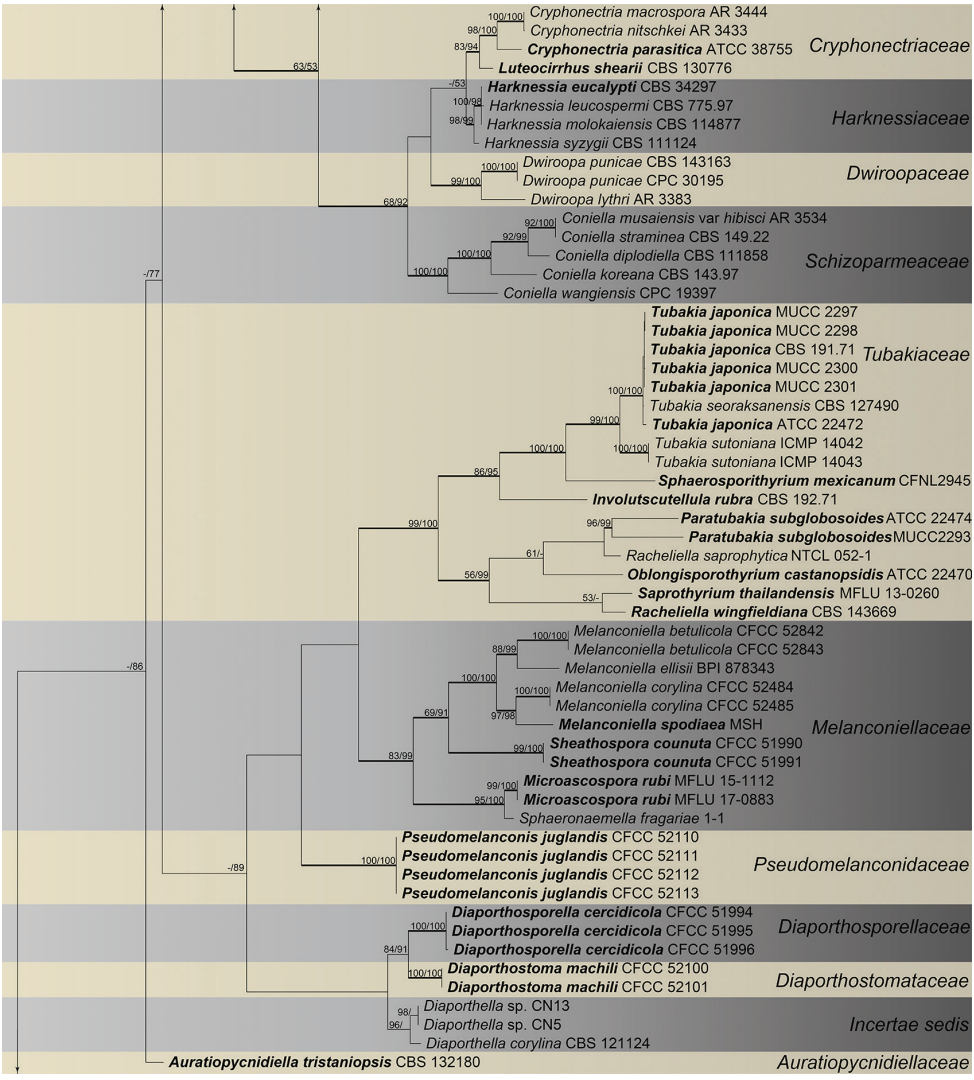

Figure 2. Continued.

For the genus *Dendrostoma* (Erythrogloeaceae), ITS, *rpb2* and *tef1-a* alignments were concatenated, including 42 ingroup accessions (three from this study and 39 retrieved from GenBank) was produced. The full matrix comprised 2,400 characters including gaps (561 characters for ITS, 1,078 for *rpb2* and 761 for *tef1-a*), of which 1,486 characters are constant, 231 variable characters are parsimony-uninformative and 683 characters are variable and parsimony-informative. The only parsimonious tree generated in MP analyses is presented in Fig. 5 (TL = 1,691, CI = 0.707, RI = 0.835, RC = 0.591). Tree topologies of ML and BI analyses were mostly similar to the MP tree. Three isolates of *Dendrostoma* represented a monophyletic clade with high support value (MP/Ml/BI = 99/99/1) (marked in blue in Fig. 5).

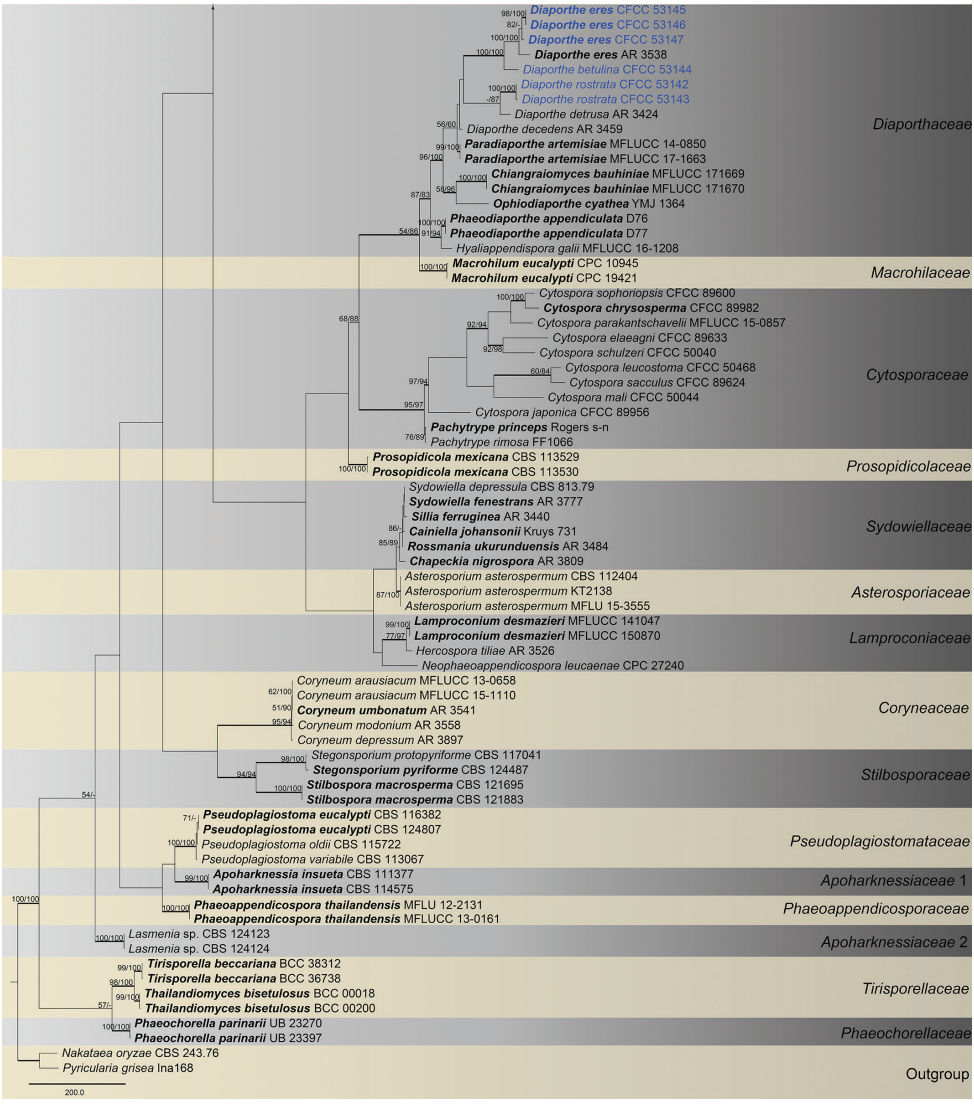

Figure 2. Continued.

Taxonomy

Diaporthaceae Höhn. ex Wehm., Am. J. Bot. 13: 638 (1926)

Type genus. *Diaporthe* Nitschke, Pyrenomyc. Germ. 2: 240 (1870).

Notes. Diaporthaceae was introduced by von Höhnel (1917) and subsequently involved in confusing the taxonomy due to many genera with wide variation of morphological characters and the majority without culture or DNA phylogeny. Senanayake et al. (2017, 2018) accepted 14 genera in Diaporthaceae, including *Allantoporthe*,

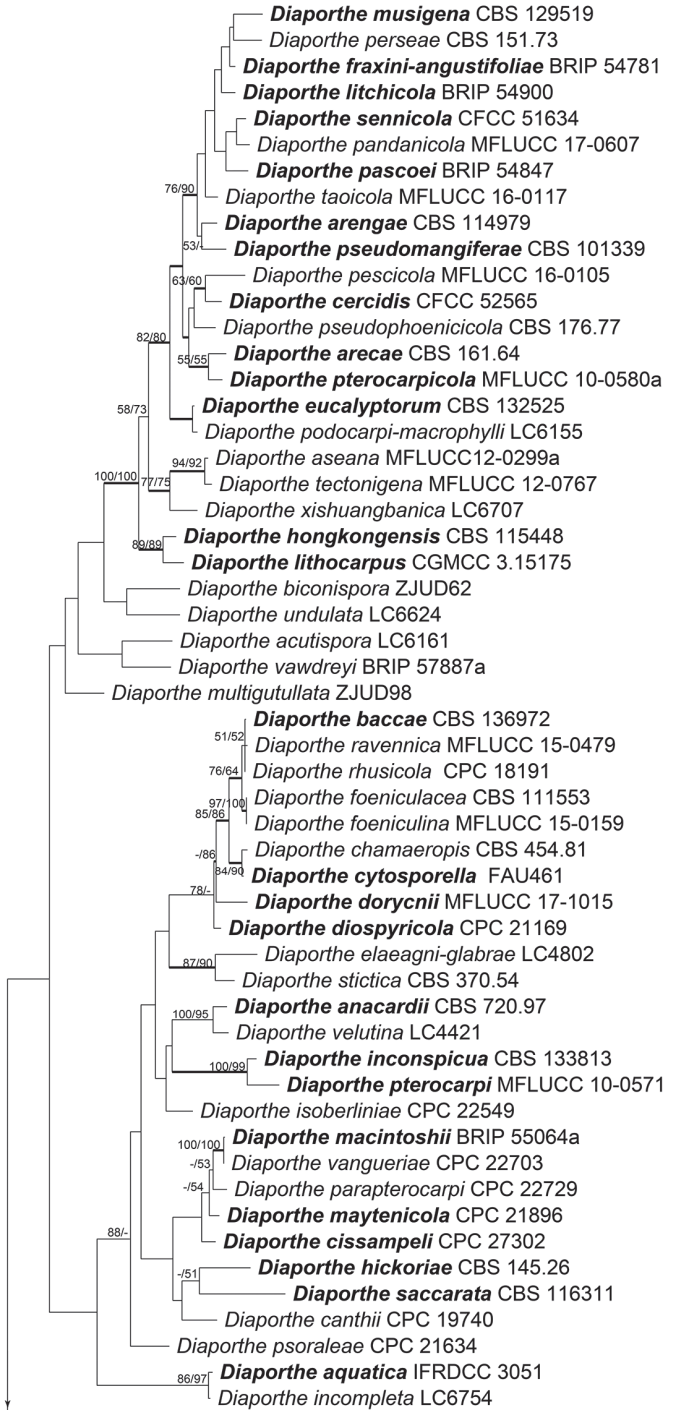

Figure 3. Phylogram of *Diaporthe* based on combined ITS, *tef1-a*, *tub2*, *cal* and *his3* genes. The MP and ML bootstrap support values above 50 % are shown at the first and second positions, respectively. Thickened branches represent posterior probabilities above 0.95 from the BI. Ex-type strains are in bold. Strains from the current study are in blue.

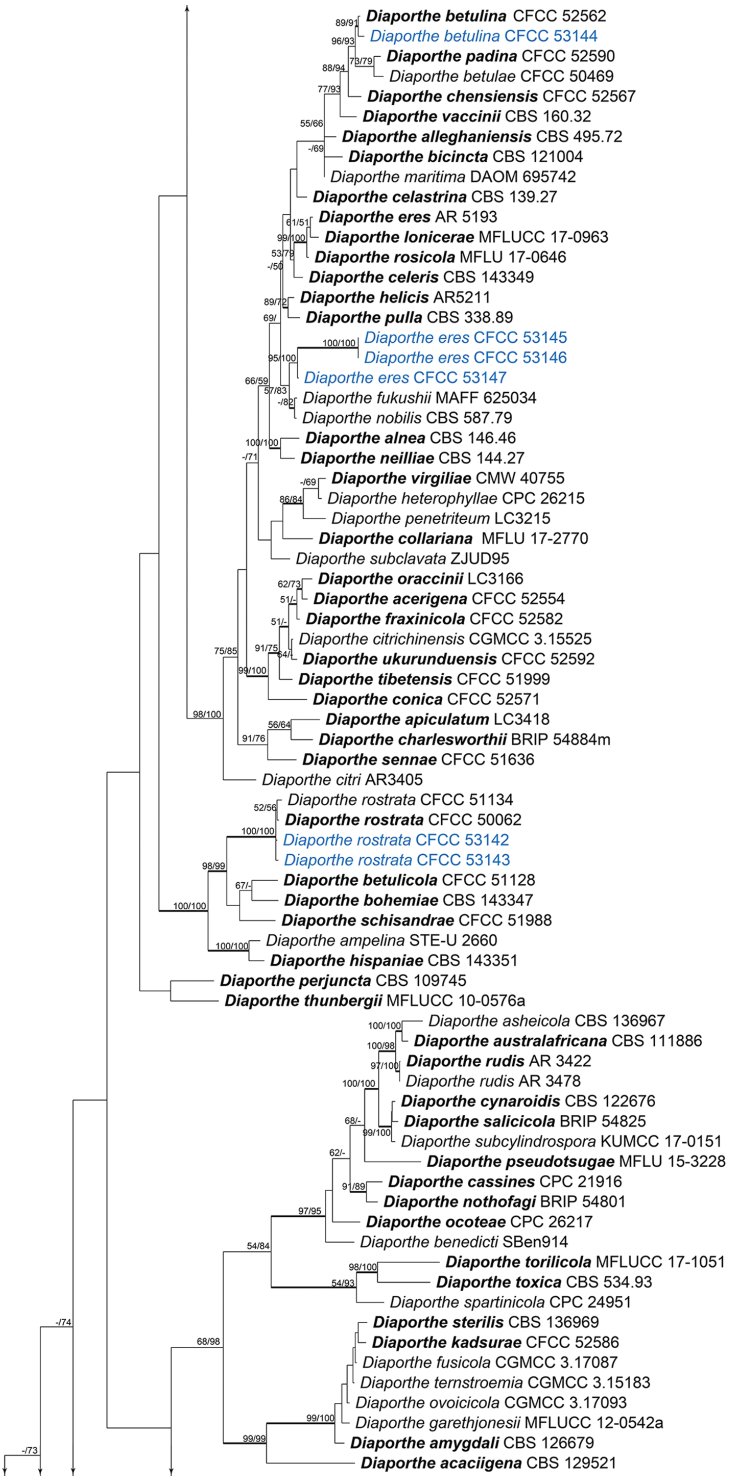

Figure 3. Continued.

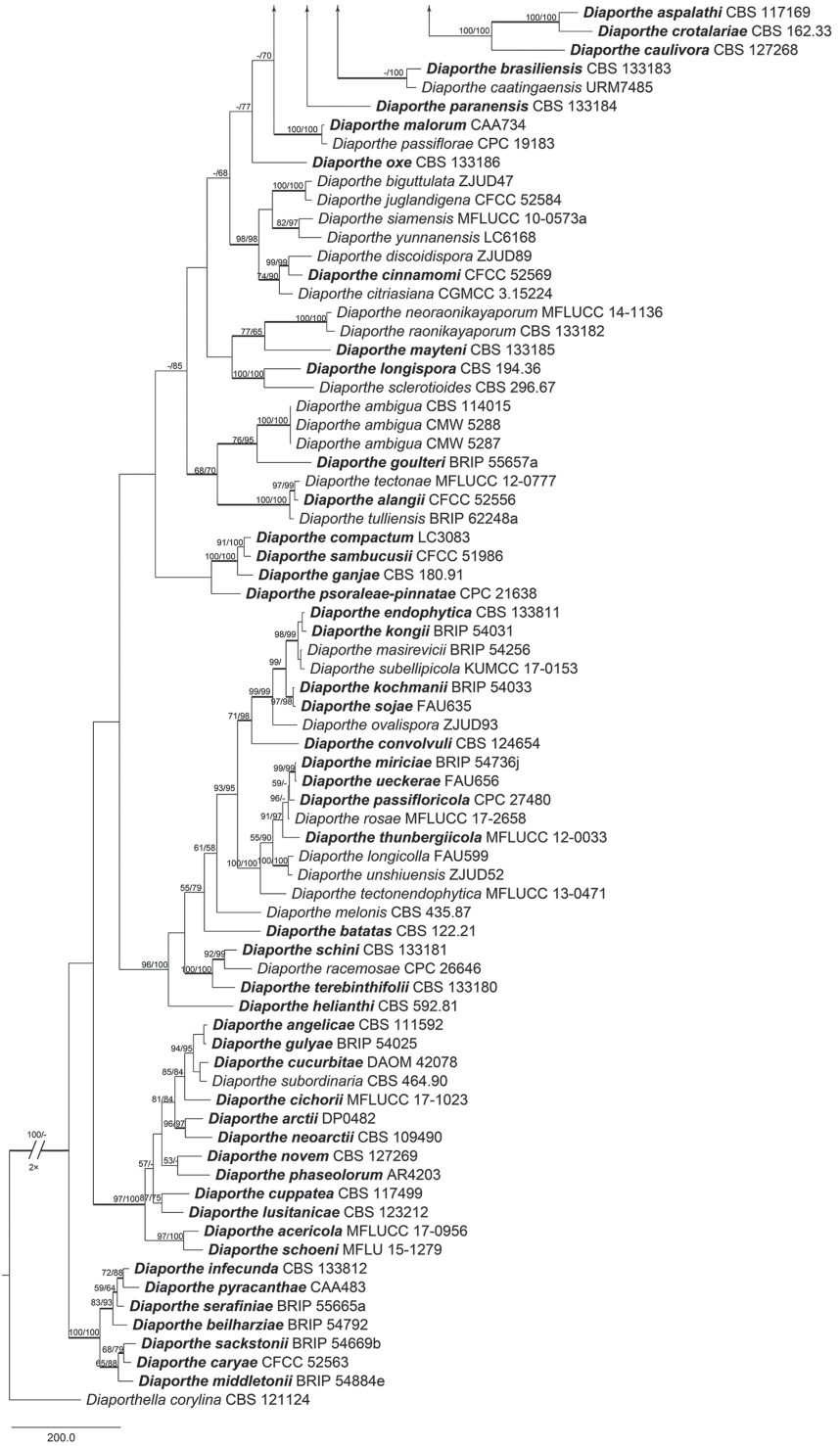

Figure 3. Continued.

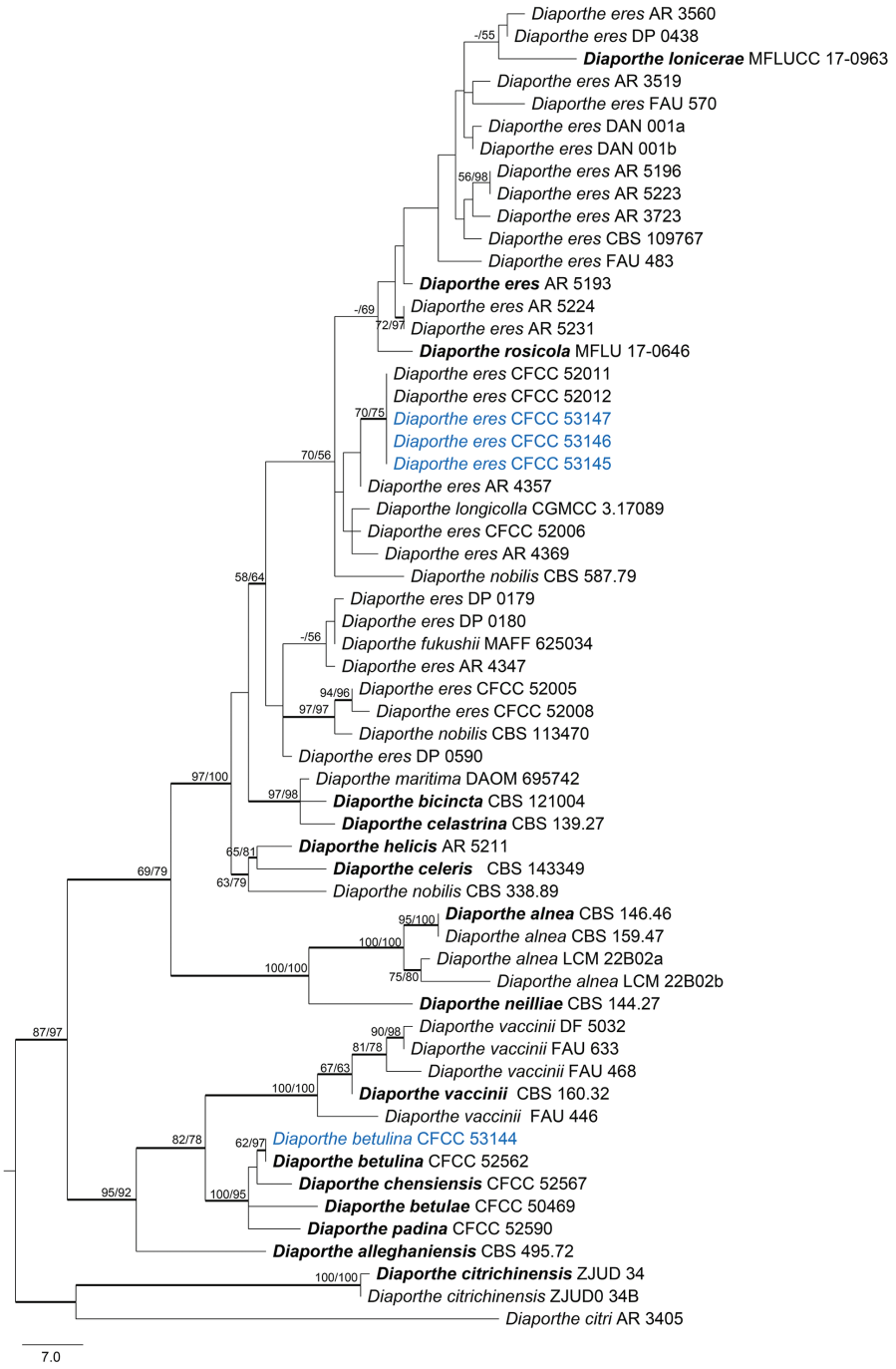

Figure 4. Phylogram of *Diaporthe eres* complex based on combined *cal*, *tef1-a* and *tub2* genes. The MP and ML bootstrap support values above 50 % are shown at the first and second positions, respectively. Thickened branches represent posterior probabilities above 0.95 from BI. Ex-type strains are in bold. Strains from the current study are in blue.

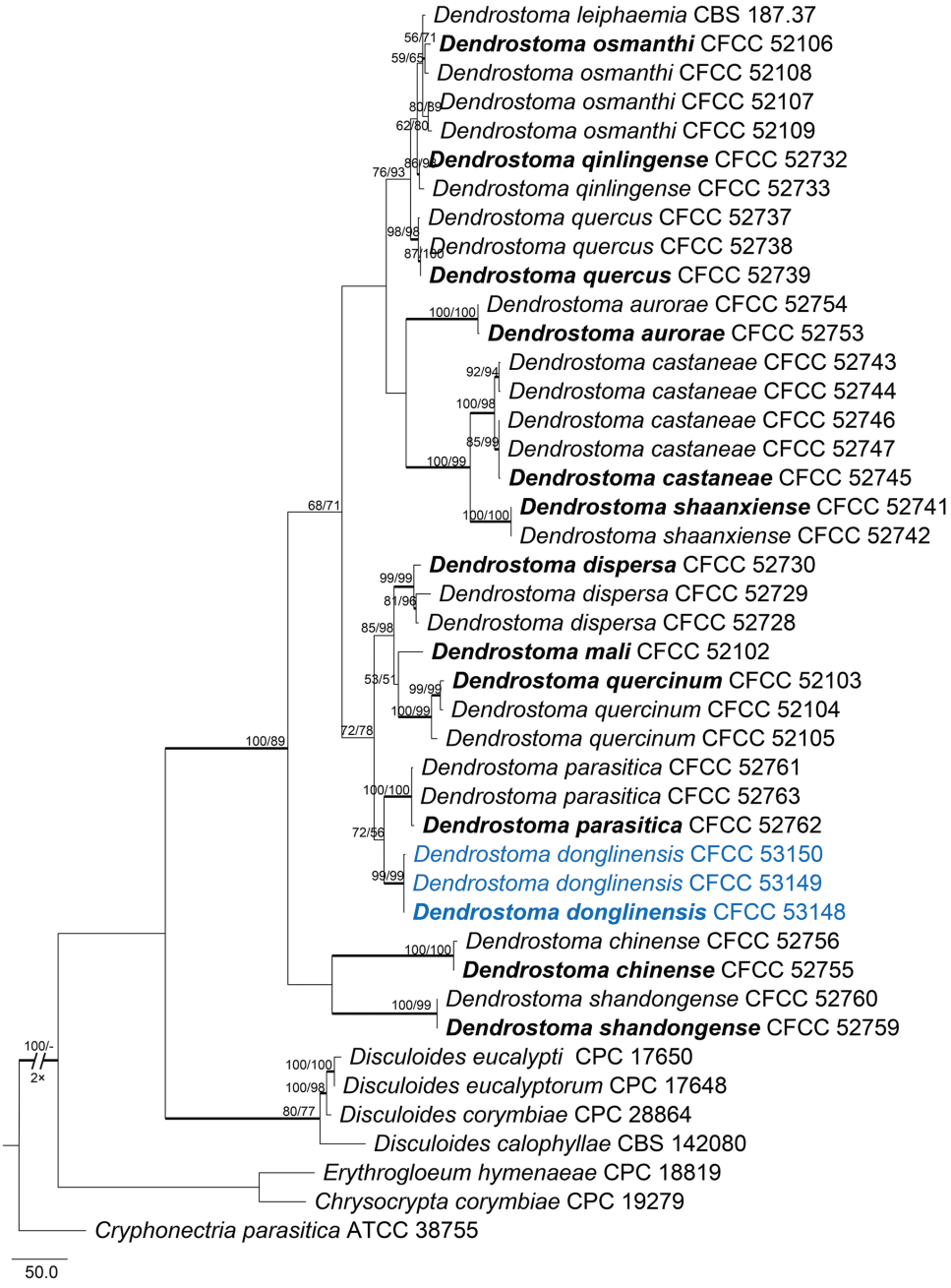

Figure 5. Phylogram of *Dendrostoma* based on combined ITS, *rpb2* and *tef1-a* genes. The MP and ML bootstrap support values above 50 % are shown at the first and second positions, respectively. Thickened branches represent posterior probabilities above 0.95 from the BI. Ex-type strains are in bold. Strains from the current study are in blue.

Apioporthella, *Chaetoconis*, *Chiangraiomyces*, *Diaporthe*, *Hyaliappendispora*, *Leucodiaporthe*, *Mazzantia*, *Ophiodiaporthe*, *Paradiaporthe*, *Phaeocytostroma*, *Phaeodiaporthe*, *Pustulomyces*, and *Stenocarpella*.

Diaporthe Nitschke, Pyrenomyc. Germ. 2: 240 (1870)

Type species. *Diaporthe eres* Nitschke, Pyrenomyc. Germ. 2: 245 (1870).

Notes. The genus *Diaporthe* (syn. *Phomopsis*) was established by Nitschke (1870). The identification of *Diaporthe* was confused due to the historical species recognition criteria based on overlapped morphology, culture characteristics and host affiliation (Dissanayake et al. 2017). The phylogenetic analysis recommended to delimitate taxa to the species level was first proposed by Udayanga et al. (2012) and later modified to include concatenated alignments of ITS, *cal1*, *his3*, *tef1-a*, *tub2* (Gomes et al. 2013). More than 1,050 epithets for *Diaporthe* and 950 for *Phomopsis* are listed in Index Fungorum (August 2019). Dissanayake et al. (2017) provided most type/ex-type species details and phylogenetic frame with 172 species in this genus. Yang et al. (2018) summarized 15 species of *Diaporthe* associated with dieback disease of tree hosts in China and introduced 12 new species.

Diaporthe betulina C.M. Tian & Q. Yang, Mycokeys 39: 97 (2018)

Description. See Yang et al. (2018).

Material examined. CHINA, Beijing City, Mentougou District, Mount Dongling, Xiaolongmen Forestry Centre (39°59'23.58"N, 115°27'05.00"E), from branches of *Betula dahurica* Pall., 17 Aug. 2017, H.Y. Zhu & X.L. Fan, deposited by X.L. Fan, CF 2019831, living culture CFCC 53144.

Notes. Yang et al. (2018) described *Diaporthe betulina* from cankers of *Betula* spp. in Heilongjiang Province. The only strain CFCC 53144 representing *D. betulina* clusters in a well-supported clade and appear most closely related to *D. betulae*, which was also isolated from *Betula platyphylla* in Sichuan Province (Du et al. 2016). *Diaporthe betulina* (strain CFCC 52562) differs from *D. betulae* by its slender alpha conidia (2.5–3 vs. 3–4 μm) (Du et al. 2016), and 13 bp for ITS, 7 bp for cal, 19 bp for his, 12 bp for tef and 6 bp for tub2 based on alignment of the concatenated five-gene deposited in TreeBASE (S24893). Both morphology and sequence data confirmed that our isolates belong to this species.

Diaporthe eres Nitschke, Pyrenomyc. Germ. 2: 245 (1870)

Fig. 6

Description. Sexual morph: not observed. Asexual morph: Pycnidial stromata immersed in bark, scattered, slightly erumpent through the bark surface, unilocular,

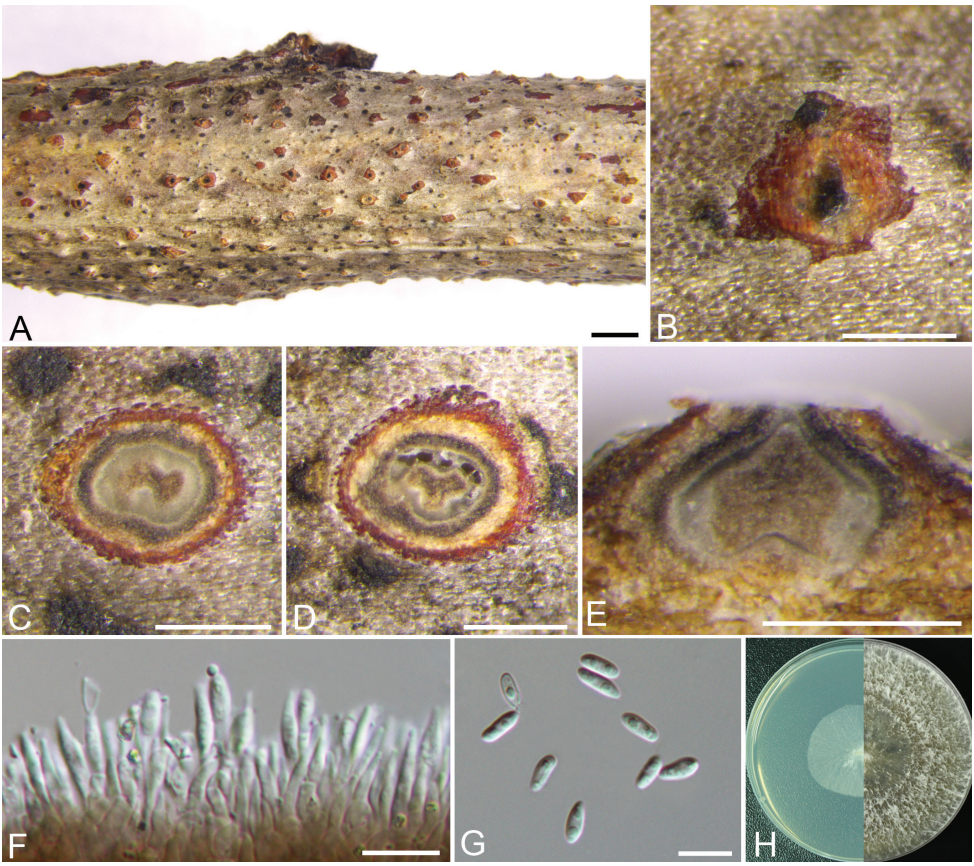

Figure 6. Morphology of *Diaporthe eres* from *Prunus davidiana* (CF 2019808). **A, B** Habit of conidiomata on twig **C, D** transverse section of conidioma **E** longitudinal section through conidioma **F** conidiophores and conidiogenous cells **G** alpha conidia **H** colonies on PDA at 3 days (left) and 30 days (right). Scale bars: 1mm (**A**); 250μm (**B–E**); 10 μm (**F, G**).

with a conspicuous central column. Central column beneath the disc more or less conical, pale grey with yellow. Ectostromatic disc orange, elliptical, 160–300 μm in diam., with one ostiole per disc. Ostiole dark brown to black, at the same level as or slightly above the disc surface, 70–80 μm in diam. Locule single, 210–260 μm in diam. Conidiophores cylindrical, hyaline, unbranched, straight or slightly curved, tapering towards the apex, 12–13.5 × 2–3 μm. Conidiogenous cells enteroblastic, phialidic. Alpha conidia hyaline, aseptate, smooth, ellipsoidal, biguttulate, rounded at both ends, 6.5–8.5 × 2.5–3 (av. = 7.3± 0.5 × 2.8 ± 0.3, n = 30) μm. Beta conidia were not observed.

Culture characteristics. Cultures on PDA are initially white, growing up to 4 cm in diam. after 3 days, and becoming yellow green to brown after 7–10 days. Colonies are flat felty with a thick texture at the marginal area, with a thin texture at the center, abundant aerial mycelium, sterile.

Material examined. CHINA, Beijing City, Mentougou District, Mount Dongling, Xiaolongmen Forestry Centre (39°58'06.45"N, 115°26'48.36"E), from branches of *Prunus davidiana* (Carr.) Franch., 20 Aug. 2017, H.Y. Zhu & X.L. Fan, deposited by X.L. Fan, CF 2019808, living culture CFCC 53146; *ibid.* CF 2019858, living culture CFCC 53145. CHINA, Beijing City, Mentougou District, Mount Dongling, Xiaolongmen Forestry Centre (39°57'47.49"N, 115°29'20.52"E), from branches of *Juglans regia* L., 20 Aug. 2017, H.Y. Zhu & X.L. Fan, deposited by X.L. Fan, CF 2019801, living culture CFCC 53147.

Notes. *Diaporthe eres* is the type species of *Diaporthe*, and is also the most common species causing canker disease on a wide range of hosts (Gomes et al. 2013, Udayanga et al. 2014, Dissanayake et al. 2017, Yang et al. 2018). Our isolates are associated with canker disease of *Prunus davidiana* in China, which belong to the *Diaporthe eres* species complex (Fig. 4). Fan et al. (2018c) treated many *Diaporthe* species as *D. eres*, and showed the combined *cal*, *tef1-a* and *tub2* genes provide a better topology than the combined five-gene phylogeny for the *D. eres* complex. Both sequence data and morphology confirm that our isolates belong to this species (Fig. 4).

Diaporthe rostrata C.M. Tian, X.L. Fan & K.D. Hyde, Mycological Progress 14: 82 (2015)

≡ *Diaporthe juglandicola* C.M. Tian & Q. Yang. Mycosphere 8(5): 821 (2017)

Description. See Fan et al. (2015).

Material examined. CHINA, Beijing City, Mentougou District, Mount Dongling, Xiaolongmen Forestry Centre (39°57'54.68"N, 115°27'45.27"E), from branches of *Juglans mandshurica* Maxim., 22 Aug. 2017, H.Y. Zhu & X.L. Fan, deposited by X.L. Fan, CF 2019807, living culture CFCC 53142; *ibid.* CF 2019910, living culture CFCC 53143.

Notes. Fan et al. (2015) introduced *Diaporthe rostrata* from *Juglans mandshurica* causing walnut dieback in China. Yang et al. (2017) introduced *D. juglandicola* as a sister clade with *D. rostrata*, but it has no conspicuous rostrate necks on the bark. However, we recommend to treat *D. juglandicola* as a synonym of *D. rostrate*, based on the same host species, and lacking of phylogenetic support to separate them after involving our current materials (CF 2019807 and CF 2019910) with conspicuous rostrate necks.

Erythrogloeaceae Senan., Maharachch. & K.D. Hyde, Stud. Mycol. 86: 258 (2017)

Type genus. *Erythrogloeum* Petr. Sydowia 7: 378 (1953).

Notes. The family *Erythrogloeaceae* was recently introduced by Senanayake et al. (2017) based on ITS, LSU, *rpb2* and *tef1-a*, and included four genera (*Chrysocrypta*, *Dendrostoma*, *Disculoides* and *Erythrogloeum*) (Fan et al. 2018a, Senanayake et al. 2018).

***Dendrostoma* X.L. Fan & C.M. Tian, Persoonia 40: 124 (2018)**

Type species. *Dendrostoma mali* X.L. Fan & C.M. Tian, Persoonia 40: 124 (2018).

Notes. *Dendrostoma* was introduced by Fan et al. (2018a) as a phytopathogenic genus, causing canker diseases on several economic hardwoods such as *Malus spectabilis*, *Osmanthus fragrans* and *Quercus acutissima*. Jiang et al. (2019b) accepted 14 species of *Dendrostoma* using a concatenated matrix of four genes (ITS, LSU, *rpb2* and *tef1-a*), including 10 new species associated with chestnut and oak canker disease in China. Here we recommend a set of three genes (ITS, *rpb2* and *tef1-a*) to separate species of this genus.

***Dendrostoma donglinensis* H.Y. Zhu & X.L. Fan, sp. nov.**
MycoBank No: 832194
Fig. 7

Etymology. Named after the location where it was collected, Mount Dongling.

Holotype. CHINA, Beijing City, Mentougou District, Mount Dongling, Xiaolongmen Forestry Centre (39°58'19.62"N, 115°26'51.27"E), from branches of *Quercus mongolica* Fisch. ex Ledeb., 18 Aug. 2017, H.Y. Zhu & X.L. Fan, deposited by X.L. Fan, holotype CF 2019903, ex-type living culture CFCC 53148.

Description. Sexual morph: not observed. Asexual morph: Pycnidial stromata immersed in the bark, scattered, erumpent through the surface of bark, unilocular, with a conspicuous central column. Central column beneath the disc more or less conical, yellow. Conceptacle absent. Ectostromatic disc hyaline, circular to ovoid, 750–1190 μm in diam., with a single ostiole per disc. Ostiole grey to black, at the same level as the disc surface, 240–270 μm in diam. Locule single, circular to irregular, undivided, 550–750 μm in diam. Conidiophores hyaline, unbranched, approximately cylindrical. Conidiogenous cells enteroblastic, phialidic. Conidia hyaline, fusoid, acute at each end, smooth or occasional not smooth, aseptate, 16.5–20.5 × 2–3.5 (av. = 18 ± 1.1 × 3 ± 0.3, n = 30) μm.

Culture characteristics. Cultures on PDA are initially white, growing slowly to 2 cm in diam. after 3 days and 4 cm after 14 days, becoming salmon in the center after 7–10 days. Growth stops when colony reaches 8 cm and cultures becoming salmon to honey after the 30 days. Colonies are felty with a uniform texture; sterile.

Additional material examined. CHINA, Beijing City, Mentougou District, Mount Dongling, Xiaolongmen Forestry Centre (39°58'19.62"N, 115°26'51.27"E), from branches of *Quercus mongolica* Fisch. ex Ledeb., 18 Aug. 2017, H.Y. Zhu & X.L. Fan, deposited by X.L. Fan, CF 2019887, living culture CFCC 53149; *ibid.* CF 2019805, living culture CFCC 53150.

Notes. *Dendrostoma donglinensis* is associated with canker disease of *Quercus mongolica* in China. It can be distinguished from its closest relative *D. parasiticum* by its

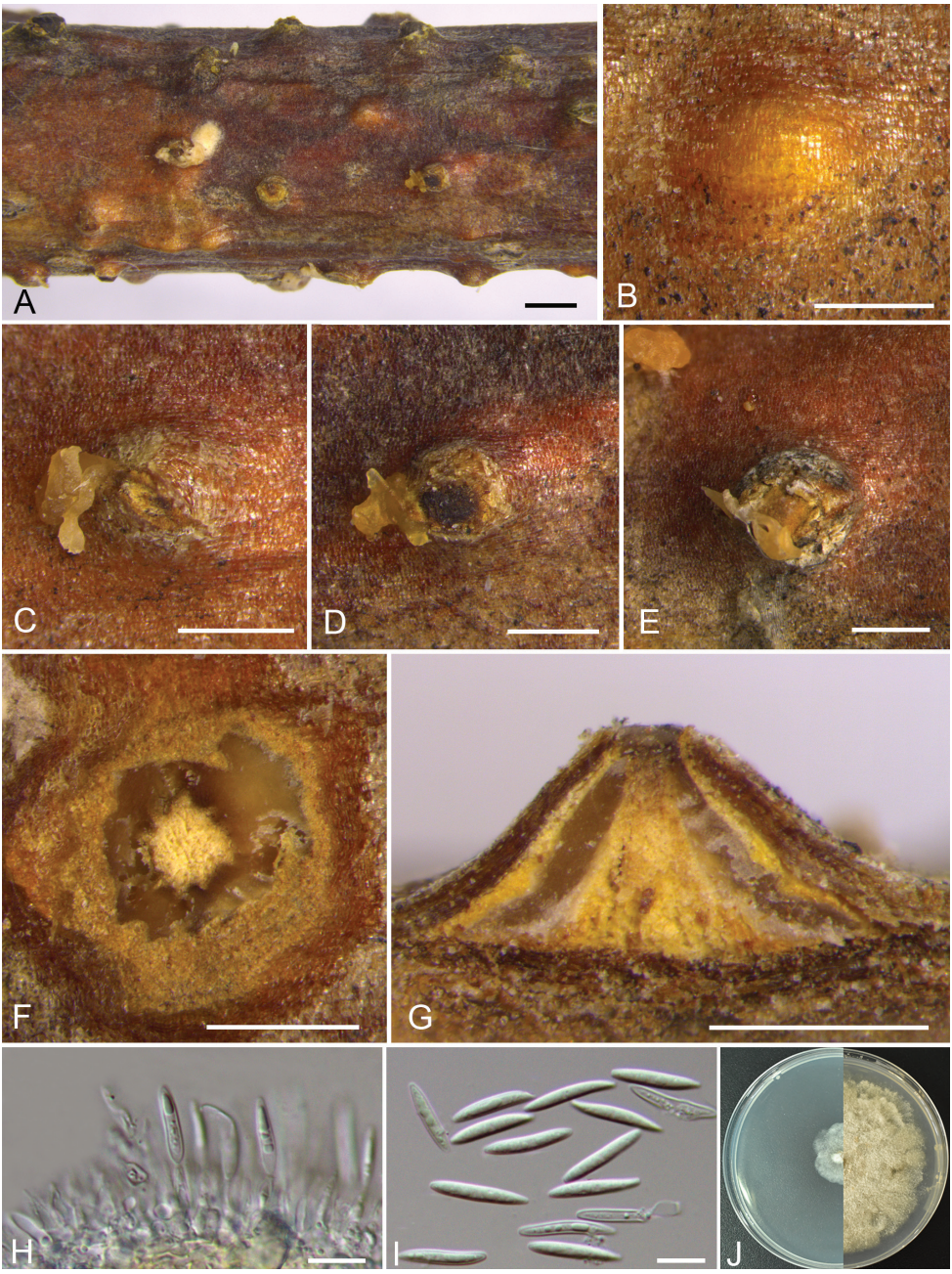

Figure 7. Morphology of *Dendrostoma donglinensis* from *Quercus mongolica* (CF 2019903). **A–E** Habit of conidiomata on twig **F** transverse section of conidioma **G** longitudinal section through conidioma **H** conidiophores and conidiogenous cells **I** conidia **J** colonies on PDA at 3 days (left) and 30 days (right). Scale bars: 1mm (**A**); 500 µm (**B–G**); 10 µm (**H, I**).

fusoid, acute at each end and larger conidia (16.5–20.5 × 2–3.5 vs. 9.3–11.7 ×2.8–3.3 μm). The isolates are phylogenetically distinct from all other available strains of *Dendrostoma* included in this study and we therefore describe this species as new, based on DNA sequence data and morphology.

Juglanconidaceae Voglmayr & Jaklitsch, Persoonia 38: 142 (2017)

Type genus. *Juglanconis* Voglmayr & Jaklitsch, Persoonia 38: 142 (2017).

Notes. Juglanconidaceae was introduced by Voglmayr et al. (2017), including a single genus *Juglanconis*.

Juglanconis Voglmayr & Jaklitsch, Persoonia 38: 142 (2017)

Type species. *Juglanconis juglandina* (Kunze) Voglmayr & Jaklitsch, *Persoonia* 38: 144 (2017).

Notes. *Juglanconis* was introduced by Voglmayr et al. (2017) to accommodate previous *Melanconium juglandinum*, *M. oblongum* and *M. pterocaryae* based on morphology and DNA data of type materials. The genus is restricted to one host in Juglandaceae, which is identified by having perithecial ascomata, 8-spored asci with an apical ring, hyaline, bicelled ascospores in the sexual morph; and acervular conidiomata, brown conidia with gelatinous sheaths in asexual morph (Voglmayr et al. 2017). *Juglanconis* includes five species (*J. appendiculata*, *J. japonica*, *J. juglandina*, *J. oblonga* and *J. pterocaryae*) (Voglmayr et al. 2019), of which *J. juglandina* and *J. oblonga* are common pathogens in *Juglans* spp. in China (Fan et al. 2018b).

Juglanconis oblonga (Berk.) Voglmayr & Jaklitsch Persoonia 38: 147 (2017)

≡ *Melanconium oblongum* Berk., Grevillea 2 (22): 153 (1874)
≡ *Diaporthe juglandis* Ellis & Everh., Proc. Acad. Nat. Sci. Philadelphia 45: 448 (1893)
≡ *Melanconis juglandis* (Ellis & Everh.) A.H. Graves, Phytopathology 13: 311 (1923)

Description. See Fan et al. (2018b).

Material examined. CHINA, Beijing City, Mentougou District, Mount Dongling, Xiaolongmen Forestry Centre (39°57'54.68"N, 115°27'45.27"E), from branches of *Juglans mandshurica* Maxim., 22 Aug. 2017, H.Y. Zhu & X.L. Fan, deposited by X.L. Fan, CF 2019906, living culture CFCC 53151; *ibid.* CF 2019909, living culture CFCC 53152.

Notes. *Juglanconis oblonga* (previous *Melanconium oblongum*) is associated with canker disease of Juglandaceae hosts in North America and Southeast Asia (Graves 1923, Voglmayr et al. 2017, Fan et al. 2018b). This species is similar to *J. juglandina* in disease symptoms but can be distinguished by its longer conidia (22 × 12.5 compared

to 20 × 13 μm) and DNA sequence data (Fan et al. 2018b). This species is a common pathogen causing walnut canker in China (Fan et al. 2018b).

Melanconidaceae G. Winter, Rabenh. Krypt. -Fl., Edn 2 (Leipzig) 1(2): 764 (1886)

Type genus. *Melanconis* Tul. & C. Tul., Select. Fung. Carpol. (Paris) 2: 115 (1863).

Notes. Melanconidaceae was introduced by Winter (1886) and has been subject to some confusion due to the overlap in morphological characters between genera and the absence of DNA sequence data supporting the family concept (Barr 1978). Castlebury et al. (2002) and Rossman et al. (2007) restricted this family to a single genus *Melanconis* based on LSU rDNA sequences, which was adapted by recent studies (Senanayake et al. 2017, Fan et al. 2018b).

Melanconis Tul. & C. Tul., Select. Fung. Carpol. (Paris) 2: 115 (1863)

Type species. *Melanconis stilbostoma* (Fr.) Tul. & C. Tul., Select. Fung. Carpol. (Paris) 2: 115 (1863).

Notes. *Melanconis* was established by Tulasne & Tulasne (1863) based on *Sphaeria stilbostoma*. *Melanconis* has approximately 105 species epithets recorded in Index Fungorum (August 2019), but for most species no living cultures or DNA sequence data are available. Rossman et al. (2007) suggested that many of the species previously residing in *Melanconis* may belong elsewhere. *Melanconis* includes five species (*Melanconis alni*, *Ms. betulae*, *Ms. marginalis*, *Ms. itoana* and the type species *Ms. stilbostoma*), which were all restricted to the hosts in Betulaceae (Fan et al. 2016, 2018b).

Melanconis stilbostoma (Fr.) Tul. & C. Tul., Select. Fung. Carpol. (Paris) 2: 115 (1863)

Description. See Fan et al. (2016).

Material examined. CHINA, Beijing City, Mentougou District, Mount Dongling, Xiaolongmen Forestry Centre (39°59'23.58"N, 115°27'05.00"E), from branches of *Betula dahurica* Pall., 22 Aug. 2017, H.Y. Zhu & X.L. Fan, deposited by X.L. Fan, CF 2019832, living culture CFCC 53128; *ibid.* CF 2019833, living culture CFCC 53129. CHINA, Beijing City, Mentougou District, Mount Dongling, Xiaolongmen Forestry Centre (39°59'23.58"N, 115°27'05.00"E), from branches of *Betula* sp., 21 Aug. 2017, H.Y. Zhu & X.L. Fan, deposited by X.L. Fan, CF 2019871, living culture CFCC 53130; *ibid.* CF 2019911, living culture CFCC 53131.

Notes. *Melanconis stilbostoma* is the type species of *Melanconis* and is thus far only known to occur on *Betula* spp. with a global distribution (Fan et al. 2016). *Betula dahurica*, *B. pendula*, *B. rotundifolia*, *B. tianschanica* and *B. platyphylla* are recorded as hosts for *Melanconis stilbostoma* in China (Zhuang 2005, Fan et al. 2016, 2018b).

Discussion

In the present work six diaporthalean species were identified residing in four families (Diaporthaceae, Erythrogloeaceae, Juglanconidaceae and Melanconidaceae) in the order Diaporthales. These include five known species (*Diaporthe betulina*, *D. eres*, *D. rostrata*, *Juglanconis oblonga* and *Melanconis stilbostoma*), and one new species (*Dendrostoma donglinensis*). All specimens in the current study were collected from symptomatic branches and twigs associated with canker or dieback diseases. *Dendrostoma* (Erythrogloeaceae) species were isolated from *Quercus mongolica* (Fagaceae). *Juglanconis* (Juglanconidaceae) species were isolated from *Juglans mandshurica* (Juglandaceae) and *Melanconis* (Melanconidaceae) species were isolated from *Betula dahurica* (Betulaceae), which suggests these fungi are host specific. *Diaporthe* (Diaporthaceae) species were isolated from *Betula dahurica* (Betulaceae), *Juglans regia*, *J. mandshurica* (Juglandaceae), *Prunus davidiana* (Rosaceae) and *Quercus mongolica* (Fagaceae). This might indicate that *Diaporthe* species are less host specific.

The classification of Diaporthales presented here follows the previous studies (Castlebury et al. 2002, Rossman et al. 2007) and discoveries of new taxa from many other works (Suetrong et al. 2015, Dissanayake et al. 2017, Voglmayr et al. 2017, Senanayake et al. 2017, 2018). We performed frequently and used four genes (ITS, LSU, *rpb2* and *tef1-a*) to evaluate the 30 families in this order, but it was found to be confusing in some taxa such as *Apoharknessia* and *Lasmenia* in Apoharknessiaceae (Fig. 2). It suggests that more studies using a multiphasic approach are still needed to clarify some issues in this order. Diaporthales includes many phytopathogenic genera such as *Dendrostoma*, *Diaporthe*, *Melanconis* and *Juglanconis*, which have been reported causing canker disease of tree hosts in China (Fan et al. 2016, 2018b, Yang et al. 2018, Jiang et al. 2019b). The current study focuses on diaporthalean fungi in Mount Dongling of Beijing, which is considered as a biodiversity hotspot with a high diversity for fungal species and (Guo et al. 2008, Zhu et al. 2018). We hope that the descriptions and molecular data of diaporthalean fungi in this study could provide a resource for future studies in this region.

Acknowledgements

This study is financed by the Fundamental Research Funds for the Central Universities (2019ZY23), the National Natural Science Foundation of China (31670647) and the College Student Research and Career-creation Program of Beijing (S201910022007).

References

Alvarez LV, Groenewald JZ, Crous PW (2016) Revising the Schizoparmaceae: *Coniella* and its synonyms *Pilidiella* and *Schizoparme*. Studies in Mycology 85: 1–34. https://doi.org/10.1016/j.simyco.2016.09.001

Alves A, Crous PW, Correia A, Phillips AJL (2008) Morphological and molecular data reveal cryptic speciation in *Lasiodiplodia theobromae*. Fungal Diversity 28: 1–13. https://doi.org/10.1002/yea.1554

Barr ME (1978) The Diaporthales in North America with emphasis on *Gnomonia* and its segregates. Mycologia Memoir 7: 1–232.

Braun U, Nakashima C, Crous PW, Groenewald JZ, Moreno-Rico O, Rooney-Latham S, Blomquist CL, Haas J, Marmolejo J (2018) Phylogeny and taxonomy of the genus *Tubakia* s. lat. Fungal Systematics and Evolution 1: 41–99. https://doi.org/10.3114/fuse.2018.01.04

Carbone I, Kohn LM (1999) A method for designing primer sets for speciation studies in filamentous ascomycetes. Mycologia 91: 553–556. https://doi.org/10.2307/3761358

Castlebury LA, Rossman AY, Jaklitsch WJ, Vasilyeva LN (2002) A preliminary overview of the Diaporthales based on large subunit nuclear ribosomal DNA sequences. Mycologia 94: 1017–1031. https://doi.org/10.1080/15572536.2003.11833157

Crous PW, Gams W, Stalpers JA, Robert V, Stegehuis G (2004) MycoBank: an online initiative to launch mycology into the 21st century. Studies in Mycology 50: 19–22.

Crous PW, Schumacher RK, Akulov A, Thangavel R, Hernández-Restrepo M, Carnegie A, Cheewangkoon R, Wingfield MJ, Summerell B, Quaedvlieg W, Coutinho TA, Roux J, Wood AR, Giraldo A, Groenewald JZ (2019) New and Interesting Fungi. 2. Fungal Systematics and Evolution 3: 57–134. https://doi.org/10.3114/fuse.2019.03.06

Crous PW, Summerell BW, Shivas RG, Burgess TI, Decock CA, Dreyer LL, Granke LL, Guest DI, Hardy GEStJ, Hausbeck MK, Hüberli D, Jung T, Koukol O, Lennox CL, Liew ECY, Lombard L, McTaggart AR, Pryke JS, Roets F, Saude C, Shuttleworth LA, Stukely MJC, Vánky K, Webster BJ, Windstam ST, Groenewald JZ (2012) Fungal Planet description sheets: 107–127. Persoonia 28: 138–182. https://doi.org/10.3767/003158512X652633

Dissanayake AJ, Phillips AJL, Hyde KD, Yan JY, Li XH (2017) The current status of species in *Diaporthe*. Mycosphere 8: 1106–1156. https://doi.org/10.5943/mycosphere/8/5/5

Doyle JJ, Doyle JL (1990) Isolation of plant DNA from fresh tissue. Focus 12: 13–15. https://doi.org/10.2307/2419362

Du Z, Fan XL, Hyde KD, Yang Q, Liang YM, Tian CM (2016) Phylogeny and morphology reveal two new species of *Diaporthe* from *Betula* spp. in China. Phytotaxa 269: 90–102. https://doi.org/10.11646/phytotaxa.269.2.2

Fan XL, Bezerra JDP, Tian CM, Crous PW (2020) *Cytospora* (Diaporthales) in China. Persoonia 45: 1–45. https://doi.org/10.3767/persoonia.2020.45.01

Fan XL, Bezerra JDP, Tian CM, Crous PW (2018a) Families and genera of diaporthalean fungi associated with canker and dieback of tree hosts. Persoonia 40: 119–134. https://doi.org/10.3767/persoonia.2018.40.05

Fan XL, Du Z, Bezerra JDP, Tian CM (2018b) Taxonomic circumscription of melanconis-like fungi causing canker disease in China. MycoKeys 42: 89–124. https://doi.org/10.3897/mycokeys.42.29634

Fan XL, Yang Q, Bezerra JDP, Alvarez LV, Tian CM (2018c) *Diaporthe* from walnut tree (*Juglans regia*) in China, with insight of the *Diaporthe eres* complex. Mycological Progress 17: 841–853. https://doi.org/10.1007/s11557-018-1395-4

Fan XL, Du Z, Liang YM, Tian CM (2016) *Melanconis* (Melanconidaceae) associated with *Betula* spp. in China. Mycological Progress 15: 1–9. https://doi.org/10.1007/s11557-016-1163-2

Fan XL, Hyde KD, Udayanga D, Wu XY, Tian CM (2015) *Diaporthe rostrata*, a novel ascomycete from *Juglans mandshurica* associated with walnut dieback. Mycological Progress 14: 1–8. https://doi.org/10.1007/s11557-015-1104-5

Glass NL, Donaldson GC (1995) Development of primer sets designed for use with the PCR to amplify conserved genes from flamentous ascomycetes. Applied and Environmental Microbiology 61: 1323–1330.

Gomes RR, Glienke C, Videira SIR, Lombard L, Groenewald JZ, Crous PW (2013) *Diaporthe*: a genus of endophytic, saprobic and plant pathogenic fungi. Persoonia 31: 1–41. https://doi.org/10.3767/003158513X666844

Graves AH (1923) The *Melanconis* disease of the butternut (*Juglans cinerra* L.). Phytopathplogy 13: 411–435.

Guarnaccia V, Crous PW (2017) Emerging citrus diseases in Europe caused by species of *Diaporthe*. IMA Fungus 8: 317–334. https://doi.org/10.5598/imafungus.2017.08.02.07

Guindon S, Dufayard JF, Lefort V, Anisimova M, Hordijk W, Gascuel O (2010) New algorithms and methods to estimate maximum-likelihood phylogenies: assessing the performance of PhyML 3.0. Systematic Biology 59: 307–321. https://doi.org/10.1093/sysbio/syq010

Guo LD, Huang GR, Wang Y (2008) Seasonal and tissue age influences on endophytic fungi of *Pinus tabulaeformis* (Pinaceae) in the Dongling Mountains, Beijing. Journal of Integrative Plant Biology 50: 997–1003. https://doi.org/10.1111/j.1744-7909.2008.00394.x

Guterres DC, Galvão-Elias S, Santos MDM, Souza BCP, Almeida CP, Pinho DB, Miller RNG, Dianese JC (2019) Phylogenetic relationships of *Phaeochorella parinarii* and recognition of a new family, Phaeochorellaceae (Diaporthales). Mycologia. https://doi.org/10.1080/00275514.2019.1603025

Hillis DM, Bull JJ (1993) An empirical test of bootstrapping as a method for assessing confidence in phylogenetic analysis. Systematic Biology 42: 182–192. https://doi.org/10.1093/sysbio/42.2.182

Hongsanan S, Maharachchikumbura SSN, Hyde KD, Samarakoon MC, Jeewon R, Zhao Q, Al-Sadi AM, Bahkali AH (2017) An updated phylogeny of Sordariomycetes based on phylogenetic and molecular clock evidence. Fungal Diversity 84: 1–17. https://doi.org/10.1007/s13225-017-0384-2

Jiang N, Fan XL, Tian CM (2019a) Identification and pathogenicity of Cryphonectriaceae species associated with chestnut canker in China. Plant Pathology 68: 1132–1145. https://doi.org/10.1111/ppa.13033

Jiang N, Fan XL, Crous PW, Tian CM (2019b) Species of *Dendrostoma* (Erythrogloeaceae, Diaporthales) associated with chestnut and oak canker diseases in China. MycoKeys 48: 67–96. https://doi.org/10.3897/mycokeys.48.31715

Katoh K, Standley DM (2013) MAFFT multiple sequence alignment software version 7: improvements in performance and usability. Molecular biology and evolution 30: 772–780. https://doi.org/10.1093/molbev/mst010

Liu YJ, Whelen S, Hall BD (1999) Phylogenetic relationships among ascomycetes: evidence from an RNA polymerse II subunit. Molecular Biology and Evolution 16: 1799–1808. https://doi.org/10.1093/oxfordjournals.molbev.a026092

Ma KP, Guo XM, Yu SL (1995) On the characteristics of the flora of Mount Dongling area and its relationship with a number of other mountainous floras in China. Bulletin Botanical Research 15: 501–515.

Nitschke T (1870) Pyrenomycetes Germanici 2. Eduard Trewendt, Breslau.

Norphanphoun C, Hongsanan S, Doilom M, Bhat DJ, Wen TC, Bulgakov TS, Hyde KD (2016) Lamproconiaceae fam. nov. to accommodate *Lamproconium desmazieri*. Phytotaxa 270: 89–102. https://doi.org/10.11646/phytotaxa.270.2.2

Posada D, Crandall KA (1998) Modeltest: testing the model of DNA substitution. Bioinformatics 14: 817–818. https://doi.org/10.1093/bioinformatics/14.9.817

Rannala B, Yang Z (1996) Probability distribution of molecular evolutionary trees: a new method of phylogenetic inference. Journal of Molecular Evolution 43: 304–311. https://doi.org/10.1007/BF02338839

Rayner RW (1970) A Mycological Colour Chart. Commonwealth Mycological Institute, Kew.

Ronquist F, Huelsenbeck JP (2003) MrBayes 3: Bayesian phylogenetic inference under mixed models. Bioinformatics 19: 1572–1574. https://doi.org/10.1093/bioinformatics/btg180

Rossman AY, Farr DF, Castlebury LA (2007) A review of the phylogeny and biology of the Diaporthales. Mycoscience 48: 135–144. https://doi.org/10.1007/S10267-007-0347-7

Senanayake IC, Crous PW, Groenewald JZ, Maharachchikumbura SSN, Jeewon R, Phillips AJL, Bhat DJ, Perera RH, Li QR, Li WJ, Tangthirasunun N, Norphanphoun C, Karunarathna SC, Erio C, Manawasighe IS, Al-Sadi AM, Hyde KD (2017) Families of Diaporthales based on morphological and phylogenetic evidence. Studies in Mycology 86: 217–296. https://doi.org/10.1016/j.simyco.2017.07.003

Senanayake IC, Jeewon R, Chomnunti P, Wanasinghe DN, Norphanphoun C, Karunarathna A, Pem D, Perera RH, Camporesi E, McKenzie EHC, Hyde KD, Karunarathna SC (2018) Taxonomic circumscription of Diaporthales based on multigene phylogeny and morphology. Fungal Diversity 93: 241–443. https://doi.org/10.1007/s13225-018-0410-z

Suetrong S, Klaysuban A, Sakayaroj J, Preedanon S, Ruang-Areerate P, Phongpaichit S, Pang KL, Jones EBG (2015) Tirisporellaceae, a new family in the order Diaporthales (Sordariomycetes, Ascomycota). Cryptogamie Mycologie 36: 319–330. https://doi.org/10.7872/crym/v36.iss3.2015.319

Sun X, Guo LD, Hyde KD (2011) Community composition of endophytic fungi in *Acer truncatum* and their role in decomposition. Fungal diversity 47: 85–95. https://doi.org/10.1007/s13225-010-0086-5

Swofford DL (2003) PAUP*: Phylogenetic Analysis Using Parsimony, * and Other Methods, Version 4.0b10, Sinauer Associates, Sunderland.

Tamura K, Stecher G, Peterson D, Filipski A, Kumar S (2013) MEGA6: molecular evolutionary genetics analysis version 6.0. Molecular Biology and Evolution 30: 2725–2729. https://doi.org/10.1093/molbev/mst197

Tulasne LR, Tulasne C (1863) Selecta Fungorum Carpologia, Vol. 2. Paris.

Udayanga D, Castlebury LA, Rossman AY, Chukeatirote E, Hyde KD (2014) Insights into the genus *Diaporthe*: phylogenetic species delimitation in the *D. eres* species complex. Fungal Diversity 67: 203–229. https://doi.org/10.1007/s13225-014-0297-2

Udayanga D, Liu XZ, Crous PW, McKenzie EHC, Chukeatirote E, Hyde KD (2012) A multilocus phylogenetic evaluation of *Diaporthe* (*Phomopsis*). Fungal Diversity 56: 157–171. https://doi.org/10.1007/s13225-012-0190-9

Vilgalys R, Hester M (1990) Rapid genetic identifcation and mapping of enzymatically amplifed ribosomal DNA from several Cryptococcus species. Journal of Bacteriology 172: 4238–4246. https://doi.org/10.1128/jb.172.8.4238-4246.1990

Voglmayr H, Castlebury LA, Jaklitsch WM (2017) *Juglanconis* gen. nov. on Juglandaceae, and the new family Juglanconidaceae (Diaporthales). Persoonia 38: 136–155. https://doi.org/10.3767/003158517X694768

Voglmayr H, Jaklitsch WM, Mohammadi H, Chakusary MK (2019) The genus *Juglanconis* (Diaporthales) on *Pterocarya*. Mycological Progress 18: 425–427. https://doi.org/10.1007/s11557-018-01464-0

Von Höhnel F (1917) System der Diaportheen. Berichte der Deutschen Botanischen Gesellschaft 35: 631–638.

White TJ, Bruns T, Lee S, Taylor J (1990) Amplifcation and direct sequencing of fungal ribosomal RNA genes for phylogenetics. PCR Protocols: a guide to methods and applications 18: 315–322. https://doi.org/10.1016/B978-0-12-372180-8.50042-1

Winter G (1886) Fungi Australienses. Revue Mycologique Toulouse 8: 207–213.

Xavier KV, KC AN, Crous PW, Groenewald JZ, Vallad GE (2019) *Dwiroopa punicae* sp. nov. (Dwiroopaceae fam. nov., Diaporthales), associated with leaf spot and fruit rot of pomegranate (*Punica granatum*). Fungal Systematics and Evolution 4: 33–41. https://doi.org/10.3114/fuse.2019.04.04

Yang Q, Fan XL, Du Z, Tian CM (2017) *Diaporthe juglandicola* sp. nov. (Diaporthales, Ascomycetes), evidenced by morphological characters and phylogenetic analysis. Mycosphere 8: 817–826. https://doi.org/10.5943/mycosphere/8/5/3

Yang Q, Fan XL, Guarnaccia V, Tian CM (2018) High diversity of *Diaporthe* species associated with dieback diseases in China, with twelve new species described. MycoKeys 39: 97–149. https://doi.org/10.3897/mycokeys.39.26914

Zhu HY, Tian CM, Fan XL (2018) Studies of botryosphaerialean fungi associated with canker and dieback of tree hosts in Dongling Mountain of China. Phytotaxa 348: 63–76. https://doi.org/10.11646/phytotaxa.348.2.1

Zhuang WY (2005) Fungi of northwestern China. Ithaca, NewYork.

Supplementary material 1

Table S1. Isolates and GenBank accession numbers used in the phylogenetic analyses of Diaporthales

Authors: Haiyan Zhu, Meng Pan, Guido Bonthond, Chengming Tian, Xinlei Fan

Data type: molecular data

Link: https://doi.org/10.3897/mycokeys.59.38055.suppl1

Supplementary material 2

Table S2. Isolates and GenBank accession numbers used in the phylogenetic analyses of *Diaporthe*

Authors: Haiyan Zhu, Meng Pan, Guido Bonthond, Chengming Tian, Xinlei Fan

Data type: molecular data

Link: https://doi.org/10.3897/mycokeys.59.38055.suppl2

Supplementary material 3

Table S3. Isolates and GenBank accession numbers used in the phylogenetic analyses of *Diaporthe eres* complex

Authors: Haiyan Zhu, Meng Pan, Guido Bonthond, Chengming Tian, Xinlei Fan

Data type: molecular data

Link: https://doi.org/10.3897/mycokeys.59.38055.suppl3

Supplementary material 4

Table S4. Isolates and GenBank accession numbers used in the phylogenetic analyses of *Dendrostoma*

Authors: Haiyan Zhu, Meng Pan, Guido Bonthond, Chengming Tian, Xinlei Fan

Data type: molecular data

Link: https://doi.org/10.3897/mycokeys.59.38055.suppl4

MycoKeys 59: 95–131 (2019)
doi: 10.3897/mycokeys.59.33182
http://mycokeys.pensoft.net

RESEARCH ARTICLE

A peer-reviewed open-access journal
MycoKeys
Launched to accelerate biodiversity research

The *Ganoderma weberianum-resinaceum* lineage: multilocus phylogenetic analysis and morphology confirm *G. mexicanum* and *G. parvulum* in the Neotropics

Milay Cabarroi-Hernández[1,2], Alma Rosa Villalobos-Arámbula[1], Mabel Gisela Torres-Torres[3], Cony Decock[2], Laura Guzmán-Dávalos[1]

1 *Universidad de Guadalajara, Apdo. postal 1–139, Zapopan, 45101, Jalisco, Mexico* **2** *Mycothèque de l'Université Catholique de Louvain (BCCM/MUCL), Croix du Sud 2 box L7.05.06, B–1348, Louvain-la-Neuve, Belgium* **3** *Universidad Tecnológica del Chocó, Ciudadela Medrano, Quibdó, Chocó, Colombia*

Corresponding author: *Cony Decock* (cony.decock@uclouvain.be); *Laura Guzmán-Dávalos* (lguzman@cucba.udg.mx)

Academic editor: *Maria-Alice Neves* | Received 18 January 2019 | Accepted 4 June 2019 | Published 29 October 2019

Citation: Cabarroi-Hernández M, Villalobos-Arámbula AR, Torres-Torres MG, Decock C, Guzmán-Dávalos L (2019) The *Ganoderma weberianum-resinaceum* lineage: multilocus phylogenetic analysis and morphology confirm *G. mexicanum* and *G. parvulum* in the Neotropics. MycoKeys 59: 95–131. https://doi.org/10.3897/mycokeys.59.33182

Abstract

Many species of *Ganoderma* exhibit a high phenotypic plasticity. Hence, particularly among them, the morphological species concept remains difficult to apply, resulting in a currently confused taxonomy; as a consequence, the geographical distribution range of many species also remains very uncertain. One of the areas with a strong uncertainty, as far as morphological species concept is concerned, is the Neotropics. It is common that names of species described from other regions, mainly from northern temperate areas, have been applied to Neotropical species. The aim of the present study was to determine which species might lay behind the *G. weberianum* complex in the Neotropics, using morphological studies and phylogenetic inferences based on both single (ITS) and multilocus (ITS, *rpb2*, and *tef1-α*) sequences. The results indicated that *G. weberianum sensu* Steyaert, which is the usually accepted concept for this taxon, was absent from the Neotropics. In this area, *G. weberianum sensu* Steyaert encompassed at least two phylogenetic species, which are tentatively, for the time being, identified as belonging to *G. mexicanum* and *G. parvulum*. These two species could be distinguished morphologically, notably by the ornamentation or its absence on their chlamydospores. The results also showed that additional species from the Neotropics might still exist, including, e.g., *G. perzonatum*, but their circumscription remains uncertain until now because of the paucity of material available. Furthermore, it was found that the current concept of *G. resinaceum* embraced a complex of species.

Keywords
Caribbean, Chlamydospores, *Fomes weberianus*, Ganodermataceae, Paleotropics, South America

Introduction

Ganoderma P. Karst. has always been considered as an extremely difficult group with many poorly circumscribed species, forming species complexes (Moncalvo and Ryvarden 1997). Early in the 20th century, Lloyd (1905) already emphasized the excessively confused taxonomy of *Ganoderma* stating "*these fungi have been described and named over and over again, until the literature has become an almost unfathomable maze of meaningless and conflicting names*".

A century later, one can deduce that the situation has improved very little, if at all. Ryvarden (1991), for instance, still concluded that the taxonomic issue of the genus worldwide was very "chaotic". Hitherto, there is no comprehensive *Ganoderma* study and the absence of a world monograph contributed to "problems with species circumscriptions and identification", *fide* Moncalvo (2000).

Nowadays, about 220 species have been described in *Ganoderma*, over 400 taxa if one includes varieties, of which 167 apply to the so-called laccate species (Ryvarden 1991, Moncalvo and Ryvarden 1997, Index Fungorum http://www.indexfungorum.org/names/names.asp). Nonetheless, estimations based on the identification of terminal clades shown by phylogenetic analysis of a large ITS sequence data set gave a range of 60–80 terminal clades or phylogenetic species within the "laccate" *Ganoderma* spp. and 10–30 within the "non-laccate" *Ganoderma* spp. (Moncalvo 2000). Over the past two decades, phylogenetic studies have tried to elucidate the status of certain species and to better circumscribe their geographic distribution (e.g., Moncalvo 2000, Wang et al. 2009, Yao et al. 2013, de Lima-Junior et al. 2014, Zhou et al. 2014, Hapuarachchi et al. 2015, Loyd et al. 2018). However, the real species number and their distribution range remain largely unknown (Moncalvo and Ryvarden 1997, Moncalvo 2000).

Alliances of taxa, taxonomically informal but morphologically homogeneous and phylogenetically (variably) supported, also have been evidenced within *Ganoderma* (e.g., Moncalvo 2000, Hong and Jung 2004). Moncalvo (2000), for instance, as a result of phylogenetic analyses based on, so far, the most comprehensive ITS DNA sequences data set, and morphological characters, identified three core groups (1–3) and a bunch of residual species of uncertain affinities. The three core groups were furthermore divided into several subgroups. The core group 1 included most of the laccate species, and was divided into *G. curtisii*, *G. lucidum*, *G. resinaceum*, and *G. tropicum* lineages (Moncalvo 2000).

The *G. resinaceum* lineage (subgroup 1.2, Moncalvo 2000) comprised species having laccate pileus, basidiospores with "extremely fine ornament" (Pegler and Young 1973), and chlamydospores formed in their basidiomes and in pure cultures on artificial media. In this lineage, Moncalvo (2000) mentioned "genetically isolated populations", from North and South America and the Old-World that could be equated to as many species or species complexes. Moncalvo (2000) also suggested that the *G. weberianum* complex would represent the tropical Asian "counterpart" of the northern temperate *G. resinaceum* complex.

Ganoderma weberianum (Bres. & Henn. ex Sacc.) Steyaert was established by Steyaert (1972) based on *Fomes weberianus* Bres. & Henn. ex Sacc. (Saccardo 1891). Steyaert (1972) built the description of this species on a presumed type specimen held in B, the type specimen of *G. rivulosum* Pat. & Har. (Patouillard and Hariot 1906), a name that he considered as a synonym, and numerous specimens from Africa and Southeast Asia. In his description, Steyaert (1972) emphasized the importance of chlamydospores or "gasterospores", both the morphology and abundance of which were variable between specimens, being mainly double-walled, smooth or ornamented with "cristae" or "columns", and scarce to extremely abundant. Steyaert (1972) then informally recognized two morphotypes within his concept of *G. weberianum*, characterized by singular combinations of cuticular cells length and abundance of chlamydospores.

Since then, the distribution range of *G. weberianum sensu* Steyaert remained uncertain as exposed by the following authors. Steyaert (1972) reported the species from Africa and Southeast Asia and suggested that it was "probably extant in tropical America". Subsequently, the species was reported from all tropical areas (e.g., Corner 1983, Quanten 1997, Pan and Dai 2001, Wang et al. 2005, Mohanty et al. 2011, Kinge et al. 2012), including the Neotropics (Torres-Torres et al. 2012, 2015, Manzano et al. 2013, López-Peña et al. 2016), up to South-eastern USA (Loyd et al. 2017, 2018). Nevertheless, Moncalvo (2000) suggested that Steyaert's concept should be narrowed to include specimens originating only from Southeast Asia, in addition to the type locality in Samoa (*G. weberianum sensu* Moncalvo). Smith and Sivasithamparam (2000, 2003) corroborated this distribution range, including also Australia. With regards to the Neotropics, Moncalvo (2000) found an isolated branch within the *G. weberianum* complex, which he tentatively identified as *G. subamboinense* Bazzalo & J.E. Wright ex Moncalvo & Ryvarden. Welti and Courtecuisse (2010) also reported *G. subamboinense* from the Lesser Antilles and suggested reassessing *G. subamboinense* var. *laevisporum* Bazzalo & J.E. Wright.

In the present study, we analyzed the status of *G. weberianum sensu* Steyaert in the Neotropics and, in particular, the statuses of *G. subamboinense* and *G. subamboinense* var. *laevisporum*. We also investigated through multilocus phylogenetic analysis, their phylogenetic relationships with specimens or species of the *G. weberianum* complex from other biogeographic zones.

Materials and methods

Studied materials

For this study, specimens from B, BAFC, BPI, ENCB, FH, IBUG, INBIO, MUCL, NY, S, and XAL herbaria (abbreviations follow Thiers, continuously updated), including the type specimens of *Fomes weberianus*, *Ganoderma argillaceum* Murrill, *G. mexicanum* Pat., *G. microsporum* R.S. Hseu, *G. parvulum* Murrill, *G. perturbatum* (Lloyd) Torrend, *G. perzonatum* Murrill, *G. pulverulentum* Murrill, *G. rivulosum*, *G. sessiliforme* Murrill,

G. stipitatum (Murrill) Murrill, *G. subamboinense* var. *subamboinense*, *G. subamboinense* var. *laevisporum*, *G. subincrustatum* Murrill, and *G. vivianimercedianum* M. Torres were re-examined. Strains examined during this study were deposited at CBS, CIRM-CF, and BCCM/MUCL. The formation of chlamydospores was examined after growing the strains on malt extract agar medium at 25 °C over four weeks according to previous results of Bazzalo and Wright (1982).

The microscopic observations procedure followed Decock et al. (2007). Specimen sections were mounted in 5% KOH solution. Melzer's reagent and cotton blue were used to test the amyloidity or dextrinoidity and cyanophyly of the microscopic structures, respectively. Microscopic characters were observed under a light microscope Axioscope 40 Carl Zeiss. Images were captured using Axio Vision 4 software on the same microscope. At least 30 structures of each mature specimen were measured. Basidiospores were measured without taking in account the apical umbo when not shrunk. Cuticular cells were measured from the middle part of the basidiome except in the case of some type materials, where only a fragment was received as loan. The 5% extremes of all microscopic measurements from each size range were given in parentheses and the arithmetic mean was provided in brackets. Color terms follow Kornerup and Wanscher (1963), and terms in descriptions are defined in Torres-Torres and Guzmán-Dávalos (2012).

DNA sequencing

Genomic DNA from herbarium specimens was extracted using three protocols: (I) CTab method with 1% PVP (Palomera et al. 2008), (II) salt-extraction method with 1% PVP (Aljanabi and Martinez 1997), and (III) Wizard Genomic DNA Purification Kit (Promega) with 1% PVP. Modifications of the protocols, following Doyle and Doyle (1987) or Palomera et al. (2008), were occasionally made. Genomic DNA was extracted from living cultures according to Amalfi et al. (2010, 2012).

The ITS region (ITS1, 5.8S, and ITS2) was amplified from dried specimens using the primer pairs G-ITS-F1/ITS4B (Cao et al. 2012) or ITS1F/ITS4B (Gardes and Bruns 1993), and from living cultures using the primer pairs ITS1F/ITS4 (White et al. 1990). The primers bRPB2–6F/bRPB2–7.1R (Matheny 2005) and CF2–EF983F/CR2–EF2218R (Rehner and Buckley 2005, Matheny et al. 2007) were used to amplify the *rpb2* and *tef1–α* regions, respectively.

Polymerase chain reaction (PCR) to amplify the ITS from dried specimens followed Guzmán-Dávalos et al. (2003) with some modifications. Each 52 µl reaction solution contained 50 µl of PCR mix [35 µl of MilliQ water, 6 µl of 10 X Taq reaction buffer without $MgCl_2$, 3 µl of 50 mM $MgCl_2$, 3 µl of 5 mM dNTP, 3 µl of 2 µg/µl Bovine Serum Albumine (BSA)], 0.5 µl of each 10 µM primer, 0.15 µl of Taq DNA polymerase (5U/µl), and 1 µl of DNA template (1:5 dilution). PCR amplifications were performed in an ESCO Swift MaxPro thermocycler as described by Guzmán-Dávalos et al. (2003), except that the annealing temperature was following Cao et al.

(2012). PCR products were purified with the GFXTM PCR DNA Purification Kit (GE Healthcare). Purified products (GFX) were sent to the Sequencing Department, University of Arizona and LaniVeg (CUCBA, University of Guadalajara). Polymerase chain reactions and amplification protocol of the ITS regions (including 5.8S), partial *tef1–α* gene, and the region of *rpb2* from cultures were described in Amalfi et al. (2010, 2012) and Decock et al. (2013). Sequences were assembled and edited with SequencherTM 4.8 software (Gene Codes Corp., Ann Arbor, Michigan).

Phylogeny

Two DNA sequence data sets were compiled: an ITS data set and a concatenated ITS, *rpb2*, and *tef1–α* data set. The combined data set comprised DNA sequences from 71 specimens/cultures from Africa, Europe, Meso– and South America, and Southeast Asia (Table 1). It included sequences from the types of *G. microsporum*, *G. subamboinense*, and *G. subamboinense* var. *laevisporum*. Sequences of 35 ITS, nine *rpb2*, and 13 *tef1–α* were downloaded from GenBank (www.ncbi.nlm.nih.gov/genbank/). It was subdivided into 11 partitions: ITS1, 5.8S, ITS2; *rpb2* and *tef1–α* introns, and –1st, –2nd, and –3rd codon positions of *rpb2* and *tef1–α*. *Ganoderma curtisii* (Berk.) Murrill and *G. lucidum* (Curtis) P. Karst. were selected as the outgroup according to results shown by Moncalvo (2000).

The ITS data set was composed by 30 specimens/cultures, of which 29 originated from the Neotropics (Table 1). It was subdivided into three partitions: ITS1, 5.8S, ITS2. In this case, *G. austroafricanum* M.P.A. Coetzee, M.J. Wingf., Marinc. & Blanchette was selected as outgroup according to the results obtained by Coetzee et al. (2015).

All sequences were automatically aligned with MUSCLE (Robert 2004) and manually adjusted using PhyDe (Müller et al. 2010). PartitionFinder (Lanfear et al. 2012) was used to determine the best evolutionary model for each gene using the corrected Akaike information criterion (AICc). Maximum Likelihood (ML) analyses were conducted using RAxML 7.0.4 (Stamatakis 2006) and Bayesian Inference (BI) analyses with MrBayes v.3.2.2 (Ronquist and Huelsenbeck 2003). In the ML analysis, the default priors were used, including individual parameters for each partition, performing 1000 replicates under the GTRGAMMA model. BI analyses were run on CIPRES Science Gateway (Miller et al. 2010). Two independent runs, with 4,000,000 generations each, were carried out with a sampling frequency every 1000 generations and a burn-in of 25%. A 50% majority rule consensus tree with posterior probabilities (PP) was obtained. Convergence of the Markov chains to a stationary distribution was assessed by visual examination of the log likelihood values in the program Tracer v1.7.1 (Rambaut et al. 2018). Nodes were considered supported when bootstrap values (BS) were ≥ 75% and the PP was ≥ 0.85. The final alignments were deposited in TreeBASE (www.treebase.org), under accession ID: 24140 (http://purl.org/phylo/treebase/phylows/study/TB2:S24140).

Table 1. DNA sequences of *Ganoderma weberianum-resinaceum* complex and outgroup used in this study, with their voucher materials and geographic origin.

Species name	Voucher/strain	Locality	GenBank accession numbers			Reference
			ITS (ITS1/ITS2)	***rpb2***	***tef1-α***	
G. austroafricanum	CBS 138724	South Africa	KM507324	**MK611970**		Coetzee et al. 2015
G. curtisii	CBS 100132	USA	JQ781848	KJ143967	KJ143927	Cao et al. 2012
G. boehnelianum	Cui 13982	China	MG279178	MG367515	MG367570	Xing et al. 2018
	Dai 11995	China	KU219988			Xing et al. 2018
	Yuan 6337	China	MG279160	MG367498	MG367551	Xing et al. 2018
G. lucidum	K 175217	UK	KJ143911	KJ143971	KJ143929	Zhou et al. 2014
	MUCL 31549	France	**MK554777**	**MK554765**	**MK554730**	This study
	MUCL 35119	France	**MK554779**	**MK554752**	**MK554719**	This study
G. mexicanum	D. Jarvio 143	Mexico	**MK531823**			This study
	MUCL 49453 SW17	Martinique	**MK531811**	**MK531836**	**MK531825**	This study
	MUCL 55832	Martinique	**MK531815**	**MK531839**	**MK531829**	This study
	MUCL 57308/ BRFM1548	Martinique	**MK531818**	**MK531842**	**MK531831**	This study
	MUCL 57309/ BRFM1830	Martinique	**MK531819**	**MK531843**	**MK531833**	This study
	MUCL 57310/ BRFM1851	Martinique	**MK531820**	**MK531844**	**MK531832**	This study
G. microsporum	RSH0821 (TYPE)	Taiwan	X78751/ X78772			Moncalvo et al. 1995
G. parvulum	E. Fletes 7619	Costa Rica	**MK531821**			This study
	MUCL 43863	Cuba	**MK554769**	**MK554745**	**MK554739**	This study
	MUCL 44148	Cuba	**MK531132**	**MK531845**	**MK531834**	This study
	MUCL 46029	Cuba	**MK554767**	**MK554749**	**MK554725**	This study
	MUCL 47074	Cuba	**MK554782**	**MK554759**	**MK554729**	This study
	MUCL 47096	Cuba	**MK554783**	**MK554742**	**MK554721**	This study
	MUCL 52655	French Guiana	**MK554770**	**MK554755**	**MK554717**	This study
	MUCL 53123	French Guiana	**MK531814**	**MK531837**	**MK531827**	This study
	MUCL 53712	French Guiana	**MK531813**	**MK531838**	**MK531828**	This study
	MUCL 57307/ BRFM1043	French Guiana	**MK531817**	**MK531841**	**MK531830**	This study
G. platense	BAFC384	Argentina	AH008109			Gottlieb et al. 2000
G. polychromum	330OR	USA	MG654196		MG754742	Loyd et al. 2018
	MS343OR	USA	MG654197		MG754743	Loyd et al. 2018
G. resinaceum	CBS 194.76	Netherlands	KJ143916		KJ143934	Zhou et al. 2014
	HMAS 86599	UK	AY884177	JF915435		Wang et al. 2012
	MUCL 38956	Netherlands	**MK554772**	**MK554747**	**MK554723**	This study
	MUCL 40604	Belgium	**MK554766**	**MK554743**	**MK554722**	This study
	MUCL 51491	Belgium	**MK554775**	**MK554741**	**MK554733**	This study
	MUCL 52253	France	**MK554786**	**MK554764**	**MK554737**	This study
	Rivoire 4150	France	KJ143915			Zhou et al. 2014
G. sessile	111TX	USA	MG654306	MG754866	MG754747	Loyd et al. 2018
	117TX	USA	MG654309	MG754868	MG754749	Loyd et al. 2018
	BAFC2373	Argentina	AH008111			Gottlieb et al. 2000
	CBS 220.36	USA	JQ520201			Park et al. 2012
	JV 1209/27	USA	KF605630	KJ143976	KJ143937	Zhou et al. 2014
	JV 1209/9	USA	KF605629		KJ143936	Zhou et al. 2014
	MUCL 38061	USA	**MK554778**	**MK554754**	**MK554736**	This study
	NY 00985711	USA	KJ143918			Zhou et al. 2014

Species name	Voucher/strain	Locality	GenBank accession numbers			Reference
			ITS (ITS1/ITS2)	***rpb2***	***tef1***-α	
G. stipitatum	THC 16	Colombia	KC884264			Submission to GenBank
G. subamboinense	Ule.2748/F 15183 (TYPE)	Brazil	**MK531824/ MK531822**			This study
G. subamboinense var. *laevisporum*	BAFC 745/ ATCC 52420	Argentina	JQ520205			Park et al. 2012
	BAFC 25225/ ATCC 52419/ BAFC 247/ (TYPE)	Argentina	X78736/ X78757			Moncalvo et al. 1995
	FLASF59210	USA	MG654371			Loyd et al. 2018
	UMNFL100	USA	MG654373		MG754762	Loyd et al. 2018
	UMNFL32	USA	MG654372		MG754761	Loyd et al. 2018
G. weberianum	15–1048	USA	KU214242			Submission to GenBank
	CBS 128581	Taiwan	**MK603805**	**MK611971**	**MK636693**	This study
	CBS 219.36	Philippines	**MK603804**	**MK611972**	**MK611974**	This study
	CCRC 37081	Taiwan	Z37064/ Z37086			Smith and Sivasithamparam, 2000
	DFP8401	Australia	EU239393			Smith and Sivasithamparam, 2000
	GanoTK16	Cameroon	JN105704			Kinge et al. 2012
	Guzmán–Dávalos 9569	Mexico	**MK554771**			This study
	GW–10	India	GU726934			Mohanty et al. 2011
	GW–11	India	GU726935			Mohanty et al. 2011
	HMAS97365	China	JF915411	JF915434		Wang et al. 2012
	SUT H2	Australia	AY569451			Submission to GenBank
	B–18	Cuba	JN637827			Manzano et al. 2013
Ganoderma sp.	MUCL 43285	Cameroon	**MK554773**	**MK554762**	**MK554731**	This study
	MUCL 43522	Cuba	**MK554792**	**MK554760**	**MK554732**	This study
	MUCL 46912	China	**MK554791**	**MK554758**	**MK554734**	This study
	MUCL 47495	Gabon	**MK554785**	**MK554753**	**MK611976**	This study
	MUCL 47536	Gabon	**MK554768**	**MK554746**	**MK554724**	This study
	MUCL 47542	Gabon	**MK554780**	**MK554757**	**MK554716**	This study
	MUCL 47543	Gabon	**MK554774**	**MK554763**	**MK554718**	This study
	MUCL 47828	China	**MK554788**	**MK554740**	**MK554728**	This study
	MUCL 47835	China	**MK554781**	**MK554756**	**MK554727**	This study
	MUCL 49266	Cameroon	**MK554784**	**MK554750**	**MK554738**	This study
	MUCL 49272	Cameroon	**MK603806**	**MK611973**	**MK611975**	This study
	MUCL 49277	Cameroon	**MK554776**	**MK554744**	**MK554720**	This study
	MUCL 49980	Congo DRC	**MK554789**	**MK554748**	**MK554735**	This study
	MUCL 49981	Congo DRC	**MK554787**	**MK554761**	**MK554726**	This study
	MUCL 51856	Taiwan	**MK554790**	**MK554751**		This study
	MUCL 52843	Gabon	**MK531812**	**MK531835**	**MK531826**	This study
	MUCL 57035	Kenya	**MK531816**	**MK531840**		This study
	UH–L	Cuba	LT726730			Torres-Farradá et al. 2017
	UH–M	Cuba	LT726731			Torres-Farradá et al. 2017

Bold names= newly generated sequences for this study.

Results

Molecular phylogeny

The combined dataset contained 172 DNA sequences: 71 ITS, 50 *rpb2*, and 51 *tef1–α*. The final alignment comprised 526 bp in the ITS, 776 in the *rpb2*, and 1123 in the *tef1–α*. The concatenated data set (ITS + *rpb2* + *tef1–α*) was 2425 bp long. From it, 23 ambiguous sites (12 from ITS1 and ITS2, 11 from *tef1–α* introns) were removed. The evolutionary models that best fit the individual dataset according to the AICc criterion were ITS1 = GTR+I+G, 5.8S = K80, ITS2 = GTR+I+G, *rpb2* 1st = GTR+I, 2nd = HKY+G, 3rd codon positions = HKY+G, *rpb2* intron= K80, *tef1–α* 1st = GTR+I, 2nd = HKY+G, 3rd codon positions = GTR+G, and *tef1–α* intron = GTR+I. In BI analyses, the average standard deviation of split frequencies was 0.008100 in the concatenated data set and 0.008875 in the ITS data set. As far as our specimens from the Neotropics are concerned, the phylogenetic trees obtained from Bayesian (not shown) and Maximum likelihood inferences using the concatenated (Fig. 1) and the ITS (Fig. 2) data sets showed overall the same two clades, except for the unsupported branch of the specimen MUCL 43522 present in the concatenated ML and BI analyses, which collapsed in the ITS tree, and the placement of the specimen UMNFL100, *G. subamboinense* var. *laevisporum*, from Florida (Figs 1–2).

The *Ganoderma weberianum-resinaceum* lineage was resolved with strong support (PP 1, BS 100%). It was divided into two major clades, I and II (Fig. 1). Clade I (PP 1, BS 98%) corresponded to the *G. resinaceum* clade as defined by Moncalvo (2000), with *G. austroafricanum*, from South Africa, located in a basal position. This was further subdivided in an unsupported clade A (PP 0.66, BS 58) and moderately supported clade B (PP 0.89, BS 82). Clade A included specimens all originated from the temperate area of the Northern Hemisphere and a specimen from the highlands of central Kenya (MUCL 57035). Clade A was structured into two subclades, A1 (PP 1, BS 100), with the Kenyan specimen (MUCL 57035) in basal position, and A2 (PP 1, BS 89), with a specimen from China (MUCL 46912) in basal position. Clade B brought together several specimens originated from both North and South America, distributed into three well-supported subclades that corresponded to *G. sessile* Murrill and *G. polychromum* (Copel.) Murrill (PP 1, BS 89; PP 0.99, BS 100), as defined by Loyd et al. (2018). Two specimens from Argentina, tentatively identified as *G. sessile* and *G. platense* Speg., formed together a third distant well-supported subclade (PP 1, BS 99).

Clade II (PP 1/BS 99) was subdivided into two major clades: clade C (PP 1, BS 95) and clade D (PP 1, BS 100). Clade C corresponded to *G. weberianum sensu* Steyaert. It was further structured into two well-supported subclades, C1 (PP 1, BS 91) and C2 (PP 1, BS 74), with a geographic dichotomic pattern opposing the New World / Neotropics (C1) to the Old World / Paleotropics (C2).

New World / Neotropical clade (C1) had two low- to moderately supported terminal clades, C1.1 (PP 0.89, BS 86) and C1.2 (PP 0.80, BS 62). C1.1 included the ex-type strain of *G. subamboinense* var. *laevisporum* (BAFC 247, Bazzalo and Wright 1982) from

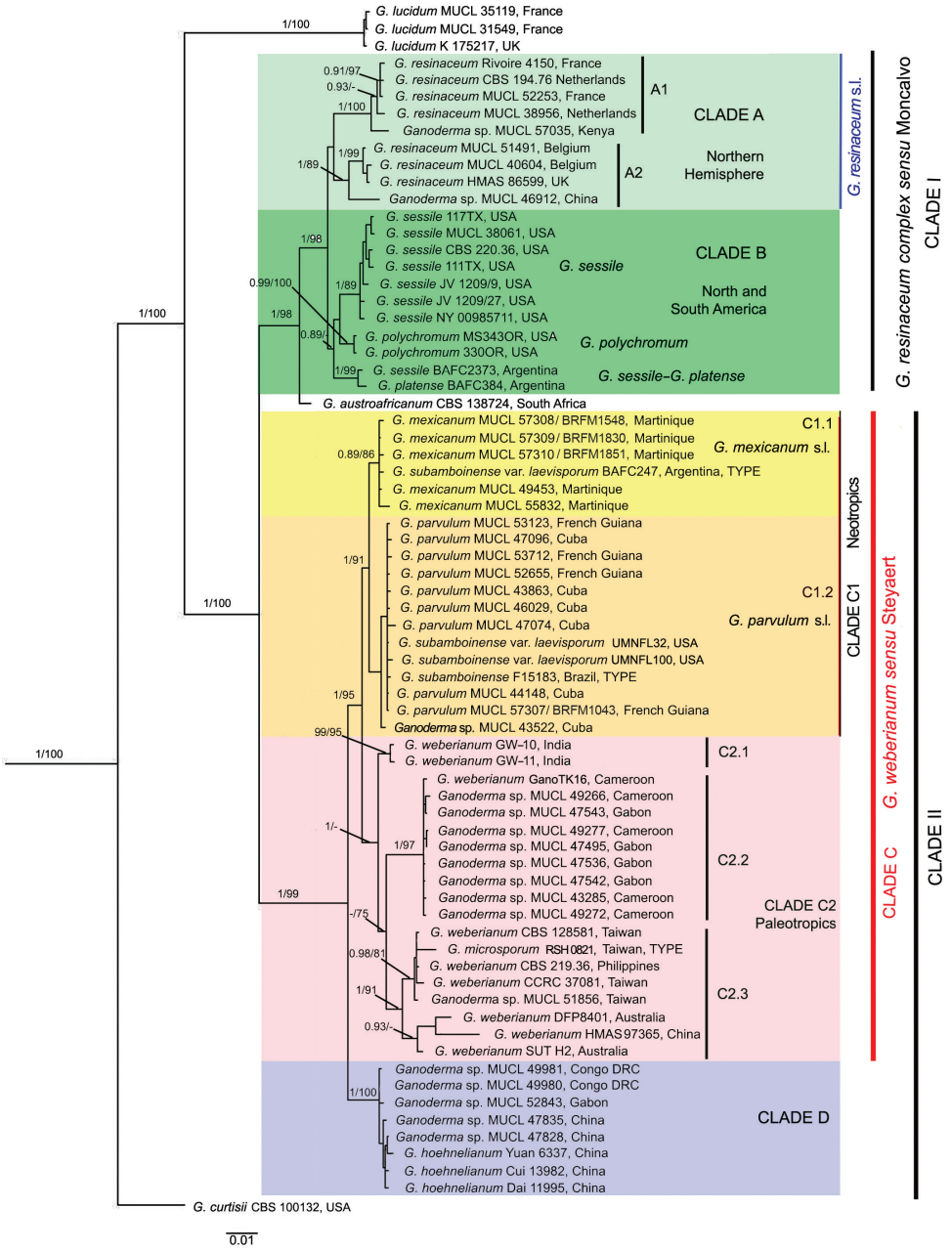

Figure 1. Phylogeny of the *Ganoderma weberianum-resinaceum* complex based on concatenated ITS, *rpb2*, and *tef1-α* sequence data obtained by Maximum Likelihood (ML). Bayesian posterior probability (PP) above 0.85 and bootstrap values (BS) from ML above 75 % are shown (PP/ BS).

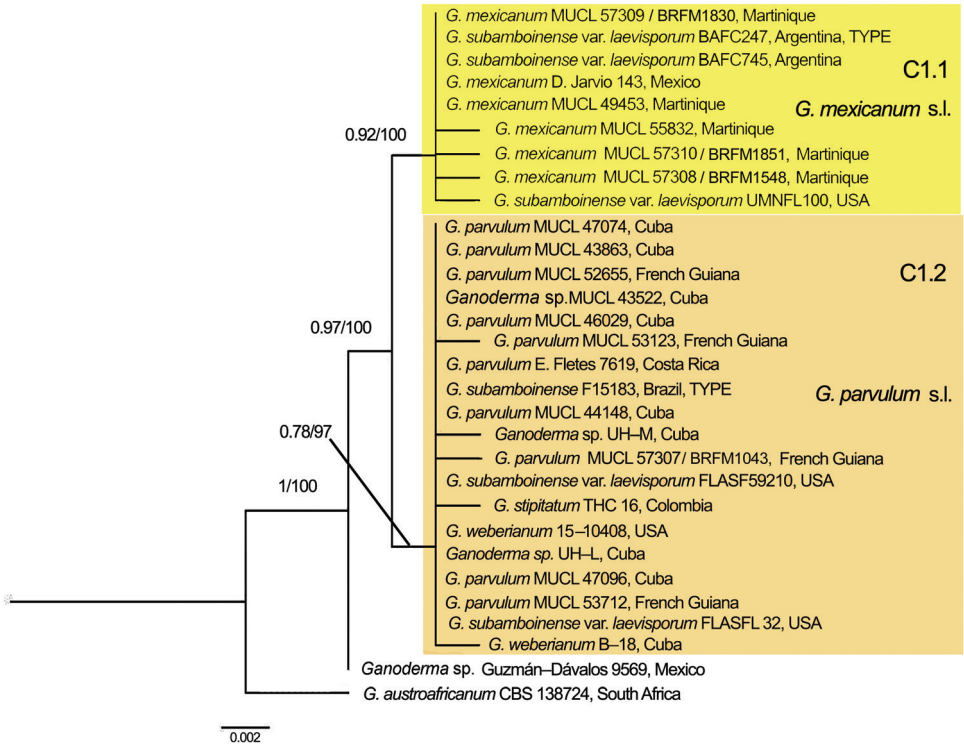

Figure 2. Phylogeny of the *Ganoderma weberianum* complex from the Neotropics based on rDNA ITS sequence data obtained by Maximum Likelihood (ML). Bayesian posterior probability (PP) above 0.85 and bootstrap values (BS) from ML above 75 % are shown (PP/BS).

Argentina and five specimens from Martinique, of which one was identified previously as *G. subamboinense* (Welti and Courtecuisse 2010) and three as *G. weberianum* (CIRM-CF, on-line catalog). Its sister clade, C1.2, comprised the type specimen of *G. subamboinense* (S F15183!) and ten specimens from Cuba and French Guiana, of which one was identified as *G. weberianum* (CIRM-CF, on-line catalog). It also comprised two specimens from Florida, which were both, alternatively identified as *G. subamboinense* var. *laevisporum* at GenBank, or as *G.* cf. *weberianum* in Loyd et al. (2018).

The Old World / Paleotropical clade (C2) contained specimens from both Africa and Asia. This clade was further subdivided into three well-supported subclades, *viz.* C2.1 (PP 0.99, BS 95), with two specimens from India, C2.2 (PP 1, BS 97) gathering specimens from Central Africa (Cameroon and Gabon), and C2.3 (PP 1, BS 91) with specimens from Australia and Southeast Asia (China, Philippines, and Taiwan). A specimen from Australia (DFP 8401) in clade C2.3 was identified as *G. rivulosum* by Steyaert (*fide* Smith and Sivasithamparam 2000) and reidentified as *G. weberianum* by Smith and Sivasithamparam (2000). The C2.3 also included the ex-type strain of *G. microsporum* (RSH0821, BPI) from Taiwan.

Finally, clade D (PP 1, BS 100) comprised specimens of *Ganoderma* sp. from Central Africa (DR Congo and Gabon) and from China, these latter tentatively identified as *G. hoehnelianum* Bres. at GenBank (Fig. 1).

The ITS data set comprised sequences from thirty specimens (Table 1) and the final alignment had 536 positions. Five positions, the alignments of which were judged to be ambiguous, were removed from the analyses. Clades C1.1 (PP 0.92, BS 100) and C1.2 (PP 0.78, BS 97) were confirmed by the ITS data set (Fig. 2). A specimen from Mexico (Guzmán-Dávalos 9569, IBUG), previously identified as *G. weberianum* by Torres-Torres et al. (2015), formed an additional branch, basal and sister to C1.1 and C1.2 (Fig.2).

Taking in account both single and multilocus phylogenetic analyses, we considered that our Neotropical specimens formed two related but distinct, well-supported terminal clades, C1.1 and C1.2 (Figs 1–2) that could be equated each to a phylogenetic species. The additional branch formed by the single specimen from Mexico also might be equated to a distinct phylogenetic species.

Morphological studies

From a morphological perspective, specimens in the phylogenetic species C1.1 and C1.2 were very similar, characterized by an overall reddish brown to violet brown pileal surface, light, cork-colored context, occasionally paler in the upper zone —described as not fully homogenous by Torres-Torres et al. (2012)—, with none to several (up to 4) dense, brown stripes or continuous lines of resinous deposits extending from the base of the context toward the margin. The cuticular cells were mainly cylindrical to clavate, apically rounded, regular, amyloid, and the basidiospores ovoid to broadly ovoid, with free to subfree pillars, and chlamydospores ("gasterospores" in Bazzalo and Wright 1982) in their context (Figs 3–4).

These chlamydospores were mostly subglobose in the context of the basidiomes and more variably shaped in pure culture on artificial media, thick-walled, hyaline to yellowish, and with dextrinoid content. In the specimens of C1.1, the chlamydospores were constantly, permanently smooth-walled (Fig. 3D–F, I) whereas in specimens of C1.2, they were smooth becoming roughened on aging, with free to partially anastomosed fine ridges with a meridian orientation (Fig. 4E–H, K). The Mexican specimen (Guzmán-Dávalos 9569, IBUG!) also presented chlamydospores in the context but they were punctuated, ornamented with thick pillars (Fig. 5).

Basidiospores were slightly wider in specimens from C1.1 compared to those of C1.2, mainly 8–9 × 6–7 µm (averaging 8.5 × 6.5 µm, Fig. 3C, H) vs. 8–9.5 × 5.5–6.5 µm (averaging 8.9 × 6.0 µm, Fig. 4C–D). Cuticular cells were moderately longer in specimens from C1.2 (up to 100 µm long, Fig. 4B, J) than specimens in C1.1 (up to 65 µm long, Fig. 3B, G).

In general, the morphology allowed the distinction of three morphotypes, which could be considered as three morphospecies. Each of these also corresponded to a phylogenetic species.

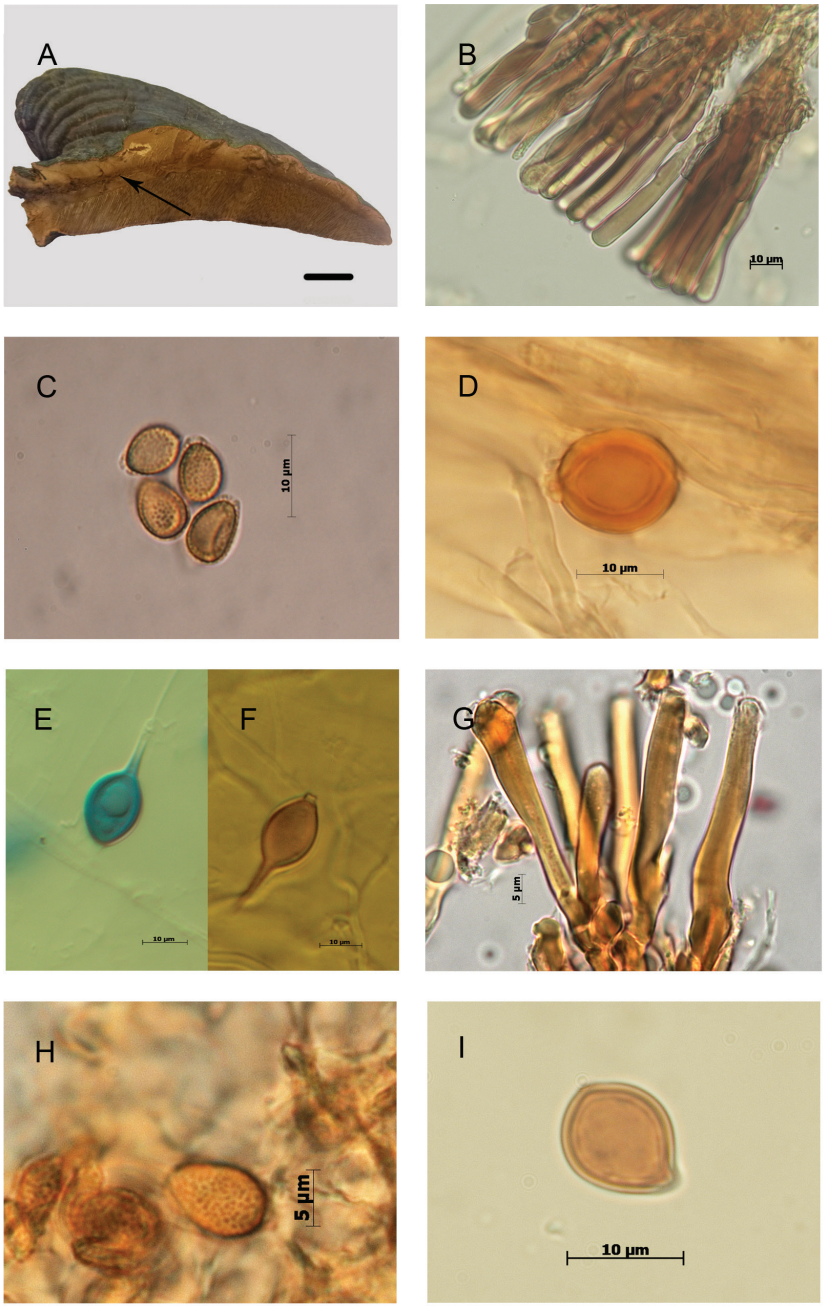

Figure 3. Morphological features and microscopic structures of *Ganoderma mexicanum* **A–F** J.P. Fiard SW 17 (as *G. subamboinense* in Welti and Courtecuisse 2010) **A** pileus and context not fully homogeneous with discrete bodies of the resin-like deposits (arrow) **B** cuticular cells **C** basidiospores with free to subfree pillars **D–F** smooth-walled chlamydospores **D** from context **E** from culture, in cotton blue **F** from culture, in Melzer reagent **G–I** BAFC 25525 (as *G. subamboinense* var. *laevisporum*, holotype) **G** cuticular cells **H** basidiospores with free to subfree pillars **I** smooth-walled chlamydospore from context.

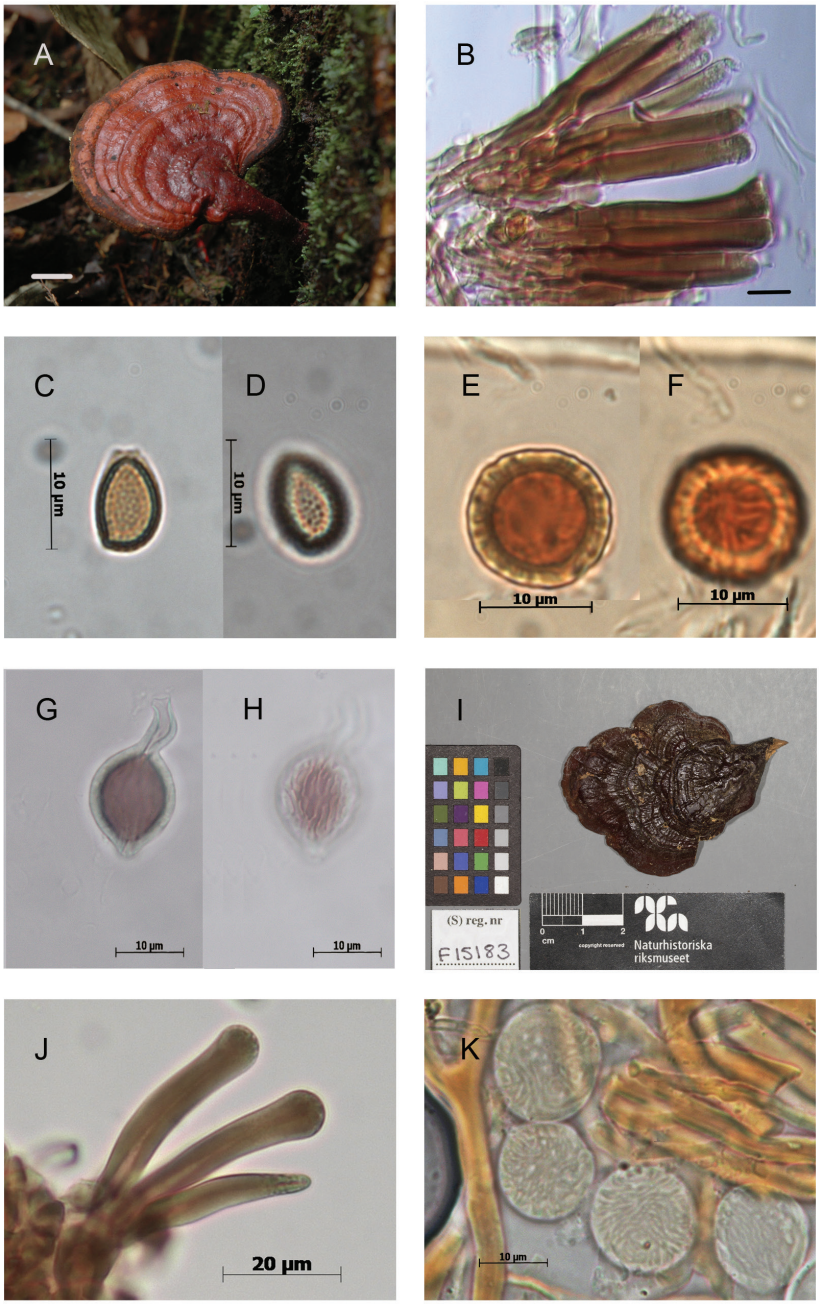

Figure 4. Morphological features and microscopic structures of *Ganoderma parvulum* **A–H** MUCL 53123 **A** pilear surface **B** cuticular cells **C–D** basidiospores with free to subfree pillars **E–H** chlamydospores ornamented with free to partially anastomosed ridges **E–F** from context **G–H** from culture **I–K** E. Ule 2748 (as *G. subamboinense*, holotype) **I** upper surface of basidiomata, copyright: Naturhistoriska riksmuseet, Stockholm **J** cuticular cells **K** chlamydospores ornamented with partially anastomosed ridges, from context, in KOH. Scale bars: 1 cm (**A**); 5 µm (**B**).

Taxonomic conclusions

The present study, using single and multilocus phylogenetic inferences combined with morphological and *in vitro* culture studies, concordantly revealed two species of *Ganoderma* in the *G. weberianum sensu* Steyaert lineage, spanning over the Neotropics. Furthermore, a specimen from Mexico, represented only by the ITS sequence (Guzmán-Dávalos 9569, Figs 2 & 5), also could be equated to a morphological and phylogenetic species, pending confirmation when additional material is available. However, none of these three species could be equated to *G. weberianum sensu* Moncalvo (Moncalvo 2000), which is restricted to tropical Asia.

Clade C1.1 contained the ex-type strain of *G. subamboinense* var. *laevisporum*; hence, it could correspond to this taxon. The sister clade C1.2 contained the ex-type strain of *G. subamboinense* var. *subamboinense*; thus, it could correspond to the typical variety. Furthermore, both the molecular and morphological data would warrant recognition of both varieties at species level.

Ganoderma subamboinense was originally described by Hennings (1904) as *Fomes subamboinense* Henn. The type specimen originated from Brazil. Bazzalo and Wright (1982) accepted the species and distinguished a var. *laevisporum* from the typical variety. Both varieties were characterized by the presence of chlamydospores in their context, which were rough-walled with "veins anastomosing to form a sort of reticulum" in the typical variety, and smooth-walled in var. *laevisporum*, what was later confirmed by Gottlieb and Wright (1999). Ryvarden (2000), based on presumed morphological resemblance, reduced *G. subamboinense* s.l. (both varieties) as a synonym of *G. multiplicatum* (Mont.) Pat. Similarities between *G. subamboinense* var. *laevisporum* and *G. multiplicatum* var. *vitalii* Steyaert were previously reported (Bazzalo and Wright 1982). Inversely, Torres-Torres et al. (2012) recognized *G. multiplicatum* as an independent species that could be differentiated from *G. subamboinense* s.l., e.g., in having apically irregular cuticular cells, with many protuberances. Steyaert (1980) had already characterized *G. multiplicatum* var. *vitalii* with "mostly irregular" cuticular cells.

The revision of a fragment of the holotype of *G. subamboinense* var. *subamboinense* (S F15183!) (Fig. 4I–K) and of the holotype of *G. subamboinense* var. *laevisporum* (BAFC 25525!) (Fig. 3G–I) confirmed the previous observations (Bazzalo and Wright 1982, Gottlieb and Wright 1999). Both varieties are mainly characterized by a pale context with resinous incrustations or thin resinous brown bands, stretching from base towards the margin, cylindrical to clavate, apically regular, amyloid cuticular cells, ovoid to broadly ovoid basidiospores with free to subfree pillars, and chlamydospores in their context. The chlamydospores were striated in the typical variety and smooth-walled in var. *laevisporum*.

The study of the holotype of *G. multiplicatum* (K 123639!), originating from French Guiana, confirmed irregular cuticular cells with both lateral and apical protuberances, distinct from those of both varieties of *G. subamboinense*. Phylogenetic analyses inferred from an ITS data set (Bolaños et al. 2016) or a combined ITS–LSU data set (de Lima-Junior et al. 2014) also showed that *G. subamboinense* var. *laevisporum* (ITS sequence from the ex-type culture ATCC 52419) and *G. multiplicatum* (that should be

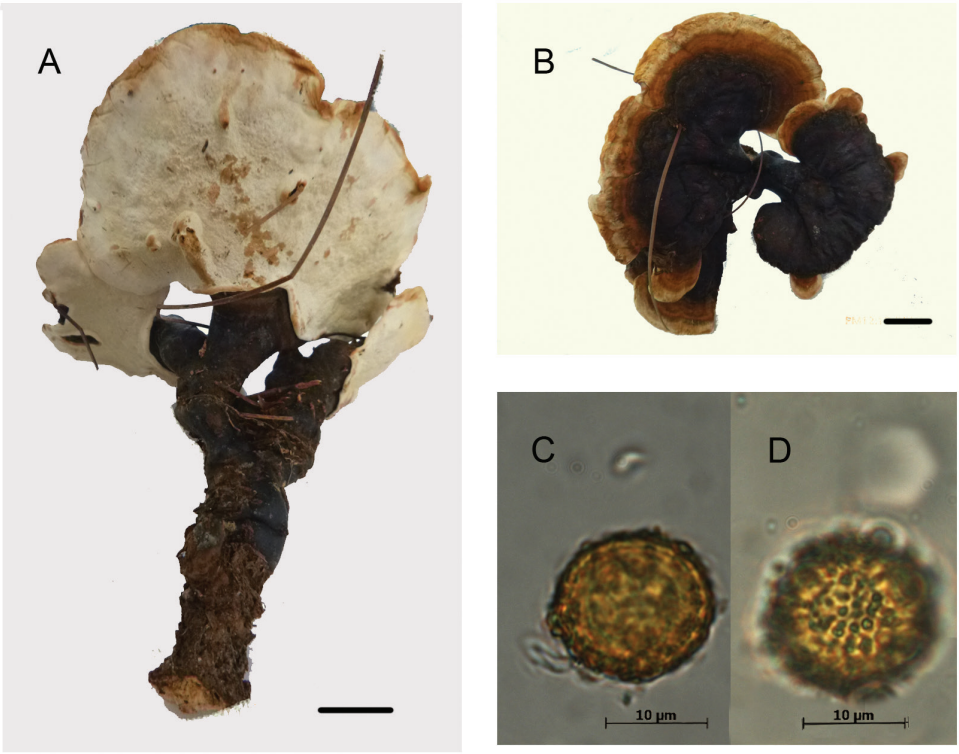

Figure 5. *Ganoderma* sp., Mexican specimen Guzmán-Dávalos 9569 (as *G. weberianum* in Torres-Torres et al. 2015) **A** stipitate basidioma **B** pilear surface **C–D** Detail of chlamydospore ornamented with pillars. Scale bar: 1 cm (**A–B**).

considered as *sensu auctores*) formed two distinct clades, in two distant lineages. Hence, the synonymy of *G. subamboinense* and *G. multiplicatum*, as suggested by Ryvarden (2000), here also is rejected.

The macro- and microscopic features of both varieties of *G. subamboinense*, overall, corresponded to those of our specimens from C1.1 and C1.2 clades, as described above. Therefore, *G. subamboinense* var. *subamboinense* (C1.2) and *G. subamboinense* var. *laevisporum* (C1.1) could be applied to the taxa shown by these clades. However, for nomenclatural reasons, the varietal epithet *laevisporum* cannot be used, at any rank. The nomenclatural status of the epithet *laevisporum* was questioned; as previously highlighted, it was invalidly published (Moncalvo and Ryvarden 1997, Welti and Courtecuisse 2010). Moncalvo and Ryvarden (1997) noted that Bazzalo and Wright (1982) did not formally propose the combination *G. subamboinense*, making it invalid; consequently, the varietal epithet also was invalid. Moncalvo and Ryvarden (1997) validated the combination *G. subamboinense* but this did not automatically validate the varietal epithet, which, therefore, cannot be used. A name, therefore, should be found for the taxon shown by the C1.1.

Furthermore, several other names whose types originate from the Neotropics but currently of uncertain status or in the limbo of the *G. weberianum-resinaceum* complex (Moncalvo and Ryvarden 1997, Ryvarden 1985, 2000, 2004) also could be reconsidered for species represented by both clades. Taking into account the main features of our specimens as described above, such as a light-colored context, *G. argillaceum*, *G. mexicanum*, *G. parvulum*, *G. perturbatum*, *G. perzonatum*, *G. praelongum* Murrill, *G. pulverulentum*, *G. sessiliforme*, *G. stipitatum*, *G. subincrustatum*, and *G. vivianimercedianum* (Patouillard 1898, Murrill 1902, 1903, 1908, 1912, Steyaert 1962, 1980, Torres-Torres et al. 2008) were worth revisiting.

Ganoderma mexicanum (holotype: FH 458184!) is the earliest name potentially available. It should be treated together with *G. sessiliforme* (holotype: NY 98713!); both type specimens are originated from neighboring localities in Morelos State, Mexico, *viz*. Tepalcingo, D. de Jonacatepec (Patouillard 1898) and Cuernacava (Murrill 1912), respectively. Torres-Torres et al. (2012) emphasized the poorly conserved type of *G. mexicanum* (Fig. 6) and reported an additional specimen from Brazil. On the basis of these two specimens, Torres-Torres et al. (2012) described clavate to narrowly clavate, 35.2–72.4 × 6.8–10.5 µm cuticular cells with very thick wall, without apical granulations, and ellipsoid basidiospores, 9.3–10.6 × 6.2–7.4 µm, with subfree pillars. Our study of the type specimen of *G. mexicanum* showed smaller, clavate to narrowly clavate cuticular cells, 25–37 × 5–7.5 µm, averaging 28.5 µm long, with occasional apical granulations. Basidiospores were ovoid with free to subfree pillars, (6.5–) 7.8–9.4 × 5.2–6.5 (–7) µm, and smooth, dextrinoid chlamydospores, 10.3–15 µm, were observed in the context (Fig. 6).

The study of the type specimen of *G. sessiliforme* (Fig. 7A–F) and of a second specimen collected in an area also neighboring the type locality (Guzmán 2078, ENCB, Fig. 7G–K, cf. Torres-Torres et al. 2015) revealed a pale context with a few resinous incrustations, scattered, smooth-walled, dextrinoid chlamydospores, (8–) 10–12 (–13.5) x 7–11 µm, clavate to narrowly clavate, smooth to sometimes faintly apically granulated cuticular cells, 25–38 × 5–9 µm, averaging 32 µm long, and ovoid basidiospores, 8–9.3 (–10.7) × 6–7.7 (–8) µm, with free to subfree pillars.

Based on these observations and inversely to the previous conclusions of Torres-Torres et al. (2012, 2015), we did not found any consistent morphological difference between *G. mexicanum* and *G. sessiliforme*. Furthermore, the type specimen of both names originated from neighboring localities and, probably, related ecosystems. Therefore, *G. sessiliforme* and *G. mexicanum* are here considered as synonyms, the latter epithet (Patouillard 1898) having priority. However, the status and affinities of *G. mexicanum* are uncertain.

Patouillard (1898) suggested that *G. mexicanum* was a sessile form of *G. lucidum* but with smooth ("*lisses*"), ovoid basidiospores. There is also a typewritten, undated note from R. Singer in the type specimen folder emphasizing "This is merely *Ganoderma sessile* Murr.", and then pencil corrected "same as [*G. sessile*]". Previously, Murrill (1902) also pointed out similarities between *G. sessiliforme* and *G. sessile*. Loyd et al. (2018) also suggested that *G. sessiliforme* might represent a synonym of *G. sessile*.

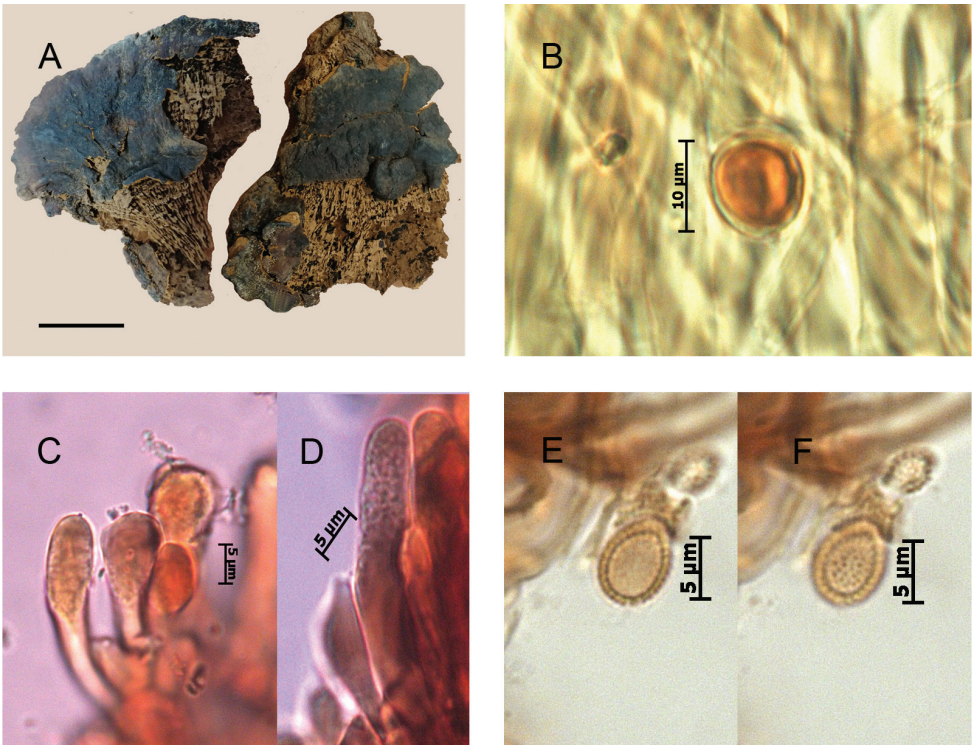

Figure 6. Morphological features and microscopic structures of the type specimen of *Ganoderma mexicanum* (P.J.B. Maury 4823, FH 458184), photographs by the authors, images courtesy of the Farlow Herbarium of Harvard University, Cambridge, Massachusetts, USA, **A** pilear surface **B** smooth chlamydospore **C–D** cuticular cells with incrustations **C** clavate **D** cylindrical **E–F** basidiospore with free to subfree pillars. Scale bars: 1 cm (**A**).

Nevertheless, *G. sessile* has distinctly larger basidiospores, 11.2–14.4 (–16.4) × 7.2–8.8 µm (*fide* Torres-Torres et al. 2015) and a duplex and spongy context (Torres-Torres et al. 2012, 2015), both features which would justify distinguishing these species.

Gottlieb and Wright (1999) and Gottlieb et al. (2000) previously compared *G. sessiliforme* with *G. subamboinense* var. *laevisporum*. They argued that *G. sessiliforme* differed from *G. subamboinense* var. *laevisporum* by the size (up to 11 mm long) and ornamentation ("semirugose" under the SEM) of its basidiospores, and the lack of chlamydospores, both features that do not stand (cf. above). The characters of *G. mexicanum*, especially the light-colored context with resinous incrustations, the basidiospores size, and the presence of smooth chlamydospores, overall remind much those of *G. subamboinense* var. *laevisporum* and of our specimens from the clade C.1.1 but for the cuticular cells. The cuticular cells are more clavate and shorter, 25–38 µm in *G. mexicanum* compared to those of *G. subamboinense* var. *laevisporum* and specimens from C1.1, 30–50 µm (Figs 3G & 6C–D).

Ganoderma parvulum (type NY 985699!) is the second earliest name potentially available. It should be treated together with *G. stipitatum*; the types of both epithets were

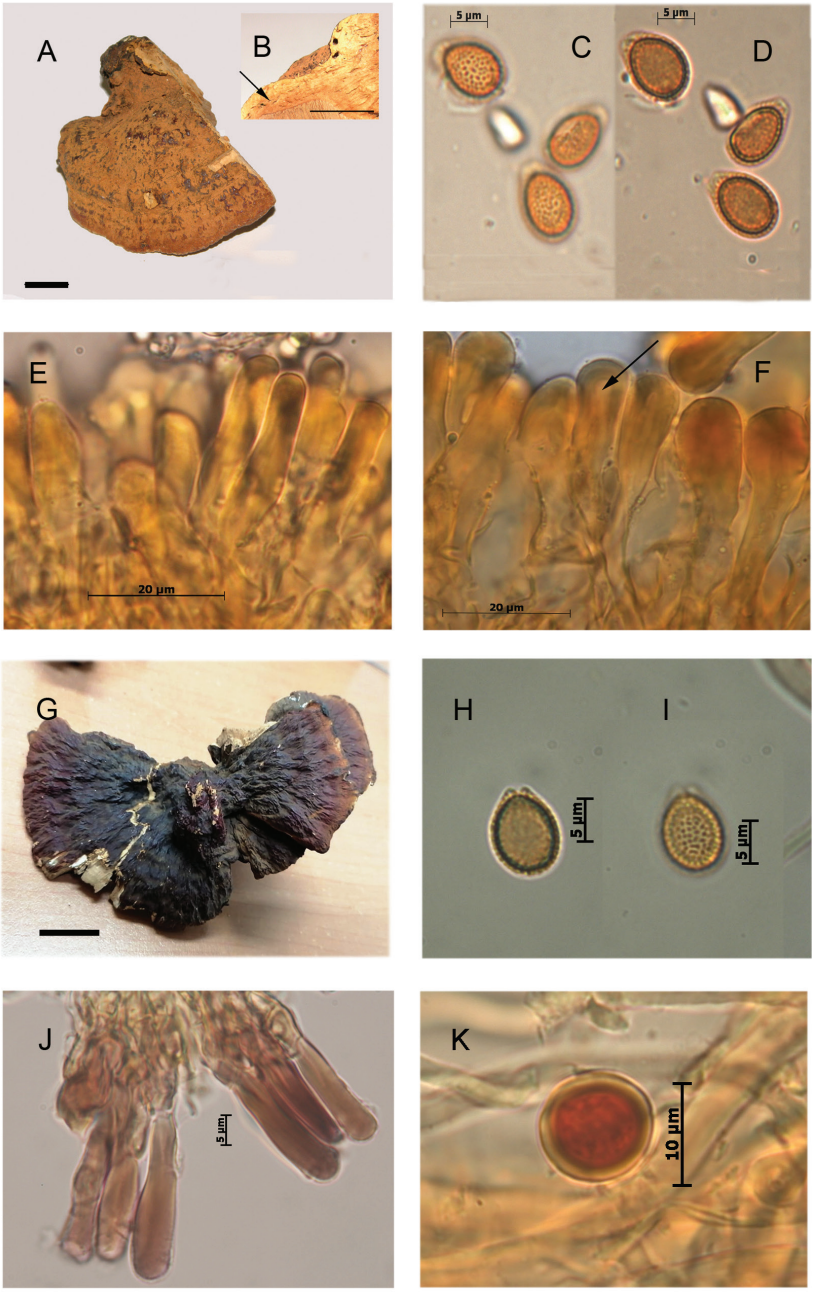

Figure 7. Morphological features and microscopic structures of *Ganoderma sessiliforme* **A–F** NY 98713 (holotype) **A** pilear surface **B** context not fully homogeneous with discrete bodies of the resin-like deposits (arrow) **C–D** basidiospores with free to subfree pillars **E–F** cuticular cells in KOH **E** cylindrical **F** clavate, with narrow lumen (arrow) **G–K** Guzmán 2078, ENCB **G** pilear surface **H–I** basidiospores with free to subfree pillars **J** cuticular cells in Melzer reagent **K** smooth-walled chlamydospore from context in Melzer reagent.

collected in Nicaragua by C.L. Smith (Murrill 1902, 1903), probably in neighboring localities. Steyaert (1980), based on type studies, although accepting these two taxa, considered they formed a species complex together with *G. bibadiostriatum* Steyaert, whose type was collected in Brazil (Steyaert 1962). Ryvarden, in a handwritten note dated from 1983, joint to the holotype of *G. stipitatum* (NY 985678!), concluded that *G. parvulum* and *G. stipitatum*, likely were synonyms ("the identity with *G. parvulum* Murr. is almost certain"), what he formalized later on, accepting a single species under *G. stipitatum*, with *G. bibadiostriatum* and *G. parvulum* as synonyms (Ryvarden 2000, 2004).

The examination of the type specimens of *G. parvulum* (NY 985699!) and *G. stipitatum* (NY 985678!) (Fig. 8A–E) revealed little developed, likely immature basidiomes. Murrill (1902) already suggested this, stating "It is possible that the specimens [of *G. parvulum*] I have are not quite mature". The type of *G. parvulum* was characterized by a pale context (pale ochraceous, *fide* Murrill 1902; light "ochraceous buff", *fide* Steyaert 1980), with resinaceous streaks, dark horny (*fide* Murrill 1902) or carob brown (*fide* Steyaert 1980). These resinaceous streaks were also present in the type of *G. stipitatum* (Murrill 1903, Steyaert 1980, Ryvarden 2004, pers. obs.). Cuticular cells were cylindrical to slightly clavate, average 50 µm long, and very few basidiospores were observed in holotype specimens. Ryvarden, in a handwritten note dated from 1983, emphasized the absence of basidiospores in the type of *G. stipitatum* ("spores are not present", NY 985678!). Nonetheless, Steyaert (1980) reported basidiospores, although without commenting on their abundance, 7.5–8.5 × 5.5–6.5 µm, averaging 8.1 × 5.9 µm in *G. parvulum* and 7.0–10.5 × 4.5–6.5 µm, averaging 7.8 × 5.5 µm in *G. stipitatum*. The few basidiospores we observed were 7–9 × 5–6.5 µm in *G. parvulum* and 7–10 × 5–6.5 µm in *G. stipitatum*, with free to subfree and very thin pillars in both.

Chlamydospores were not reported in the literature for *G. parvulum* nor for *G. stipitatum* (Steyaert 1972, 1980, Gottlieb and Wright 1999, Ryvarden 2000, 2004, Welti and Courtecuisse 2010), with the sole exception of Torres-Torres et al. (2012). Torres-Torres et al. (2012) reported and illustrated double-walled chlamydospores with "inter-walled, very thick pillars" presumably from the type of *G. parvulum* (cf. Torres-Torres et al. 2012, fig. 22d). However, their fig. 8, which is captioned as type of *G. parvulum*, actually corresponds to the type of *G. stipitatum* (NY 985678!). The voucher specimen from which these punctuated chlamydospores were observed remained uncertain. Nonetheless, our study of the type of *G. parvulum* and *G. stipitatum* revealed scattered chlamydospores in the context of both. These chlamydospores were smooth-walled or also ornamented with anastomosed ridges (Fig. 8D–E).

The likely immaturity of the type of *G. parvulum* and *G. stipitatum*, to a certain extent, could prevent definitive taxonomic interpretations. Notwithstanding, we would follow Ryvarden (2000, 2004) in considering that these two epithets represent a single species. Furthermore, the main macro- and microscopic characteristics of *G. stipitatum* and to a lesser extent, of *G. parvulum*, as described above, overall, also correspond to those of *G. subamboinense* var. *subamboinense.* Therefore, *G. parvulum*, *G. stipitatum*, and *G. subamboinense* could be considered synonymous. In this case, the epithet *parvulum*

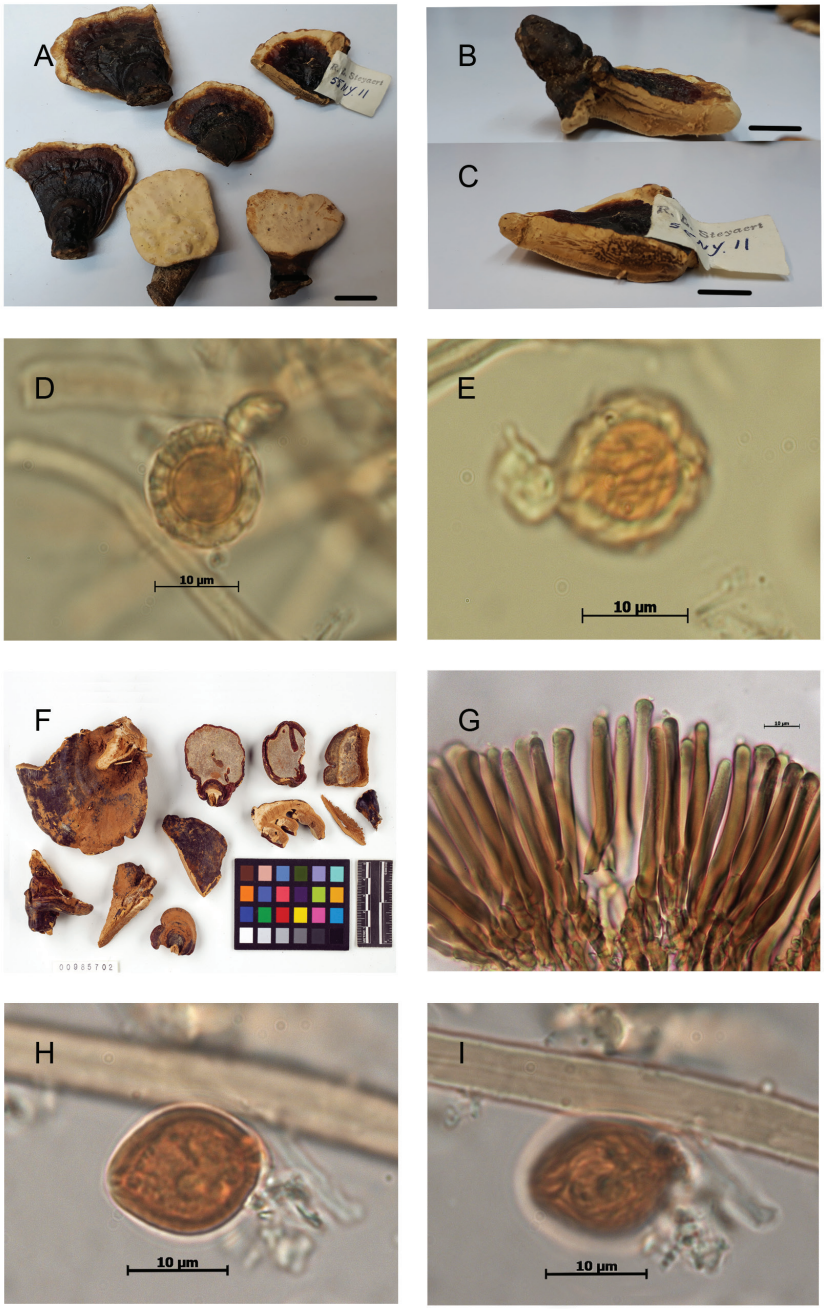

Figure 8. Morphological features and microscopic structures of type specimens of *Ganoderma* **A–E** *Ganoderma stipitatum* (NY 985678, holotype) **A** basidiomata **B–C** context **B** brown stripes of resinous deposits **C** numerous bodies of the resin-like deposits **D–E** chlamydospore, ornamented with partially anastomosed ridges, from context **F–I** *Ganoderma perzonatum* (NY 985702, holotype), **F** basidiomata, copyright: NY Botanical Garden **G** cuticular cells, cylindrical, with incrustations **H–I** chlamydospore with fine longitudinal ridges, from context. Scale bar: 1 cm (**A–C**).

(Murrill 1902) has priority over *subamboinense* (Hennings 1904) and *stipitatum* (basionym: *Fomes stipitatus* Murrill 1903), contrary to the conclusion of Ryvarden (2004).

Steyaert (1962, 1980), Bazzalo and Wright (1982), and Gottlieb and Wright (1999) recognized *G. bibadiostriatum* as a distinct species. *Ganoderma bibadiostriatum* was characterized by a distinctly brown (*fide* Bazzalo and Wright 1982, or cinnamon, *fide* Steyaert 1962, 1980) context and basidiospores 7.0–11.0 × 5.5–7.5 µm, averaging 9.3 × 6.5 µm (*fide* Steyaert 1980), or 9–11 × 6–8 µm (*fide* Gottlieb and Wright 1999). These features differed from those of *G. parvulum*. Through phylogenetic inferences based on ITS and LSU, de Lima-Junior et al. (2014) showed that Brazilian specimens identified as either *G. parvulum* or *G. stipitatum* (identifications that should be considered as *sensu auctores*) were gathered into a single clade, which nested within the *G. tropicum* clade sensu Moncalvo (2000), and were unrelated to *G. subamboinense* var. *laevisporum*, hence unrelated to the *G. weberianum-resinaceum* lineage. Therefore, contrary to Ryvarden (2000, 2004) but following Gottlieb and Wright (1999), we also rejected the synonymy of *G. bibadiostriatum* with *G. parvulum* and *G. stipitatum*. We suggest that the identity of the *G. parvulum–G. stipitatum* clade shown by de Lima-Junior et al. (2014) should be re-evaluated, and that it might well represent *G. bibadiostriatum*.

The status and affinities of *G. perzonatum* have been debated and still are uncertain. *Ganoderma perzonatum* was described from Cuba (Murrill 1908). Moncalvo and Ryvarden (1997) first related it to *G. parvulum*. Previously, Steyaert in 1962 and Wright in 1967, in two notes joint to the type specimen of *G. stipitatum* (NY 985678!) and to a second specimen annotated "probable type" [of *G. stipitatum*] (NY 985716!) also informally suggested that *G. perzonatum* and *G. parvulum* were synonymous. However, later on, Ryvarden (2004) retained the species that he associated to the *G. resinaceum* complex. The revision of the type specimen (NY 985702!) (Fig. 8F–I) confirmed the main features (Ryvarden 2004): a sessile, dimidiate habit with superposed pilei, a pale corky context with dark, resinous streaks, cuticular cells up to 100 µm long, and basidiospores 8.5–9.5 (–10) × 6–7 µm. Furthermore, chlamydospores with smooth or then ornamented with fine longitudinal ridges (Fig. 8H–I), also were observed, a feature previously unnoticed. These characteristics brought it back to *G. parvulum*, as first suggested by Moncalvo and Ryvarden (1997).

However, *G. perzonatum* would differ from *G. parvulum* in having larger, sessile, dimidiate basidiomes and markedly cylindrical, longer cuticular cells. A specimen originating from the type locality of *G. perzonatum* (MUCL 43522, La Havana, Cuba, Fig. 9) shared these characters. It also produced striated chlamydospores, both in the context of the basidiome and in pure culture, similar to those of *G. parvulum*. However, this specimen formed a short, isolated branch, basal to the C1.2 clade, in phylogenetic inferences of the combined data set (Fig. 1). *Ganoderma perzonatum* remains of uncertain interpretation. It could be included, for the time being, in the concept of *G. parvulum* (hence *G. parvulum* s.l.).

The taxonomic statuses of *G. argillaceum*, *G. perturbatum*, *G. praelongum*, *G. pulverulentum*, and *G. subincrustatum* also were widely debated. *Ganoderma argillaceum* and *G. praelongum* were considered as synonyms of *G. resinaceum* by

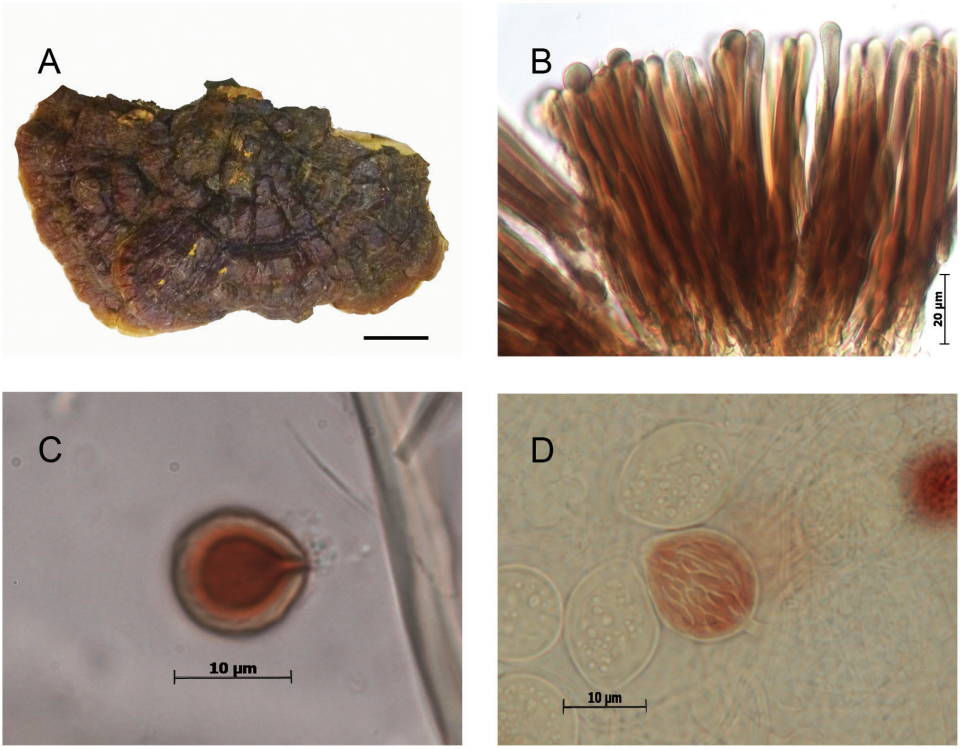

Figure 9. Morphological features and microscopic structures of the Cuban specimen of *Ganoderma* MUCL 43522 **A** upper surface of basidiomata **B** cuticular cells **C–D** chlamydospore with longitudinal ridges **C** from context **D** from culture. Scale bar: 1 cm (**A**).

Steyaert (1980). Bazzalo and Wright (1982) also included *G. pulverulentum* and *G. subincrustatum* to the list of the *G. resinaceum* presumed synonyms, to which Ryvarden (2000) added *G. perturbatum* and *G. sessiliforme.* Inversely, at the other extreme, Torres-Torres and Guzmán-Dávalos (2012) recognized under these epithets as many independent species. Gottlieb and Wright (1999) accepted *G. praelongum* with *G. pulverulentum* (Murrill 1908) as a synonym, whereas Welti and Courtecuisse (2010) recognized *G. pulverulentum* as an independent species.

Ganoderma argillaceum, *G. praelongum*, and *G. pulverulentum* differed from *G. parvulum*, *G. mexicanum*, and our Neotropical specimens in having larger basidiospores (respectively 9–11 × 6–8 µm, *fide* Gottlieb and Wright 1999; 9–11 × 6–8.5 µm, *fide* Gottlieb and Wright 1999; 9.6–12.8 × 6.2–8 µm, *fide* Torres-Torres et al. 2012). *Ganoderma argillaceum* (holotype NY, 01293316!) had basidiospores with abundant and thin pillars and lacked chlamydospores (Gottlieb and Wright 1999), whereas *G. praelongum* and *G. pulverulentum* had basidiospores with partially anastomosed pillars (Gottlieb and Wright 1999, Torres-Torres et al. 2012). *Ganoderma vivianimercedianum* also differed from our specimens in having larger basidiospores,

8.8–11.2 (–12) × 6.5–8 µm, and absence of chlamydospores (Torres-Torres et al. 2008). These names remained of uncertain status and affinities. They are most likely not synonyms of *G. resinaceum* s.s. from Europe (Bazzalo and Wright 1982) but affinities with North American species of the *G. resinaceum* clade, *viz*. *G. sessile* and *G. polychromum* (Loyd et al. 2018), should not be excluded.

Ganoderma perturbatum (BPI!) differs from our specimens from both clades (C1.1 and C1.2) in having larger basidiospores 10–12.8 × 8–9.4 µm with subacute apex and partially anastomosed pillars or short crest-like ornamentations. *Ganoderma subincrustatum* has cuticular cells generally with short and thick protuberances and basidiospores with partially anastomosed pillars (Torres-Torres and Guzmán-Dávalos 2012, Torres-Torres et al. 2015, pers. obs.). Their status and affinities also remained uncertain.

In conclusion, we are of the opinion that *G. mexicanum* could be selected as the earliest name available for the specimens of the clade C1.1. It is morphologically very similar if not identical to *G. subamboinense* var. *laevisporum*. We therefore suggest, for the time being, pending new material and DNA sequences data, to apply *G. mexicanum* to the clade C1.1. We also concluded that the name *G. parvulum* could be retained as the earliest name available for the taxa represented by the clade C1.2, previously reported in the literature as *G. subamboinense* var. *subamboinense*. *Ganoderma perzonatum* could represent another closely related taxon in the vicinity of *G. mexicanum* / *G. parvulum*.

Taxonomy

Ganoderma mexicanum **Pat., Bull. Soc. Mycol. Fr. 14: 54 (1898)**
Mycobank: MB469325
Figs 3, 6–7

≡ *Fomes mexicanus* (Pat.) Sacc., Syll. Fung. 14: 184 (1899) [MB166450]
= *Ganoderma sessiliforme* Murrill, Bull. New York Bot. Gard. 8: 149 (1912) [MB469342]
= *Ganoderma subamboinense* var. *laevisporum* Bazzalo & J.E. Wright, Mycotaxon 16(1): 302 (1982) [MB117102], invalid.

Description. *Basidiome* annual, sessile, occasionally stipitate, solitary, light in weight, consistency corky-woody; *pileus* projecting 4–8 cm, 6–14 cm wide, up to 1.5–1.8 cm thick at the base, 0.3–0.4 cm at the margin, dimidiate, flabelliform to conchate in pole view, applanate or slightly convex in section; *stipe* absent or 2 × 0.5–3 cm, horizontal, short and thick, slightly swollen at the base, laccate, smooth, reddish brown (8F6) to violet brown (11F7); *pileal surface* laccate, smooth, radially zonate, with dark lines or with concentric variably deep sulcations, reddish brown (8F6) to dark brown (8F5), lighter towards the margin; *margin* likely white when young, entire to slightly lobulated, sometimes incurved; *pore surface* yellowish white to greyish yellow (4C7), yellowish brown (5E7), or brownish orange (5C3), bruising dark brown (6F5), sometimes marked with spots of same aspect as pilear surface (laccate, reddish brown, 8F6); *pores* round, 4–6

(–7) per mm; *context* 0.2–1 cm thick, fibrous, homogeneous to slightly heterogeneous (not fully homogeneous *fide* Torres-Torres et al. 2012), almost overall white to light yellow (4A4) or light yellow (4A4) to greyish orange (5B4) toward the crust, yellowish brown (5D6) to light brown (7D3) in a narrow zone above the tubes, with few to several resinous incrustations or thin resinous dark bands stretching from the basis to the margin; *tubes* 0.1–0.8 cm long, unstratified, concolorous with lower part of the context.

Hyphal system dimitic; *generative hyphae* 1–3 µm diam., septate, thin-walled with clamp connections, little branched, hyaline to yellowish; *somatic hyphae* as arboriform skeleto-binding hyphae, golden yellow, composed of a basal stalk arising from a clamp, unbranched, thick-walled but with a visible lumen, with several secondary processes, branches gradually tapering from 6 µm wide in the primary processes to 1.5–2 µm wide at the thin-walled apices, thick-walled to solid. *Pileipellis* a crustohymeniderm; *cuticular cells* clamped at the basal septum, shortly to moderately pedicelated then cylindrical a clavate, occasionally slightly apically capitate, rarely with 1–2 lateral branches, with rounded apices, thick-walled, smooth or with a fine apical granulation, amyloid, 25- [~ 40] -50 (-65) × 5-7 um. *Hymenium: basidia* not seen; *basidiospores* ovoid to broadly ovoid, the apex shrunken, appearing truncate, exosporium with thick, free to subfree pillars, (7.5–) 8– [8.5] –9 (–10.5) × (4.2–) 6– [6.5] –7 (–8) µm, Q = 1.33– [1.30] –1.28; spore print light brown (6E5) (estimated from spore deposit on the pileus). *Chlamydospores* in the basidiomata absent, rare, to variably abundant, only in the context, subspherical, ellipsoid, or citriform, terminal or intercalated; with smooth thick-wall; sometimes guttulate, dextrinoid, 9.5–13 (–16) × 8–10 µm. Chlamydospores always abundant in pure culture on malt agar, spherical to more often ellipsoid, terminal or intercalary, when terminal with the apex occasionally papillated; with smooth, hyaline to pale golden brown, single or double wall; sometimes with densely guttulate contents, often dextrinoid, 11–16 × 9.5–12 µm.

Holotype. MEXICO. Estado de México: D. de Jonacatepec, Tepalcingo, 22 Oct 1890, P.J.B. Maury 4823 (FH 458184!).

Known distribution. Argentina, Brazil, Martinique, Mexico.

Specimens examined. ARGENTINA. Buenos Aires: Tigre, on *Platanus* sp., 15 May 1980, Connon (as holotype of *G. subamboinense* var. *laevisporum*, BAFC 25525, culture ex. type BAFC n° 247 = ATCC 52419). MARTINIQUE. Prêcheur: Anse Couleuvre, sentier de la cascade de la rivière Couleuvre, on *Artocarpus altilis*, in mature, secondary mesophylic forest, 13 Aug 2007, J.P. Fiard SW 17 (LIP, culture ex. MUCL 49453). Rivière–Pilote: Morne Aca, on a lying trunk, in meso-xerophylic forest, 14 Aug 2007, S. Welti, SW 19 (LIP). La Caravelle, xerophylic forest, on dead fallen trunk, 12 Aug 2015, C. Decock, MA/15–45 (MUCL 55832, culture ex. MUCL 55832). MEXICO. Morelos: Municipality of Cuernavaca, on dead wood, 24–27 December 1909, W.A. & E.L. Murrill 392 (as holotype of *G. sessiliforme*, NY 985713). Mpio. of Tepoztlán, Tepoztlán, Estación del Ferrocarril El Parque, w/o date, G. Guzmán 2078 (ENCB). Veracruz: San Andrés Tlalnelhuayocan, alrededores de San Antonio Hidalgo, bosque mesófilo de montaña, 1400 m, D. Jarvio 143 (XAL).

Ganoderma parvulum **Murrill, Bull. Torrey Bot. Club. 29: 605 (1902)**
Mycobank: MB241944
Figs 4, 8

≡ *Fomes parvulus* (Murrill) Sacc. & D. Sacc, Syll. Fung. (Abellini). 17: 123 (1905) [MB241944]
= *Fomes stipitatus* Murrill, Bull. Torrey Bot. Club. 30(4): 229 (1903) [MB241804]
≡ *Ganoderma stipitatum* (Murrill) Murrill, N. Amer. Fl. (New York) 9(2): 122 (1908) [MB451185]
= *Fomes subamboinensis* Henn., Hedwigia 43(3): 175 (1904) [MB148868]
≡ *Ganoderma subamboinense* (Henn.) Bazzalo & J.E. Wright ex Moncalvo & Ryvarden, Synopsis Fungorum 11: 82 (1997) [MB249603]
≡ *Ganoderma subamboinense* var. *subamboinense* Bazzalo & J.E. Wright Mycotaxon 16(1): 302 (1982) [MB417363] (invalid)

Description. *Basidiome* annual, sessile or stipitate, solitary or sometimes concrescent or forming several (up to 3) pileus, light in weight, consistency corky-woody; *pileus* projecting 4.5–8 cm, 6.5–15 cm wide, up to 0.8–3 cm thick at the base, 0.5–0.7 cm at the margin; dimidiate, flabelliform to conchate in pole view, applanate or convex in section; *stipe* absent or 1.5–4.5 (–8) × 0.5–3 cm, horizontal or dorsally lateral, short and thick or long and tortuous, slightly swollen at the base, laccate, reddish brown (9F6) to dark brown (9F4) or violet brown (10F8) to almost black, stumpy or cylindrical, sometimes with laterals branches; *pileal surface* smooth, laccate, radially rugose or with concentric deep sulcations or occasionally, slightly zonate with dark lines, fully reddish brown (9F8) to violet brown (10F8), or gradually lighter towards the margin with a yellowish orange (5A7) band; *margin* white to pale yellow (4A3) or greyish yellow (4C7) to yellowish orange (5A7), entire to slightly lobulated, sometimes incurved; *pore surface* white, yellowish white (3A2), dull yellow (3B3), or sun yellow (2A5) when fresh and actively growing, greyish yellow (4C7), yellowish brown (5E7), or brownish orange (5C3) on drying, bruising dark brown (6F5), sometimes marked with spots of same aspect than pilear surface (laccate, reddish brown, 9F8); *pores* 4–5 per mm, round to mainly angular; *context* 0.3–2.4 cm thick, fibrous, homogeneous to slightly heterogeneous, sometimes zonate, greyish yellow (4B5) to greyish orange (5B3) toward the crust, and brownish orange (6C4) to light brown (6D4) in a narrow zone above the tubes, changing to yellow when cut in fresh specimens, with none to few to several (up to 4) resinous incrustations or occasionally resinous bands (up to 4), sometimes with yellow (3B8) spots throughout the context, with a yellow (3B8) to yellowish orange (4A7) thin line just below the crust; *tubes* 0.2–0.6 cm long, unstratified, concolorous with lower part of the context.

Hyphal system dimitic; *generative hyphae* 1.6–3.2 µm diam., septate, thin-walled with clamp connections, non-branched, hyaline to yellowish; *somatic hyphae* as arboriform skeleto–binding hyphae, golden yellow, composed of a basal stalk arising from a

clamp, with several secondary processes, branches gradually tapering from 6 µm wide in the primary processes to 1.5–2 µm wide at the thin-walled apices, thick-walled to solid. *Pileipellis* a crustohymeniderm; *cuticular cells* clamped at the basal septum, pedicelated, mainly cylindrical to clavate, occasionally slightly apically capitate, rarely with 1–2 lateral protuberances, with regular, rounded end, thick-walled to almost solid, amyloid, the apex occasionally with a radial fine granulation, 40- [~ 60] -75 (-100) x 5-10 um. *Hymenium*: *basidia* not seen; *basidiospores* ovoid to broadly ovoid, the apex shrunken, appearing truncate, exosporium with thick, free to subfree pillars, (6–) 8– [8.9] –9.5 × (4.8–) 5.5– [6.0] –6.5 (–7) µm, Q = 1.45– [1.48] –1.46, ovoid; spore print (6E5), light brown (estimated from spore deposit on the pileus). *Chlamydospores* in the basidiomata absent, rare, to variably abundant, only in the context, subspherical, ellipsoid, or citriform, sometimes spindle-shaped, terminal or intercalated; smooth-walled to roughened with fine, isolated to partially anastomosed ridges, having a meridian orientation, variably stretching between the two extremities, totally dextrinoid or with dextrinoid content and golden wall, 7–13 × 6–12 µm. Chlamydospores always abundant in pure culture on malt agar, spherical to ellipsoid, sometimes spindle-shaped, often truncated at both ends; terminal or intercalary; when terminal with the apex occasionally papillated; single or golden double walled; with several large guttulae, with dextrinoid contents; smooth first then variably roughened, ornamented with fine partial or continuous ridges, isolated to partially anastomosed, 11–16 (–17.5) × 9–14.5 (–16) µm.

Holotype. NICARAGUA. C.L. Smith s.n. (NY 985699!).

Known distribution. Brazil, Colombia, Costa Rica, Cuba, French Guiana, Mexico, Nicaragua, South–eastern USA (Florida).

Specimens examined. BRAZIL. St. Clara: Río Juruá, Oct 1900, E. Ule 2748, (under *Fomes subamboinensis* as type of *G. subamboinense*, F15183 (S). COSTA RICA. Puntarenas: Isla del Coco, orilla del río Genio, represa hidroeléctrica, 0–100 m s.n.m., 5 Jun 2005, E. Fletes–7619, Lote: 84813 (INB 3976555); Osa, P.N. Corcovado, Estación Sirena, Sendero Guanacaste, bosque primario, 10 m s.n.m., E. Fletes–266, Lote: 53967 (INB 1546586), río Madrigal, quebrada Ceniza, 200 a 300 m s.n.m., 19 Mar 2003, E. Fletes–4943, Lote: 73208 (INB 3700175). CUBA. Province La Habana: Municipality Boyeros, Zoológico Nacional de Cuba, on base of a living trunk, 22 Aug 2001, C. Decock and S. Oliva, MUCL 43522 (culture ex. MUCL 43522); Finca La Chata, on base of a living trunk of *Casuarina equisetifolia*, 27 May 2002, C. Decock w/o #, MUCL 43863 (culture ex. MUCL 43863); Province Villa Clara: Falcon, Carretera Central, dead stump of *Casuarina equisetifolia*, Aug 2002, C. Decock, CU–02/14, MUCL 44148 (culture ex 44148 = CRGF 715); Province Sancti Spiritus: Topes de Collantes, on the way to the Caburni, dead trunk, unidentified angiosperm, Sep 2004, C. Decock, CU–04/12, MUCL 46029 (culture ex 46029 = CRGF 202); Sep 2005, C. Decock, CU–05/196 (MUCL 47074, culture ex 47074 = CRGF 719); Province Pinar del Río: La Palma, near the Motel La Ciguaraya, decaying stump, unidentified angiosperm, Oct 2005, C. Decock, CU–05/246, MUCL 47096 (culture ex 47096 = CRGF 722). FRENCH GUIANA. Nouragues

National Reserve, Inselberg CNRS research station, dead fallen trunk, unidentified angiosperm, Aug 2010, C. Decock, FG/10-283, MUCL 53123 (culture ex. 53123); 2011, C. Decock, FG/11–481, MUCL 53712 (culture ex. 53712). MEXICO. State of Veracruz: Zentla, camino Huatusco–Maromilla, a la altura de Puentecilla, bosque mesófilo de montaña, alt. 860 m s.n.m. (as *G. lucidum*), A. Sampieri 84 (XAL). NICARAGUA. C.L. Smith s.n., as *F. stipitatus* (holotype of *G. stipitatum*, NY 985678); C.L. Smith s.n., as *F. stipitatus* ("TYPE" of *G. stipitatum*, NY 985679); without data, C.L. Smith s.n., as *F. stipitatus* ("Probable TYPE" of *F. stipitatus*, det. as *G. parvulum* by Steyaert 1961, NY 985716).

Additional species examined. BRAZIL. Rio Grande do Sul: Lageado, without date, R. Rick s.n. (holotype of *G. perturbatum*) (BPI). CUBA. Province La Habana: Municipality Santiago de Las Vegas, on mango log, 1904, F.S. Earle 309 (holotype of *G. perzonatum*, NY 985702); on dead mango, 5 Jul 1904, F.S. Earle 658 (holotype of *G. argillaceum*, NY 01293316). GRENADA. Without data, on dry manchinell, 14 Sep 1905, W.E. Broadway s.n. (holotype of *G. pulverulentum*, NY 00985705). INDONESIA. Java: without data, P. Serre s.n. (type of *G. rivulosum*, F181158, S). MEXICO. Estado de México: valle del Tepeite, 10 km NE of Santa María, 10 Aug 1986, E. Bastidas-Varela s.n. (holotype of *G. vivianimercedianum*, ENCB). SAMOA ISLAND. Without data, Weber s.n. (as "TYPUS" of *Fomes weberianus* F15098, S); without data, Weber s.n., as *Fomes weberianus* (B 700021870), *"Fomes weberi"*), without data, Weber s.n., as *Fomes weberianus* (B 700007410, "TYPE" of *G. weberianum*). TAIWAN. Taipei: on *Salix babylonica* Linn. (Salicaceae), 21 Aug 1983, R.-S. Hseu (isotype of *G. microsporum*, HMAS 57945, frag. in BR!).

Remarks: *Ganoderma mexicanum* and *G. parvulum* have sessile to stipitate basidiomes, more frequently stipitate in the latter, with a basal and horizontal stipe. The type specimens of *G. subamboinense* (Fig. 4I–K) and of *G. stipitatum* (Fig. 8A–E), overall, have the same basidiome habit. The two specimens of *G. parvulum* from the rainforest of French Guiana also were morphologically very homogeneous, stipitate, with a basal and horizontal stipe. In the Greater Antilles (Cuba), *G. parvulum* was found mostly in anthropic or urban environment and had sessile, dimidiate basidiomes.

The context of both *G. mexicanum* and *G. parvulum* was light-colored, usually very pale toward the crust and darker just above the tubes, with none to several brown resinous incrustations or resinous bands variably stretching through the context from the base to the margin. The context in *G. parvulum* sometimes showed yellow, scattered spots and a thin yellow line just below the crust. Both species have chlamydospores in their context and in pure culture on artificial media. There are not many morphological characters to differentiate them except for the ornamentation of their chlamydospores. However, chlamydospores are sometimes very scarce and difficult to observe in the basidiome. Nonetheless, they are always present, and frequent, in pure culture on artificial media.

The basidiospores were, on average, marginally wider in *G. mexicanum* in comparison to those of *G. parvulum*, *viz.* on average 8.6 × 6.4 µm or 9.0 × 6.0 µm, respectively. The cuticular cells were cylindrical to claviform, occasionally with 1–2

short lateral branches, strongly amyloid, usually smooth or with a fine apical granulation, which was more consistently present in *G. parvulum*. The cuticular cells also were marginally longer in *G. parvulum* (up to 100 µm long) compared to those of *G. mexicanum* (up to 65 µm long).

The distribution ranges and ecologies of both species are still little known. *Ganoderma parvulum*, as here interpreted, had been observed from the Brazilian Amazon, Colombia, and French Guiana in South America, Costa Rica and Nicaragua in Mesoamerica, and up to Cuba in the Caribbean. Loyd et al. (2017, 2018) reported *G.* cf. *weberianum* from the subtropical southern Florida (USA) on the basis of two specimens (UMNFL 32 and UMNFL 100), which DNA sequences, nevertheless, were deposited in GenBank under *G. subamboinense* var. *laevisporum*. Loyd et al. (2018) described striated chlamydospores in the context of these specimens, which points toward *G. parvulum*. Our multilocus phylogenetic inferences showed that these Florida specimens nested within the *G. parvulum* clade (Fig. 1). However, there was incongruence between the topology resulting from the multilocus-based phylogenies and the ITS-based inferences (Fig. 2) regarding the position of UMNFL 100. The ITS sequences of this showed a change in three nucleotide positions, that could represent a misreading of the sequencer. Notwithstanding, these reports extend the distribution range of *G. parvulum* northerly to the subtropical, south–eastern USA. This ample distribution would imply a broad ecological range, but also could encompass a hidden diversity.

In French Guiana, *G. parvulum* has been observed at the Nouragues Nature Reserve (~4°04'18"N, 52°43'57"W), a spot of primary, very humid (3000 mm of rain / year), tropical rainforest characteristic of the Guianas shield, which belongs to the larger Amazonian rain forest phytochorion. Locally, this species was uncommon; three basidiomes only were observed during six, two- to three-weeks long surveys of polypores. These three specimens were found emerging from dead, fallen trunks. In French Guiana, it has been observed also once in an anthropic, semi-urban environment (culture BRFM 1043, voucher specimen and data on the substrate and host unavailable). The type specimen of *G. parvulum*, originating from Brazil, was also, most likely, collected in the same phytochorion. In Cuba, Greater Antilles, the species has been observed mostly in anthropic, urban or semi-urban environments (cf. list of specimens examined).

Ganoderma mexicanum, as here interpreted, has been observed from Argentina, Brazil, Martinique (Lesser Antilles), and Mexico. In Mexico, the species is known from a rather restricted area of the Morelos State, which is the type locality of *G. mexicanum* and *G. sessiliforme*, and of a third additional specimen collected in secondary tropical forest with *Quercus* sp. (Torres-Torres et al. 2015). Raymundo et al. (2013) and López-Peña et al. (2016) also reported *G. sessiliforme* from xerophylic vegetation with *Quercus* sp. in Sonora, but the voucher specimens were not available for confirmation. In Martinique, the species was found in mesophylic to distinctly xerophylic forests, which could represent, locally, its preferential habitat. Several collections came from The Caravelle Peninsula, which is characterized by a seasonally dry season.

Discussion

The current morphological concept of *Ganoderma weberianum* dated back from Steyaert (1972) and was based on *Fomes weberianus*. However, on one hand, the very identification of *F. weberianus* remained questioned. As raised by Yombiyeni and Decock (2017), there was confusion around the modern interpretation of this taxon and its generic placement was debated; the species was either considered in *Ganoderma*, following Steyaert (1972), or in *Phylloporia*, following Ryvarden (1972). On another hand, the circumscription of *G. weberianum sensu* Steyaert remained questioned and, consequently, its distribution range remained uncertain.

Fomes weberianus, originating from Samoa ("*in insula Samoa*"), was first described by Saccardo (1891). This author did not specify a type or any reference specimens, mentioning only "*Exempl. in Museo berolin*" (nowadays B). The current concept of *G. weberianum* was developed based on a specimen held in B (#700007410) stamped as type; this specimen represents indeed a species of *Ganoderma*, hence *G. weberianum sensu stricto* (Steyaert 1972). However, the same year, Ryvarden (1972) recombined *F. weberianus* into *Phylloporia*, although without citing any reference specimen.

Nonetheless, in addition to the type cited by Steyaert (1972), two other specimens annotated as "*Fomes weberianus*, Weber, Samoa" exist, of which one also is stamped as type. One of these two specimens is located at B [Samoa Island, Weber "*Fomes Weberi*" det. P. Henn., *Fomes weberianus* (#700021870!)], and the second in the Bresadola herbarium in S [Samoa Island, Weber, det. P. Henn. and Bresadola as *Fomes weberianus* "n. sp." "*Typus*!" F15098!]. These two latter specimens do not represent a species of *Ganoderma* but a species of *Phylloporia*; their morphological features agree very well with the modern, morphological concept of this genus (e.g., Wagner and Ryvarden 2002). Moreover, and essentially, the morphological characters of these two specimens are in complete agreement with the original diagnosis of *F. weberianus* (Saccardo 1891).

This diagnosis was, partly, a copy of a handwritten description, contemporary to, or previous to Saccardo (1891), and which is still present within the folder #700007410 in B. It emphasized a duplex context ("*strato duplice*") made of an upper tomentose to floccose layer ("*superiori tomentoso–floccoso*") and a lower, corky layer ("*inferiori suberoso–lignoso*"), separated one from the other by a thin black line ("*a superiore linea nigra limitato*"). Saccardo (1891), following the above-cited note, related *F. weberianus* to *Polyporus circinatus* (Fr.) Fr. and *P. tomentosus* Fr., two Hymenochaetaceae nowadays accepted in *Onnia* (Ryvarden 1990). Subsequent early interpretations of *F. weberianus* (e.g., Bresadola 1914, 1916, 1925, Lloyd 1915, Cunningham 1950) also associated this species to taxa that are, mainly, akin to species of *Phylloporia* as currently accepted. As far as we had been able to ascertain, there was no pre-Steyaert (1972) interpretation of this taxon as a species of *Ganoderma*.

This casted doubts on the interpretation of *F. weberianus*; considering the original diagnosis and both specimens from B and Bresadola herbarium in S, *Phylloporia weberiana sensu* Ryvarden (1972), most likely, is the correct interpretation. Hence, a lectotype should be designated. This will be discussed in more detail later on.

Our results, following Moncalvo (2000), confirmed that *G. weberianum sensu* Steyaert was polyphyletic and encompassed several species. Multilocus phylogenetic inferences had shown distinct, well-supported clades and an overall phylogenetic structure corresponding to a geographical pattern (Fig. 1). The *G. weberianum sensu* Steyaert lineage was divided into two main sublineages, *viz*. a Neotropical and Paleotropical sublineages.

As far the Neotropics are concerned, at least two species were confirmed, *G. mexicanum* (previously variably reported as *G. sessiliforme* and *G. subamboinense* var. *laevisporum*) and *G. parvulum* (previously known as *G. subamboinense*). Furthermore, the specimen MUCL 43522 from Cuba could represent *G. perzonatum*. Although we are of the opinion that *G. perzonatum* may well represent a species on its own, more material, ideally from various localities, and DNA sequences, is necessary to draw a definitive conclusion. On the other hand, the specimen Guzmán-Dávalos 9569 (IBUG!) from Mexico, basal to the *G. parvulum* s.l. / *G. mexicanum* s.l. clade in the ITS-based phylogenetic inferences (Fig. 2) and with chlamydospores ornamented with isolated pillars, also could represent a distinct taxon. This demonstrates a likely higher than known phylogenetic and morphological diversity and, ahead, taxonomic diversity. Several additional names also remain of uncertain status and, if any, unknown affinities; it includes *G. argillaceum* and *G. praelongum*, or still *G. multiplicatum* and *G. vivianimercedianum*. Collections from their type localities and DNA sequences data are highly needed.

The Paleotropical sublineage was further divided into three clades, including an African, an Indian, and a tropical Asian / Australasian clade, representing, at the least, as many phylogenetic species or species complexes. As regard to the situation in Central Africa, at least one species could be segregated from the *G. weberianum sensu* Steyaert. *Ganoderma carocalcareum* Douanla-Meli (Douanla-Meli and Langer 2009) could apply for this taxon but three previous priority names might apply too, which will require a revision of their type specimens.

On the basis of our phylogenetic inferences, we conclude that *G. weberianum* in Southeast Asia and Australia (which would correspond to *G. weberianum sensu* Moncalvo 2000) also is a complex of species. It would include, at least, *G. rivulosum* (S F181158!) and *G. microsporum* (isotype BPI!). Moncalvo et al. (1995) suggested that there are few differences between *G. microsporum* and *G. weberianum*, and later on, Moncalvo (2000) considered both names as synonyms (Moncalvo 2000), which was also the opinion of Smith and Sivasithamparam (2003) and Wang et al. (2005). However, this synonymy needs to be ascertained.

The sister clade of *G. weberianum sensu* Steyaert lineage is, in our phylogenetic analyses, hitherto, the clade D, which comprised specimens from Central Africa and China, the latter referenced at GenBank as *G. hoehnelianum*. *Ganoderma hoehnelianum* was described by Bresadola (1912) from Java (Indonesia) having basidiomes with a "*crusta*, *tenui*, *opaca*". This "crust" was observed in the type specimen (S F181067!) and is different from the laccate pileal surface of the *G. weberianum* complex, made of cuticular cells organized in a dense palisade. Therefore, the identity of this clade also should be ascertained.

This study also confirmed that *G. resinaceum sensu auctores* from China, East Africa, Europa, and both North and South America represented a species complex. Loyd et al. (2018) showed that *G. resinaceum sensu* American *auctores* encompassed at least two distinct species, *viz*. *G. polychromum* and *G. sessile*. These results agreed with those of Moncalvo (2000), who distinguished European and North American "populations" of *G. resinaceum*, on the basis of which it was proposed that these "disjunct and genetically isolated [populations]" "may warrant recognition at the species level". Our study showed that the *G. resinaceum sensu* European auctores also represented a species complex, with two well-supported phylogenetic species (Fig. 1); thus *G. resinaceum* in Europe also could hide a larger than expected diversity.

As emphasized by Moncalvo (2000) and Richter et al. (2015), the identification of species in *Ganoderma* was commonly based on the microanatomy of the pileus surface, the basidiospores morphology and size, and in some cases, the host relationships. The occurrence of chlamydospores in the basidiomes or in *in vitro* cultures also was highlighted as a valuable feature (Moncalvo 2000, Hong and Jung 2004, Richter et al. 2015, Loyd et al. 2019), although this character, as suggested by Steyaert (1980), also could be environment dependent. Our results concerning the Neotropical species of the *G. weberianum* complex confirmed the presence of chlamydospores, in basidiomes and in *in vitro* cultures, and their ornamentation, as pertinent taxonomic features for the systematic of this group. Three ornamentation types, smooth, with pillars, or with ridges have been observed in the Neotropical species. A similar situation could occur in *G. weberianum sensu* Moncalvo in Southeast Asia. Steyaert (1972) described *G. weberianum* with both smooth and ornamented chlamydospores with pillars, "columns", or "partitions". Smith and Sivasithamparam (2003) confirmed these observations based on examination of the type specimen (cited by Steyaert 1972) and specimens from Australia and the south Pacific regions.

Acknowledgments

The authors thank the curators of the following herbaria for the loan of types and other materials, B, BAFC, BPI, ENCB, FH, IBUG, INBIO, MUCL, NY, S, and XAL. Milay Cabarroi Hernández gratefully acknowledges financial support received from the Rufford Foundation, UK (project 17535–2), from the *Université Catholique de Louvain*, Belgium (Scholarship from the *Conseil de l'Action Internationale (CAI): Coopération au développement*), the University of Guadalajara, and the CONACYT, Mexico (National Scholarship). Cony Decock gratefully acknowledges the financial support received from the Belgian State – Belgian Federal Science Policy through the BCCM research program, the FNRS / FRFC (convention FRFC 2.4544.10) and the Nouragues Travel Grant "MYcorrhizal COmmon network of Trees on INselbergs" (program 2013) that allowed fungal diversity studies in French Guiana, and the CIUF/CUD through a PIC program (project CIUF–CUD–MUCL–Cuba) that allowed fungal diversity studies in Cuba. Cony Decock also thanks Dr. Anne Corval

and Dr. Annaïg Le Guen, respectively previous and present Director of the "CNRS Guiana", for granting authorization and facilities for field research at the CNRS Nouragues "Inselberg" and "Pararé" forest plots, and the CNRS staff members in Cayenne and at both camps, *viz*. Dorothée Deslignes, Laeticia Proux, Philippe Gaucher, Patrick Châtelet, Gilles Peroz, Wemo Betian, and Stéphane Ricatte. Cony Decock also thanks Prof. Régis Courtecuisse for his invitation to participate to the Mycoflora of Martinique project, and Dr. Anne Favel for providing strains from CIRM-CF Marseille. Laura Guzmán-Dávalos recognizes the support of the University of Guadalajara, Mexico. Our gratitude also is extended to Dr. Pilar Zamora Tavares from LaNiVeg at University of Guadalajara who provided Sanger Sequencing. Thanks are extended also to Stéphanie Huret for her help in the sequencing program and Philipe Charue for his help in the laboratory work, as well as Dr. Eduardo Ruiz and Dr. Gerardo Hernández Vera for their advice about the phylogenetic work.

References

Aljanabi SM, Martinez I (1997) Universal and rapid salt extraction of high quality genomic DNA for PCR-based techniques. Nucleic Acids Research 25: 4692–4693. https://doi.org/10.1093/nar/25.22.4692

Amalfi M, Yombiyeni P, Decock C (2010) *Fomitiporia* in sub-Saharan Africa: morphology and multigene phylogenetic analysis support three new species from the Guineo-Congolian rainforest. Mycologia 102: 1303–1317. https://doi.org/10.3852/09-083

Amalfi M, Raymundo T, Valenzuela R, Decock C (2012) *Fomitiporia cupressicola* sp.nov., a parasite on *Cupressus arizonica*, and additional unnamed clades in the southern USA and northern Mexico, determined by multilocus phylogenetic analyses. Mycologia 104: 880–893. https://doi.org/10.3852/11-196

Bazzalo ME, Wright JE (1982) Survey of the Argentine species of the *Ganoderma lucidum* complex. Mycotaxon 16: 293–325.

Bolaños AC, Bononi VLR, Gugliotta AM, Muñoz JE (2016) New records of *Ganoderma multiplicatum* (Mont.) Pat. (Polyporales, Basidiomycota) from Colombia and its geographic distribution in South America. Check List 12(4): 1948 https://doi.org/10.15560/12.4.1948

Bresadola G (1912) Polyporaceae Javanicae. Annales Mycologici 10: 492–508.

Bresadola G (1914) Fungi nonnulli exotici ex Museo Berolinensi. Annales Mycologici 12: 539–544.

Bresadola G (1916) Synonymia et adnotanda mycologia. Annales Mycologici 14: 221–242.

Bresadola G (1925) New species of fungi. Mycologia 17: 68–77. https://doi.org/10.1080/00275514.1925.12020457

Cao Y, Wu S, Dai Y (2012) Species clarification of the prize medicinal *Ganoderma* mushroom "Lingzhi". Fungal Diversity 56: 49–62. https://doi.org/10.1007/s13225-012-0178-5

Coetzee MPA, Marincowitz S, Muthelo VG, Wingfield MJ (2015) *Ganoderma* species, including new taxa associated with root rot of the iconic *Jacaranda mimosifolia* in Pretoria, South Africa. IMA Fungus 6: 249–256. https://doi.org/10.5598/imafungus.2015.06.01.16

Corner EJH (1983) Ad Polyporaceas I, *Amauroderma* and *Ganoderma*. Beihefte zur Nova Hedwigia 75: 1–182.

Cunningham GH (1950) Australian Polyporaceae in herbaria of Royal Botanic Gardens, Kew, and British Museum of Natural History. Proceedings of the Linnean Society of New South Wales 75: 214–249.

Decock C, Herrera-Figueroa S, Robledo G, Castillo G (2007) *Fomitiporia punctata* (Basidiomycota, Hymenochaetales) and its presumed taxonomic synonyms in America: taxonomy and phylogeny of some species from tropical/subtropical area. Mycologia 99: 733–752. https://doi.org/10.1080/15572536.2007.11832537

Decock C, Amalfi M, Robledo G, Castillo G (2013) *Phylloporia nouraguensis* (Hymenochaetales, Basidiomycota), an undescribed species from the Neotropics. Cryptogamie, Mycologie 34: 15–27. https://doi.org/10.7872/crym.v34.iss1.2013.15

Douanla-Meli C, Langer E (2009) *Ganoderma carocalcareus* sp. nov., with crumbly-friable context parasite to saprobe on *Anthocleista nobilis* and its phylogenetic relationship in *G. resinaceum* group. Mycological Progress 8: 145–155. https://doi.org/10.1007/s11557-009-0586-4

Doyle JJ, Doyle JL (1987) A rapid isolate procedure from small quantities of fresh leaf tissue. Phytochemical Bulletin 19: 11–15.

Gardes M, Bruns TD (1993) ITS primers with enhanced specificity for basidiomycetes – application to the identification of mycorrhizae and rusts. Molecular Ecology 2: 113–118. https://doi.org/10.1111/j.1365-294X.1993.tb00005.x

Gottlieb AM, Wright JE (1999) Taxonomy of *Ganoderma* from South America: subgenus *Ganoderma*. Mycological Research 103: 661–673. https://doi.org/10.1017/S0953756298007941

Gottlieb AM, Ferrer E, Wright JE (2000) rDNA analyses as an aid to the taxonomy of species of *Ganoderma*. Mycological Research 104: 1033–1045. https://doi.org/10.1017/S095375620000304X

Guzmán-Dávalos L, Mueller GM, Cifuentes J, Miller AN, Santerre A (2003) Traditional infrageneric classification of *Gymnopilus* is not supported by ribosomal DNA sequence data. Mycologia 95: 1204–1214. https://doi.org/10.1080/15572536.2004.11833028

Hapuarachchi KK, Wen TC, Deng CY, Kang JC, Hyde KD (2015) Mycosphere essays 1: taxonomic confusion in the *Ganoderma lucidum* species complex. Mycosphere 6: 542–559. https://doi.org/10.5943/mycosphere/6/5/4

Hennings P (1904) Fungi amazonici I. a cl. Ernesto Ule collection. Hedwigia 43: 154–186.

Hong SG, Jung HS (2004) Phylogenetic analysis of *Ganoderma* based on nearly complete mitochondrial small-subunit ribosomal DNA sequences. Mycologia 96: 742–755. https://doi.org/10.1080/15572536.2005.11832922

Kinge TR, Mih AM, Coetzee MPA (2012) Phylogenetic relationships among species of *Ganoderma* (Ganodermataceae, Basidiomycota) from Cameroon. Australian Journal of Botany 60: 526–538. https://doi.org/10.1071/BT12011

Kornerup A, Wanscher JH (1981) Methuen handbook of colour. 3rd ed. Methuen, London, 252 pp.

Lanfear R, Calcott B, Ho S Y, Guindon S (2012) PartitionFinder: combined selection of partitioning schemes and substitution models for phylogenetic analyses. Molecular Biology and Evolution, 29: 1695–1701. https://doi.org/10.1093/molbev/mss020

de Lima-Junior N, Baptista G, Malosso E (2014) Delimitation of some Neotropical laccate *Ganoderma* (Ganodermataceae): molecular phylogeny and morphology. Revista de Biología Tropical 62: 1197–1208. https://doi.org/10.15517/rbt.v62i3.12380

Lloyd CG (1905) Synopsis of the genus *Ganoderma*. Mycological Writings 1.

Lloyd CG (1915) Synopsis of the genus *Fomes*. Mycological Writings 4: 209–288.

López-Peña D, Gutiérrez A, Hernández-Navarro E, Valenzuela R, Esqueda M (2016) Diversidad y distribución de *Ganoderma* (Polyporales: Ganodermataceae) en Sonora, México. Botanical Sciences 94: 431–439. https://doi.org/10.17129/botsci.463

Loyd AL, Smith JA, Richter BS, Blanchette RA, Smith ME (2017) The laccate *Ganoderma* of the Southeastern United States: a cosmopolitan and important genus of wood decay fungi. UF's EDIS. http://edis.ifas.ufl.edu.

Loyd AL, Held BW, Barnes CW, Schink MJ, Smith ME, Smith JA, Blanchette RA (2018) Elucidating '*lucidum*': distinguishing the diverse laccate *Ganoderma* species of the United States. PLoS One 13(7): e0199738. https://doi.org/10.1371/journal.pone.0199738

Loyd AL, Linder ER, Smith ME, Blanchette RA, Smith JA (2019) Cultural characterization and chlamydospore function of the Ganodermataceae present in the eastern United States. Mycologia 111: 1–12. https://doi.org/10.1080/00275514.2018.1543509

Manzano AM, Torres G, González A, Banguela A, Ramos-González PL, Valiente PA, Sánchez MI, Sánchez-Lamar Á, Rochefort D, Mclean MD, Ramos-Leal M, Guerra G (2013) Role of laccase isozymes in textile dye decolorization and diversity of laccase genes from *Ganoderma weberianum* B–18. Journal of Applied Sciences in Environmental Sanitation 8: 237–242.

Matheny PB (2005) Improving phylogenetic inference of mushrooms with RPB1 and RPB2 nucleotide sequences (*Inocybe*, Agaricales). Molecular Phylogenetics and Evolution 35: 1–20. https://doi.org/10.1016/j.ympev.2004.11.014

Matheny PB, Wang Z, Binder M, Curtis JM, Lim YW, Nilsson RH, Hughes KW, Petersen RH, Hofstetter V, Ammirati JF, Schoch C, Langer GE, Mclaughlin DJ, Wilson AW, Crane PE, Frøslev T, Ge ZW, Kerrigan RW, Slot JC, Vellinga EC, Liang ZL, Aime MC, Baroni TJ, Fischer M, Hosaka K, Matsuura K, Seidl MT, Vaura J, Hibbett DS (2007) Contributions of *rpb2* and *tef1* to the phylogeny of mushrooms and allies (Basidiomycota, Fungi). Molecular Phylogenetics and Evolution 43: 430–451. https://doi.org/10.1016/j.ympev.2006.08.024

Miller MA, Pfeiffer W, Schwartz T (2010) Creating the CIPRES Science Gateway for inference of large phylogenetic trees. Proceedings of the Gateway Computing Environments Workshop (GCE), New Orleans, pp. 1–8. https://doi.org/10.1109/GCE.2010.5676129

Mohanty PS, Harsh NSK, Pandey A (2011) First report of *Ganoderma resinaceum* and *G. weberianum* from north India based on ITS sequence analysis and micromorphology. Mycosphere 2: 469–474.

Moncalvo JM (2000) Systematics of *Ganoderma*. In: Flood P, Bridge D, Holderness M (Eds) *Ganoderma* diseases of perennial crops. CABI, Wallingford, 23–45. https://doi.org/10.1079/9780851993881.0023

Moncalvo JM, Ryvarden L (1997) A nomenclatural study of the Ganodermataceae Donk. Synopsis Fungorum 11: 1–114.

Moncalvo JM, Wang HH, Hseu RS (1995) Phylogenetic relationships in *Ganoderma* inferred from the internal transcribed spacers and 25S ribosomal DNA sequences. Mycologia 87: 223–238. https://doi.org/10.1080/00275514.1995.12026524

Müller J, Müller K, Neinhuis C, Quandt D (2010) PhyDe® Phylogenetic Data Editor. http://www.phyde.de

Murrill WA (1902) The Polyporaceae of North America, part I. The genus *Ganoderma*. Bulletin of the Torrey Botanical Club 29: 599–608. https://doi.org/10.2307/2478682

Murrill WA (1903) The Polyporaceae of North America. III. The genus *Fomes*. Bulletin of the Torrey Botanical Club 30: 225–232. https://doi.org/10.2307/2478780

Murrill WA (1908) Additional Philippine Polyporaceae. Bulletin of the Torrey Botanical Club 35: 391–416. https://doi.org/10.2307/2479285

Murrill WA (1912) Polyporaceae of Mexico. Bulletin of New York Botanical Garden 8: 137–153.

Palomera V, Castro-Félix P, Villalobos-Arámbula AR (2008) High yield of high quality DNA from vegetative and sexual tissues of Mexican white pine (*Pinus ayacahuite*). African Journal of Biotechnology 7: 51–54.

Pan HY, Dai YC (2001) *Ganoderma weberianum* newly recorded from mainland of China. Fungal Science 16: 31–34.

Park YJ1, Kwon OC, Son ES, Yoon DE, Han W, Yoo YB, Lee CS (2012) Taxonomy of *Ganoderma lucidum* from Korea Based on rDNA and Partial β-Tubulin Gene Sequence Analysis. Mycobiology 40(1): 71–5. https://doi.org/10.5941/MYCO.2012.40.1.071

Patouillard N (1898) Quelques champignons nouveaux récoltés au Mexique par Paul Maury. Bulletin de la Société mycologique de France 14: 54.

Patouillard N, Hariot P (1906) Fungorum novorum. Decas secunda. Bulletin de la Société mycologique de France 22: 118–119.

Pegler DN, Young TWK (1973) Basidiospore form in the British species of *Ganoderma* Karst. Kew Bulletin 28: 351–364. https://doi.org/10.2307/4108879

Quanten E (1997) The polypores (Polyporaceae s.l.) of Papua New Guinea. Opera Botanica Belgica 11: 1–352.

Rambaut A, Drummond AJ, Xie D, Baele G, Suchard MA (2018) Posterior summarisation in Bayesian phylogenetics using Tracer 1.7. Systematic Biology. https://doi.org/10.1093/sysbio/syy032

Raymundo T, Valenzuela R, Gutiérrez A, Coronado ML, Esqueda M (2013) Agaricomycetes xilófagos de la planicie central del desierto Sonorense. Revista Mexicana de Biodiversidad 84: 417–424. https://doi.org/10.7550/rmb.30828

Rehner SA, Buckley E (2005) A *Beauveria* phylogeny inferred from nuclear ITS and EF1–a sequences: evidence for cryptic diversification and links to *Cordyceps* teleomorphs. Mycologia 97: 84–98. https://doi.org/10.3852/mycologia.97.1.84

Richter C, Wittstein K, Kirk P, Stadler M (2015) An assessment of the taxonomy and chemotaxonomy of *Ganoderma*. Fungal Diversity 71: 1–15. https://doi.org/10.1007/s13225-014-0313-6

Robert EC (2004) MUSCLE: multiple sequence alignment with high accuracy and high throughput. Nucleic Acids Research 32: 1792–1797. https://doi.org/10.1093/nar/gkh340

Ronquist F, Huelsenbeck JP (2003) MrBayes 3: Bayesian phylogenetic inference under mixed models. Bioinformatics 19: 1572–1574. https://doi.org/10.1093/bioinformatics/btg180

Ryvarden L (1972) A critical checklist of the Polyporaceae in tropical East Africa. Norwegian Journal of Botany 19: 229–238.

Ryvarden L (1985) Type studies in the Polyporaceae. 17. Species described by W.A. Murrill. Mycotaxon 23: 169–198.

Ryvarden L (1990). Type studies in the Polyporaceae. 22. Species described by C.G. Lloyd in *Polyporus*. Mycotaxon 38: 83–102.

Ryvarden L (1991) Genera of polypores. Nomenclature and taxonomy. Synopsis Fungorum 5: 1–363.

Ryvarden L (2000) Studies in Neotropical polypores. 2. A preliminary key to Neotropical species of *Ganoderma* with a laccate pileus. Mycologia 92: 180–191. https://doi.org/10.1080/00275514.2000.12061142

Ryvarden L (2004) Neotropical polypores. Part 1. Introduction, Ganodermataceae and Hymenochaetaceae. Synopsis Fungorum 19: 1–229.

Saccardo PA (1891) *Sylloge Fungorum IX.* – [*Hymenomyceteae*, *Polyporeae*, Fomes]. Padua, 174.

Smith BJ, Sivasithamparam K (2000) Internal transcribed spacer ribosomal DNA sequence of five species of *Ganoderma* from Australia. Mycological Research 104: 943–951. https://doi.org/10.1017/S0953756200002458

Smith BJ, Sivasithamparam K (2003) Morphological studies of *Ganoderma* (Ganodermataceae) from the Australasian and Pacific regions. Australian Systematic Botany 16: 487–503. https://doi.org/10.1071/SB02001

Stamatakis A (2006) RAxML-VI-HPC: maximum likelihood-based phylogenetic analyses with thousands of taxa and mixed models. Bioinformatics 22: 2688–2690. https://doi.org/10.1093/bioinformatics/btl446

Steyaert RL (1962) Genus *Ganoderma* (Polyporaceae). Taxa nova 2. Bulletin du Jardin Botanique de l'État à Bruxelles 32: 89–104. https://doi.org/10.2307/3667315

Steyaert RL (1972) Species of *Ganoderma* and related genera mainly of the Bogor and Leiden Herbaria. Persoonia 7: 55–118.

Steyaert RL (1980) Study of some *Ganoderma* species. Bulletin du Jardin Botanique National de Belgique 50: 135–186. https://doi.org/10.2307/3667780

Thiers B (continuously updated) Index Herbariorum: a global directory of public herbaria and associated staff. New York Botanical Garden's Virtual Herbarium. http://sweetgum.nybg.org/science/ih/. Accessed 2018.

Torres-Farradá G, Manzano León AM, Rineau F, Ledo Alonso LL, Sánchez-López MI, Thijs S, Colpaert J, Ramos-Leal M, Guerra G, Vangronsveld J (2017) Diversity of ligninolytic enzymes and their genes in strains of the genus *Ganoderma*: Applicable for biodegradation of xenobiotic compounds. Frontiers in Microbiology 8: 898. https://doi.org/10.3389/fmicb.2017.00898

Torres-Torres MG, Guzmán-Dávalos L (2012) The morphology of *Ganoderma* species with a laccate surface. Mycotaxon 119: 201–216. https://doi.org/10.5248/119.201

Torres-Torres MG, Guzmán-Dávalos L, Guggliota AM (2008) *Ganoderma vivianimercedianum* sp. nov. and the related species, *G. perzonatum*. Mycotaxon 105: 447–454.

Torres-Torres MG, Guzmán-Dávalos L, Guggliota AM (2012) *Ganoderma* in Brazil: known species and new records. Mycotaxon 121: 93–132. https://doi.org/10.5248/121.93

Torres-Torres MG, Guzmán-Dávalos L, Ryvarden L (2015) *Ganoderma* subgénero *Ganoderma* en México. Revista Mexicana de Micología 41: 27–45.

Wagner T, Ryvarden L (2002) Phylogeny and taxonomy of the genus *Phylloporia* (Hymenochaetales). Mycological Progress 1: 105–116. https://doi.org/10.1007/s11557-006-0009-8

Wang DM, Wu SH, Su CH, Peng JT, Shih YH (2009) *Ganoderma multipileum*, the correct name for "*G. lucidum*" in tropical Asia. Botanical Studies 50: 451–458.

Wang DM, Zhang XQ, Yao YJ (2005) Type studies of some *Ganoderma* species from China. Mycotaxon 93: 61–70.

Wang XC, Xi RJ, Li Y, Wang DM, Yao YJ (2012) The species identity of the widely cultivated *Ganoderma*, '*G. lucidum*' (Ling-zhi), in China. PLoS ONE 7(7): e40857. https://doi.org/10.1371/journal.pone.0040857

Welti S, Courtecuisse R (2010) The Ganodermataceae in the French West Indies (Guadeloupe and Martinique). Fungal Diversity 43: 103–126. https://doi.org/10.1007/s13225-010-0036-2

White TJ, Bruns T, Lee S, Taylor JW (1990) Amplification and direct sequencing of fungal ribosomal RNA genes for phylogenetics. In: Innis MA, Gelfand DH, Sninsky JJ, White TJ (Eds) PCR protocols: a guide to methods and applications. Academic Press, New York, 315–322. https://doi.org/10.1016/B978-0-12-372180-8.50042-1

Xing JH, Sun YF, Han YL, Cui BK, Dai YC (2018) Morphological and molecular identification of two new *Ganoderma* species on *Casuarina equisetifolia* from China. MycoKeys 34: 93–108. https://doi.org/10.3897/mycokeys.34.22593

Yao YJ, Wang XC, Ang B (2013) Epitypification of *Ganoderma sichuanense* J.D. Zhao & X.Q. Zhang (Ganodermataceae). Taxon 62: 1025–1031. https://doi.org/10.12705/625.10

Yombiyeni P, Decock C (2017) Hymenochaetaceae (Hymenochaetales) from the Guineo-Congolian phytochorion: *Phylloporia littoralis* sp. nov. from coastal vegetation in Gabon, with an identification key to the local species. Plant Ecology and Evolution 150: 160–172. https://doi.org/10.5091/plecevo.2017.1289

Zhou LW, Cao Y, Wu SH, Vlasák J, Li DW, Li MJ, Dai YC (2014) Global diversity of the *Ganoderma lucidum* complex (Ganodermataceae, Polyporales) inferred from morphology and multilocus phylogeny. Phytochemistry 114: 7–15. https://doi.org/10.1016/j.phytochem.2014.09.023